

# MODELLING SEDIMENT YIELD FROM NATURAL WATERSHEDS

## A THESIS

*Submitted in partial fulfilment of the  
requirements for the award of the degree*

*of*

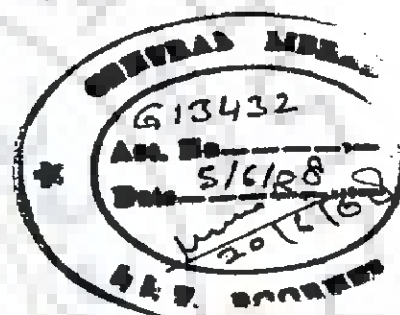
DOCTOR OF PHILOSOPHY

*in*

HYDROLOGY

By

**JAIVIR TYAGI**



DEPARTMENT OF HYDROLOGY  
INDIAN INSTITUTE OF TECHNOLOGY ROORKEE  
ROORKEE-247 667 (INDIA)

JULY, 2007

**© INDIAN INSTITUTE OF TECHNOLOGY ROORKEE, ROORKEE, 2007  
ALL RIGHTS RESERVED**





# INDIAN INSTITUTE OF TECHNOLOGY ROORKEE ROORKEE

## CANDIDATE'S DECLARATION

I hereby certify that the work which is being presented in the thesis entitled **MODELLING SEDIMENT YIELD FROM NATURAL WATERSHEDS** in partial fulfilment of the requirements for the award of the Degree of Doctor of Philosophy and submitted in the Department of Hydrology of the Indian Institute of Technology Roorkee, Roorkee is an authentic record of my own work carried out during a period from August 2002 to July 2007 under the supervision of Dr. Ranvir Singh, Professor, Department of Hydrology and Dr. S. K. Mishra, Assistant Professor, Department of Water Resources Development and Management, Indian Institute of Technology Roorkee, Roorkee.

The matter presented in this thesis has not been submitted by me for the award of any other degree of this or any other Institute.

(JAI VIR TYAGI)

This is to certify that the above statement made by the candidate is correct to the best of our knowledge



(Dr. S. K. Mishra)

Assistant Professor

Department of WRD&M

Indian Institute of Technology Roorkee

Roorkee - 247 667, INDIA



(Dr. Ranvir Singh)

Professor

Department of Hydrology

Indian Institute of Technology Roorkee

Roorkee - 247 667, INDIA

Date: July 16, 2007

The Ph.D. Viva-Voce Examination of **Mr. JAI VIR TYAGI**, Research Scholar, has been held on .....

## ABSTRACT

---

The rainfall-runoff-soil erosion process in a watershed is a very complicated phenomenon that is controlled by a large number of known and unknown climatic, geologic and physiographic factors that vary both in time and space. Several models, varying in complexity from lumped empirical to physically based, time and space distributed, are available in literature to model soil erosion and consequent sediment yield. The physically based models have proved very useful as a research tool but are of limited use in field, especially in developing countries like India, because they require large amount of data. Nevertheless, search is still continuing for developing new and simple models. In the present research work, an attempt has therefore been made to develop event-based, lumped and time-distributed simple sediment yield models using the well-accepted hydrologic concept of proportional equality of the Soil Conservation Service Curve Number (SCN-CN) method and the upland potential erosion, normally estimated by erosion equations such as the Universal Soil Loss Equation (USLE).

To start with, a detailed survey of the published works relating to rainfall-runoff-erosion modelling was carried out. Because of the close dependence of sediment yield process on surface runoff, a sediment yield model utilizes either a lumped estimate of surface runoff for computing total sediment yield from a storm event or a suitable infiltration model is employed to generate temporally varying rainfall-excess (or runoff rate) that is primarily responsible for delivering the sediment at the watershed outlet.

The SCS-CN method is well established in hydrologic engineering and is one of the most popular methods for computing the volume of direct surface runoff for a given rainfall event from small agricultural, forest and urban watersheds. The direct surface runoff generated by

SCS-CN method is closely linked with infiltration. The SCS-CN method accounts for most of the runoff producing watershed characteristics, viz., soil type, land use/treatment, surface condition, and antecedent moisture condition through curve number. The USLE, used to compute the potential soil erosion from small watersheds, also accounts for these watershed characteristics, albeit differently. Thus, the processes of runoff generation and soil erosion are closely interrelated. Further, the sediment yield is generally determined from the USLE computed potential erosion using the sediment delivery ratio (DR). It is therefore conjectured that by coupling the SCS-CN method and the USLE, one can compute the sediment yield from the knowledge of rainfall, soil type, land use and antecedent soil moisture condition, for sediment yield greatly depends on runoff. In developing the time-distributed sediment yield model, the rainfall-excess rate was computed using the SCS-CN based infiltration model. In order to have confidence in its simulation ability, the SCS-CN based infiltration model was first evaluated for its performance in comparison with other infiltration models. The following text briefly presents development of the sediment yield models.

### **Comparative Evaluation of SCS-CN Based Infiltration Model**

Since the present research work uses the SCS-CN based infiltration model for computation of event sedimentographs, it was evaluated for its performance in comparison to other popular infiltration models. A total of fourteen infiltration models including Philip Model, Green and Ampt model, linear and nonlinear Smith-Parlange models, Singh-Yu model, SCS-CN based Mishra-Singh model, Smith model, Horton model, Holtan model, Overton model, Kostiaikov model, modified Kostiaikov model, Huggins-Monke model, and Collis-George model were evaluated using the Nash and Sutcliffe efficiency criterion and compared for their performance on 243 sets of infiltration data collected from field and laboratory tests conducted in India and USA on soils ranging from coarse sand to fine clay. Based on a relative grading scale,

the semi-empirical Singh-Yu general model, Holtan model, and Horton model were graded respectively as 6.52, 5.57, and 5.48 out of 10. The empirical Huggins-Monke model, modified-Kostiakov model, Kostiakov model, and SCS-CN based model were graded as 5.57, 5.30, 5.22, and 4.96 respectively. The physically-based non-linear and linear models of Smith-Parlange were graded as 5.48 and 5.22, respectively. Other models were ranked lower than these models. In general, the above ranked models exhibited a satisfactory to very good performance on laboratory-tests; and poor to very good on field-tests in India. All the models generally performed poorly on field-tests on Georgia sandy soils, except the Robertsdale Loamy sand. The study indicated that the SCS-CN based infiltration model, with its performance comparable with other frequently used models, can be used satisfactorily for further applications.

#### **SCS-CN Based Lumped Sediment Yield Model**

The model for computing total sediment yield from a rainfall event was derived by coupling the SCS-CN method with USLE. The coupling is based on three hypotheses: (1) the runoff coefficient,  $C$  (dimensionless), is equal to the degree of saturation,  $S_r$  (dimensionless); (2) the USLE can be signified in terms of SCS-CN parameter potential maximum retention,  $S$  (L); and (3) the sediment delivery ratio,  $DR$  (dimensionless), can be equated to  $C$  or  $S_r$ . The volumetric analysis of the potential erosion led to the inference that the ratio of actual potential maximum erosion,  $A$  (M), per unit area to actual potential maximum retention,  $S$  ( $= A/S$  ratio) is constant for a watershed. Based on the analytical development, seven variations of the sediment yield model were formulated for different combinations of initial abstraction,  $I_a$ , antecedent moisture,  $M$ , and initial flush,  $I_f$ . These model variations were applied to the rainfall-runoff-sediment yield data of 98 rainfall events observed on 12 watersheds, located in India and USA. The watersheds varying from 300 m<sup>2</sup> to a few km<sup>2</sup> in size represented different land uses viz., urban, agricultural, and forest. The parameters  $I_a$ ,  $A$ ,  $S$ ,  $M$ , and  $I_f$  as applicable to different

model variations were calibrated using non-linear Marquardt optimization technique. For all the watersheds, the computed sediment yield was found to be in good agreement with the observed values. The Nash and Sutcliffe (1970) efficiency exhibited that the performance of the model directly based on the existing SCS-CN method was comparable with that showing the highest performance, and therefore, it was recommended for computing the sediment yield,  $Y$  (M), as:

$$Y = \frac{(P - 0.2S)A}{P + 0.8S} \quad (1)$$

where  $P$  is the total rainfall (L) from the storm event. The CN values computed from the sediment yield model and from the existing SCS-CN method exhibited a quadratic relationship. The A/S ratios were also determined for each of the study watersheds, and a procedure is suggested for computation of sediment yield from the storm events using these ratios.

#### SCS-CN Based Time-Distributed Sediment Yield Model

An event based, time-distributed sediment yield model for computation of sedimentograph was developed using the SCS-CN based infiltration model. The rainfall-excess rate (or the direct surface runoff rate),  $q_t$  ( $L T^{-1}$ ), at any time 't' was computed by subtracting the infiltration rate ( $L T^{-1}$ ) from the rainfall intensity,  $i$  ( $L T^{-1}$ ), as:

$$q_t = (i - f_c) \left[ 1 - \frac{S^2}{(P + S - \lambda S)^2} \right] \quad (2)$$

which is valid for  $P > \lambda S$ ,  $q_t = 0$  otherwise. Here,  $f_c$  is the steady or constant infiltration rate ( $L T^{-1}$ ),  $P$  is the cumulative rainfall (L) up to time 't' since the start of rainfall, and  $\lambda S$  represents initial abstraction (L). The value of  $\lambda$  was taken as 0.2 (a standard value). The sediment-excess rate,  $y_t$  ( $M T^{-1}$ ), was computed by coupling the rainfall-excess rate,  $q_t$ , with the actual potential maximum erosion using the proportionality concept of SCS-CN method as follows:

$$\frac{y_t}{A} = \frac{q_t}{P_{\Delta t}} \quad (3)$$

where  $A$  = actual potential maximum erosion ( $M$ ) of the watershed, dependent on soil properties and actual potential maximum retention,  $S$ ; and  $P_{\Delta t}$  = rainfall amount ( $L$ ) during time interval  $\Delta t$ .

Rearranging Eq. 3 as:

$$y_t = \frac{A}{P_{\Delta t}} \left[ 1 - \frac{S^2}{(P + S - \lambda S)^2} \right] (i - f_c) \quad (4)$$

enables determination of sediment-excess rate from watershed characteristics and temporal distribution of rainfall. The sedimentograph at the watershed outlet was computed by routing the sediment-excess rate using simple single linear reservoir technique.

The model was calibrated and validated on a number of events using the data of seven watersheds from India and USA. Representative values of  $A/S$  ratios computed for the watersheds from calibration were used for validation of the model. The efficiencies of computation of sedimentographs in both calibration and validation were reasonably high to show satisfactory model performance.

Finally, it was concluded that both lumped and time-distributed sediment yield models, developed using the SCS-CN proportionality concept, performed satisfactorily well on all the study watersheds. Being simple, the proposed models have ample potential for field applications, for these have only a few parameters determinable from watershed characteristics.



## ACKNOWLEDGEMENTS

---

It is my proud privilege to express my heartfelt gratitude and sincere thanks to my supervisors, Dr. Ranvir Singh, Professor, Department of Hydrology and Dr. S.K. Mishra, Assistant Professor, Department of Water Resources Development and Management, Indian Institute of Technology, Roorkee for their efforts, inputs and patience in bringing out the scholar in me. I am highly obliged to them for their keen interest, able guidance and encouragement throughout this research study.

I am extremely thankful to Dr. N.K. Goel, Professor and Head, Department of Hydrology, for extending the help, support and facilities during the course of this research work. I am grateful to Prof. B.S. Mathur, Prof. D.K. Srivastava, Prof. D.C. Singhal and Dr. M. Perumal in the Department of Hydrology for their constant encouragement, guidance and cooperation.


I express my sincere thanks to Dr. K.D. Sharma, Director, National Institute of Hydrology, Roorkee for permitting me to carry out this work and extending the necessary research facilities. I am also thankful to Dr. K.K.S. Bhatia, Mr. R.D. Singh, Dr. Sharad K. Jain, Dr. Bhisim Kumar, Dr. Sanjay K. Jain, Dr. Sudhir Kumar and my other colleague Scientists in NIH Roorkee who were helpful in many ways.

I am obliged to Mr. C.M. Pandey, Deputy Commissioner and Mr. R.K. Tiwari, Assistant Commissioner, Ministry of Agriculture, Govt. of India, New Delhi and Mr. G. Honore, *RODECO Consulting Germany at New Delhi, for providing hydrological data of the watersheds* monitored under 'Indo-German Bilateral Project on Watershed Management' for use in the present research study. I also gratefully acknowledge Dr. Latif Kalin, National Risk management Research laboratory, Cincinnati, USA, for providing rainfall, runoff and sediment yield data of W2 Treynor watershed.

I am also thankful to Mr. Raveendra Kumar Rai, Mr. Ashoke Basistha and other fellow research scholars in the Department of Hydrology, who have shared parts of their time with me, filling me with knowledge, togetherness and support.

I am short of words to express my feelings for all my family members, who stood besides me during the present work at various stages. My mother, brothers, sister and in-laws were always source of inspiration for the completion of this work in time. I am extremely grateful to my wife Anita, and both the children, Manila and Shubham for their persuasive inspiration, love, affection and patience throughout the study.

Lastly, the greatest of my gratitude is towards the Almighty for giving me the power to fulfill the promises He entrusted to me as a human being. All the efforts that could be made in this study have been possible by the grace of God who is the Author and Finisher of every good work.



(Jaivir Tyagi)

# CONTENTS

<b>Chapters</b>	<b>Page No.</b>
<b>CANDIDATE'S DECLARATION</b>	(i)
<b>ABSTRACT</b>	(ii)
<b>ACKNOWLEDGEMENTS</b>	(vii)
<b>CONTENTS</b>	(ix)
<b>LIST OF FIGURES</b>	(xii)
<b>LIST OF TABLES</b>	(xiv)
<b>LIST OF SYMBOLS AND ABBREVIATIONS</b>	(xv)
<b>1. INTRODUCTION</b>	<b>1</b>
1.1 BACKGROUND	1
1.2 OBJECTIVES OF THE STUDY	5
1.3 PLAN OF DISSERTATION	5
<b>2. REVIEW OF LITERATURE</b>	<b>7</b>
2.1 SCS-CN METHOD	7
2.2 FACTORS AFFECTING CURVE NUMBERS	9
2.2.1 Soil Type	9
2.2.2 Land Use/Treatment	10
2.2.3 Hydrologic Condition	11
2.2.4 Agricultural Management Practices	12
2.2.5 Antecedent Moisture Condition	12
2.3 APPLICATIONS OF SCS-CN METHOD IN WATERSHED HYDROLOGY	14
2.4 MODELLING INFILTRATION PROCESS	16
2.5 MECHANICS OF SOIL EROSION BY WATER	21
2.6 FACTORS AFFECTING EROSION AND SEDIMENT YIELD	22
2.6.1 Climate	22
2.6.2 Soil Properties	23
2.6.3 Catchment Characteristics	24
2.6.4 Land Cover	25

2.7	MODELLING SOIL EROSION AND SEDIMENT YIELD	25
2.7.1	Empirical Erosion Models	26
2.7.2	Conceptual Erosion Models	31
2.7.3	Physically Based Erosion Models	32
2.8	CONCEPT OF SEDIMENT DELIVERY RATIO	41
2.9	SOME USEFUL WATERSHED MODELS FOR RAINFALL-RUNOFF- SEDIMENT YIELD MODELLING	42
2.10	SUMMARY	44
<b>3.</b>	<b>COMPARISON OF INFILTRATION MODELS</b>	<b>45</b>
3.1	GENERAL	45
3.2	INFILTRATION MODELS	46
3.3	APPLICATION OF INFILTRATION MODELS	52
3.3.1	Infiltration Data	52
3.3.2	Parameter Estimation	53
3.3.3	Performance Evaluation	53
3.4	DISCUSSION OF RESULTS	60
3.5	SUMMARY	67
<b>4.</b>	<b>DESCRIPTION OF STUDY WATERSHEDS</b>	<b>70</b>
4.1	GENERAL	70
4.2	STUDY WATERSHEDS	71
4.2.1	IGBP Watersheds	71
4.2.2	USDA-ARS Watersheds	73
4.2.3	Cincinnati Watershed	75
4.3	DATA STATUS	76
<b>5.</b>	<b>SCS-CN BASED LUMPED SEDIMENT YIELD MODEL</b>	<b>85</b>
5.1	INTRODUCTION	85
5.1.1	SCS-CN Method	86
5.1.2	Universal Soil Loss Equation	88
5.1.3	Computation of Sediment Yield	88
5.2	DEVELOPMENT OF SEDIMENT YIELD MODEL	90
5.2.1	Hypothesis: $C = S_r$	90
5.2.2	Hypothesis: Physical Significance of S	91

5.2.3	Hypothesis: $DR = C$	93
5.2.4	Coupling of the SCS-CN Method with USLE	94
5.3	MODEL APPLICATION	97
5.3.1	Data Used	97
5.3.2	Model Formulations	97
5.3.3	Goodness of Fit Statistics	97
5.4	RESULTS AND DISCUSSION	97
5.4.1	Model Calibration and Verification	97
5.4.2	Determination of the A/S Ratio	107
5.5	SUMMARY	108
<b>6.</b>	<b>SCS-CN BASED TIME-DISTRIBUTED SEDIMENT YIELD MODEL</b>	<b>113</b>
6.1	INTRODUCTION	113
6.2	MODEL DEVELOPMENT	114
6.2.1	Relationship of USLE with S	114
6.2.2	Derivation of Infiltration Model and Computation of Rainfall-Excess Rate	114
6.2.3	Coupling of Rainfall-Excess Rate with Upland Erosion	118
6.2.4	Routing of Sediment-Excess Rate	119
6.3	HYDROLOGICAL DATA FOR MODEL APPLICATION	119
6.4	RESULTS AND DISCUSSION	120
6.4.1	Model Calibration	120
6.4.2	Determination of A/S Ratio	129
6.4.3	Model Validation	130
6.5	SUMMARY	132
<b>7.</b>	<b>SUMMARY AND CONCLUSIONS</b>	<b>137</b>
7.1	EVALUATION OF SCS-CN BASED INFILTRATION MODEL	138
7.2	SCS-CN BASED LUMPED SEDIMENT YIELD MODEL	139
7.3	SCS-CN BASED TIME-DISTRIBUTED SEDIMENT YIELD MODEL	140
7.4	MAJOR CONTRIBUTIONS OF THE STUDY	141
	<b>REFERENCES</b>	<b>143</b>
	<b>LIST OF PUBLICATIONS</b>	<b>166</b>

## LIST OF FIGURES

Figures	Page No.
3.1 Simulation of infiltration data of Plainfield sand (PFS)	68
3.2 Simulation of infiltration data of Robertsdale loamy sand (RLS)	68
3.3 Simulation of infiltration data of Dudhnai silty sand (DUSS)	69
3.4 Simulation of infiltration data of Cowarts loamy sand (COWLS)	69
4.1 Drainage map of Nagwa watershed	80
4.2 Drainage map of Karso watershed	80
4.3 Drainage map of Banha watershed	81
4.4 Drainage map of Mansara watershed	81
4.5 Drainage map of W-2 Treynor watershed	82
4.6 Drainage map of W6 Goodwin creek watershed	82
4.7 Drainage map of W7 Goodwin creek watershed	83
4.8 Drainage map of W14 Goodwin creek watershed	83
4.9 Drainage map of Cincinnati watershed	84
4.10 Drainage map of 123 NAEW	84
4.11 Drainage map of 129 NAEW	84
4.12 Drainage map of 182 NAEW	84
5.1 Proportionality concept	87
5.2 Schematic diagram showing soil-water-air	91
5.3 Relationship between curve numbers derived from (a) the rainfall-sediment yield model and (b) the existing SCS-CN method (using rainfall-runoff data)	104
5.4 Comparison of observed and computed (a) sediment yield (b) runoff using model S2 and R2 for Nagwa watershed	109
5.5 Comparison of observed and computed (a) sediment yield (b) runoff using model S2 and R2 for Karso watershed	109
5.6 Comparison of observed and computed (a) sediment yield (b) runoff using model S2 and R2 for Banha watershed	109
5.7 Comparison of observed and computed (a) sediment yield (b) runoff using model S2 and R2 for Mansara watershed	110

5.8	Comparison of observed and computed (a) sediment yield (b) runoff using model S2 and R2 for W2 Treynor watershed	110
5.9	Comparison of observed and computed (a) sediment yield (b) runoff using model S2 and R2 for W6 Goodwin creek watershed	110
5.10	Comparison of observed and computed (a) sediment yield (b) runoff using model S2 and R2 for W7 Goodwin creek watershed	111
5.11	Comparison of observed and computed (a) sediment yield (b) runoff using model S2 and R2 for W14 Goodwin creek watershed	111
5.12	Comparison of observed and computed (a) sediment yield (b) runoff using model S2 and R2 for Cincinnati watershed	111
5.13	Comparison of observed and computed (a) sediment yield (b) runoff using model S2 and R2 for 182 NAEW watershed	112
5.14	Comparison of observed and computed (a) sediment yield (b) runoff using model S2 and R2 for 129 NAEW watershed	112
5.15	Comparison of observed and computed (a) sediment yield (b) runoff using model S2 and R2 for 123 NAEW watershed	112
6.1	Comparison of observed and computed sedimentographs for the calibration events	125
6.2	Relationship between curve numbers derived from (a) the time-distributed rainfall-sediment yield model and (b) the existing SCS-CN method (using rainfall-runoff data)	128
6.3	Comparison of observed and computed sedimentographs for the validation events	135

## LIST OF TABLES

---

	<b>Tables</b>	<b>Page No.</b>
2.1	Important relationships available for the inter-rill erosion computation	34
2.2	Important relationships available for the rill erosion process	37
2.3	Important relationships available for the transport process	40
3.1	Infiltration data	55
3.2	Statistics of optimized parameters on various soil types	56
3.3	Models performance on various soils	62
4.1	Hydro-climatic characteristics of the watersheds selected for the study	78
5.1	Formulation of rainfall-sediment yield and rainfall-runoff models	98
5.2	Results of various model applications to study watersheds	100
5.3	Runoff computation using transformed S-values and model R2	107
6.1	Optimized values of parameters of sediment yield model for calibration events	122
6.2	Characteristics of observed and computed sedimentographs for calibration events	124
6.3	Parameter values of sediment yield model for validation events	131
6.4	Characteristics of observed and computed sedimentographs for validation events	134



## LIST OF SYMBOLS AND ABBREVIATIONS

---

A	actual potential maximum erosion; a hydrologic soil group; a parameter of Green-Ampt model ( $A_t$ = potential maximum erosion of completely dry soil)
AMC	antecedent soil moisture condition (AMC I for dry, AMC II for normal, and AMC III for wet soil)
b	a parameter of Mockus method
B	a hydrologic soil group; a parameter of the Green-Ampt model
C	runoff coefficient; a hydrologic soil group; cover management factor
CN	curve number ( $CN_{II}$ = curve number for AMC II)
D	a hydrologic soil group
DR	sediment delivery ratio
f	infiltration rate
$f_c$	final or minimum infiltration rate
$f_d$	dynamic rate of infiltration rate
$f_o$	initial infiltration rate
F	cumulative infiltration
$F_c$	cumulative static (steady) portion of total infiltration
$F_d$	cumulative dynamic portion of total infiltration
h	hour
ha	hectare
i	rainfall intensity
I	Inflow rate
$I_a$	initial abstraction
$i_e$	effective rainfall intensity
$I_f$	initial flush
k	Horton's infiltration decay parameter
K	storage coefficient of linear reservoir; soil erodibility factor
$K_s$	Saturated hydraulic conductivity
KN	kilo newton
LS	slope length and steepness factor
M	antecedent moisture amount

mm	millimeter
MUSLE	modified universal soil loss equation
n	soil porosity
NEH	National Engineering Handbook
O	outflow rate
P	cumulative rainfall depth; supporting practice factor
$P_{\Delta t}$	rainfall amount during time interval $\Delta t$
$P_c$	cumulative effective rainfall depth
Q	cumulative direct surface runoff
$q_t$	rainfall-excess rate
R	rainfall erosivity factor
S	actual potential maximum retention ( $S_1 = S$ of completely dry soil)
$S_c$	potential maximum storage space available for steady portion of infiltration
$S_d$	potential maximum storage space available for dynamic portion of infiltration
$S_r$	degree of saturation
$S_{ro}$	initial degree of saturation
SCS	Soil Conservation Service
t	time coordinate
V	total volume of soil column; storage of linear reservoir
$V_a$	volume of air
$V_{ao}$	initial volume of air in the soil
$V_{pe}$	actual potential maximum erodible soil depth
$V_s$	volume of solids
$V_v$	volume of voids
$V_w$	volume occupied by infiltrated water
$V_{wo}$	initial volume of water in the soil
USLE	universal soil loss equation
Y	total sediment yield; land gradient over the runoff length
$y_t$	sediment-excess rate
$\lambda$	initial abstraction coefficient
$\lambda_1$	initial flush coefficient
$\rho_s$	density of solids

# CHAPTER 1

## INTRODUCTION

---

### 1.1 BACKGROUND

Land degradation from water-induced soil erosion is a serious global problem, which is not only eroding the top fertile soil but is also responsible for swelling of river beds and reservoirs thereby causing floods and reduction in the life span of costly reservoirs and dams. Though it is difficult to assess reliably and accurately the rate and magnitude of runoff and associated soil loss, the information available in literature, which is often based on reconnaissance surveys and extrapolations, provides an idea of the severity of this problem. Judson (1981) estimated that river-borne sediments carried into the oceans increased from 10 billion tones per year before the introduction of intensive agriculture, grazing, and other activities to 25-50 billion tones per year thereafter. Dudal (1981) reported that the current rate of agricultural land degradation worldwide by soil erosion along with other factors led to an irreversible loss in annual productivity of about six million ha of fertile land. Narayana and Babu (1983) estimated that about 5334 million tones of soil is being eroded annually in India, due to which 8.4 million tones of nutrients are lost. Another estimate reveals that the average soil loss in India is about 16.3 tones per ha per year against the permissible range of 5-12.5 tones per ha per year for various regions (Narayana, 1993).

Reliable estimates of soil erosion and sediment yield are, therefore, required for design of efficient erosion control measures, reservoir sedimentation assessment, water quality management, and evaluation of watershed management strategies. The detachment and displacement of soil particles over short distances, referred to as erosion, do not wholly represent

the sediment delivered at the watershed outlet known as sediment yield. Much deposition and reduction in sediment load occurs between the sediment sources and the outlet (Narayana and Babu, 1983). Sediment yield is limited by the transport capacity of runoff (Beasley and Huggins, 1981; Morgan, 1995). Measurement of sediment yield on a number of watersheds is operationally difficult, expensive, time consuming, and tedious, and therefore modelling is carried out for simulating, generating or augmenting the sediment yield data base.

The rain falling on a watershed undergoes a number of transformations and abstractions through various component processes of hydrologic cycle, viz., interception, detention, evaporation and evapotranspiration, overland flow, infiltration, interflow, percolation, base flow etc., and finally emerges as runoff at the watershed outlet. These component processes are functions of various climatic and watershed characteristics, such as rainfall intensity and duration, topography, land use and vegetation cover, drainage pattern, drainage density, geology etc., which are not uniform in time and space. Soil erosion by water that refers to the removal of soil particles from the land surface due to erosive action of water depends on both rainfall intensity and consequent runoff. When raindrops fall on the surface, soil particles are detached due to the kinetic energy of drops. The higher the rainfall intensity, the greater will be the amount of the soil detached. When the rainfall-excess (or direct runoff) flows downhill, it gets concentrated. During the process of overland flow, soil particles are detached when shear stress of the flow exceeds the gravitational and cohesive forces of the soil mass. The movement of detached soil particles depends on the sediment load in the flow and the flow's sediment transport capacity. Once a soil particle has been detached, sufficient energy must be available to transport it or the particle will be deposited. Thus, the soil loss is greatly influenced by the intensity of rainfall, rate of overland flow, vegetation cover, and soil texture.

Several models, varying in complexity from lumped empirical to physically based, have been developed by various researchers to model the soil erosion and consequent sediment yield (Wischmeier and Smith, 1965, 1978; Foster and Meyer, 1972a; Nearing et al., 1989; Woolhiser et al., 1990; Govindaraju and Kavvas, 1991; Kothyari et al., 1997; Tayfur, 2001; Su et al., 2003; Kalin et al., 2004; Jain et al., 2005). A common approach to the assessment of soil erosion and sediment yield is the use of empirical equations, such as the Universal Soil Loss Equation (USLE) (Wischmeier and Smith, 1965; 1978) or its extensions viz., Modified Universal Soil Equation (MUSLE) (Williams, 1975) and Revised Universal Soil Equation (RUSLE) (Renard et al., 1991). The USLE predicts sheet and rill erosion and does not take into account the deposition of sediment enroute. Therefore, a concept of sediment delivery ratio has been used with USLE for estimation of sediment discharge from large watersheds (Hadley et al, 1985). The sediment delivery ratio, DR, represents the ratio of the sediment yield to the gross upland erosion in the watershed and depends on many factors, including watershed physiography, sediment source, transport system, texture of eroded material and depositional areas (Dendy, 1982).

Because of the close dependence of sediment yield process on the surface runoff, the erosion models, or the component processes of detachment, transport and deposition thereof, are coupled with models capable of simulating the rainfall-runoff response of a watershed (Knisel, 1980; Leonard et al., 1987; Rode and Frede, 1997). Examples of such a coupling include a number of models, such as empirical Modified Universal Soil Loss Equation (MUSLE) (Williams, 1975) and the model of Williams and Berndt (1977); physically based Water Erosion Prediction Project (WEPP) (Nearing et al., 1989), Areal Nonpoint Source Watershed Environment Response Simulation (ANSWERS) (Beasley and Huggins, 1980), Agricultural Nonpoint Source Pollution Model (AGNPS) (Young et al., 1987), and SWAT (Arnold et al., 1993) models, among others.

Thus, quite a good deal of literature is available on rainfall-runoff-erosion modelling to simulate the complex processes of soil erosion and sediment yield under different field conditions. These models have also proved very useful as a research tool but are of limited use in field, especially in developing countries, because they require sufficient skill and large amount of data. Nevertheless, search is still continuing for developing new and simpler models which, at the same time, should retain their prediction ability as close to the reality as possible. In the present study, an attempt has therefore been made to develop simple sediment yield models using the well-accepted hydrologic concept of proportional equality of the Soil Conservation Service Curve Number (SCN-CN) method (SCS, 1956). The SCS-CN method is a popular method for computing the volume of direct surface runoff for a given rainfall event from small agricultural, forest, and urban watersheds. The method is simple, easy to understand and apply, and useful for ungauged watersheds. The method utilizes proportional equality hypothesis in combination with water balance equation for computing the direct surface runoff.

The soil texture determines both permeability and erodibility of soils. Permeability describes infiltration, which, in turn, determines hydrologic activeness of the soil surface in terms of both runoff generation and soil erosion. The direct surface runoff generated by SCS-CN method is closely linked with infiltration. The method accounts for most of the runoff producing watershed characteristics, viz., soil type, land use/treatment, surface condition, and antecedent moisture condition through curve number. The USLE, used to compute the potential soil erosion from small watersheds, also accounts for these watershed characteristics, albeit differently. Thus, the processes of runoff generation and soil erosion are closely interrelated. However, the SCS-CN method and USLE have not yet been investigated for their interrelationship. The SCS-CN proportionality concept can be extended to the sediment delivery ratio to allow a coupling of the SCS-CN method with the USLE and to compute the sediment yield from the knowledge of

rainfall, soil type, land use and antecedent soil moisture condition, since the sediment yield greatly depends on runoff.

## **1.2 OBJECTIVES OF THE STUDY**

Based on the above discussion, the specific objectives set out for the present research work are summarized as follows.

- (i) To collect and compile the data available in literature on infiltration tests for various soils, and hydrological and sediment yield for a number of watersheds;
- (ii) To apply the SCS-CN based infiltration model along with other popular infiltration models to the infiltration data and assess the performance of the SCS-CN based model in simulating the infiltration rates in comparison to other models;
- (iii) To develop SCS-CN based lumped sediment yield model for estimating the sediment yield from a rainfall event;
- (iv) To develop SCS-CN based time-distributed sediment yield model for computing event sedimentograph from rainfall event at watershed scale;
- (v) To calibrate and validate the models developed herein and assess their general applicability using the available hydrological and sediment yield data of a number of watersheds.

The proposed simple models may be useful for field engineers and conservation workers in estimation of the sediment yield required for conservation planning, project planning, and soil erosion inventories.

## **1.3 PLAN OF DISSERTATION**

The thesis presents a systematic review of various approaches employed in erosion and sediment yield modelling, and the development of suitable event based, lumped and time-

distributed sediment yield models applicable to natural watersheds. The contents of this thesis are divided into seven chapters. A brief account of the chapter-wise contents is given as follows.

**Chapter 1:** It presents a brief introduction of erosion and sediment yield modelling and its need, followed by the objectives of the study.

**Chapter 2:** It brings out literature survey relevant to the study. Besides presenting a brief review of the SCS-CN method and infiltration modelling, the chapter also discusses the pertinent aspects of soil erosion by water and the erosion and sediment yield modelling reported by various researchers.

**Chapter 3:** Since the SCS-CN based infiltration model was employed in computation of temporal rates of sediment yield, it was evaluated for its performance in comparison to other popular infiltration models and the results are discussed in Chapter 3.

**Chapter 4:** The details of the watersheds and availability of their hydrologic and sediment yield data that have been used for application of the proposed sediment yield models are discussed.

**Chapter 5:** It deals with the analytical development and application of the event-based lumped sediment yield model. The pertinent aspects of SCS-CN method, the USLE, and their coupling, crucial to the model development, are presented in this chapter.

**Chapter 6:** It presents a detailed description of the SCS-CN based infiltration model and its coupling with the potential erosion leading to the development of the time-distributed sediment yield model. The results of model calibration and validation are also discussed in this chapter.

**Chapter 7:** Finally, the summary and conclusions of the study have been presented in this chapter.



## **CHAPTER 2**

### **REVIEW OF LITERATURE**

---

The process of sediment yield closely depends on the direct surface runoff. Therefore, a sediment yield model utilizes either a lumped estimate of direct surface runoff for computing total sediment yield from a storm event or, as in most cases, a suitable infiltration model to generate the temporal rainfall-excess rate (or runoff rate) that is primarily responsible for delivering the temporally varying sediment rate at the watershed outlet. The present research work is carried out with an objective to develop event based lumped and time-distributed sediment yield models for natural watersheds by coupling the upland potential erosion with the SCS-CN (SCS, 1956) method through its proportional equality hypothesis. Accordingly, in the present work the review of literature has been carried out with a focus on SCS-CN methodology and its applications in watershed hydrology for computation of surface runoff; modelling the infiltration process; pertinent aspects of soil erosion by water, and; the erosion and sediment yield modelling as reported by various researchers.

#### **2.1 SCS-CN METHOD**

The Soil Conservation Service (now called the Natural Resources Conservation Service) Curve Number (SCS-CN) method was developed in 1954 and is documented in Section 4 of the National Engineering Handbook (NEH-4) published by the Soil Conservation Service, U.S. Department of Agriculture in 1956. The document has since been revised in 1964, 1971, 1972, 1985 and 1993. The SCS-CN method is the result of exhaustive field investigations carried out during late 1930s and early 1940s and the works of several early investigators, including Mockus (1949), Sherman (1949), Andrews (1954) and Ogrosky (1956). The method is well established in

hydrologic engineering and environmental impact analysis (Ponce and Hawkins, 1996) and is one of the most popular methods for computing the volume of direct surface runoff for a given rainfall event from small agricultural, forest and urban watersheds (Mishra and Singh, 2003).

The SCS-CN method is based on the water balance equation and two fundamental hypotheses. The first hypothesis equates the ratio of the actual amount of direct surface runoff (Q) to total rainfall (P) (or potential maximum surface runoff) to the ratio of the amount of actual infiltration (F) (or actual retention) to amount of potential maximum retention (S). The second hypothesis relates the initial abstraction ( $I_a$ ) to the potential retention. Expressed mathematically, the water balance equation and the two hypotheses, respectively, are:

$$P = I_a + F + Q \quad (2.1)$$

$$\frac{Q}{P - I_a} = \frac{F}{S} \quad (2.2)$$

$$I_a = \lambda S \quad (2.3)$$

The initial abstraction accounts for the short-term losses, such as interception, surface storage and initial infiltration. Parameter  $\lambda$  is frequently viewed as a regional parameter dependent on geologic and climatic factors (Bosznay, 1989). The existing SCS-CN method assumes  $\lambda$  to be equal to 0.2 for practical applications. Many other studies carried out in the United States and other countries (SCD, 1972; Springer et al., 1980; Cazier and Hawkins, 1984; Bosznay, 1989) report  $\lambda$  to vary in the range of (0-0.3). Combining Eq. 2.1 and Eq. 2.2, the popular form of SCS-CN method is obtained:

$$Q = \frac{(P - I_a)^2}{P - I_a + S} \quad (2.4)$$

Eq. 2.4 is valid for  $P > I_a$ ,  $Q = 0$ , otherwise. For  $\lambda = 0.2$ , Eq. 2.4 can be re-written as:

$$Q = \frac{(P - 0.2S)^2}{P + 0.8S} \quad (2.5)$$

Thus, the existing SCS-CN method (Eq. 2.5) has only one parameter, S, for computing surface runoff from storm event. Since S can vary in the range of  $0 \leq S \leq \infty$ , it is mapped into a dimensionless curve number (CN), varying in a more appealing range  $0 \leq CN \leq 100$ , as follows:

$$S = \frac{25400}{CN} - 254 \quad (\text{for } S \text{ expressed in mm}) \quad (2.6)$$

Although CN theoretical varies from 0 to 100, the practical design values validated by experience lie in the range (40-98) (Van Mullem, 1989; Mishra and Singh, 2003).

## 2.2 FACTORS AFFECTING CURVE NUMBERS

The curve number (CN) indicates the runoff response characteristics of a drainage basin and is affected by soil type, land use/treatment, hydrologic condition, antecedent moisture condition, and climate of the watershed (SCS, 1956; Mishra and Singh, 2003). The combination of soil type, hydrologic condition, and land use/treatment is referred to as Hydrological Soil-Cover Complex (Miller and Cronshey, 1989). These characteristics primarily affect the infiltration potential of a watershed. NEH-4 (SCS, 1956) presents CN values for several typical Hydrological Soil-Cover Complexes.

### 2.2.1 Soil Type

Soil properties such as texture, organic matter, aggregation, soil structure and tilth greatly influence the amount of runoff. In the SCS-CN method, these properties are represented by a hydrological parameter: the minimum rate of infiltration obtained for a bare soil after prolonged wetting. The influence of both the soil's surface condition (infiltration rate) and its horizon (transmission rate) are thereby included. The Soil Conservation Service identified four hydrologic groups of soils based on their infiltration and transmission rates as given below.

**Group A:** The soils falling in this group exhibit high infiltration rates even when they are thoroughly wetted, high rate of water transmission, and low runoff potential. Such soils include primarily deep, well to excessively drained sands or gravels.

**Group B:** These soils have moderate infiltration rates when thoroughly wetted and a moderate rate of water transmission. They include moderately deep to deep, moderately well to well drained soils with moderately fine to moderately coarse textures, for example, shallow loess and sandy loam.

**Group C:** Soils in this group have low infiltration rates when thoroughly wetted and a low rate of water transmission. These soils primarily contain a layer that impedes downward movement of water. Such soils are of moderately fine to fine texture as, for example, clay loams, shallow sandy loam, and soils in low organic content.

**Group D:** These soils have very low infiltration rates when thoroughly wetted and a very low rate of water transmission. Such soils are primarily clay soils with a high swelling potential, soils with a permanently high water table, soils with a clay pan or clay layer at or near the surface, or shallow soils over nearly impervious material.

### **2.2.2 Land Use/Treatment**

The land use characterizes the uppermost surface of the soil system and has a definite bearing on infiltration. It describes watershed cover and includes every kind of vegetation, litter and mulch, and fallow as well as nonagricultural uses, such as water surfaces, roads, roofs, etc. A forest soil, rich in organic matter, allows greater infiltration than a paved one in urban areas. On an agricultural land or a land surface with loose soil whose particles are easily detached by the impact of rainfall, infiltration is affected by the process of rearrangement of these particles in the upper layers such that the pores are clogged and lead to reduction in infiltration rate. A grassy or vegetated land will help reduce such a clogging and allow more infiltration. Land treatment

applies mainly to agricultural land uses and includes mechanical practices such as contouring or terracing, and management practices such as rotation of crops, grazing control, or burning. In the SCS-CN method, the following categories of land use are distinguished:

- *Fallow* is the agricultural land use with the highest potential for runoff because the land is kept bare;
- *Row crops* are field crops planted in rows far enough apart that most of the soil surface is directly exposed to rainfall;
- *Small grain* is planted in rows close enough that the soil surface is not directly exposed to rainfall;
- *Close-seeded legumes or rotational meadow* are either planted in close rows or broadcasted. This kind of cover usually protects the soil throughout the year;
- *Pasture range* is native grassland used for grazing, whereas meadow is grassland protected from grazing and generally mown for hay;
- *Woodlands* are usually small isolated groves of trees being raised for farm use.

### **2.2.3 Hydrologic Condition**

The hydrologic condition of an agricultural watershed is defined in terms of the percent area of grass-cover. The larger the area of grass cover in a watershed, the lesser will be the runoff potential of the watershed and more will be infiltration. Such a situation describes the watershed to be in a good hydrologic condition. It is good because it favours the protection of watershed from erosion for soil conservation purposes. Similarly, a watershed having lesser acreage of grass cover can be defined to be in a poor hydrologic condition. Alternatively, a good hydrologic condition allows more infiltration than does a poor hydrologic condition. Thus, the hydrologic condition of a forest area also represents its runoff-producing potential. The curve number will be the highest for poor, average for fair, and the lowest for good condition, leading to

### **2.3 APPLICATIONS OF SCS-CN METHOD IN WATERSHED HYDROLOGY**

Since its development, the SCS-CN method has witnessed myriad applications all over the world (Mishra and Singh, 2003). The method has been used in long-term hydrologic simulation and several models have been developed in the past three decades (Huber et al. 1976; Hawkins, 1978; Williams and LaSeur 1976; Knisel 1980; Soni and Mishra 1985; Mishra and Singh 2004a). A significant literature has also been published on the SCS-CN method in the recent past, and several recent articles have reviewed the method at length. For example, McCuen (1982) provided guidelines for practical application of the method to hydrologic analyses. Ponce and Hawkins (1996) critically examined this method; discussed its empirical basis; delineated its capabilities, limitations, and uses; and identified areas of research in the SCS-CN methodology. Hjelmfelt (1991), Hawkins (1993), Bonta (1997), McCuen (2002), Bhunya et al. (2003), and Schneider and McCuen (2005), suggested procedures for determining curve numbers for a watershed using field data. Steenhuis et al. (1995) used SCS-CN method to predict the contributing area of a watershed and concluded that the SCS-CN equation is directly based on principles used in partial-area hydrology. Yu (1998) derived the SCS-CN method analytically assuming the exponential distribution for the spatial and temporal variation of the infiltration capacity and rainfall rate, respectively. Mishra and Singh (1999, 2002a) derived the method from the Mockus (1949) method and from linear and non-linear concepts, respectively. Mishra and Singh (2003) presented a state-of-the-art account and a mathematical treatment of the SCS-CN methodology, and its application to several areas, other than the originally intended one.

Mishra and Singh (2002b) developed a modified SCS-CN method to incorporate the antecedent soil moisture in the existing method. Jain et al. (2006a) applied existing SCS-CN method, its variant and the modified Mishra and Singh (2002 b) model to a large set of rainfall-

applies mainly to agricultural land uses and includes mechanical practices such as contouring or terracing, and management practices such as rotation of crops, grazing control, or burning. In the SCS-CN method, the following categories of land use are distinguished:

- *Fallow* is the agricultural land use with the highest potential for runoff because the land is kept bare;
- *Row crops* are field crops planted in rows far enough apart that most of the soil surface is directly exposed to rainfall;
- *Small grain* is planted in rows close enough that the soil surface is not directly exposed to rainfall;
- *Close-seeded legumes or rotational meadow* are either planted in close rows or broadcasted. This kind of cover usually protects the soil throughout the year;
- *Pasture range* is native grassland used for grazing, whereas meadow is grassland protected from grazing and generally mown for hay;
- *Woodlands* are usually small isolated groves of trees being raised for farm use.

### 2.2.3 Hydrologic Condition

The hydrologic condition of an agricultural watershed is defined in terms of the percent area of grass-cover. The larger the area of grass cover in a watershed, the lesser will be the runoff potential of the watershed and more will be infiltration. Such a situation describes the watershed to be in a good hydrologic condition. It is good because it favours the protection of watershed from erosion for soil conservation purposes. Similarly, a watershed having lesser acreage of grass cover can be defined to be in a poor hydrologic condition. Alternatively, a good hydrologic condition allows more infiltration than does a poor hydrologic condition. Thus, the hydrologic condition of a forest area also represents its runoff-producing potential. The curve number will be the highest for poor, average for fair, and the lowest for good condition, leading to

categorizing the hydrologic condition into three groups: good, fair, and poor, depending on the areal extent of grasslands or native pasture or range. These conditions are based on cover effectiveness. Grazing on dry soils generally results in lowering of infiltration rates due to the compaction of the soil by hooves. Determination of CN for forest areas for various hydrologic conditions is primarily guided by the U.S. Forest Service (USFS) (1959). SCS (1985) has also briefly described it.

#### **2.2.4 Agricultural Management Practices**

Agricultural management systems involve different types of tillage, vegetation and surface cover. Freebairn et al. (1989) illustrated the effects of tillage practices (mouldboard plough, chisel plough, and no till) on infiltration. Such practices primarily alter the porosity of the soils. Brakensiek and Rawls (1988) reported that mouldboard increases soil porosity from 10-20%, depending on the soil texture and, in turn, increases infiltration rates over non-tilled soils. It is shown (Rawls, 1983) that an increase in organic matter in the soil lowers bulk density or increases porosity, and hence increases infiltration and, in turn, decreases the runoff potential.

#### **2.2.5 Antecedent Moisture Condition**

The antecedent moisture condition (AMC) refers to the wetness of the soil surface or the amount of moisture available in the soil profile, or alternatively the degree of saturation before the start of the storm. In the event that the soil is fully saturated, the whole amount of rainfall will directly convert to runoff without infiltration losses and if the soil is fully dry, it is possible that the whole rainfall amount is absorbed by the soil, leading to no surface runoff. Thus, the AMC affects the process of rainfall-runoff significantly. In the SCS-CN method, the soil moisture condition is classified in three AMC classes: AMC I, AMC II, and AMC III. AMC I refers to practically dry condition of a soil (i.e. the soil moisture content is at wilting point), AMC II to normal or average, and AMC III to the wet situation (i.e. the soil moisture content is



at field capacity). Thus, the CN corresponding to AMC I refers to the dry CN or the lowest runoff potential while the CN corresponding to AMC III refers to the wet CN or the highest runoff potential. AMC classes are based on the 5-day antecedent rainfall (i.e. the accumulated total rainfall preceding the runoff under consideration). In the original SCS method, a distinction was made between the dormant and the growing season to allow for differences in evapotranspiration. Using the NEH-4 tables (SCS, 1956; 1985), the CN is first computed for AMC II which is later converted to AMC I or III depending on the AMC of the watershed.

In an attempt to justify the rationale for developing individual curve numbers, Mockus (1964) explained: "The CN associated with the soil-cover complexes are median values, roughly representing average conditions of a watershed. We took the average condition to mean average soil moisture condition because we had to ignore rainfall intensity". Since the sample variability in CN can be due to infiltration, evapotranspiration, soil moisture, lag time, rainfall intensity, etc., the AMC was supposedly used to represent this variability (Mishra and Singh, 2003).

Even though the CN is treated as an exact value for a watershed, experience (SCS, 1985; Hjelmfelt, 1991) indicates that a set of curve numbers can exist for a given watershed. Ponce and Hawkins (1996) summarized the likely sources to lie in the spatial and temporal variability of rainfall, quality of measured rainfall-runoff data, and the variability of antecedent rainfall and the associated soil moisture amount. Until individual effects of each cause are investigated, the variation of CN can be attributed to random variation, which implies that confidence intervals are appropriate for characterizing the variation (Hjelmfelt, 1982; Hawkins et al., 1985). McCuen (2002) in his approach to estimate confidence interval for CN used the method of moments for parameter estimation and pooled data for assigning confidence intervals. Bhunya et al. (2003) described the random variation of CN as Gamma distributed for estimation of confidence intervals for CN-values ranging from 65 to 95.

### **2.3 APPLICATIONS OF SCS-CN METHOD IN WATERSHED HYDROLOGY**

Since its development, the SCS-CN method has witnessed myriad applications all over the world (Mishra and Singh, 2003). The method has been used in long-term hydrologic simulation and several models have been developed in the past three decades (Huber et al. 1976; Hawkins, 1978; Williams and LaSeur 1976; Knisel 1980; Soni and Mishra 1985; Mishra and Singh 2004a). A significant literature has also been published on the SCS-CN method in the recent past, and several recent articles have reviewed the method at length. For example, McCuen (1982) provided guidelines for practical application of the method to hydrologic analyses. Ponce and Hawkins (1996) critically examined this method; discussed its empirical basis; delineated its capabilities, limitations, and uses; and identified areas of research in the SCS-CN methodology. Hjelmfelt (1991), Hawkins (1993), Bonta (1997), McCuen (2002), Bhunya et al. (2003), and Schneider and McCuen (2005), suggested procedures for determining curve numbers for a watershed using field data. Steenhuis et al. (1995) used SCS-CN method to predict the contributing area of a watershed and concluded that the SCS-CN equation is directly based on principles used in partial-area hydrology. Yu (1998) derived the SCS-CN method analytically assuming the exponential distribution for the spatial and temporal variation of the infiltration capacity and rainfall rate, respectively. Mishra and Singh (1999, 2002a) derived the method from the Mockus (1949) method and from linear and non-linear concepts, respectively. Mishra and Singh (2003) presented a state-of-the-art account and a mathematical treatment of the SCS-CN methodology, and its application to several areas, other than the originally intended one.

Mishra and Singh (2002b) developed a modified SCS-CN method to incorporate the antecedent soil moisture in the existing method. Jain et al. (2006a) applied existing SCS-CN method, its variant and the modified Mishra and Singh (2002 b) model to a large set of rainfall-

runoff data from small to large watersheds and concluded that the existing SCS-CN method was more suitable for high runoff producing agricultural watersheds than to watersheds showing pasture/range land use and sandy soils. This was in conformity with Ponce and Hawkins (1996) that the SCS-CN method performs best on agricultural watersheds, fairly on range sites and poorly on forest sites (Hawkins, 1984; 1993). Mishra et al. (2006) investigated a number of initial abstraction-potential maximum retention relations incorporating antecedent moisture as a function of antecedent precipitation.

Bhuyan et al. (2003) evaluated the use of individual-event watershed-scale AMC values to adjust field-scale CN using the stream flow data. For individual runoff events, calibration was achieved with AMCs that averaged 1.5 and ranged from 0.9 to 2.4. It was concluded that an AMC of 2, as used in many hydrologic models, would overestimate the surface runoff amounts in the sub-humid Kansas watershed, U.S.A.

Yuan et al. (2001) modified the SCS-CN method to estimate subsurface drainage flow for five drainage monitoring stations. The flows predicted during calibration and validation were not significantly different from the observed subsurface flows. Jain et al. (2006b) incorporated storm duration and a nonlinear relation for initial abstraction ( $I_a$ ) to present an enhanced version of the SCS-CN-based Mishra–Singh model (2002 b). The proposed version was found to perform better than all other existing versions on watershed of USDA-ARS. Sahu et al. (2006) suggested a soil moisture accounting procedure for SCS curve number method.

SCS-CN method is also construed as an infiltration model (Aron et al., 1977; Chen, 1982; Ponce and Hawkins 1996). Hjelmfelt (1980) proposed an SCS-CN based infiltration equation comparable with Holtan and Overton infiltration equations, to compute the infiltration rate from rainfall of uniform intensity. Mishra (1998) and Mishra and Singh (2002b) introduced a term for

steady state infiltration rate and proposed an infiltration equation by expressing the SCS-CN method in the form of the Horton method and assuming constant rainfall intensity. It has been employed for determination of infiltration and runoff rates (Mishra 1998; Mishra and Singh 2002b, 2004b).

Besides above applications, the SCS-CN method has also been used in association with erosion models for computation of sediment yield. The Modified Universal Soil Loss Equation, MUSLE (Williams, 1975), Agricultural Non Point Source Model, AGNPS (Young, et al., 1987), Soil and Water Assessment Tool, SWAT (Arnold et al., 1993, 1998), Erosion-Productivity Impact Calculator, EPIC (Williams et al., 1983), are, but a few examples. Sharda et al. (2002) used SCS-CN method in combination with USLE to compare runoff and soil loss from conservation bench terrace system and the conventional farming system.

To conclude, the SCS-CN method is a well accepted technique in applied hydrology and has been extensively used for determining direct surface runoff from the given rainfall on a watershed. Since the method relies only on one parameter, it is simple, easy to understand and applicable to those watersheds with a minimum of hydrologic information.

#### **2.4 MODELLING INFILTRATION PROCESS**

Infiltration refers to the process of water entering the soil at the ground surface. The major abstraction from rainfall during a significant runoff producing storm is infiltration of water into the soil. Many factors influence the infiltration rate, including the condition of soil surface and its vegetative cover; soil properties such as its texture, porosity and hydraulic conductivity; antecedent soil water conditions; and rainfall intensity. The process of infiltration of water and subsequent water movement within the soil zone is a complex process (Haan et al., 1994). The soils exhibit great spatial variability even with relatively small areas such as a field. As a result

of these great spatial variations in soil properties and the time variations in soil properties that occur as the soil moisture content changes, infiltration becomes a very complex process that can be described only approximately with mathematical equations (Chow et al., 1988).

A great deal of efforts has been extended in developing the mathematical theory of infiltration of water into the soils and subsequent movement of this water within the soil. The continuity equation and Darcy's law, which govern unsaturated flow through soil medium, are expressed mathematically as Eq. 2.7 and Eq. 2.8 respectively:

$$\frac{\partial \theta}{\partial t} + \frac{\partial q}{\partial z} = 0 \quad (2.7)$$

$$q = -K(\theta) \frac{\partial h}{\partial z} \quad (2.8)$$

where  $\theta$  is the soil water content,  $K$  is the hydraulic conductivity as a function of the soil water content,  $q$  is the Darcy flux,  $h$  is the hydraulic head composed of the capillary head and elevation head expressed as:

$$h = \psi + z \quad (2.9)$$

where  $\psi$  is the capillary head,  $z$  is the vertical or elevation head, and  $t$  is the time. The capillary head in the soil at any time depends on the soil moisture at that time. This means that the hydraulic conductivity can also be expressed as a function of soil moisture content. Introducing a quantity called diffusivity ( $L^2/T$ ):

$$D = K \frac{\partial \psi}{\partial \theta} \quad (2.10)$$

and combining Eqs. 2.7 to 2.9, one obtains:

$$\frac{\partial \theta}{\partial t} = \frac{\partial}{\partial z} \left( D \frac{\partial \theta}{\partial z} \right) - \frac{\partial K}{\partial z} \quad (2.11)$$

Eq. 2.11 is known as the Fokker-Planck equation and is based on the following assumptions (Smith, 1972): (a) only vertical flow is considered, (b) the water table is very deep and changes in air pressure under infiltration are insignificant, and (c) the saturation increases everywhere monotonically with time. For solving Eq. 2.11, the following initial and boundary conditions can be specified:

$$t = 0, z > 0, \theta = \theta_i; 0 < t \leq t_p, z = 0, K - D \left( \frac{\partial \theta}{\partial z} \right) = r(t) \quad (2.12)$$

where  $\theta_i$  = initial water content,  $t_p$  = time to ponding, and  $r(t)$  = time-varying rainfall intensity pattern. Assuming that  $D(\theta)$  varies rapidly with  $\theta$ , Philip (1969) transformed Eq. 2.11 into:

$$\frac{\partial \theta}{\partial t} + \frac{\partial}{\partial \theta} \left( D \frac{\partial \theta}{\partial z} \right) = \frac{dK}{d\theta} \quad (2.13)$$

Eq. 2.13 constitutes the basis of physically-based infiltration models. Depending on the considerations of dimensionality, flow dynamics, hydraulic conductivity-capillary head (or moisture content) retention relation, and initial and boundary conditions, physically-based models of varying complexity have been derived. Examples of such models are the models of Green and Ampt (1911), Philip (1957, 1969), Mein and Larson (1971, 1973), Smith (1972), Smith and Parlange (1978), among others.

Considering a soil column of unit area for vertical infiltration, Eq. 2.7 can be integrated over space and expressed in spatially lumped form as:

$$\frac{dS(t)}{dt} = f(t) - f_s(t) \quad (2.14)$$

where  $S(t)$  is the potential water storage space available at any time  $t$ ,  $f_s$  is the seepage rate or rate at which water comes out of the soil element, and  $f$  is the rate of infiltration or the rate at which water enters the soil element. One can express  $S(t)$  as:

$$S(t) = S(f, f_s, t) \quad (2.15)$$

Eq. 2.15 is a general expression relating  $S$  to  $f$  and  $f_s$  and is analogous to a flux-concentration relation. Eqs. 2.14 and 2.15 constitute the basis of several semi-empirical infiltration models (Singh and Yu, 1990). These models are based on systems approach popularly employed in surface water hydrology and are a compromise between empirical and physically-based models. Examples of semi-empirical models are the models of Horton (1938), Holtan (1961), Overton (1964), Singh and Yu (1990), Grigorjev and Iritz (1991), among others.

Empirical models do not directly use any of the above equations. These models are based on data derived from either field or laboratory experiments. Examples of such models are the SCS-CN, Kostiakov (1932), Huggins and Monke (1966), modified Kostiakov (Smith, 1972), Collis-George (1977) models, among others.

Obviously, there are a large number of infiltration models but their suitability for real world data is less than clear. Hence, it is not always evident as to which model is better and under what conditions. Using large field plot data, Skaggs et al. (1969) evaluated Green-Ampt, Holtan, Horton and Philip models for infiltration. Model parameters for several different soils at varying initial water contents and surface conditions were obtained. Adequate fits to experimental infiltration data were obtained for all the four models. However, the Green-Ampt and Philip models predicted infiltration rates that were too low for times greater than the duration of experimental data. The Holtan and Horton models predicted steady state infiltration rates accurately. The model parameters varied widely due to soil variations, crusting effects, and initial non-uniform soil water content. Whisler and Bower (1970) compared the Green-Ampt, Philip and numerical models for calculating infiltration into the soil profiles and found that numerical models produced best agreement with observations but these required considerable input data. Swartzendruber and Youngs (1974) compared the Green-Ampt and Philip models and reasoned a preference for the Philip model. Comparing the Green-Ampt and Philip models, Fok

(1975) showed the latter model can be derived from the former one and the maximum difference between the two models was less than 17%.

Rawls et al. (1976) calibrated and compared the infiltration models of Green-Ampt, Horton, Holtan, Philip, and Snyder for the Georgia coastal plain. It was found that the models of Horton and Snyder best represented the infiltration capacity curves. The models of Green and Ampt, Holtan and Philip consistently over-estimated the early part of the infiltration capacity curves and underestimated the later portion. Gifford (1976) examined the suitability of Horton, Kostiakov and Philip models for infiltration data collected from a variety of mostly semi-arid rangeland plant communities from both Australia and the USA. Nearly 1100 infiltrometer plots were included in the analysis. The results indicated that the Horton's model best fits the infiltrometer data, but only under certain conditions.

Innes (1980) compared the Horton, Holtan, Green-Ampt, Philip, Mein-Larson, and SCS-CN models for 10 different types of Hawaiian soils varying from clay to sand loam to silty clay loam. The Horton, Green-Ampt, and Philip models did not fit well. The Mein-Larson model was found to be the best and SCS-CN performed well for dry soils but poorly for wet conditions. Idike et al. (1980) experimentally evaluated the Holtan and Green-Ampt models. Both models predicted infiltration rates satisfactorily during the latter and middle portions of the experimental runs. The Green-Ampt model adequately predicted the time to start of runoff while the Holtan model generally failed to predict the delay in ponding.

Wilson et al. (1982) compared three versions of the combined Green-Ampt and Mein-Larson model on four different soil types using soil properties determined from laboratory techniques and analytical methods. The observed infiltration data were divided into wet and dry runs. All three models failed to satisfactorily predict the wet runs, probably because of changed



soil properties due to reconsolidation and/or formation of a surface seal. Only the version accounting for the entrapped air predicted infiltration satisfactorily. Singh et al. (1992) evaluated the Horton and Philip models for determining the optimum slope of graded check borders. Field evaluation revealed that the Philip model yielded values of slope closer to the observed field values than did the Horton model.

Chahinian et al. (2005) compared Philip, SCS-CN, Morel-Seytoux, and Horton models in simulating the Hortonian overland flow at the field scale. These models were coupled with a unit hydrograph transfer function. The results indicated that Morel-Seytoux's model performed better than the other models.

From the above discussion it can be inferred that the performance of different infiltration models varied from one application to other depending on soil properties, initial moisture and surface conditions etc.

## **2.5 MECHANICS OF SOIL EROSION BY WATER**

Mechanics of water erosion is often a two-fold process. Raindrops falling on soil surface can cause particles to detach and splash upward. Upon returning to the soil, splashed particles disperse and clog soil pores, causing surface crusting and a reduction in the soil's infiltration rate. The pounding action of rain may also compact the soil, further decreasing infiltration. When water is applied in excess of the soil's infiltration rate, water will puddle and the runoff leads to additional detachment of soil particles due to shear stress of flow and transport of these particles by the flowing water. Particle transport by water requires a critical speed to effectively carry sediment; when water velocity slows below this speed, deposition occurs. Because coarse particles fall out of suspension sooner than fine particles as runoff velocity slows down, they are more apt to remain on the field while fine particles are moved farther downstream.

capacity, and soil fertility. Moldenhauer and Long (1964) studied the effect of different textures of soil on erosion under simulated rainfall. The relative soil loss at high intensity rainfall varied as follows: soil loss from silty clay > silty clay loam > silt > loam > fine sand. However, at low intensity rainfall the order of soil loss was as follows: soil loss from silty clay loam > silty clay > loam > silt > fine sand. With equal water loss, the order of erodibility was as follows. Soil loss from fine sand > silty clay > silty clay loam > silt > loam. The works of Wischmeier and Mannering (1969), Wischmeier et al. (1971), and Alberts et al. (1980) on soil erodibility factor and its relationship with soil texture and available organic contents are worth mentioning. Flaxman (1972) included percent of soil particles greater than 1.0 mm in his annual sediment yield equation.

### **2.6.3 Catchment Characteristics**

Catchment area, slope, and drainage density are some of the catchment characteristics that influence the runoff production and thus the sediment yield (Jansen and Painter, 1974; Garde and Kothyari, 1987). Because fast moving water can carry more sediment than slow moving water, there is a greater potential to lose a larger amount of material on steep slopes than gradual slopes (Morgan, 1979). In an analysis of data from 27 catchments in India, Garde et al. (1983) concluded that the catchment slope was an important variable and established a relationship between the soil erosion per unit area ( $A$ ) and the topographic factor, given by: ( $A = f(S^m L^n)$ ), where  $S$  is the slope and  $L$  is slope length,  $m$  and  $n$  are the exponents ranging respectively, between 1.3 to 2.0 and 0.3 to 0.7. Many researchers have investigated the effect of slope steepness on the erosion and found a power relationship of the form of ( $y = ax^b$ ); where  $y$  is the erosion,  $x$  is the slope steepness,  $a$  and  $b$  are, respectively, the constant and exponent of the power relationship (Zingg, 1940). Schumm (1954) demonstrated the variation of sediment delivery ratio with catchment area and derived an inverse correlation between sediment yield per

unit area and the area. A similar effect was observed by several other investigators (Roehl, 1962; Wilson, 1973; Taylor, 1983).

#### **2.6.4 Land Cover**

Vegetative cover reduces detachment of soil particles by intercepting raindrops and dissipating their energy. Type of land use and vegetative cover also influence the overland flow in terms of the roughness (Chow, 1959). Surface vegetation and residue act as dams that slow down flow velocity and promote deposition. Roots of vegetation play significant role in reducing the soil erosion by binding the soil mass to increase its resistance to flow (Wischmeier, 1975). This factor was included in the Universal Soil Loss Equation as Cover Management Practice Factor, 'C'. A wider range of the literature is available on the studies of the effects of residue on soil erosion rates (Meyer et al., 1975a; Laflen and Colvin, 1981; Foster, 1982; Hussein and Laflen, 1982; Cogo et al., 1984; Dickey et al., 1985; Norton et al., 1985; Gilley et al., 1986; Franti et al., 1996).

### **2.7 MODELLING SOIL EROSION AND SEDIMENT YIELD**

The processes controlling sediment detachment, transport, and deposition on the hill slope scale, lumped under the term erosion processes, are complex and interactive (Lane et al., 1988). This complexity leads to the need for upland erosion models as tools in resource management. Since runoff is the main carrier of sediment, the erosion models are used in combination with a hydrologic model to estimate the sediment yield at the outlet of the watershed. The models are simplified representations of the actual physical processes of the rainfall-runoff-soil erosion mechanism. Several models have been developed over the last three to four decades that vary greatly in complexity and range from simple regression models to physically based models. More precisely, these models may be categorized into: (i) empirical soil erosion models, for example, the equation of Musgrave (1947), USLE -Wischmeier and

Smith (1965, 1978), MUSLE - Williams (1975), Brown and Foster (1987), RUSLE - Renard et al., 1991; (ii) conceptual soil erosion models, for example, the models of Johnson (1943), Rendon-Herrero (1978), Williams (1978), Kalin et al. (2004); and (iii) physically based erosion models, for example the models of Meyer and Wischmeier (1969), Foster and Meyer (1972a, b), Bennett (1974), Hjelmfelt et al. (1975), Meyer et al. (1975a), Foster et al. (1977a), Shirley and Lane (1978), Foster (1982), Singh and Regi (1983), CREAMS (Knisel, 1980), WEPP (Nearing et al., 1989), ANSWERS (Beasley et al., 1980), KINEROS (Woolhiser, et al., 1990), and SHESED (Wicks and Bathurst, 1996). Empirical models are developed using long records of observed data and are spatially lumped. In reality, the physically based models still rely on empirical equations to describe erosion process and, therefore, they are termed as physically process based models.

### **2.7.1 Empirical Erosion Models**

The development of erosion prediction technology perhaps began with analysis such as the one by Cook (1936) who identified three major variables that affect soil erosion as (i) susceptibility of soil to erosion, (ii) potential erosivity of rainfall and runoff, and (iii) soil protection afforded by plant cover. Later, Zingg (1940) published the first equation for soil erosion that described the effects of slope steepness and slope length on erosion. Smith (1941) added factors for cropping systems and supporting practices to this equation. Browning et al. (1947) added soil erodibility and management factors to Smith equation and prepared extensive tables for relative factor values for different soils, rotations, and slope lengths. Smith and Whitt (1947) presented a method for estimating soil losses from fields of claypan soils. The following year, Smith and Whitt (1948) presented a rational erosion-estimating equation,  $A=CSLKP$ . The C factor was the average annual soil loss for a specific rotation, slope length, slope steepness, and row direction. The other factors for slope (S), slope length (L), soil group (K), and supporting practice (P) were dimensionless multipliers to adjust value of C to other conditions.

soil properties due to reconsolidation and/or formation of a surface seal. Only the version accounting for the entrapped air predicted infiltration satisfactorily. Singh et al. (1992) evaluated the Horton and Philip models for determining the optimum slope of graded check borders. Field evaluation revealed that the Philip model yielded values of slope closer to the observed field values than did the Horton model.

Chahinian et al. (2005) compared Philip, SCS-CN, Morel-Seytoux, and Horton models in simulating the Hortonian overland flow at the field scale. These models were coupled with a unit hydrograph transfer function. The results indicated that Morel-Seytoux's model performed better than the other models.

From the above discussion it can be inferred that the performance of different infiltration models varied from one application to other depending on soil properties, initial moisture and surface conditions etc.

## **2.5 MECHANICS OF SOIL EROSION BY WATER**

Mechanics of water erosion is often a two-fold process. Raindrops falling on soil surface can cause particles to detach and splash upward. Upon returning to the soil, splashed particles disperse and clog soil pores, causing surface crusting and a reduction in the soil's infiltration rate. The pounding action of rain may also compact the soil, further decreasing infiltration. When water is applied in excess of the soil's infiltration rate, water will puddle and the runoff leads to additional detachment of soil particles due to shear stress of flow and transport of these particles by the flowing water. Particle transport by water requires a critical speed to effectively carry sediment; when water velocity slows below this speed, deposition occurs. Because coarse particles fall out of suspension sooner than fine particles as runoff velocity slows down, they are more apt to remain on the field while fine particles are moved farther downstream.

Thus, for a given physiography, the energy required for the detachment and the transportation of soil particles is supplied by raindrops and the overland flow. Besides acting as energy source, raindrops also act as wetting source. Mode of detachment of soil particles by impact of raindrops varies with the degree of wetness of land surface (Garde and Kothyari, 1987). The shear strength of soil decreases with increasing wetness. The overland flow exerts shear stress on the surface thereby inducing both the detachment and transportation of soil particles. Maximum soil splash takes place when the land surface is covered by overland flow of small depth (Mutchler and Young, 1975). Deposition of detached material takes place when the transport capacity of flow is less than the sediment load being transported.

Three main forms of water erosion are sheet, rill and gully erosion. Sheet erosion is the removal of a thin layer of soil from the surface and is caused by overland flow moving uniformly across the surface. As the sheet erosion continues, water begins to concentrate in small channels or rills, and rill erosion occurs. Rills tend to be uniformly distributed over the field and are defined as being small enough to be smoothed over by cultivation practices. The concentration of running water causes rill erosion to be more erosive than sheet erosion. Gully erosion occurs when large quantities of runoff concentrate and create large channels in the landscape. Gullies are relatively permanent features that cannot be removed by tillage.

## **2.6 FACTORS AFFECTING EROSION AND SEDIMENT YIELD**

The four principal factors that affect soil erosion and quantity of sediment that may reach the outlet of a watershed are climate, soil properties, watershed characteristics and land cover characteristics. The effects of these factors on erosion and sediment yield are reviewed below.

### **2.6.1 Climate**

Climate has always been observed to have a strong influence on erosion and sediment yield. Intensity, duration and frequency of rain events all appear to play a role in the amount of

soil that erodes. In general, the most severe erosion occurs when rains are of relatively short duration, but high intensity. Heavy raindrop action coupled with higher rain intensity than the soil infiltration capacity can lead to high surface runoff and large soil loss. Long, low intensity storms can also be highly erosive due to saturated soil conditions causing increased runoff (Morgan, 1995). Soil detachment by wind driven rain is different from that by rain falling under calm air (Lal, 1976). The wind action on rain drops may add to their erosive energy and also may increase the velocity of flow and thereby its transport capacity. The temperature plays an important role in the process of weathering which leads to disintegration of rocks. For the same rainfall, temperature also affects runoff and hence the sediment yield.

### **2.6.2 Soil Properties**

Soil properties affecting water erosion and sediment yield include those that influence infiltration and soil stability, such as texture, organic matter, aggregation, soil structure and tilth. The effect of these properties in terms of infiltration/runoff were presented in Section 2.2.1. Soil erodibility or the vulnerability of soil to erosion refers to the resistance of soil to both detachment and transportation (Wischmeier and Smith, 1978). Key factors that affect erodibility are soil texture, soil permeability, soil structure, and amount of organic matter. Because water readily infiltrates into sandy soils, the runoff, and consequently the erosion potential, is relatively low. Clay, because of its stickiness, binds soil particles together and makes it resistant to erosion. However, once heavy rain or fast flowing water erodes the fine particles, they will travel great distances before settling. The soils with 40 to 60 percent silt content are more erodible in spite of large particles being resistant to transport and the fine particles offer resistance to detachment due to their cohesiveness. Soil with clay fraction between 9 to 30 percent is more susceptible to erosion (Evans, 1980). Organic matter consists of plant and animal litter in various stages of decomposition. Organic matter improves soil structure and increases permeability, water holding

capacity, and soil fertility. Moldenhauer and Long (1964) studied the effect of different textures of soil on erosion under simulated rainfall. The relative soil loss at high intensity rainfall varied as follows: soil loss from silty clay > silty clay loam > silt > loam > fine sand. However, at low intensity rainfall the order of soil loss was as follows: soil loss from silty clay loam > silty clay > loam > silt > fine sand. With equal water loss, the order of erodibility was as follows. Soil loss from fine sand > silty clay > silty clay loam > silt > loam. The works of Wischmeier and Mannering (1969), Wischmeier et al. (1971), and Alberts et al. (1980) on soil erodibility factor and its relationship with soil texture and available organic contents are worth mentioning. Flaxman (1972) included percent of soil particles greater than 1.0 mm in his annual sediment yield equation.

### **2.6.3 Catchment Characteristics**

Catchment area, slope, and drainage density are some of the catchment characteristics that influence the runoff production and thus the sediment yield (Jansen and Painter, 1974; Garde and Kothiyari, 1987). Because fast moving water can carry more sediment than slow moving water, there is a greater potential to lose a larger amount of material on steep slopes than gradual slopes (Morgan, 1979). In an analysis of data from 27 catchments in India, Garde et al. (1983) concluded that the catchment slope was an important variable and established a relationship between the soil erosion per unit area ( $A$ ) and the topographic factor, given by: ( $A = f(S^m L^n)$ ), where  $S$  is the slope and  $L$  is slope length,  $m$  and  $n$  are the exponents ranging respectively, between 1.3 to 2.0 and 0.3 to 0.7. Many researchers have investigated the effect of slope steepness on the erosion and found a power relationship of the form of ( $y = ax^b$ ); where  $y$  is the erosion,  $x$  is the slope steepness,  $a$  and  $b$  are, respectively, the constant and exponent of the power relationship (Zingg, 1940). Schumm (1954) demonstrated the variation of sediment delivery ratio with catchment area and derived an inverse correlation between sediment yield per



unit area and the area. A similar effect was observed by several other investigators (Roehl, 1962; Wilson, 1973; Taylor, 1983).

#### **2.6.4 Land Cover**

Vegetative cover reduces detachment of soil particles by intercepting raindrops and dissipating their energy. Type of land use and vegetative cover also influence the overland flow in terms of the roughness (Chow, 1959). Surface vegetation and residue act as dams that slow down flow velocity and promote deposition. Roots of vegetation play significant role in reducing the soil erosion by binding the soil mass to increase its resistance to flow (Wischmeier, 1975). This factor was included in the Universal Soil Loss Equation as Cover Management Practice Factor, 'C'. A wider range of the literature is available on the studies of the effects of residue on soil erosion rates (Meyer et al., 1975a; Laflen and Colvin, 1981; Foster, 1982; Hussein and Laflen, 1982; Cogo et al., 1984; Dickey et al., 1985; Norton et al., 1985; Gilley et al., 1986; Franti et al., 1996).

### **2.7 MODELLING SOIL EROSION AND SEDIMENT YIELD**

The processes controlling sediment detachment, transport, and deposition on the hill slope scale, lumped under the term erosion processes, are complex and interactive (Lane et al., 1988). This complexity leads to the need for upland erosion models as tools in resource management. Since runoff is the main carrier of sediment, the erosion models are used in combination with a hydrologic model to estimate the sediment yield at the outlet of the watershed. The models are simplified representations of the actual physical processes of the rainfall-runoff-soil erosion mechanism. Several models have been developed over the last three to four decades that vary greatly in complexity and range from simple regression models to physically based models. More precisely, these models may be categorized into: (i) empirical soil erosion models, for example, the equation of Musgrave (1947), USLE -Wischmeier and

Smith (1965, 1978), MUSLE - Williams (1975), Brown and Foster (1987), RUSLE - Renard et al., 1991; (ii) conceptual soil erosion models, for example, the models of Johnson (1943), Rendon-Herrero (1978), Williams (1978), Kalin et al. (2004); and (iii) physically based erosion models, for example the models of Meyer and Wischmeier (1969), Foster and Meyer (1972a, b), Bennett (1974), Hjelmfelt et al. (1975), Meyer et al. (1975a), Foster et al. (1977a), Shirley and Lane (1978), Foster (1982), Singh and Regi (1983), CREAMS (Knisel, 1980), WEPP (Nearing et al., 1989), ANSWERS (Beasley et al., 1980), KINEROS (Woolhiser, et al., 1990), and SHESED (Wicks and Bathurst, 1996). Empirical models are developed using long records of observed data and are spatially lumped. In reality, the physically based models still rely on empirical equations to describe erosion process and, therefore, they are termed as physically process based models.

### **2.7.1 Empirical Erosion Models**

The development of erosion prediction technology perhaps began with analysis such as the one by Cook (1936) who identified three major variables that affect soil erosion as (i) susceptibility of soil to erosion, (ii) potential erosivity of rainfall and runoff, and (iii) soil protection afforded by plant cover. Later, Zingg (1940) published the first equation for soil erosion that described the effects of slope steepness and slope length on erosion. Smith (1941) added factors for cropping systems and supporting practices to this equation. Browning et al. (1947) added soil erodibility and management factors to Smith equation and prepared extensive tables for relative factor values for different soils, rotations, and slope lengths. Smith and Whitt (1947) presented a method for estimating soil losses from fields of claypan soils. The following year, Smith and Whitt (1948) presented a rational erosion-estimating equation,  $A=CSLKP$ . The C factor was the average annual soil loss for a specific rotation, slope length, slope steepness, and row direction. The other factors for slope (S), slope length (L), soil group (K), and supporting practice (P) were dimensionless multipliers to adjust value of C to other conditions.

Erosion experiment stations were established in the 1930's by the U.S Soil Conservation Services, which were concerned about the conservation of agricultural lands. These stations were responsible for measuring rainfall, runoff, and soil erosion from small plots. As a result of the plot erosion research, the first erosion models (equations) were developed. Ellison (1944) showed the effect of rainfall energy on sheet erosion by the equation  $E = KV^{4.33} d^{1.07} I^{0.65}$ , where E is the grams of soil intercepted in splash sampler during a 30 minute period, V is the velocity of drops in ft/sec, d is the diameter of the drops in mm, I is the intensity of rainfall in in/hr, and K is a constant. Musgrave (1947) analyzed 40000 plot-years of data to develop his relationship to incorporate the land characteristics, and expressed the relationship as:

$$A_L = C_s R_g S^{1.35} L^{0.35} P_{30}^{1.75} \quad (2.16)$$

where,  $A_L$  = long term average soil loss from sheet and rill erosion (acre-inch per year),  $C_s$  = soil erodibility factor (inch per year),  $R_g$  = crop management factor, S = slope (percent), L = length of slope (feet), and  $P_{30}$  = two year, 30 minutes rainfall amount (inches).

Graphs to solve the Musgrave equation were prepared by Lloyd and Eley (1952). Van Doren and Bartelli (1956) proposed an erosion equation for different soils and cropping conditions that estimated annual soil loss as a function of nine factors. Einstein (1950) developed methodology for bedload functions and bedload transport for rivers and streams.

Wischmeier and Smith (1958) re-examined the erosion plot data used by Musgrave and the US Weather Bureau rainfall data and published their first results which ultimately led to the development of the Universal Soil Loss Equation (USLE). USLE was published by Wischmeier and Smith (1965) based on over 10,000 plot years of natural and simulated runoff data, expressed as:

$$A = R K L S C P \quad (2.17)$$

where A is the annual potential soil erosion ( $t\ ha^{-1}\ year^{-1}$ ); R is the rainfall erosivity factor ( $MJ\ mm\ ha^{-1}\ hr^{-1}\ year^{-1}$ ) taken as the long term average of the summation of the product of total rainfall energy (E) and maximum 30 minute rainfall intensity ( $I_{30}$ ), i.e.  $EI_{30}$ ; K is the soil erodibility factor ( $t\ ha\ hr\ ha^{-1}\ MJ^{-1}\ mm^{-1}$ ); LS is the slope length and steepness factor (dimensionless); C is the cover management factor (dimensionless); and P is the supporting practice factor (dimensionless). The dimensions used here are consistent with the work of Renard et al. (1991). The R factor of USLE can be computed from:

$$R = \frac{\sum_{i=1}^j (EI_{30})}{N} \quad (2.18)$$

where,  $(EI_{30})_i = EI_{30}$  for storm i, j = number of storms in an N year period and  $I_{30}$  is maximum 30 minute rainfall intensity. The kinetic energy, E can be computed using Laws and Parsons (1943) equations. The soil erodibility factor (K), a function of soil texture, is a measure of the potential erodibility of soil. The slope length and steepness factor (LS) accounts for the overland runoff length and slope. For slopes > 4%, it can be determined as:

$$LS = L^{1/2} (0.0138 + 0.00974Y + 0.001138Y^2) \quad (2.19)$$

where Y is the gradient (%) over the runoff length and L is the length (m) of slope from the point of origin of the overland flow to the point where the slope decreases to the extent that sedimentation begins. The cover management factor (C) estimates the effect of ground cover conditions, soil conditions, and general management practices on erosion rates. The supporting conservation practice factor (P) accounts for the effectiveness of erosion control practices, such as land treatment by contouring, compacting, establishing sedimentation basins, and other control structures. Generally, C reflects the protection of the soil surface against the impact of rain drops and subsequent loss of soil particles, whereas P includes treatments that retain eroded particles and prevent them from further transport. The experimentally derived values of the

above factors for various soil-vegetation-land use complexes are available elsewhere (Ponce, 1989; Singh, 1992; Novotny and Olem, 1994; Singh and Singh, 2001).

Three major limitations of the USLE restricted its application in many modelling analysis. First, it was not intended for estimating soil loss from single storm events (Haan et al., 1994); second, it was an erosion equation, and consequently did not estimate the deposition (Wischmeier, 1976); and third, it did not estimate gully or channel erosion.

Since 1965, efforts have been to improve the USLE and it has been expanded for additional types of land use, climatic conditions and management practices. Renard et al. (1974) modified the USLE to approximate soil loss from rangeland watersheds by including an additional term in the USLE to accommodate channel erosion. Williams (1975) presented a Modified Universal Soil Loss Equation (MUSLE) for predicting sediment yield from individual storm events. The rainfall energy term of the USLE was replaced by the runoff energy factor because the runoff is more closely related to the sediment yield than the rainfall energy, as the former is responsible for transporting detached sediment to the catchment outlet. The MUSLE is expressed as,

$$Y = 11.8(V \cdot Q_p)^{0.56} KLSCP \quad (2.20)$$

where, Y is the sediment yield (t), V is the storm runoff volume (m<sup>3</sup>), Q<sub>p</sub> is the peak runoff rate (m<sup>3</sup> s<sup>-1</sup>), and other factors are same as that of USLE.

Since the procedure suggested by Wischmeier and Smith (1965) for determining R-values of USLE is applicable for computation of annual erosion, its use in estimation of soil loss from a single storm would yield errors (Haan et al., 1994). Foster et al. (1977b) suggested a modification of R-values applicable to individual storm events as:

$$R = 0.5R_r + 0.35Qq^{1/3} \quad (2.21)$$

where  $R_e$  is the rainfall energy factor for the storm ( $= EI_{30}$  for the storm) ( $N \text{ hr}^{-1}$ ),  $Q$  is the runoff volume (mm), and  $q$  is the peak runoff rate (mm/hr). Since  $q$  is related to the detachment of soil particles more than is  $Q$ , a reduction in peak discharge by the vegetative cover will also reduce sediment transport (Williams and Berndt, 1977).

The USDA Forest service, under an interagency agreement with USEPA compiled a set of watershed analyses and prediction procedures (Snyder, 1980). These state-of-the-art techniques are collectively referred to as WRENSS (Water Resources Evaluation of Nonpoint Sources-Silvicultural). The objective of the soil erosion component in WRENSS was to estimate the quantity of accelerated soil loss under given silvicultural activity condition. An empirical procedure was chosen for estimating soil loss using the USLE, modified for use in forest environments. The cropping management factor and the erosion control practice factor have been replaced by a vegetation management factor to form the Modified Soil Loss Equation (MSLE).

Renard et al. (1991) proposed revised USLE (RUSLE) incorporating a method for computing kinetic energy of rainfall for individual storm events using the equation proposed by Brown and Foster (1987):

$$e = 1099[1 - 0.72\exp(-1.27 i)] \quad (2.22)$$

The total energy in the storm is computed by multiplying the above computed  $e$ -value with the depth of rainfall (i.e.  $E = e.P$ ).

USLE so far remains the well accepted and most widely used empirical approach for estimation of upland erosion despite the development of a number of conceptual and physically process based models (Lane et al., 1988; Narula et al., 2002). Researches and investigators have applied USLE with suitable modifications for estimation of annual soil loss and sediment yield as well as its temporal variation on single storm event basis, and to study the effect of various

parameters that affect the soil loss. The works of Foster and Wischmeier (1974), Onstad and Foster (1975), Onstad and Bowie (1977), Cooley (1980), Hadley et al. (1985), McCool et al. (1987), Liu et al. (1994), Jain and Kothyari (2000), Kothyari et al. (1996) are worth mentioning.

### **2.7.2 Conceptual Erosion Models**

The conceptual models lie somewhere between empirical and physically based models and are based on spatially lumped forms of continuity equations for water and sediment and some other empirical relationships. Although highly simplified, they do attempt to model the sediment yield, or the components thereof, in a logical manner. To summarize, conceptual models of sediment are analogous in approach to those of surface runoff, and hence, embody the concepts of the unit hydrograph theory.

Johnson (1943) was perhaps the first to derive a distribution graph for suspended sediment concentration employing the hypothesis analogous to that embodied in the unit hydrograph. Rendon-Herrero (1978) extended the unit hydrograph method to directly derive a unit sediment graph (USG) for a small watershed. The sediment load considered in the USG is the wash load only.

Williams (1978) extended the concept of an instantaneous unit hydrograph (IUH) to instantaneous unit sediment graph (IUSG) to determine the sediment discharge from an agricultural catchment. The concept of USG has been also employed by Singh et al. (1982), Chen and Kuo (1986), Kumar and Rastogi (1987), Raghuwanshi et al. (1994), Banasik and Walling (1996), among others, for the purpose of estimating the temporal variation of sediment yield.

Kalin et al. (2004) developed a modified unit sedimentograph approach for identification of sediment source areas within a watershed. The watershed was partitioned into a number of

elements. The sediment flux response of the elements at the basin outlet was computed by characterizing the rainfall event by the pulses of excess rainfall depths. The application of these methods requires considerable input data for their calibration and they inherit the limitations of unit hydrograph theory.

### **2.7.3 Physically Based Erosion Models**

Significant research and understanding of basic processes of erosion and sediment yield led to the development of more complicated, physically based sediment yield models. These models have been developed in a coupled structure such that the algorithms for computing runoff are combined with the algorithms for computing sediment detachment, deposition and their transport. In physically based sediment yield models, the simulation of hydrological and erosion processes involves solutions to the simultaneous partial differential equations of mass, momentum and energy conservation, which being non-linear in nature are difficult to solve. However, the kinematic wave simplification of the Saint Venant equations of flow is adequate to describe the process of surface runoff in upland areas of a watershed (Bennett, 1974; Woolhiser, 1977; Laguna and Giraldez, 1993). Physically based models are expected to provide reliable estimates of sediment yield. However, these models require a large number of input parameters and, therefore, the practical application of these models is still limited because of uncertainty in specifying model parameter values and also due to the difference between the scales of application i.e. a catchment versus a field (Hadley, et al., 1985; Wu, et al., 1993).

The physically based models generally separate the ground surface into inter-rill and rill erosion areas (Wu et al., 1993; Meyer et al., 1975b; Kothyari and Jain, 1997). Detachment over inter-rill areas is considered to be by the impact of rain drops because flow depths are shallow, while runoff is considered to be the dominant factor in rill detachment and sediment transport over both rill and inter-rill areas. During the last four decades, the development of mathematical



theory to describe the mechanics of soil erosion, sedimentation, and their interrelationship, provide the needed foundation for the development of physically based models (Bennett, 1974; Foster et al., 1977a; Foster, 1982; Hirschi and Barfield, 1988; Nearing et al., 1989; Elliot and Laflen, 1993). Ellison (1947) presented a comprehensive analysis of various soil erosion sub-processes, an essential requirement for more recent soil erosion modelling. Meyer and Wischmeier (1969) formulated the latest concept using mathematical descriptions of rainfall and runoff detachment and transport processes. Foster and Meyer (1972a) described the relationship for runoff detachment where its rate is a function of the ratio of sediment flux to the sediment transport capacity of the flow. Many more relationships developed by various researchers and subsequently used by many other investigators are available for estimation of the inter-rill detachment, rill detachment, and transport of the detached sediment. The works of David and Beer (1975a, b), Foster and Meyer (1975), Mutchler and Young (1975), Foster et al. (1977 a, b), Meyer (1981), Foster and Lane (1983), Schultz (1985), Nearing et al. (1989), Watson and Laflen (1986), Woolhiser et al. (1990), Govindaraju and Kavvas (1991), Haan et al. (1994), Sharda and Singh (1994), Tayfur and Kavvas (1994), Foster et al. (1995), Sander et al. (1996), Hjelmfelt and Wang (1999), Tayfur (2001, 2002), Hogarth et al. (2004 a, b), and Jain et al. (2005) are worth mentioning. A summary of some important relationships proposed by various investigators for inter-rill process, rill process and the transport process are presented in Tables 2.1, 2.2 and 2.3 respectively.

Table 2.1: Important relationships available for the inter-rill erosion computation

S.No	Authors with Year	Relationship	Parameters
(1)	(ii)	(iii)	(iv)
1.	Ellison (1947)	$D_R = f(I^{2.14})$	$D_R$ = soil splash loss; $I$ = 30 min rainfall intensity
2.	Meyer and Wischmeier (1969)	$D_R = S_{DR} A_i I^2$	$D_R$ = soil detachment due to rainfall; $S_{DR}$ = a constant for the soil effect; $A_i$ = the incremental area; $I$ = 30 min rainfall intensity
3.	David and Beer (1975)	$D_R = SC_F \cdot LS_F \cdot I^a \cdot \exp(-k y)$	$SC_F$ = soil and soil cover factor; $LS_F$ = land slope factor; $k$ = exponent greater than one; $y$ = overland flow depth; $I$ = rainfall intensity; $a$ = exponent (= 1).
4.	Foster et al. (1977a)	$D_i = K_i I (bS + c)$	$D_i$ = soil detachment due the rainfall; $I$ = rainfall intensity; $S$ = slope steepness; and $a$ and $b$ are the constant determined from experiments and analysis.
5.	CREAMS (Knisel, 1980)	$D_i = 4.57(EI)(\sin\theta + 0.014)K_c P(Q_p / Q_w)$	$D_i$ = interrill detachment rate [ $g s^{-1} m^{-2}$ ]; $EI = EI_{30}$ value of storm [ $MJ m^{-2} mm^{-1} h$ ]; $\theta$ = slope angle (degree); $Q_p$ = peak runoff rate ( $m s^{-1}$ ); $Q_w$ = discharge rate per unit area [ $m^3 s^{-1} m^{-2}$ ]; and $K$ ( $g EI_{30}^{-1}$ ), $C_u$ and $P$ are the soil erodibility, cover and management, and supporting conservation practice factors, respectively, from the USLE. P factor is used in the presence of contouring.
6.	Meyer (1981)	$D_i = a I^b$	$D_i$ = inter-rill erosion; $I$ = rainfall intensity; $a$ = coefficient; $b$ = exponent (ranges between 1.6 and 2.1 depending upon the clay content of the soil).
7.	Singh and Prasad (1982); Blau et al. (1988); Shirley and Lane (1978)	$E_i = K_i R^m$	$E_i$ = interrill erosion rate ( $kg m^2 s^{-1}$ ); $K_i$ = interrill erodibility factor ( $kg m^3$ ); $R$ = rainfall excess rate ( $m s^{-1}$ ); and $m$ is an exponent taken to be unity
8.	Croley (1982); Foster (1982); Croley and Foster (1984)	$E_i = K_i R^m$	$E_i$ = interrill erosion rate ( $kg m^2 s^{-1}$ ); $K_i$ = interrill erodibility factor ( $kg m^3$ ); $R$ = rainfall excess rate ( $m s^{-1}$ ); and $m = 2$
9.	Gilley et al. (1986)	$D_s = 0.2 K_d \rho \cos^2 \theta a_i V_i^2 (d_i / Y)^{1.83}$ $Y = \{[(b I^c + K_w)(v I x)] / 8 g S\}^{1/3}$	$D_s$ = soil detachment ( $kg m^2 s^{-1}$ ); $K_d$ = soil detachment factor ( $s m^{-1}$ ); $\rho$ = density of soil ( $kg m^3$ ); $\theta$ = slope angle; $a_i$ = number of drops in the $i^{th}$ class; $V_i$ = velocity of drop ( $m s^{-1}$ ) with diameter $d_i$ ; $d_i$ = mean drop diameter of class $i$ (m); and $Y$ = depth of overland flow (m). $I$ = rainfall intensity ( $m s^{-1}$ ); $b$ and $c$ are the regression coefficients; $K_w$ = 24 for laminar flow over smooth surface; $v$ = kinematic viscosity of water ( $mm^2 s^{-1}$ ); $x$ = distance in flow direction (m); and $S$ = channel bottom slope ( $m m^{-1}$ )

(i)	(ii)	(iii)	(iv)
10.	Schultz, (1985)	For $t \leq t_p$ : $\ln(SR) = 4.27 - 0.339 \ln(\tau - 3.22)$ $\ln(SR) = 17.2 \ln(10.3 - D) - 35.0$ $\tau = 3.22 + 15.4 \exp(-2.68 t)$	$SR$ = soil splash rate ( $\text{kg ha}^{-1} \text{min}^{-1}$ ); and $D$ = depth of ponded water (mm); $t_p$ = time of initial ponding (equal to 1.5); $\tau$ = shear strength of the soil.
11.	Watson and Laflen (1986)	$D_i = A \tau_a^B I^C S$	$D_i$ = soil detachment; $\tau_a$ = soil shear strength after rainfall (Pa); $I$ = rainfall intensity; $S$ = slope; and $A$ , $B$ and $C$ are the constants
12.	Hirschi and Barfield (1988)	$SSR = C R^{e_1} E^{e_2} P_d^{e_3} S^{e_4}$	$SSR$ = soil splash ( $\text{g cm}^{-2}$ ) during $\Delta t$ ; $C$ = empirical constant; $e_1, \dots, e_4$ are the exponents; $R$ = rainfall intensity ( $\text{cm h}^{-1}$ ); $E$ = applied rainfall energy during $\Delta t$ (joules $\text{cm}^{-2}$ ); $P_d$ = percent clay of the surface layer; and $S$ = soil surface slope.
13.	Nearing et al. (1989)	$D_i = K_i I_e^2 C_e G_e (R_s / w)$ $w = c Q_e^d$ $C_e = 1 - F_c \exp(-0.34 H_c)$ $G_e = \exp(-2.5 g_i)$	$D_i$ = interrill erosion rate ( $\text{kg m}^{-2} \text{s}^{-1}$ ); $K_i$ = baseline interrill erodibility; $I_e$ = effective rainfall intensity; $C_e$ = effect of canopy on interrill erosion; $G_e$ = effect of ground cover on interrill erosion; $R_s$ = spacing of rills, and $w$ is the computed rill width. $Q_e$ = flow discharge at the end of slope; $c$ and $d$ are the coefficient derived from Laflen et al. (1987). $F_c$ = fraction of the soil protected by canopy cover; $H_c$ = effective canopy height (m) (Laflen et al., 1985). $g_i$ = fraction of interrill surface covered by residue
14.	Laguna and Giraldez (1993)	$D_i = 0.0138 K_i \cdot C \cdot r^2$	$D_i$ = interrill erosion rate ( $\text{kg m}^{-2} \text{h}^{-1}$ ); $K_i$ = soil erodibility factory for raindrop impact ( $\text{kg h N}^{-1} \text{m}^{-2}$ ); $C$ = USLE' C parameter; $r$ = rainfall intensity ( $\text{mm h}^{-1}$ ).
15.	Foster et al. (1995)	$D_i = K_{iadj} I_e \sigma_{IR} SDR_{RR} (R_s / w)$	$K_{iadj}$ = interrill erodibility adjusted for consolidation effects ( $\text{kg s m}^{-4}$ ); $I_e$ = effective rainfall intensity ( $\text{m s}^{-1}$ ) ( $= \int Idt / t_e$ ); $I$ = breakpoint rainfall intensity ( $\text{m s}^{-1}$ ); $t_e$ = duration for which rainfall exceeds the infiltration rate (s); $\sigma_{IR}$ = interrill runoff rate ( $\text{m s}^{-1}$ ); $SDR_{RR}$ = sediment delivery ratio; $R_s$ = rill spacing (m); and $w$ = rill width (m)
16.	Sander et al. (1996)	$e_i = \frac{(1-H) a P}{I}$	$e_i$ = rate of rainfall detachment of sediment of settling class $i$ ( $\text{kg m}^{-2} \text{s}^{-1}$ ); $H$ = fraction of surface shields due to raindrop effect; $a$ = rainfall detachability ( $\text{kg m}^{-1}$ ); $P$ = rainfall rate ( $\text{m s}^{-1}$ ); and $I$ = number of classes.

(i)	(ii)	(iii)	(iv)
17.	Wicks and Bathurst (1996)	$D_i = K_r F_w (1 - C_G) [(1 - C_C) M_R + M_D]$ $M_R = \alpha I^\beta$ $M_D = \frac{(V \rho \pi D^3 / 6)^2 \text{DRIP \%} \cdot \text{DRAIN}}{(\pi D^3 / 6)}$ $F_w = \exp(1 - h / D_m) \quad \text{if } h > D_m$ $F_w = 1.0 \quad \text{if } h \leq D_m$ $D_m = 0.00124 I^{0.182}$	<p><math>D_i</math> = soil detached by raindrop impact (<math>\text{kg m}^{-2} \text{s}^{-1}</math>); <math>K_r</math> = raindrop soil erodibility coefficient (<math>\text{J}^{-1}</math>); <math>C_G</math> = e proportion of soil covered by ground cover; <math>C_C</math> = proportion of ground covered by canopy cover; <math>F_w</math> = flow depth correction factor; <math>M_R</math> = momentum squared for rain [<math>(\text{kg m s}^{-1})^2 \text{m}^{-2} \text{s}^{-1}</math>]; and <math>M_D</math> = momentum squared for leaf drip [<math>(\text{kg m s}^{-1})^2 \text{m}^{-2} \text{s}^{-1}</math>].</p> <p><math>I</math> = rainfall intensity (<math>\text{mm/h}</math>); <math>\alpha</math> and <math>\beta</math> are the empirical coefficient which vary with rainfall intensity.</p> <p><math>V</math> = leaf drip fall velocity (<math>\text{m s}^{-1}</math>); <math>\rho</math> = density of water (<math>\text{kg m}^{-3}</math>); <math>D</math> = leaf drip diameter (m) taken between 5-6 mm; <math>\text{DRIP \%}</math> = proportion of drainage which falls as leaf drip; and <math>\text{DRAIN}</math> is the canopy drainage (<math>\text{m s}^{-1}</math>).</p> <p><math>h</math> = water depth (m); and <math>D_m</math> = median raindrop diameter (m) which is computed from Laws and Parsons (1943); <math>I</math> = rainfall intensity (<math>\text{mm h}^{-1}</math>).</p>
18.	Li (1979); Tayfur and Kavvas (1994); Tayfur (2001); Tayfur (2002)	$D_{rd} = \alpha r^b \left( 1 - \frac{Z_w}{Z_m} \right) \quad \text{if } Z_w < Z_m$ $D_{rd} = 0 \quad \text{Otherwise}$ $Z_m = 3 (2.23 r^{0.182})$	<p><math>D_{rd}</math> = soil detachment rate (<math>\text{kg m}^{-2} \text{h}</math>); <math>\alpha</math> = soil detachability coefficient that depends on the soil characteristics (<math>\text{kg m}^{-2} \text{mm}</math>); <math>r</math> = rainfall intensity (<math>\text{mm h}^{-1}</math>); <math>Z_w</math> = flow depth plus loose soil depth (mm); and <math>Z_m</math> = maximum penetration depth of the raindrop splash (mm) which is given by (Li, 1979).</p>
19.	Jain et al. (2005)	$D_i = \omega F_w C_F K_F I^a (2.96 S_o^{0.79} + 0.56)$	<p><math>\omega</math> = coefficient for rainfall detachment; <math>F_w</math> = flow correction factor computed using the relationship proposed by Park et al. (1982); <math>C_F</math> = cover management factor of the USLE; <math>K_F</math> = soil erodibility factor of the USLE (<math>\text{kg h N}^{-1} \text{m}^{-2}</math>); <math>I</math> = rainfall intensity (<math>\text{mm/h}</math>); and <math>a</math> = exponent of rainfall intensity (=2).</p>

Table 2.2: Important relationships available for the rill erosion process

S.No	Authors with Year	Relationship	Parameters
(i)	(ii)	(iii)	(iv)
1.	Meyer (1964)	$D_r = K_r (\tau - \tau_c)^a$ $\tau = \gamma_w r_h S$	$D_r$ = rill detachment rate ( $\text{g m}^2 \text{ s}^{-1}$ ); $K_r$ = soil erodibility ( $\text{g m}^{-1} \text{ s}^{-1} \text{ Pa}^{-1}$ ); $\tau$ = average shear stress (Pa); $\tau_c$ = critical shear stress (Pa); $\gamma_w$ = specific weight of water ( $\text{N m}^{-3}$ ); $r_h$ = rill hydraulic radius (m); $S$ is the hydraulic gradient ( $\text{m m}^{-1}$ ); and $a$ is an exponent equal to 1.0 (Foster et al., 1977a), 1.05 (Knisel, 1980), 1.5 (Foster and Meyer, 1972).
2.	Meyer and Wischmeier (1969)	$D_F = S_{DF} A_I \{ [S_s^{2/3} Q_s^{2/3} + S_c^{2/3} Q_c^{2/3}] / 2 \}$	$D_F$ = detachment due to runoff; $S_{DF}$ = constant for detachment due to runoff; $A_I$ = incremental area; $S$ = slope steepness; $Q$ = flow rate, and subscripts $s$ and $c$ represents for starting and end values.
3.	Meyer et al. (1975a); Priest et al. (1975)	$D_r = a_s (\tau_e - \tau_{cr})^\xi$	$a_s$ = factor related to the soil's susceptibility to rilling; $\tau_e$ = effective shear stress; $\tau_{cr}$ = critical shear stress; and $\xi$ = exponent.
4.	David and Beer (1975)	$E_r = C' \gamma^{\beta 6}$	$E_r$ = amount of overland flow scour, $\beta 6$ = an exponent ( $\geq 1$ ); $C'$ = constant representing soil characteristics and the overland flow surface slope. If the flow is concentrated along well-defined rills and the actual flow depth is greater than the average overland flow depth, $\gamma$ , the value of $\beta 6$ will be greater than one.
5.	Foster (1976)	$D_F = 0.90 \cdot C_F \cdot K_F \cdot A_I \cdot S \cdot Q$	$D_F$ = detachment due to runoff ( $\text{kg/min}$ ); $A_I$ = incremental area ( $\text{m}^2$ ); $S$ = slope steepness; $Q$ = flow rate ( $\text{m}^3 \text{ min}^{-1}$ ); $C_F$ = cropping and management factor from USLE; $K_F$ = soil erodibility factor from USLE.
6.	Foster et al. (1977)	$D_r = a_s C_\tau^{3/2} \gamma^{3/2} (f_c / 2g)^{1/2} S \sigma x$ $D_r = 2K_r (a S^e) \sigma x$	$a_s$ = factor related to the soil's susceptibility to rilling; $C_\tau^{3/2}$ = lumped equal to $(2K_r)$ ; $\gamma$ = weight density of water; $f_c$ = coefficient of friction; $g$ = acceleration due to gravity; $S$ = slope steepness; $\sigma$ = excess rainfall rate (rainfall rate - infiltration rate); $x$ = distance along the slope. The portion of $C_\tau^{3/2}$ ( $= a S^e$ ) where $a$ and $e$ are function of tillage pattern, soil roughness, and other factors that interact with slope steepness to influence rill pattern.

(i)	(ii)	(iii)	(iv)
7. Foster et al. (1981)		$D_r = 6.86 \times 10^6 m Q_w Q_p^{1/3} \left( \frac{x}{22.1} \right)^{m_c - 1}$ $\times \sin^2 \theta K C_u P \left( \frac{Q_p}{Q_w} \right)$	<p><math>D_r</math> = rill detachment rate [<math>g \ s^{-1} \ m^{-3}</math>]; <math>m_c</math> = slope length exponent from USLE (0.5 for straight slope), and <math>x</math> = slope length (m), <math>\theta</math> = slope angle (degree); <math>Q_p</math> = peak runoff rate (<math>m^3 \ s^{-1}</math>); <math>Q_w</math> = discharge rate per unit area [<math>m^3 \ s^{-1} \ m^{-2}</math>]; and <math>K</math> (g <math>EL_{30}^{-1}</math>), <math>C_u</math>, and <math>P</math> are the soil erodibility, cover and management, and supporting conservation practice factors, respectively, from the USLE. <math>P</math> factor is used in the presence of contouring.</p>
8. Foster (1982)		$D_{RC} = \xi C_F K_F \tau^{1.5}$	<p><math>C_F</math> = cover management factor of USLE; <math>K_F</math> = soil erodibility factor of USLE; <math>\xi</math> = coefficient; and <math>\tau = \rho h S_f</math></p>
9. Foster (1982); Woolhiser et al., (1990)		$D_{fd} = \beta (T_c - q_s)$ $\beta = 0.5 V_f / q$ $V_f^2 = [4g(S_s - 1)d] / (3D_c)$ $D_c = 24 / R_{pn} + 3 / R_{pn}^{0.5} + 0.34$ $R_{pn} = V_f d / \nu$	<p><math>D_r</math> = rill erosion rate [<math>ML^{-2}T^{-1}</math>]; <math>\beta</math> = a first order reaction coefficient for deposition [<math>L^{-1}</math>]; <math>T_c</math> = transport capacity [<math>ML^{-1}T^{-1}</math>]; <math>q_s</math> = sediment load [<math>ML^{-1}T^{-1}</math>]; <math>V_f</math> = fall velocity [<math>LT^{-1}</math>]; <math>q</math> = discharge per unit width [<math>L^2T^{-1}</math>]; <math>g</math> = gravitational acceleration [<math>LT^{-2}</math>]; <math>S_s</math> = particle specific gravity; <math>d</math> = particle diameter [L]; <math>D_c</math> = drag coefficient; <math>R_{pn}</math> = particle Reynolds number; and <math>\nu</math> = kinematic viscosity of water [<math>L^2T^{-1}</math>].</p>
10. Hirschi and Barfield (1988)		$D_r = (1 - G_f / T_c) \alpha (\tau - \tau_c)^\beta$ $D_r = (1 - \frac{G_f}{T_c}) \alpha (\tau - \tau_c)^\beta (1 - f_{cd})$	<p><math>D_r</math> = actual detachment rate; <math>G_f</math> = flow sediment load; <math>T_c</math> = flow sediment transport capacity; <math>\alpha</math> and <math>\beta</math> are empirical constants; <math>\tau</math> and <math>\tau_c</math> are bed shear stress and critical bed shear stress (<math>N \ m^{-2}</math>), respectively. <math>f_{cd}</math> = a fraction of the bed.</p>
11. Blau et al. (1988)		$D_f = (B/k)q - cq$	<p><math>D_f</math> = rill erosion rate (<math>g \ m^{-2} \ s^{-1}</math>); <math>B</math> = a sediment transport parameter; <math>k</math> = a slope resistance parameter; <math>q</math> = discharge per unit width (<math>m^3 \ s^{-1} \ m^{-1}</math>); and <math>c</math> = sediment concentration (<math>g \ m^{-1}</math>).</p>
12. Nearing et al. (1989); Wicks and Bathurst (1996); Laguna and Giraldez (1993)		$D_f = D_c [1 - G / T_c]$ $D_c = K_r (\tau_f - \tau_c)$ $D_F = K_f [(\tau_f / \tau_c) - 1]; K_f = K_r / \tau_c$ $\tau_f = \gamma ((P_r / C) x s)^{2/3}$	<p><math>D_r</math> = rill erosion rate (<math>kg \ s^{-1} \ m^{-2}</math>); <math>D_c</math> = detachment at capacity rate (<math>kg \ s^{-1} \ m^{-2}</math>); <math>G</math> = sediment load (<math>kg \ s^{-1} \ m^{-1}</math>); and <math>T_c</math> = transport capacity in the rill (<math>kg \ s^{-1} \ m^{-1}</math>); <math>K_r</math> = rill soil erodibility parameter (<math>s/m</math>), <math>\tau_f</math> = flow shear stress (Pa); <math>\tau_c</math> = critical shear stress (Pa); <math>K_f</math> = overland flow erodibility coefficient; <math>P_r</math> = peak flow rate (<math>m \ s^{-1}</math>); <math>\gamma</math> = specific weight of water (<math>kg \ m^{-2} \ s^{-2}</math>); <math>x</math> = distance down slope (m), <math>s</math> = slope gradient.</p>

(i)	(ii)	(iii)	(iv)
13.	Elliot and Lafien (1993)	$D_c = K_p [(\gamma_w Q_s / w_r) - P_c]$	$D_c$ = detachment capacity ( $\text{gm}^2 \text{s}^{-1}$ ); $K_p$ = soil erodibility coefficient ( $\text{g j}^{-1}$ ) (= 2.19 to 51.97); $w_r$ = rill width; and $P_c$ = critical stream power ( $\text{w m}^{-2}$ ) below which no detachment (varies between 0.14 to 1.36).
14.	Govindaraju and Kavvas, (1991); Tayfur (2001, 2002)	$D_{fd} = \beta(T_c - q_s)$ $q_s = \rho_s c q$	$D_{fd}$ = soil detachment/deposition rate by sheet flow [ $\text{ML}^2 \text{T}^{-1}$ ]; $\rho_s$ = sediment article density [ $\text{ML}^{-3}$ ]; $q$ = unit flow discharge [ $\text{L}^2 \text{T}^{-1}$ ]; $c$ = sediment concentration by volume [ $\text{L}^3 \text{L}^{-3}$ ]; $T_c$ = transport capacity of sheet flow [ $\text{ML}^{-1} \text{T}^{-1}$ ]; $q_s$ = unit sediment discharge [ $\text{ML}^{-1} \text{T}^{-1}$ ]; and $\beta$ = transfer rate coefficient may vary over a wide range depending on the soil type [ $\text{L}^{-1}$ ].
15.	Zhang et al. (2002)	$D_c = 5.43 \times 10^6 q^{2.04} S^{1.27}$ $R^2 = 0.97$ $D_c = 1.17 \times 10^3 h^{4.62} S^{2.37}$ $R^2 = 0.92$ $D_c = 6.20 V^{4.12}$ $R^2 = 0.90$ $D_c = 0.0429 \omega^{1.62}$ $R^2 = 0.89$	$D_c$ = detachment rate ( $\text{kg m}^2 \text{s}^{-1}$ ); $q$ = flow discharge ( $\text{m}^3 \text{s}^{-1}$ ); $S$ = slope gradient; $h$ = depth of flow; $V$ = flow velocity ( $\text{m s}^{-1}$ ); $\tau$ = shear stress (Pa); $\rho$ = density of water ( $\text{kg m}^{-3}$ ); $g$ = acceleration due to gravity ( $\text{m s}^{-2}$ ); and $\omega$ is stream power ( $\text{kg s}^{-3}$ ).

Table 2.3: Important relationships available for the transport process

S.No	Authors with Year	Relationship	Parameters
(i)		(iii)	(iv)
1.	Meyer and Wischmeier (1969)	$T_R = S_{TR} S^I$	$T_R$ = transport capacity due to rainfall; $S_{TR}$ = constant that include soil effect; $S$ = slope steepness; and $I$ = rainfall intensity.
2.	Meyer and Wischmeier (1969)	$T_F = S_{TF} S^{5/3} Q^{5/3}$	$T_F$ = transport capacity due to flow; $S_{TF}$ = constant depends on effect of particle size and density of soil to account soil's transportability; $S$ = slope steepness; and $Q$ = flow rate.
3.	David and Beer (1975)	$T = n S^\delta y^K$	$n$ = Manning's roughness coefficient; $S$ = overland flow surface slope, $y$ = depth of flow, $\delta$ = an exponent, and $K$ = a constant.
4.	Foster (1982); Tayfur 2001, 2002)	$T_c = \eta(\tau_f - \tau_{cr})^{3/2}$ ; $\tau_{cr} = \delta_s(\gamma_s - \gamma_w)d$ $\tau_f = \gamma_w h S$	$T_c$ = transport capacity; $\eta$ = soil erodibility coefficient, $\tau_f$ = flow shear stress; $\tau_{cr}$ = critical shear stress, $\delta_s$ = constant dependent on flow conditions (= 0.047), $\gamma_s$ = specific weight of sediment, $\gamma_w$ = specific weight of water, $d$ = particle diameter, $h$ = depth of overland flow, $S$ = slope
5.	Foster (1982); Yalin (1963)	$T_c = 0.635 \delta V_c S_u \rho_w d [1 - (1/\sigma) \log(1 + \sigma)]$ $\sigma = A_s \delta$ ; $A_s = 2.45 S_g^{-0.4} Y_c^{0.5}$ ; $\delta = 0$ , if $Y < Y_c$ ; $V_c = (\tau / \rho_w)^{0.5}$ ; $\delta = (Y / Y_c) - 1$ , if $Y \geq Y_c$ ; $V_c = (\tau / \rho_w)^{0.5}$ ; $Y = V_c^2 / (S_g - 1) g$ ; $V_c = (\tau / \rho_w)^{0.5}$ ; $\tau = \gamma h S_f (n_b / n_r)^{0.9}$ ; $h = (Q_w n_b / S_f)^{1/2}$ , $0.6$	$T_c$ = transport capacity in mass per unit width per unit time [ $ML^{-1}T^{-1}$ ]; $S_g$ = particle specific gravity; $\rho_w$ = mass density of water; $d$ = diameter of the particle; $V_c$ = shear velocity; $Y_c$ = critical lift force obtained from Shield's diagram; $g$ = acceleration due to gravity; $h$ = flow depth; $S_f$ = energy slope; $\gamma$ = specific weight of water; $n_b$ = Manning's roughness coefficient for bare soil; $n_r$ = Manning's roughness coefficient for rough or vegetated surface; and $Q_w$ = discharge rate per unit area.
6.	Beasley et al. (1980)	$T_F = 161 \cdot S \cdot Q^{0.5}$ for $Q \leq 0.046 \text{ m}^2 \text{ min}^{-1}$ $T_F = 16320 \cdot S \cdot Q^2$ for $Q > 0.046 \text{ m}^2 \text{ min}^{-1}$	$T_F$ = transport capacity ( $\text{kg m}^{-1} \text{ min}^{-1}$ ); $S$ = slope steepness ( $\text{m m}^{-1}$ )
7.	Nearing et al. (1989)	$T_c = k_t \cdot \tau_f^{3/2}$	$T_c$ = transport capacity; $\tau_f$ = hydraulic shear acting on the slope; and $k_t$ = transport coefficient. Transport capacity at the end of the slope is computed using Yalin equation and the coefficient $k_t$ is calibrated from the transport capacity (Finkner et al., 1989)



## 2.8 CONCEPT OF SEDIMENT DELIVERY RATIO

The concept of sediment delivery ratio, DR, owes its origin to the observation that the erosion predicted by the USLE overestimates the amount of sediment delivered from hillslopes because sediment deposition often occurs on hillslopes whereas the USLE does not account for deposition. The sediment yield of a catchment is only a part of gross erosion that equals the gross erosion minus sediment deposited enroute to the point of reference. Sediment produced by sheet and rill erosion often move only short distances and may get deposited away from the stream system. They may remain in the areas of their origin or be deposited on a milder slope downstream. Therefore, sediment yield is often computed based on the use of a sediment delivery ratio, DR, which is defined as the ratio of the sediment reaching the watershed outlet to the gross surface erosion. The dimensionless ratio, DR, is expressed mathematically as:

$$DR = \frac{Y}{A} \quad (2.23)$$

where, Y is the total sediment yield at watershed outlet, and A is the total material eroded (gross erosion) on the watershed area above the outlet. Many factors including catchment physiography, sediment source, proximity and magnitude of source, transport system, texture of eroded material, depositional areas and land cover etc. affect sediment delivery ratio (Dendy, 1982; Walling, 1983, 1988). However, variables such as catchment area, land slope, and land cover have been mainly used as parameters in empirical equations for DR (Hadley et al., 1985; Roehl, 1962; Williams and Berndt, 1972; Kothyari and Jain, 1997). The U.S. Soil Conservation Service has developed a generalized relationship between delivery ratio and catchment area. The inverse relationship between delivery ratio and catchment area has been explained in terms of decreasing slope and channel gradients and the increasing opportunity for deposition associated with increasing catchment size. Schumm (1954) also demonstrated an inverse correlation between

sediment yield per unit area and the catchment area. Walling (1983, 1988) has summarized some of the relationships between sediment delivery ratio and the catchment characteristics.

## **2.9 SOME USEFUL WATERSHED MODELS FOR RAINFALL-RUNOFF-SEDIMENT YIELD MODELLING**

In earlier times, hydrology and erosion/sediment transport models were generally developed independently. It was not until the development of the digital computers that these components were put together to develop comprehensive watershed models for simulation of runoff and sediment yield behaviour of watersheds with varying complexities. Some of the watershed models that are in common use around the world (Wurbs, 1994; Narula et al., 2002) are briefly presented below.

Areal Non Point Source Watershed Environment Response Simulation (ANSWERS) (Beasley et al., 1980) is an event based, distributed parameter watershed model to simulate the runoff and sediment yield from agricultural watersheds and to evaluate the effect of various management practices on the runoff and sediment response of the watershed. ANSWERS-2000 (Bouraoui and Dillaha, 1996), a recent version of the ANSWERS model is capable of simulating the runoff and sediment yield on continuous basis.

Williams and Hann (1978) developed a basin scale model to consider surface runoff, sedimentation, and plant nutrients. The hydrologic component is a modification of the SCS-CN model. The USLE was modified for the erosion component by replacing rainfall energy term with a product of storm runoff volume and peak rate of discharge raised to a power.

Agricultural Non-point Source Pollution Model (AGNPS) (Young, et al., 1987) is a distributed parameter, single event model that simulates runoff, sediment and nutrient transport from agricultural watersheds. The model uses the SCS-CN method and the revised version of the USLE to estimate runoff and upland erosion respectively. Erosion-Productivity Impact

Calculator (EPIC) (Williams et al., 1983) is a continuous model that uses a modified SCS method for computing surface runoff by estimating S as a function of NEH-4 CN value and soil moisture parameters. Subsurface flow is computed separately based on soil moisture parameters.

Soil and Water Assessment Tool (SWAT) (Arnold et al., 1993, 1998) is a distributed parameter, continuous simulation model designed to evaluate the long-term impacts of management of water, chemicals, and sediment in large ungauged watersheds. The model utilizes the Modified Universal Soil Loss Equation (MUSLE) (Williams, 1975) to compute the sediment yield. Runoff volume and peak rate of runoff, as required in the MUSLE, are calculated using the SCS-CN method and a modified rational formula respectively. Muttiah and Wurbs (2002) used SWAT model on large watersheds to study the change in water balance components due to variability of soils and climate. Gosain and Rao (2004) employed SWAT model to simulate the quantity of water and sediment erosion for local level planning, incorporating the sustainability aspects of watershed development.

Water Erosion Prediction Project (WEPP) (Nearing et al., 1989) is a continuous simulation, field or watershed scale model that incorporates new erosion prediction technology developed by the USDA. The model requires input data of rainfall amount and intensity; soil texture; plant growth; residue decomposition; effects of tillage implements on soil properties, slope shape, steepness, and orientation; and soil erodibility parameters. The watershed version of WEPP routes runoff and sediment from fields and incorporates channel scour based on the work of Foster and Meyer (1972b), and Knisel (1980).

Chemicals, Runoff, and Erosion from Agricultural Management Systems (CREAMS) (Knisel, 1980), a physically based daily simulation model maintains the elements of USLE, but includes sediment transport capacity of flow. KYERMO (Hirschi and Barfield, 1988), an event

based model that isolates important sub-processes within the overall erosion process; STAND model (Zeng, 2000; Zeng and Beek, 2001) for simulation of stream flows, sediment transport and interactions of sediment with other attributes of water quality; EUROSEM (Morgan et al., 1998), a dynamic distributed model capable to simulate sediment transport, erosion and deposition over the land surface by rill and interrill processes in single storm for both individual fields and small watersheds are some of the useful watershed models, among others.

## **2.10 SUMMARY**

In Summary, the review of literature reveals that there exists a considerable interest in estimation of soil erosion throughout the world. As a result, a number of approaches that vary from simple empirical to physically based models involving mathematical treatment of detachment, transport and deposition processes have been used to estimate the sediment yield. The complex physically based models are expected to provide reliable estimates of the sediment yield. However, these models require the coordinated use of various sub-models related to meteorology, hydrology, hydraulics, and soil erosion. As such, the large input parameter requirement and uncertainty in estimation of these parameters limit the practical applications of physically based models to those areas which have little or no data. More often, USLE based approaches have been successfully used to estimate the sediment yield from the watersheds. The SCS-CN method has also been used in many of the sediment yield models to simulate the surface runoff. The main reason the SCS-CN method has been well received by most hydrologists lies in its simplicity and applicability to those watersheds with a minimum of hydrologic information. It relies only on one parameter that relates runoff to the most runoff producing watershed characteristics and the required inputs can easily be estimated. In the present study, an attempt has, therefore, been made to develop SCS-CN based simple sediment yield models to suit the data availability of watersheds in developing countries like India.

## **CHAPTER 3**

### **COMPARISON OF INFILTRATION MODELS**

---

#### **3.1 GENERAL**

Infiltration models play a key role in rainfall-runoff modelling. Runoff estimation procedure based on infiltration approach, known as Hortonian approach, is most commonly used in the area of hydrological analysis. It is evident from the review of literature that a number of infiltration models, classified into three general groups, viz., physically based, semi-empirical, and empirical, are available for simulation of infiltration rates. In the present work, the SCS-CN based infiltration model is utilized for the development of time-distributed sediment yield model. This chapter presents a comparative evaluation of the SCS-CN based infiltration model. The review of literature reveals that in studies on comparative evaluation, only two to four infiltration models have been considered using either laboratory experiments or field experiments and the results obtained have been mixed. The models perform differently when applied to the data derived in the laboratory and in the field. In the present study, it was therefore felt that the comparative evaluation be based on an exhaustive infiltration data set considering a sufficient number of infiltration models. To this end, fourteen popular infiltration models, representing physically-based, semi-empirical, and empirical, were identified for assessment of their performance and comparative evaluation on 243 sets of infiltration data collected from field and laboratory tests conducted in India and USA on soils ranging from coarse sand to fine clay. A brief account of the selected models, the data used, and the results of application of these models are discussed.

### Singh-Yu Model

Singh and Yu (1990) derived a model based on two postulates: (1) the rate of infiltration in excess of the final infiltration rate, called excess infiltration, at any time is directly proportional to the  $m^{\text{th}}$  power of the available storage space in the soil column at that time; (2) the rate of excess infiltration is inversely proportional to the  $n^{\text{th}}$  power of the cumulative infiltration up to that time. Expressed mathematically:

$$f(t) = f_c + \frac{a[S(t)]^m}{[S_o - S(t)]^n} \quad (3.6)$$

where  $f(t)$  is the infiltration rate ( $LT^{-1}$ ) at time  $t$ ;  $f_c$  is the final infiltration rate;  $(f - f_c)$  is the excess infiltration rate;  $S(t)$  is the available storage for water retention in the soil column at time  $t$  (L);  $S_o$  is the potential storage space available for moisture retention in soil column (L) at the beginning; and  $a$ ,  $m$ , and  $n$  are, respectively, the coefficient and exponents of the variables  $S(t)$  and  $(S_o - S(t))$ . The cumulative infiltration ( $F$ ) is equal to  $S_o - S(t)$ . Singh and Yu (1990) provided several relations for variation of  $S$  with time. Parameters  $f_c$  and  $S_o$  are determined from available infiltration data and soil properties, such as soil porosity  $\phi$  and initial moisture content  $\theta_o$ ; and the parameters  $a$ ,  $m$ , and  $n$  can be computed using a least squares approach. The Singh-Yu model is a general model and specializes into the models of Green and Ampt (1911), Holtan (1961), Horton (1938), Kostiaikov (1932), modified Kostiaikov, Overton (1964), and Philip (1969).

### SCS-CN Based Mishra-Singh Model

By expressing the popular SCS-CN method in the form of the Horton method assuming a linear variation of the cumulative precipitation with time (or constant rainfall intensity), Mishra (1998) and Mishra and Singh (2002b) developed an infiltration equation:

$$f = f_c + \frac{S k}{(1 + kt)^2} \quad (3.7)$$

where  $S$  is the potential maximum retention parameter of the SCS-CN model, identical to the Singh-Yu (1990) general model parameter  $S_o$ , and  $k$  is the decay coefficient identical to the Horton model parameter. The parameter  $S$  is derivable from physical properties of the soil. However,  $k$ ,  $S$ , and  $f_c$  are best estimated by empirical fitting of Eq. 3.7 to observed infiltration data. The mathematical expression of Eq. 3.7 is a specific form of the retention model proposed by van Genuchten (1980) relating  $\theta$  with  $\psi$ .

### Smith Model

Under the assumption of uniform rainfall, Smith (1972) developed an infiltration model expressed mathematically as:

$$f = f_c + A(t - t_o)^{-b} \quad (3.8)$$

where  $t_o$  is the initial time when runoff started (or time to ponding), and  $A$  and  $b$  are parameters which depend on soil type, initial moisture, and rainfall rate. During ponded infiltration (rainfall rate  $\rightarrow \infty$  and time to ponding  $\rightarrow 0$ ), Smith found  $A$  to vary from 0.149 to 0.493  $\text{cm min}^{-1}$  and  $b$  from 0.537 to 0.585 (non-dimensional) for the soils ranging from Poudre sand to Muren clay. For  $t_o$  equal to 0, Eq. 3.8 reduces to the Kostiakov model.

### Horton Model

Horton (1938) developed an infiltration equation:

$$f = f_c + (f_o - f_c)e^{-kt} \quad (3.9)$$

where  $f_c$  is the steady state value of  $f$ ,  $f_o$  is the value of  $f$  at  $t = 0$ , and  $k$  is the infiltration decay factor. Eq. 3.9 is derived from simple assumption that the reduction in infiltration capacity during rain is directly proportional to the rate of infiltration and is applicable only when the effective rainfall intensity is greater than  $f_c$  (Linsley et al., 1975). Maidment (1993) provided generalized estimates of  $f_o$  varying from 210 to 900  $\text{mm h}^{-1}$ ,  $f_c$  from 2 to 290  $\text{mm h}^{-1}$ , and  $k$  from

0.8 to 2.0 min<sup>-1</sup> for soils ranging from fine sandy clay to standard turfed agricultural soil. For field applications, the model parameters are usually estimated by empirical fitting.

### Holtan Model

Using a storage exhaustion concept, Holtan (1961) derived an infiltration equation expressed as:

$$f = f_c + a(S_o - F)^n \quad (3.10)$$

where 'a' and 'n' are constants dependent on soil type, surface, and cropping conditions, and S<sub>o</sub> is the storage potential of the soil above the impeding layer (total porosity, φ, minus the antecedent soil moisture, θ<sub>o</sub>). The quantity (S<sub>o</sub> - F) represents potential infiltration. For four different soils, the value of parameter n was found to be 1.387 and the parameter a varied from 0.25 to 0.80 with the average value of 0.62 (when f was measured in inches h<sup>-1</sup>). To account for the effect of vegetation, a vegetative factor k is introduced for vegetated soils and the parameter a is replaced by 0.62 k. Like other models, the model parameters are best determined by empirical fitting.

### Overton Model

Using the Holtan model with n = 2, Overton (1964) derived an infiltration equation expressed as:

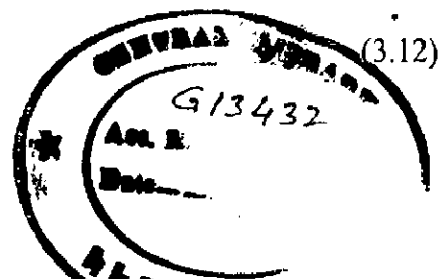
$$f = f_c \sec^2[(a f_c)^{1/2}(t_c - t)] \quad (3.11)$$

where a is a constant which varies with antecedent soil moisture, and t<sub>c</sub> is a time parameter. From Eq. 3.11 it is possible to compute infiltration rate at any time during a storm, even when rainfall does not exceed the infiltration capacity or when there is a temporary interruption in rainfall.

### Kostiakov Model

The general form of the infiltration equation given by Kostiakov (1932) is:

$$F = a t^b \quad (3.12)$$





## CHAPTER 3

### COMPARISON OF INFILTRATION MODELS

---

#### 3.1 GENERAL

Infiltration models play a key role in rainfall-runoff modelling. Runoff estimation procedure based on infiltration approach, known as Hortonian approach, is most commonly used in the area of hydrological analysis. It is evident from the review of literature that a number of infiltration models, classified into three general groups, viz., physically based, semi-empirical, and empirical, are available for simulation of infiltration rates. In the present work, the SCS-CN based infiltration model is utilized for the development of time-distributed sediment yield model. This chapter presents a comparative evaluation of the SCS-CN based infiltration model. The review of literature reveals that in studies on comparative evaluation, only two to four infiltration models have been considered using either laboratory experiments or field experiments and the results obtained have been mixed. The models perform differently when applied to the data derived in the laboratory and in the field. In the present study, it was therefore felt that the comparative evaluation be based on an exhaustive infiltration data set considering a sufficient number of infiltration models. To this end, fourteen popular infiltration models, representing physically-based, semi-empirical, and empirical, were identified for assessment of their performance and comparative evaluation on 243 sets of infiltration data collected from field and laboratory tests conducted in India and USA on soils ranging from coarse sand to fine clay. A brief account of the selected models, the data used, and the results of application of these models are discussed.

## 3.2 INFILTRATION MODELS

### Philip Model

Using Eq. 2.13, Philip (1957, 1969) derived the following infiltration model:

$$f = st^{-1/2} + C \quad (3.1)$$

where  $f$  is the infiltration rate and  $s$  and  $C$  are parameters dependent on soil diffusivity and moisture retention characteristic. Parameter  $s$  is referred to as the soil sorptivity (Philip, 1957). After a long period of time,  $f$  becomes approximately constant and may generally equal the saturated hydraulic conductivity,  $K_s$ . However, Philip noted that this equality did not exist. Rather, parameter  $C$  varies from half to three-quarters of the value of  $K_s$ . The sorptivity parameter can be expressed in terms of  $K_s$ , effective capillary drive, the difference between saturated and initial soil-water content (White and Sully, 1987; Nachabe et al., 1997). In practice, however, these parameters are estimated either empirically or by optimization.

### Green-Ampt Model

Green and Ampt (1911) presented a model based on the assumption that soil may be regarded as a bundle of tiny capillary tubes irregular in area, direction, and shape. Assuming a homogeneous, deep soil with uniform initial moisture content, and ponded surface, the Green-Ampt infiltration equation takes the form:

$$f = A \left[ 1 + \frac{B(H_c + H)}{F} \right] \quad (3.2)$$

where  $A$  and  $B$  are parameters which depend on soil characteristics,  $H_c$  is capillary potential at wetting front ( $L$ ),  $H$  is the head of water on the surface ( $L$ ), and  $F$  is the cumulative infiltration. Smith and Parlange (1978) have shown that for initially ponded conditions (ponding time = 0) with rainfall rate approaching infinity and  $K$  varying slowly near saturation, Eq. 3.2 can be derived from Eq. 2.11. The Green-Ampt model has been subject to a resurgence of interest and

application, largely because its parameters can be obtained from physically measurable quantities as discussed by Brakensiek and Onstad (1977), Brakensiek et al. (1981), Rawls et al. (1983), and Ogden and Sagafian (1997). Nevertheless, for field applications or fitting to infiltration data, parameters are often estimated by empirical fitting. To that end, Eq. 3.2 can be re-written as:

$$f = A + \frac{C}{F} \quad (3.3)$$

where  $C=AB(H_c + H)$ . Parameters A and C can be estimated using observed infiltration data.

### **Linear Smith-Parlange Model**

By neglecting the first partial differential term on the left-hand side of Eq. 2.13 and then integrating it, Smith and Parlange (1978) derived an infiltration model expressed as:

$$f = K_s \left[ \frac{C}{K_s F} + 1 \right] \quad (3.4)$$

where  $K_s$  is the saturated hydraulic conductivity and C is a parameter which is related to the soil sorptivity and varies linearly with the initial moisture and also depends on the amount and pattern of rainfall intensity. The neglect of the first differential terms was based on the proviso that  $D(\theta)$  in Eq. 2.13 varies rapidly with  $\theta$  (Parlange, 1971). Parameters C and  $K_s$  can be determined either graphically or using a regression approach utilizing infiltration data. For field applications, this is the most viable way to estimate parameters.

### **Nonlinear Smith-Parlange Model**

Smith and Parlange (1978) also derived a non-linear infiltration model expressed as:

$$f = K_s \frac{e^{(FK_s/c)}}{e^{(FK_s/c)} - 1} \quad (3.5)$$

where C has the same connotation as in Eq. 3.4. Both parameters  $K_s$  and C can be derived from physical properties of soils. However, for practical applications, parameters are estimated empirically by fitting.

### Singh-Yu Model

Singh and Yu (1990) derived a model based on two postulates: (1) the rate of infiltration in excess of the final infiltration rate, called excess infiltration, at any time is directly proportional to the  $m^{\text{th}}$  power of the available storage space in the soil column at that time; (2) the rate of excess infiltration is inversely proportional to the  $n^{\text{th}}$  power of the cumulative infiltration up to that time. Expressed mathematically:

$$f(t) = f_c + \frac{a[S(t)]^m}{[S_0 - S(t)]^n} \quad (3.6)$$

where  $f(t)$  is the infiltration rate ( $LT^{-1}$ ) at time  $t$ ;  $f_c$  is the final infiltration rate;  $(f - f_c)$  is the excess infiltration rate;  $S(t)$  is the available storage for water retention in the soil column at time  $t$  (L);  $S_0$  is the potential storage space available for moisture retention in soil column (L) at the beginning; and  $a$ ,  $m$ , and  $n$  are, respectively, the coefficient and exponents of the variables  $S(t)$  and  $(S_0 - S(t))$ . The cumulative infiltration ( $F$ ) is equal to  $S_0 - S(t)$ . Singh and Yu (1990) provided several relations for variation of  $S$  with time. Parameters  $f_c$  and  $S_0$  are determined from available infiltration data and soil properties, such as soil porosity  $\phi$  and initial moisture content  $\theta_0$ ; and the parameters  $a$ ,  $m$ , and  $n$  can be computed using a least squares approach. The Singh-Yu model is a general model and specializes into the models of Green and Ampt (1911), Holtan (1961), Horton (1938), Kostiaikov (1932), modified Kostiaikov, Overton (1964), and Philip (1969).

### SCS-CN Based Mishra-Singh Model

By expressing the popular SCS-CN method in the form of the Horton method assuming a linear variation of the cumulative precipitation with time (or constant rainfall intensity), Mishra (1998) and Mishra and Singh (2002b) developed an infiltration equation:

$$f = f_c + \frac{Sk}{(1 + kt)^2} \quad (3.7)$$

where  $S$  is the potential maximum retention parameter of the SCS-CN model, identical to the Singh-Yu (1990) general model parameter  $S_0$ , and  $k$  is the decay coefficient identical to the Horton model parameter. The parameter  $S$  is derivable from physical properties of the soil. However,  $k$ ,  $S$ , and  $f_c$  are best estimated by empirical fitting of Eq. 3.7 to observed infiltration data. The mathematical expression of Eq. 3.7 is a specific form of the retention model proposed by van Genuchten (1980) relating  $\theta$  with  $\psi$ .

### Smith Model

Under the assumption of uniform rainfall, Smith (1972) developed an infiltration model expressed mathematically as:

$$f = f_c + A(t - t_0)^{-b} \quad (3.8)$$

where  $t_0$  is the initial time when runoff started (or time to ponding), and  $A$  and  $b$  are parameters which depend on soil type, initial moisture, and rainfall rate. During ponded infiltration (rainfall rate  $\rightarrow \infty$  and time to ponding  $\rightarrow 0$ ), Smith found  $A$  to vary from 0.149 to 0.493  $\text{cm min}^{-1}$  and  $b$  from 0.537 to 0.585 (non-dimensional) for the soils ranging from Poudre sand to Muren clay. For  $t_0$  equal to 0, Eq. 3.8 reduces to the Kostiakov model.

### Horton Model

Horton (1938) developed an infiltration equation:

$$f = f_c + (f_0 - f_c)e^{-kt} \quad (3.9)$$

where  $f_c$  is the steady state value of  $f$ ,  $f_0$  is the value of  $f$  at  $t = 0$ , and  $k$  is the infiltration decay factor. Eq. 3.9 is derived from simple assumption that the reduction in infiltration capacity during rain is directly proportional to the rate of infiltration and is applicable only when the effective rainfall intensity is greater than  $f_c$  (Linsley et al., 1975). Maidment (1993) provided generalized estimates of  $f_0$  varying from 210 to 900  $\text{mm h}^{-1}$ ,  $f_c$  from 2 to 290  $\text{mm h}^{-1}$ , and  $k$  from

0.8 to 2.0 min<sup>-1</sup> for soils ranging from fine sandy clay to standard turfed agricultural soil. For field applications, the model parameters are usually estimated by empirical fitting.

### Holtan Model

Using a storage exhaustion concept, Holtan (1961) derived an infiltration equation expressed as:

$$f = f_c + a(S_o - F)^n \quad (3.10)$$

where 'a' and 'n' are constants dependent on soil type, surface, and cropping conditions, and  $S_o$  is the storage potential of the soil above the impeding layer (total porosity,  $\phi$ , minus the antecedent soil moisture,  $\theta_o$ ). The quantity  $(S_o - F)$  represents potential infiltration. For four different soils, the value of parameter n was found to be 1.387 and the parameter a varied from 0.25 to 0.80 with the average value of 0.62 (when f was measured in inches h<sup>-1</sup>). To account for the effect of vegetation, a vegetative factor k is introduced for vegetated soils and the parameter a is replaced by 0.62 k. Like other models, the model parameters are best determined by empirical fitting.

### Overton Model

Using the Holtan model with  $n = 2$ , Overton (1964) derived an infiltration equation expressed as:

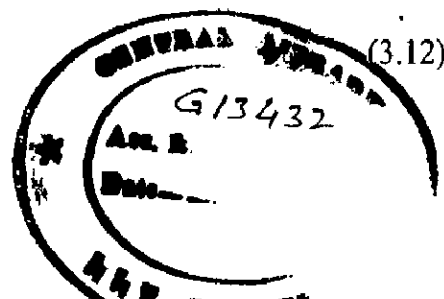
$$f = f_c \sec^2[(a f_c)^{1/2} (t_c - t)] \quad (3.11)$$

where a is a constant which varies with antecedent soil moisture, and  $t_c$  is a time parameter. From Eq. 3.11 it is possible to compute infiltration rate at any time during a storm, even when rainfall does not exceed the infiltration capacity or when there is a temporary interruption in rainfall.

### Kostiakov Model

The general form of the infiltration equation given by Kostiakov (1932) is:

$$F = a t^b \quad (3.12)$$



where  $a$  and  $b$  are constants ( $0 < b < 1$ ). For three different soils (silt loam, fine sandy loam, and gravelly clay), Kincaid et al. (1969) found the value of  $a$  to vary from 0.225 to 1.1 and the value of  $b$  from 0.458 to 0.669. By differentiating Eq. 3.12 (Rode, 1965),  $f$  can be written as:

$$f = \alpha (t)^{-\beta} \quad (3.13)$$

where  $\alpha = ab$  and  $\beta = (1 - b)$ . Eqs. 3.12 and 3.13 are applicable for  $t \neq 0$ . Eq. 3.13 is simple and has primarily been used for irrigation applications (Maidment, 1993). The values of parameters  $\alpha$  and  $\beta$  are determined experimentally.

### Modified Kostiakov Model

Smith (1972) modified the Kostiakov equation (3.13) by including the term  $f_c$  as:

$$f = f_c + \alpha(t)^{-\beta} \quad (3.14)$$

where  $\alpha$  and  $\beta$  are the same as above. Cahoon (1998) derived parameters of Eq. 3.14 from the kinematic wave model.

### Huggins-Monke Model

By introducing porosity in the Holtan model, Huggins and Monke (1966) proposed an infiltration model expressed as:

$$f = f_c + \frac{a (S_o - F)^n}{\phi^m} \quad (3.15)$$

where  $S_o$  and  $\phi$  are the Holtan model parameters and  $a$  is another model parameter, which depend on the soil type, surface, and cropping conditions. It is noted that for a given soil stratum,  $\phi$  is constant and 'm' is the model parameter. Therefore,  $a/\phi^m$  is also a constant, leading to the Holtan model. Furthermore, since  $S_o$  bears the dimension of length, it cannot be equal to a non-dimensional quantity, i.e.,  $(\phi - \theta_o)$ , as originally hypothesized, rather it is equal to  $(\phi - \theta_o)$  times the depth of soil stratum above the impeding layer. The model parameters are determined experimentally.

## Collis-George Model

Collis-George (1977) found that the Green and Ampt model did not mimic the observed behavior of simple soils at long times and the Horton model did not at short times. He, therefore, proposed a model which would work well at all times:

$$f = f_c + \frac{0.5 i_o [1 - \tanh (t/t_c)^2]}{\tanh (t/t_c)^{0.5}} \quad (3.16)$$

where  $i_o = s(t_c)^{1/2}$  and  $t_c$  is a time parameter. On clayey soils, Collis-George found  $i_o$  to vary from 1.5 to 6.6 cm and  $t_c$  from 750 to 13000 s. The model parameters can be determined from soil properties experimentally.

### 3.3 APPLICATION OF INFILTRATION MODELS

#### 3.3.1 Infiltration Data

The data employed in this study are shown in Table 3.1. These data were derived from infiltration tests done in the laboratory and field in the USA and India. The infiltration data for the first five soils were generated from several laboratory tests reported by Mein and Larson (1971). The data from Sl. No. 6 to 17 belong to the Tifton Upland Physiographic Region of the Georgia Coastal Plain in the USA. Specifically, these tests were conducted in South-Central Georgia near Tifton in the vicinity of the Little River Experimental Watershed. These data have been published by Agriculture Research Service (ARS, 1976) of the U.S. Department of Agriculture.

The infiltration tests carried out in India were from two catchments: (a) Sher basin in Madhya Pradesh and (b) Dudhnai catchment in Assam and Meghalaya. The tests in Madhya Pradesh were conducted in Narsinghpur district and the data were reported by Roy and Singh (1995). The Dudhnai catchment is bounded by the River Brahmaputra in the north, the Garo Hills in the south, the Kulsi Deosila sub-basin in the east, and the Jinari sub-basin in the west.



The soils of this basin are mostly new alluvium usually found in riverine tracts, generally sandy loam and silty loam. The infiltration data for these soils have been reported by Kumar et al. (1995). What follows utilizes the abbreviated names of various soils given in Table 3.1.

### 3.3.2 Parameter Estimation

Optimal values of the parameters of the aforementioned models for each infiltration data set were estimated using the non-linear Marquardt algorithm of the least squares procedure of the Statistical Analysis System (SAS, 1988). The algorithm is quite efficient and in most cases, approximately three to five iterations were required to obtain the final estimates of parameters of each model. To get an idea about the model parameters, the minimum, maximum, and average parameter values of eight top-ranked models (as discussed in the following section) for each soil are given in Table 3.2.

It is apparent from Table 3.2 that for various soils, the average values of the Horton model parameter  $f_0$  vary from 2.73 to 689.73  $\text{cm h}^{-1}$ ,  $k$  from 0.01 to 98.66  $\text{min}^{-1}$ , and  $f_c$  from 0.08 to 18.08  $\text{cm h}^{-1}$ . The Holtan model parameter  $S_0$  varies from 2.25 to 45.35 cm, 'a' from 0.08 to 2.12, and 'n' from 0 to 3.55. The Kostiakov model parameter  $\alpha$  varies from 7.76 to 333.92, and  $\beta$  from 0 to 0.77. In general, the parameter values however differ significantly from those reported in the literature and presented above, because the present analysis considers a much wider range of soils.

### 3.3.3 Performance Evaluation

Several statistical measures are available for evaluating the performance of a model. These include correlation coefficient, relative error, standard error, volume error, coefficient of efficiency (Hsu et al., 1995), among others. The Nash and Sutcliffe (1970) efficiency is one of the most frequently used criteria and was employed in this study. This criterion is analogous to the coefficient of determination and is expressed in percentage form as:

$$\text{Efficiency} = (1 - D_1/D_o) \times 100 \quad (3.17)$$

where  $D_1$  is the sum of the squares of deviations between computed and observed data:

$$D_1 = \sum (Y_o - \hat{Y})^2 \quad (3.18)$$

and  $D_o$  is the initial variance which is the sum of the squares of deviations of the observed data about the observed mean, expressed as:

$$D_o = \sum (Y_o - \bar{Y})^2 \quad (3.19)$$

where  $Y_o$  is the observed data,  $\hat{Y}$  and  $\bar{Y}$  stand for computed data and mean of the observed data, respectively. The efficiency varies on a scale of 0 to 100. It can also assume a negative value if  $D_1 > D_o$ , implying that the variance in the observed and computed values is greater than the model variance. In such a case, the mean of the observed data fits better than the model. The efficiency of 100 implies that the computed values are in perfect agreement with the observed data. In the present study, negative efficiencies were assigned a zero value for describing the model performance at the scale of 0 – 100.

For evaluation of model performance, infiltration was computed for each soil test using the above 14 models and efficiencies were computed. The average of these efficiencies for a soil type was taken as a measure of the model performance on that soil type for the following reason. The efficiency is a kind of weight (if efficiency is divided by 100) or marks assigned to a model for how well the model performed on a test without any bias. Thus, the overall performance of a model on a soil type is the sum of the marks scored on each test. The division of total marks by the number of tests leads to an average model efficiency, which is an unbiased indicator of the model performance.

Table 3.1: Infiltration data

Sl. No.	Soil	Region	Country	Number of tests	$K_s$ (cm s <sup>-1</sup> )	Porosity	Hydrologic Group	Reference
1.	Plainfield Sand (PFS) (disturbed sample)	Minnesota	USA	12	$3.44 \times 10^{-3}$	0.477		Black et al. (1969)
2.	Columbia Sandy Loam (CSL) (disturbed sample)	Minnesota	USA	36	$1.39 \times 10^{-3}$	0.518		Laliberte et al. (1966)
3.	Guelph Loam (GL) (air dried, sieved)	Minnesota	USA	12	$3.67 \times 10^{-4}$	0.523		Elrick and Bowman (1964)
4.	Ida Silt Loam (ISL) (undisturbed sample)	Minnesota	USA	42	$2.92 \times 10^{-5}$	0.530		Green (1962)
5.	Yolo Light Clay (YLC) (disturbed sample)	Minnesota	USA	12	$1.23 \times 10^{-5}$	0.499		Moore (1939)
6.	Alapaha Loamy Sand (ALS)	Georgia	USA	4			D	ARS (1976)
7.	Carnegie Sandy Loam (CASL)	Georgia	USA	4			C	ARS (1976)
8.	Cowarts Loamy Sand (COWLS)	Georgia	USA	20			C	ARS (1976)
9.	Dothan Loamy Sand (DLS)	Georgia	USA	4			B	ARS (1976)
10.	Fuquay Loamy Sand (FLS)	Georgia	USA	4			B	ARS (1976)
11.	Fuquay Pebbly Loamy Sand (FPLS)	Georgia	USA	6			B	ARS (1976)
12.	Kershaw Coarse Sand (KCS)	Georgia	USA	3			A	ARS (1976)
13.	Leefield Loamy Sand (LLS)	Georgia	USA	4			C	ARS (1976)
14.	Robertsdale Loamy Sand (RLS)	Georgia	USA	4			C	ARS (1976)
15.	Stilson Loamy Sand (SLS)	Georgia	USA	4			B	ARS (1976)
16.	Troup Sand (TS)	Georgia	USA	12			A	ARS (1976)
17.	Tifton Loamy Sand (TLS)	Georgia	USA	9			B	ARS (1976)
18.	Narsinghpur Clay (NC)	Madhya Pradesh	India	24				Roy and Singh (1995)
19.	Narsinghpur Sandy Clay Loam (NSCL)	Madhya Pradesh	India	2				Roy and Singh (1995)
20.	Narsinghpur Silty Clay (NSIC)	Madhya Pradesh	India	2				Roy and Singh (1995)
21.	Dudhnai Silty Sand (DUSS)	Assam	India	8				Kumar et al. (1995)
22.	Dudhnai Sandy Loam (DUSL)	Assam	India	6				Kumar et al. (1995)
23.	Dudhnai Loamy Sand (DULS)	Assam	India	9				Kumar et al. (1995)

Table 3.2: Statistics of optimized parameters on various soil types

Soil	Statistics	Smith - Parlange (l)			Smith-Parlange (nl)			Singh and Yu Model			Horton Model		
		$K_s$ ( $\text{cm h}^{-1}$ )	$C$ ( $\text{cm}^2 \text{h}^{-1}$ )	$C$ ( $\text{cm}^2 \text{h}^{-1}$ )	$K_s$ ( $\text{cm h}^{-1}$ )	$C$ ( $\text{cm}^2 \text{h}^{-1}$ )	$C$ ( $\text{cm}^2 \text{h}^{-1}$ )	$f_c$ ( $\text{cm h}^{-1}$ )	$S_0$ (cm)	$a$	$m$	$n$	$f_c$ ( $\text{cm h}^{-1}$ )
PFS	Minimum	7.10	26.81	12.79	33.32	10.60	5.43	3.79	0.00	0.64	10.60	44.49	0.00
	Maximum	20.51	65.17	26.14	65.64	22.16	8.90	40.88	1.51	1.38	22.16	140.17	1.19
	Average	10.58	49.52	16.32	51.88	18.08	6.67	11.42	0.91	1.06	18.08	91.57	0.62
CSL	Minimum	2.73	18.87	5.12	24.93	9.47	3.95	0.61	0.15	0.19	9.47	18.19	0.00
	Maximum	11.42	56.29	14.27	56.48	20.03	9.51	14.09	2.44	1.33	20.03	124.38	12.42
	Average	5.17	40.38	8.27	42.04	12.16	6.62	4.83	1.25	0.92	12.16	49.95	1.09
GL	Minimum	0.50	7.17	0.96	7.46	3.07	3.82	0.34	0.81	0.00	3.07	14.60	0.07
	Maximum	1.25	11.48	2.03	11.62	3.85	5.27	7.06	2.11	2.19	3.85	25.27	0.16
	Average	0.96	9.22	1.66	9.37	3.33	4.37	1.81	1.40	0.93	3.33	18.38	0.11
ISL	Minimum	0.00	0.08	0.00	0.08	0.06	1.54	0.04	0.00	0.05	0.06	0.27	0.00
	Maximum	0.08	0.43	0.14	0.41	0.21	3.20	2.38	1.12	5.30	0.21	30.43	0.97
	Average	0.03	0.22	0.06	0.23	0.12	2.25	0.21	0.15	1.57	0.12	2.73	0.04
YLC	Minimum	0.00	0.13	0.00	0.14	0.06	1.77	0.07	0.00	0.00	0.06	0.39	0.00
	Maximum	0.04	0.43	0.06	0.38	0.09	3.33	1.46	1.22	4.16	0.09	23.27	0.01
	Average	0.01	0.26	0.01	0.25	0.08	2.48	0.28	0.38	1.55	0.08	5.72	0.01
ALS	Minimum	0.00	3.05	0.02	2.00	0.61	2.49	0.06	0.00	1.31	0.61	12.94	0.06
	Maximum	4.97	9.33	5.83	9.46	5.15	14.98	7.74	0.13	8.91	5.15	163.53	0.94
	Average	1.43	5.76	1.85	5.75	2.00	6.81	3.68	0.03	4.14	2.00	65.78	0.45
CASL	Minimum	3.20	1.20	3.93	4.76	2.68	8.39	0.36	0.00	0.00	2.68	7.77	0.00
	Maximum	9.20	10.76	9.23	12.62	6.40	21.43	125.26	1.23	3.49	6.40	53.32	0.26
	Average	5.64	4.81	6.19	8.21	4.79	15.01	32.20	0.45	1.24	4.79	19.87	0.09
COWLS	Minimum	0.00	0.00	0.03	1.30	2.07	5.02	0.00	0.00	0.00	2.07	6.89	0.00
	Maximum	10.83	25.18	10.97	26.65	10.69	28.80	22.19	4.05	2.70	10.69	3150.97	326.05
	Average	6.85	5.54	6.44	9.78	5.99	16.04	3.47	0.63	0.57	5.99	173.16	16.39
DLS	Minimum	5.34	1.74	6.68	3.63	5.88	14.79	0.03	0.08	0.03	5.88	8.98	0.02
	Maximum	9.49	15.02	10.04	18.23	9.08	30.72	12.36	1.42	1.15	9.08	21.22	0.08
	Average	7.68	7.30	8.39	10.66	7.38	20.14	3.22	0.83	0.40	7.38	14.12	0.04
FLS	Minimum	1.36	0.72	2.27	7.28	3.26	9.75	0.83	0.00	0.00	3.26	11.38	0.01
	Maximum	13.22	20.80	13.60	21.23	8.08	28.03	3.03	1.33	1.85	8.08	18.79	0.09
	Average	7.82	7.65	8.29	11.29	6.14	21.16	1.64	0.58	0.61	6.14	15.16	0.04
FPLS	Minimum	5.66	0.50	5.80	3.12	5.03	12.04	0.66	0.00	0.00	5.03	7.91	0.01
	Maximum	9.07	3.36	9.10	5.20	8.00	32.10	15.30	0.47	1.51	8.00	37.25	0.57
	Average	7.14	1.37	7.32	3.72	6.45	18.54	5.20	0.08	0.50	6.45	15.04	0.16
KCS	Minimum	15.11	0.00	0.00	12.53	13.30	26.40	0.10	0.00	0.00	13.30	15.76	0.00
	Maximum	15.78	0.00	15.02	23.12	15.60	69.67	1.67	0.00	0.00	15.60	22.90	0.60
	Average	15.43	0.00	5.01	17.22	14.49	42.99	0.73	0.00	0.00	14.49	18.63	0.24

Table 3.2: Statistics of optimized parameters on various soil types (contd...)

Soil	Statistics	Smith - Parlange (l)			Smith-Parlange (nl)			Singh and Yu Model				Horton Model		
		K <sub>s</sub> (cm h <sup>-1</sup> )	C (cm <sup>2</sup> h <sup>-1</sup> )	C	K <sub>c</sub> (cm h <sup>-1</sup> )	C (cm <sup>2</sup> h <sup>-1</sup> )	f <sub>c</sub> (cm h <sup>-1</sup> )	S <sub>o</sub> (cm)	a	m	n	f <sub>c</sub> (cm h <sup>-1</sup> )	f <sub>o</sub> (cm h <sup>-1</sup> )	k (min <sup>-1</sup> )
LLS	Minimum	0.00	3.39	0.09	5.99	2.19	5.99	0.10	0.08	0.13	2.19	8.28	0.00	
	Maximum	7.68	12.38	8.44	14.70	6.00	22.23	8.00	1.10	2.44	6.00	26.92	0.16	
	Average	5.01	7.33	5.49	9.82	3.85	14.59	4.62	0.45	0.80	3.85	14.28	0.05	
RLS	Minimum	0.84	3.48	1.47	3.49	1.92	4.90	1.70	0.00	0.88	1.92	10.10	0.05	
	Maximum	2.48	8.11	3.17	8.44	2.35	9.17	6.52	0.28	2.44	2.35	24.73	0.23	
	Average	1.63	5.69	2.39	5.95	2.14	7.31	4.18	0.08	1.48	2.14	15.63	0.13	
SLS	Minimum	0.00	5.19	0.00	7.65	2.74	7.04	0.48	0.58	0.03	2.74	9.94	0.01	
	Maximum	9.78	22.77	10.29	21.26	7.99	31.25	2.65	1.30	1.42	7.99	26.26	0.10	
	Average	5.82	10.38	6.33	12.13	5.50	17.23	1.26	0.88	0.61	5.50	16.50	0.04	
TS	Minimum	0.02	0.00	0.17	1.50	1.95	3.12	0.37	0.00	0.00	1.95	7.32	0.01	
	Maximum	10.21	26.67	10.32	30.38	9.20	20.81	906.97	1.49	12.78	9.20	109.14	0.54	
	Average	4.41	6.80	4.96	8.52	4.47	12.70	79.64	0.50	1.86	4.47	24.55	0.16	
TLS	Minimum	0.00	1.76	0.07	2.77	0.24	3.25	0.02	0.00	0.00	0.24	6.89	0.01	
	Maximum	9.56	19.02	9.84	23.31	8.90	21.38	18.05	1.98	3.42	8.90	25.19	0.16	
	Average	4.48	8.87	5.08	9.27	4.30	12.22	4.01	0.62	0.96	4.30	14.10	0.06	
NC	Minimum	0.00	0.02	0.00	0.03	0.02	1.00	0.03	0.00	0.00	0.02	0.64	0.02	
	Maximum	6.68	1846.55	8.10	1725.49	14.35	109.60	76.68	6.18	7.84	14.35	224.49	0.84	
	Average	0.52	84.30	0.69	78.63	1.36	9.71	5.49	2.00	1.62	1.36	28.43	0.35	
NSCL	Minimum	0.43	0.10	0.51	0.12	0.25	2.05	0.19	0.56	0.00	0.25	1.68	0.72	
	Maximum	1.92	8.11	2.37	9.06	0.25	17.60	1.64	2.59	0.20	0.25	23.58	1.49	
	Average	1.17	4.10	1.44	4.59	0.25	9.83	0.91	1.57	0.10	0.25	12.63	1.10	
NSIC	Minimum	0.55	0.26	0.69	0.29	0.35	3.00	0.30	0.91	0.49	0.35	2.20	0.02	
	Maximum	10.94	75.05	13.71	89.61	11.95	33.50	1.93	0.93	0.62	11.95	1377.25	197.30	
	Average	5.74	37.65	7.20	44.95	6.15	18.25	1.11	0.92	0.56	6.15	689.73	98.66	
DUSS	Minimum	0.00	375.39	0.01	213.75	1.20	19.50	0.36	0.76	0.00	1.20	83.44	0.04	
	Maximum	20.84	2121.57	31.99	2199.54	32.00	107.00	10.11	1.72	0.72	32.00	215.35	0.09	
	Average	2.60	929.21	4.73	781.83	6.50	45.35	4.13	1.26	0.27	6.50	123.69	0.06	
DUSL	Minimum	0.00	0.18	0.25	0.20	0.40	1.80	0.00	0.72	0.20	0.40	16.64	0.04	
	Maximum	1.42	320.73	2.52	278.45	5.20	29.30	39.28	5.66	2.97	5.20	79.05	0.14	
	Average	0.28	162.81	0.74	134.75	2.12	18.57	10.08	1.71	1.24	2.12	53.09	0.09	
DULS	Minimum	0.00	55.65	0.02	63.58	0.90	11.20	0.79	0.59	0.00	0.90	78.07	0.04	
	Maximum	0.00	3368.64	2.22	2699.40	10.50	84.10	94.37	1.52	5.66	10.50	181.45	42.04	
	Average	0.00	924.58	1.02	670.74	3.49	41.31	12.37	1.22	0.86	3.49	123.86	4.76	

Table 3.2: Statistics of optimized parameters on various soil types (contd...)

Soil	Statistics	Holtan Model				Kostiakov Model			Modified Kostiakov Model				Huggins and Monke Model			
		$f_c$ ( $\text{cm h}^{-1}$ )	$S_0$ (cm)	$a$	$n$	$\alpha$	$\beta$		$f_c$ ( $\text{cm h}^{-1}$ )	$\alpha$	$\beta$	$f_c$ ( $\text{cm h}^{-1}$ )	$S_0$ (cm)	$(a/\phi^m)$	$n$	
PFS	Minimum	10.60	5.43	0.33	0.40	47.81	0.28		10.60	27.99	0.42	10.60	5.43	0.33	0.40	
	Maximum	22.16	8.90	14.45	2.94	60.92	0.58		22.16	60.90	1.25	22.16	8.90	14.45	2.94	
	Average	18.08	6.67	2.12	2.09	55.18	0.48		18.08	40.37	1.01	18.08	6.67	2.12	2.09	
CSL	Minimum	9.47	3.95	0.17	0.50	24.19	0.00		9.47	31.62	0.61	9.47	3.95	0.17	0.50	
	Maximum	20.03	9.51	5.00	2.76	69.54	0.68		20.03	476.46	2.32	20.03	9.51	5.00	2.76	
	Average	12.16	6.62	0.74	2.17	53.11	0.48		12.16	145.05	1.46	12.16	6.62	0.74	2.17	
GL	Minimum	3.07	3.82	0.13	1.87	15.14	0.44		3.07	25.85	0.77	3.07	3.82	0.06	1.87	
	Maximum	3.85	5.27	0.53	3.68	40.22	0.61		3.85	145.38	1.81	3.85	5.27	0.53	4.05	
	Average	3.33	4.37	0.27	2.55	29.92	0.58		3.33	63.81	1.28	3.33	4.37	0.25	2.69	
ISL	Minimum	0.06	1.54	0.02	0.82	2.25	0.46		0.06	3.55	0.70	0.06	1.54	0.02	0.82	
	Maximum	0.21	3.20	0.17	6.95	28.45	0.81		0.21	7365.05	1.81	0.21	3.20	0.17	6.95	
	Average	0.12	2.25	0.08	2.95	7.76	0.62		0.12	348.64	1.04	0.12	2.25	0.08	2.95	
YLC	Minimum	0.06	1.77	0.07	0.86	5.40	0.63		0.06	17.54	0.85	0.06	1.77	0.07	0.86	
	Maximum	0.09	3.33	0.14	2.06	29.14	0.83		0.09	4863.40	1.69	0.09	3.33	0.14	2.06	
	Average	0.08	2.48	0.10	1.40	17.10	0.74		0.08	463.62	1.10	0.08	2.48	0.10	1.40	
ALS	Minimum	0.61	2.49	0.08	1.40	13.89	0.25		0.61	27.13	0.84	0.61	2.49	0.08	1.40	
	Maximum	5.15	14.98	0.45	5.75	28.10	0.91		5.15	441.88	3.48	5.15	14.98	0.45	5.75	
	Average	2.00	6.81	0.23	2.66	20.34	0.59		2.00	145.43	1.81	2.00	6.81	0.23	2.66	
CASL	Minimum	2.68	8.39	0.01	0.03	9.81	0.01		2.68	7.52	0.29	2.68	8.39	0.01	0.03	
	Maximum	6.40	21.43	2.81	2.64	16.10	0.29		6.40	63.45	1.30	6.40	21.43	2.81	2.64	
	Average	4.79	15.01	1.09	1.12	12.40	0.17		4.79	26.00	0.67	4.79	15.01	1.09	1.12	
COWLS	Minimum	2.07	5.02	0.00	0.00	5.88	0.00		2.07	0.80	0.00	2.07	5.02	0.00	0.00	
	Maximum	10.69	28.80	5.16	2.58	49.28	0.64		10.69	188.86	2.09	10.69	28.80	5.16	2.58	
	Average	5.99	16.04	0.92	1.05	15.97	0.17		5.99	30.96	0.70	5.99	16.04	0.92	1.05	
DLS	Minimum	5.88	14.79	0.02	1.14	10.16	0.08		5.88	7.03	0.48	5.88	14.79	0.02	1.14	
	Maximum	9.08	30.72	0.18	1.67	24.19	0.89		9.08	47.89	0.92	9.08	30.72	0.18	1.67	
	Average	7.38	20.14	0.10	1.34	16.20	0.36		7.38	21.51	0.70	7.38	20.14	0.10	1.34	
FLS	Minimum	3.26	9.75	0.01	0.33	14.39	0.09		3.26	11.12	0.18	3.26	9.75	0.01	0.33	
	Maximum	8.08	28.03	2.70	2.02	41.28	0.88		8.08	85.53	1.50	8.08	28.03	2.70	2.02	
	Average	6.14	21.16	1.00	1.00	23.61	0.43		6.14	34.96	0.76	6.14	21.16	1.00	1.00	
FPLS	Minimum	5.03	12.04	0.10	0.00	6.07	0.00		5.03	1.52	0.00	5.03	12.04	0.10	0.00	
	Maximum	8.00	32.10	1.56	1.03	11.30	0.12		8.00	12.74	0.85	8.00	32.10	1.56	1.03	
	Average	6.45	18.54	0.58	0.35	9.05	0.05		6.45	5.79	0.47	6.45	18.54	0.58	0.35	
KCS	Minimum	13.30	26.40	0.17	0.00	14.25	0.00		13.30	0.16	0.00	13.30	26.40	0.17	0.00	
	Maximum	15.60	69.67	1.83	0.00	15.78	0.00		15.60	1.86	0.00	15.60	69.67	1.83	0.00	
	Average	14.49	42.99	0.83	0.00	15.01	0.00		14.49	0.82	0.00	14.49	42.99	0.83	0.00	

Table 3.2: Statistics of optimized parameters on various soil types (contd....)

Soil	Statistics	Holtan Model			Kostiakov Model			Modified Kostiakov Model			Huggins and Monke Model			
		$f_c$ (cm h <sup>-1</sup> )	$S_0$ (cm)	$a$	$n$	$\alpha$	$\beta$	$f_c$ (cm h <sup>-1</sup> )	$\alpha$	$\beta$	$f_c$ (cm h <sup>-1</sup> )	$S_0$ (cm)	$(a/\phi^n)$	$n$
LLS	Minimum	2.19	5.99	0.01	0.20	10.46	0.11	11.11	0.19	2.19	5.99	0.01	0.20	
	Maximum	6.00	22.23	4.43	4.53	34.55	0.66	126.49	1.52	6.00	22.23	4.43	4.53	
	Average	3.85	14.59	1.31	1.72	19.84	0.29	41.14	0.73	3.85	14.59	1.31	1.72	
RLS	Minimum	1.92	4.90	0.01	1.20	13.97	0.36	15.12	0.63	1.92	4.90	0.01	1.20	
	Maximum	2.35	9.17	0.30	4.35	20.68	0.48	52.43	1.50	2.35	9.17	0.30	4.35	
	Average	2.14	7.31	0.17	2.30	17.25	0.44	30.56	0.95	2.14	7.31	0.17	2.30	
SLS	Minimum	2.74	7.04	0.02	0.81	13.88	0.13	11.72	0.38	2.74	7.04	0.02	0.81	
	Maximum	7.99	31.25	0.76	2.97	60.27	0.75	262.62	1.53	7.99	31.25	0.76	2.97	
	Average	5.50	17.23	0.28	1.73	28.54	0.34	88.14	0.88	5.50	17.23	0.28	1.73	
TS	Minimum	1.95	3.12	0.02	0.00	5.47	0.00	1.41	0.00	1.95	3.12	0.02	0.00	
	Maximum	9.20	20.81	2.22	4.59	40.62	0.62	664.56	2.37	9.20	20.81	2.22	4.59	
	Average	4.47	12.70	0.45	1.63	17.53	0.27	84.47	0.90	4.47	12.70	0.45	1.63	
TLS	Minimum	0.24	3.25	0.02	0.41	8.47	0.07	0.67	0.00	0.24	3.25	0.02	0.41	
	Maximum	8.90	21.38	1.00	4.34	74.57	1.19	91.10	1.34	8.90	21.38	1.00	4.34	
	Average	4.30	12.22	0.33	1.72	25.02	0.39	32.76	0.72	4.30	12.22	0.29	1.86	
NC	Minimum	0.02	1.00	0.01	1.06	0.81	0.25	1.06	0.42	0.02	1.00	0.01	1.06	
	Maximum	14.35	109.60	5.63	10.26	413.62	1.86	355.06	2.18	14.35	109.60	5.63	10.26	
	Average	1.36	9.71	0.57	3.55	44.87	0.67	61.12	0.98	1.36	9.71	0.57	3.55	
NSCL	Minimum	0.25	2.05	0.20	0.84	2.41	0.34	2.48	0.43	0.25	2.05	0.20	0.84	
	Maximum	0.25	17.60	0.68	2.36	21.27	0.41	21.54	0.48	0.25	17.60	0.68	2.36	
	Average	0.25	9.83	0.44	1.60	11.84	0.38	12.01	0.46	0.25	9.83	0.44	1.60	
NSIC	Minimum	0.35	3.00	0.11	1.44	3.83	0.34	3.82	0.52	0.35	3.00	0.11	1.44	
	Maximum	11.95	33.50	0.13	2.38	60.21	0.38	92.38	0.83	11.95	33.50	0.13	2.38	
	Average	6.15	18.25	0.12	1.91	32.02	0.36	48.10	0.67	6.15	18.25	0.12	1.91	
DUSS	Minimum	1.20	19.50	0.20	1.08	242.23	0.52	12.78	0.69	1.20	19.50	0.20	1.08	
	Maximum	32.00	107.00	1.49	1.86	450.76	0.93	482.50	1.02	32.00	107.00	1.49	1.86	
	Average	6.50	45.35	0.69	1.44	333.92	0.75	327.14	0.84	6.50	45.35	0.69	1.44	
DUSL	Minimum	0.40	1.80	0.01	1.14	3.08	0.45	12.74	0.70	0.40	1.80	0.01	1.14	
	Maximum	5.20	29.30	1.29	12.48	181.21	0.86	207.32	2.54	5.20	29.30	1.29	12.48	
	Average	2.12	18.57	0.63	3.18	87.91	0.67	116.21	1.25	2.12	18.57	0.63	3.18	
DULS	Minimum	0.90	11.20	0.29	1.09	41.13	0.00	13.58	0.68	0.90	11.20	0.29	1.09	
	Maximum	10.50	84.10	1.21	1.59	458.85	1.52	717.65	1.89	10.50	84.10	1.21	1.59	
	Average	3.49	41.31	0.72	1.37	276.52	0.77	342.80	0.91	3.49	41.31	0.72	1.37	

### 3.4 DISCUSSION OF RESULTS

Table 3.3 presents a qualitative assessment of the model performance, assuming the following criteria: the model performance on a data set is very good (VG) if the average efficiency  $\geq 95\%$ , good (G) if  $90\% \leq \text{efficiency} < 95\%$ , satisfactory (ST) if  $75\% \leq \text{efficiency} < 90\%$ , and poor (P) if  $\text{efficiency} < 75\%$ . These are based on the average of the efficiencies derived from a model application to all infiltration data sets on a soil type. The overall grading (last row of Table 3.3) was taken for all the soils as the average of marks assigned to each of P, ST, G, and VG as equal to 4, 6, 8, and 10, respectively. It is evident from Table 3.3 that the Philip model performed satisfactorily only on soils NSIC, DUSS, DULS and RLS; and poorly on all other soils. The model exhibited an overall performance indicated by the relative grading equal to 4.35, reflecting an overall poor performance. Similarly, the performance of all other models on all the soils was evaluated.

Except for the Philip, Green-Ampt, and Collis-George models, all other models generally exhibited a satisfactory, good or very good performance on the laboratory-tested soils of PFS, CSL, GL and ISL. Specifically, the physically-based (both linear and non-linear) Smith-Parlange models and the semi-empirical Singh-Yu model exhibited a good to very good performance on all laboratory-tested soils except YLC on which their performance was satisfactory. The performance of SCS-CN based Mishra-Singh model was either good or satisfactory on all the laboratory-tested soils. All the models exhibited a poor performance on Georgia soils of CASL, COWLS, FLS, FPLS, KCS, LLS, and TS. On other Georgia soils too, the performance of the models was otherwise generally poor to satisfactory. As shown later, the infiltration data sets of Georgia soils generally showed an erratic behaviour of the infiltration decay pattern, which can not be simulated using the above-described simple models. Based on this discussion, it is inferred that the models were generally not amenable to Georgia sandy soils, and less to YLC. In



simulating the infiltration rates for the tests carried out in India, the Singh-Yu model exhibited satisfactory to very good performance on all six types of soils; Huggins-Monke model and Holtan model exhibited a very good performance on DUSS, satisfactory on four soils viz., NSCL, NSIC, DUSL, DULS, and poor on NC soils; and SCS-CN based model showed satisfactory performance on five soils and poor on NSIC soils. The other models showing a poor performance on two or more soils indicated a mixed performance on these soils.

Based on the relative grading, the models were ranked in the decreasing order of their performance as: Singh-Yu model, Holtan model, Huggins-Monke model, Smith-Parlange model (non-linear), Horton model, modified Kostiakov model, Smith-Parlange model (linear), Kostiakov model, SCS-CN based model, Collis-George model, Overton model, Green-Ampt model, Smith model, and Philip model. The semi-empirical Singh-Yu general model outweighed all other models in performance, for it was graded as 6.52 out of 10 whereas all other models were graded as 5.57 (for example, Holtan and Huggins models) or less, up to 4.35 (for example, Philip model). This might suggest that postulates 1 and 2 of Singh-Yu model are justified. The high ranking of Holtan or Huggins-Monke model suggests that the first postulate of the Singh-Yu model outweighs the second postulate, for the Green-Ampt model (derived for  $m=0$  and  $n=1$  from the Singh-Yu model) is significantly low ranked (last third). This discussion shows that the semi-empirical Singh-Yu model performed better than the others on the maximum number of soils under examination, except for CASL, COWLS, FLS, FPLS, KCS, LLS, and TS, where it performed poorly. Furthermore, except for the linear and non-linear Smith-Parlange models, the semi-empirical models (viz., Singh-Yu, Holtan and Horton model) and empirical models (viz., Huggins-Monke, modified Kostiakov, Kostiakov, SCS-CN based Mishra-Singh, and Collis-George model) performed better than other physically-based models (viz., Green-Ampt, Smith, and Philip model), which were apparently better for laboratory-tested soils than for field soils.

Table 3.3: Models performance on various soils

Soils	Efficiency Statistics	Philip	Green -Ampt	Smith-Parlange (l)	Smith-Parlange (nl)	Singh -Yu	Mishra -Singh	Smith	Horton	Holtan	Overton	Kostiakov	Modified Kostiakov	Huggins -Monke	Collis-George
PFS	Minimum	26.87	14.40	27.14	28.61	22.10	22.04	0.00	0.00	15.25	17.89	27.05	27.64	15.25	27.17
	Maximum	88.73	97.49	99.92	99.90	99.92	87.94	99.85	98.61	95.84	95.70	98.49	99.68	95.84	96.54
	Average	71.58	83.03	91.83	91.96	91.60	75.94	81.23	80.79	76.98	70.09	90.44	91.82	76.98	87.61
	Performance	P	ST	G	G	G	ST	ST	ST	ST	ST	P	G	G	ST
CSL	Minimum	10.51	6.13	6.87	5.85	8.84	13.32	0.00	0.00	12.48	13.27	0.00	0.00	12.48	0.00
	Maximum	81.73	94.06	99.88	99.85	99.95	97.32	99.41	99.77	99.98	99.24	99.87	99.54	99.98	99.62
	Average	56.25	72.98	96.26	96.17	96.22	84.82	85.10	70.93	92.53	79.03	84.71	89.62	92.53	55.97
	Performance	P	P	VG	VG	VG	ST	ST	P	G	ST	ST	ST	G	P
GL	Minimum	31.99	47.96	98.19	98.22	81.02	88.06	7.16	96.99	94.25	77.49	19.21	0.00	94.74	0.00
	Maximum	70.23	84.97	99.91	99.89	99.75	99.18	99.29	99.22	99.74	99.71	99.86	99.33	99.74	98.07
	Average	50.12	66.60	99.03	99.03	97.54	93.72	83.13	98.10	97.83	90.13	91.53	62.05	98.15	36.68
	Performance	P	P	VG	VG	VG	G	ST	VG	VG	G	G	P	VG	P
ISL	Minimum	25.38	40.69	59.26	59.33	0.00	56.72	0.00	0.00	54.95	0.00	0.00	54.03	54.95	0.00
	Maximum	91.30	99.54	99.91	99.90	100.00	98.75	99.95	99.64	99.39	99.35	99.90	99.98	99.39	90.71
	Average	73.50	86.23	95.53	95.60	90.64	86.66	82.85	78.70	89.52	78.98	89.62	95.62	89.52	9.43
	Performance	P	ST	VG	VG	G	ST	ST	ST	ST	ST	ST	VG	ST	P
YLC	Minimum	14.94	24.13	0.00	24.58	49.81	51.54	38.71	0.00	49.82	0.00	38.24	23.64	49.82	0.00
	Maximum	79.53	93.04	99.81	99.81	99.95	97.86	99.72	99.03	99.86	97.63	99.83	99.79	99.86	0.00
	Average	56.20	72.78	85.71	87.61	86.21	86.24	77.61	74.77	87.43	65.31	88.45	82.90	87.43	0.00
	Performance	P	P	ST	ST	ST	ST	ST	P	ST	P	ST	ST	ST	P
ALS	Minimum	44.46	38.15	34.37	46.25	77.71	21.84	0.00	63.95	15.41	41.16	57.18	84.77	15.41	58.72
	Maximum	69.20	77.62	78.05	79.97	93.13	73.70	0.64	92.93	77.66	53.53	85.02	95.16	77.66	92.65
	Average	57.74	55.86	56.93	63.10	85.53	39.53	0.16	80.46	50.80	46.92	74.17	89.31	50.80	79.95
	Performance	P	P	P	P	ST	P	P	ST	P	P	P	ST	P	ST
CASL	Minimum	0.00	0.00	0.60	8.31	0.00	0.00	0.00	0.00	0.00	0.00	0.18	0.00	0.00	0.00
	Maximum	54.25	77.94	89.97	92.51	91.41	52.89	91.27	93.19	82.33	74.47	81.99	91.95	82.33	93.20
	Average	36.26	33.70	42.59	43.69	37.92	20.22	38.33	27.65	25.96	31.23	43.61	46.17	25.96	23.30
	Performance	P	P	P	P	P	P	P	P	P	P	P	P	P	P
COWLS	Minimum	0.00	0.00	0.00	0.00	0.00	0.00	0.00	0.00	0.00	0.00	0.00	0.00	0.00	0.00
	Maximum	87.98	94.81	94.90	94.35	96.99	92.25	93.01	98.09	95.52	91.89	97.31	95.84	95.52	97.41
	Average	43.02	37.83	50.05	45.06	55.87	30.95	39.13	51.26	50.66	49.82	48.97	46.74	50.66	30.65
	Performance	P	P	P	P	P	P	P	P	P	P	P	P	P	P

Table 3.3: Models performance on various soils (contd...)

Soils	Efficiency Statistics	Philip	Green-Ampt	Smith-Parlange (l)	Smith-Parlange (nl)	Singh -Yu	Mishra -Singh	Smith	Horton	Holtan	Overton	Kostiakov	Modified Kostiakov	Huggins -Monke	Collis-George
DLS	Minimum	55.12	5.35	37.05	13.99	79.77	0.00	51.96	76.59	45.15	45.69	0.00	55.13	45.15	0.00
	Maximum	67.89	77.49	79.62	80.55	91.32	84.40	78.95	94.40	92.25	69.15	91.42	82.55	92.25	92.22
	Average	62.74	49.59	61.24	37.36	87.21	51.60	66.36	86.21	78.69	57.97	58.82	71.20	78.69	27.74
	Performance	P	P	P	P	ST	P	P	ST	ST	P	P	P	ST	P
FLS	Minimum	0.00	0.00	10.39	4.42	23.64	0.00	24.26	33.18	13.38	0.00	0.00	24.62	13.38	0.00
	Maximum	61.79	75.80	88.53	88.36	91.07	85.79	88.66	95.09	90.19	89.20	92.97	89.92	90.19	93.03
	Average	27.83	30.30	40.62	45.53	64.14	21.45	46.40	62.57	68.16	38.68	42.02	51.42	68.16	23.26
	Performance	P	P	P	P	P	P	P	P	P	P	P	P	P	P
FPLS	Minimum	0.00	0.00	4.76	22.32	0.00	0.00	0.00	0.00	0.00	0.00	0.00	0.00	0.00	0.00
	Maximum	52.37	38.85	54.94	67.45	67.93	0.11	49.57	54.45	67.74	28.58	49.56	51.82	67.74	34.69
	Average	26.03	14.55	32.76	48.75	18.51	0.02	17.40	19.64	19.28	9.80	24.52	28.86	19.28	8.12
	Performance	P	P	P	P	P	P	P	P	P	P	P	P	P	P
KCS	Minimum	0.00	0.00	0.00	0.00	0.00	0.00	0.00	0.00	0.00	0.00	0.00	0.00	0.00	0.00
	Maximum	0.00	0.00	0.00	9.49	0.00	0.00	0.00	0.00	0.00	0.00	0.00	0.00	0.00	0.00
	Average	0.00	0.00	0.00	3.16	0.00	0.00	0.00	0.00	0.00	0.00	0.00	0.00	0.00	0.00
	Performance	P	P	P	P	P	P	P	P	P	P	P	P	P	P
LLS	Minimum	0.00	0.00	16.54	15.24	7.87	13.79	0.00	17.44	5.44	0.00	26.54	0.00	5.44	0.00
	Maximum	70.06	72.21	80.47	81.67	95.78	62.50	76.57	98.41	96.58	51.04	92.43	97.06	96.58	98.34
	Average	44.80	37.92	58.00	49.76	64.46	44.32	19.14	64.04	59.37	22.40	66.56	60.18	59.37	24.58
	Performance	P	P	P	P	P	P	P	P	P	P	P	P	P	P
RLS	Minimum	54.81	63.34	81.81	83.33	92.51	37.16	0.00	77.80	27.38	53.22	80.98	95.07	27.38	82.56
	Maximum	90.93	94.17	95.94	95.77	96.08	79.18	96.70	98.19	82.50	78.76	95.28	97.86	82.50	97.88
	Average	75.20	83.19	89.76	90.11	94.79	57.42	24.17	87.25	63.43	66.08	88.40	96.21	63.43	90.83
	Performance	ST	ST	ST	G	G	P	P	ST	P	P	ST	VG	P	G
SLS	Minimum	44.78	0.00	28.23	8.43	86.43	0.00	0.00	79.55	91.12	47.63	10.82	49.77	91.12	0.00
	Maximum	56.18	84.35	95.22	90.56	95.43	87.90	93.47	98.41	95.21	90.92	94.16	96.44	95.21	97.83
	Average	50.04	35.12	60.18	51.51	91.49	61.56	44.21	89.50	92.23	70.55	57.56	73.62	92.23	62.56
	Performance	P	P	P	P	G	P	P	ST	G	P	P	P	G	P
TS	Minimum	0.00	0.00	0.00	8.09	0.00	0.00	0.00	0.00	0.00	0.00	0.00	0.00	0.00	0.00
	Maximum	79.14	87.51	93.39	91.77	97.78	88.19	91.37	97.02	91.69	94.43	97.82	99.25	91.69	97.59
	Average	43.32	46.83	55.98	57.73	64.71	33.03	28.66	60.47	46.15	36.12	57.15	64.42	46.15	55.49
	Performance	P	P	P	P	P	P	P	P	P	P	P	P	P	P

Table 3.3: Models performance on various soils (contd...)

Soils	Efficiency Statistics	Philip	Green-Ampt	Smith-Parlange (f)	Smith-Parlange (nl)	Singh -Yu	Mishra -Singh	Smith	Horton	Holtan	Overton	Kostiakov	Modified Kostiakov	Huggins -Monke	Collis-George
TLS	Minimum	0.00	0.00	21.00	32.14	7.58	0.00	40.99	16.46	7.25	39.84	0.00	16.46	0.00	
	Maximum	76.79	82.51	91.17	97.47	96.98	86.12	97.73	97.48	96.91	94.92	97.32	97.48	97.85	
	Average	58.20	54.36	61.97	59.04	83.09	64.00	56.59	82.17	71.04	45.11	78.24	69.44	71.07	58.97
	Performance	P	P	P	ST	P	P	P	ST	P	P	ST	P	P	P
NC	Minimum	39.05	7.63	0.00	34.46	32.42	0.00	0.00	20.22	16.32	0.00	0.00	20.22	0.00	
	Maximum	93.20	93.52	95.65	99.50	99.02	99.84	99.86	99.17	96.24	99.72	99.78	99.17	97.37	
	Average	73.50	65.18	61.21	68.17	87.75	78.51	49.25	62.20	70.88	70.09	82.62	84.96	70.88	40.00
	Performance	P	P	P	P	ST	ST	P	P	P	P	ST	ST	P	P
NSCL	Minimum	62.73	28.15	46.48	37.70	71.62	76.92	39.55	0.00	72.15	71.05	67.21	62.85	72.15	0.00
	Maximum	76.53	35.38	59.83	53.22	93.10	91.78	78.60	0.00	93.09	79.14	79.66	78.72	93.09	0.00
	Average	69.63	31.77	53.15	45.46	82.36	84.35	59.07	0.00	82.62	75.10	73.43	70.78	82.62	0.00
	Performance	P	P	P	P	ST	ST	P	P	ST	ST	P	P	ST	P
NSIC	Minimum	71.79	72.19	79.41	74.24	86.84	59.94	0.00	0.00	76.19	70.71	87.88	85.43	76.19	0.00
	Maximum	85.34	87.11	88.66	81.75	95.30	78.03	84.74	78.36	82.67	93.08	96.70	89.89	82.67	78.57
	Average	78.57	79.65	84.03	78.00	91.07	68.99	42.37	39.18	79.43	81.89	92.29	87.66	79.43	39.28
	Performance	ST	ST	ST	ST	G	P	P	P	ST	ST	G	ST	ST	P
DUSS	Minimum	70.21	66.08	6.53	66.05	95.13	0.00	0.00	95.64	78.70	0.00	90.88	0.00	78.70	0.00
	Maximum	86.19	88.60	90.78	90.21	99.97	99.87	96.94	99.86	99.49	99.19	98.42	96.81	99.49	99.22
	Average	77.44	75.77	54.82	76.79	98.28	86.80	64.88	98.91	95.53	72.76	94.55	76.75	95.53	85.77
	Performance	ST	ST	P	ST	VG	ST	P	VG	VG	P	G	ST	VG	ST
DUSL	Minimum	27.76	38.65	33.37	57.11	93.69	43.00	1.27	94.41	37.87	8.40	0.00	0.00	37.87	91.61
	Maximum	85.36	85.87	97.11	97.39	99.86	99.87	99.42	99.93	99.65	84.36	95.04	99.42	99.65	99.51
	Average	68.28	70.78	68.75	75.79	98.17	81.20	48.00	97.17	78.35	57.14	70.80	57.04	78.35	95.72
	Performance	P	P	P	ST	VG	ST	P	VG	ST	P	P	P	ST	VG
DULS	Minimum	63.45	50.52	21.11	0.00	0.00	0.00	0.00	0.00	33.87	0.00	0.00	0.00	33.87	93.85
	Maximum	89.34	90.52	92.15	93.27	99.93	99.75	95.03	99.75	99.95	96.42	94.86	96.69	99.95	99.10
	Average	78.08	73.84	65.02	60.89	86.56	75.74	54.57	87.42	84.22	46.01	74.14	82.69	84.22	97.89
	Performance	ST	P	P	P	ST	ST	P	ST	ST	P	P	ST	ST	VG
<b>Relative Grading</b>		4.35	4.43	5.22	5.48	6.52	4.96	4.43	5.48	5.57	4.52	5.22	5.30	5.57	4.96

The less-than-satisfactory performance of all the above models on some soils, for example Georgia sandy soils except RLS, can largely be attributed to the fact that the final infiltration rates ( $f_c$ ) in all model runs on all the soils were derived from the observed data rather than optimization, wherein these may assume unrealistic negative values to enhance the model performance. Here, it is noted that different models can assume different  $f_c$  values for a soil in optimization, which appears to be unrealistic, for  $f_c$  is generally considered as a soil dependent parameter (Singh, 1992). To make the comparison of the basic model formulations more logical, the variation of  $f_c$  was restricted to the observed one. Exceptions were the linear and non-linear Smith-Parlange models, where parameter  $K_s$  was optimized because its observed values for all the soils were not available. Similarly, parameter  $S_o$  was taken as equal to the maximum cumulative infiltration for models of Singh-Yu, Holtan, and Huggins-Monke. Furthermore, the parameters of all the above models were restricted to realistic non-negative ( $\geq 0$ ) values. In general, an *a priori* fixing of the crucial parameters  $f_c$  and  $S_o$  and restricting the variation of parameters affected the model performance adversely. Secondly, the less satisfactory performance can also be attributed to the assumptions involved in the model derivation. For example, the Philip model is derived for time to ponding equal to zero. The data, however, exhibited a significant time to ponding, for example, the data of GL showed a time to ponding in the range of (4.56, 29.99) minutes. On the other hand, the Smith model which accounts for time to ponding performed satisfactorily on all the laboratory-tested soils including GL, indicating an improved model performance. In addition, the Smith model assumes uniform rainfall intensity that was true for laboratory tests. Similarly, other models were compared as discussed below.

Since the Smith-Parlange (non-linear) model also accounts for the non-linearity existing in the infiltration phenomenon, it shows an improved performance over the linear version of the model. The Singh-Yu model specializing into the above-described models performed better than

all its specific versions. Since the reformulated mathematical expressions of Holtan and Huggins-Monke models for optimization are the same, their relative grading is also equal to 5.57. It, however, does not hold for other models showing equal grades. As shown by Mishra (1998), the SCS-CN based model yielded a higher  $f_c$  value in optimization on an infiltration data set than the observed one and that due to the Horton model, an *a priori* fixing of  $f_c$  values yielded poorer performance of the former than the latter. In the present case too, an *a priori* fixing of  $f_c$  values led to the lower performance of the SCS-CN model than the Horton model. The non-variation of parameter 'a' of the Overton model with the antecedent moisture in optimization led to a poorer performance than did the Holtan model, from which it was derived. Since the Collis-George model is appropriate for simple soil systems, it also ranked low (Table 3.3). The modified Kostiakov model accounting for  $f_c$  ranked higher than the Kostiakov model, which excludes  $f_c$ . Figs. 3.1 through 3.3 show typical fits of some top-ranked models to the data sets of three sample soils, PFS, RLS, and DUSS, derived from laboratory-tests, Georgia, and India, respectively.

The infiltration data collected in the field generally represented soil heterogeneity, existence of macro-pores or secondary pores, and most of the available models are not designed to account for these local features. This is indirectly supported by an improved performance exhibited by several models on laboratory-tested soils. An example of the possible macro-pore development for COWLS soil of Georgia is illustrated in Fig. 3.4. The observed infiltration rates, having followed an exponential decay pattern, started to increase after about 10 min, perhaps because of macro-pores, increased till 50 min, and then gradually decreased following an almost sinusoidal pattern. Although most of the models followed the observed pattern at long times while a few followed the initial decay, the consequent efficiencies were much lower than desired according to the assumed criterion. The reason for the low efficiency might be the rising pattern of infiltration rates after 10 min.

Since the SCS-CN based infiltration model is used in the present research work for computation of event sedimentograph from the storm events on the watersheds, it is further assessed for its field applicability. Based on the results and the foregoing discussion, it is inferred that the SCS-CN based model performed satisfactorily on both laboratory-test data (USA) and field-test data (India), exhibiting the Nash and Sutcliffe efficiency  $\geq 75\%$  on these soils. The poor performance of the model on Georgia soils was no exception as almost all the models exhibited a poor performance on these soils for the possible reasons of existence of macro-pores or secondary porosity as described above. The overall relative grading (Table 3.3) also places the SCS-CN model at ninth rank amongst fourteen models. The added advantage with the use of the SCS-CN based model is that it has only three parameters for calibration and a backing of widely used SCS-CN method in surface hydrology analysis.

### 3.5 SUMMARY

Fourteen physically-based, semi-empirical and empirical infiltration models were evaluated and compared for their performance on a large set of infiltration data collected from field and laboratory tests on various soils types. The models were ranked on a relative grading scale based on their performance on these soils. In general, the Singh-Yu model, Holtan model, Huggins-Monke model, Smith-Parlange model (non-linear), Horton model, modified Kostiakov model, Smith-Parlange model (linear), Kostiakov model, and SCS-CN based model exhibited a satisfactory to very good performance on laboratory-tests; and poor to very good on field-tests in India. Other models were ranked lower than these models. All the models generally performed poorly on field-tests on Georgia's sandy soils. The study indicated that the SCS-CN based model, with its performance comparable with other frequently used models, can be used satisfactorily for further applications.

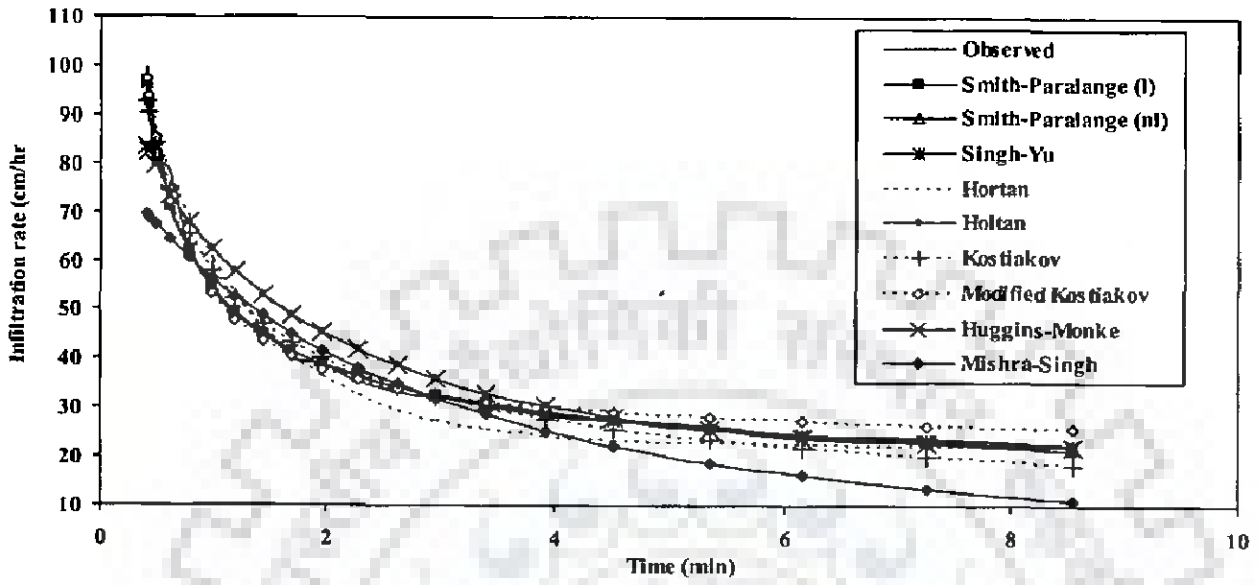


Fig. 3.1: Simulation of infiltration data of Plainfield sand (PFS)

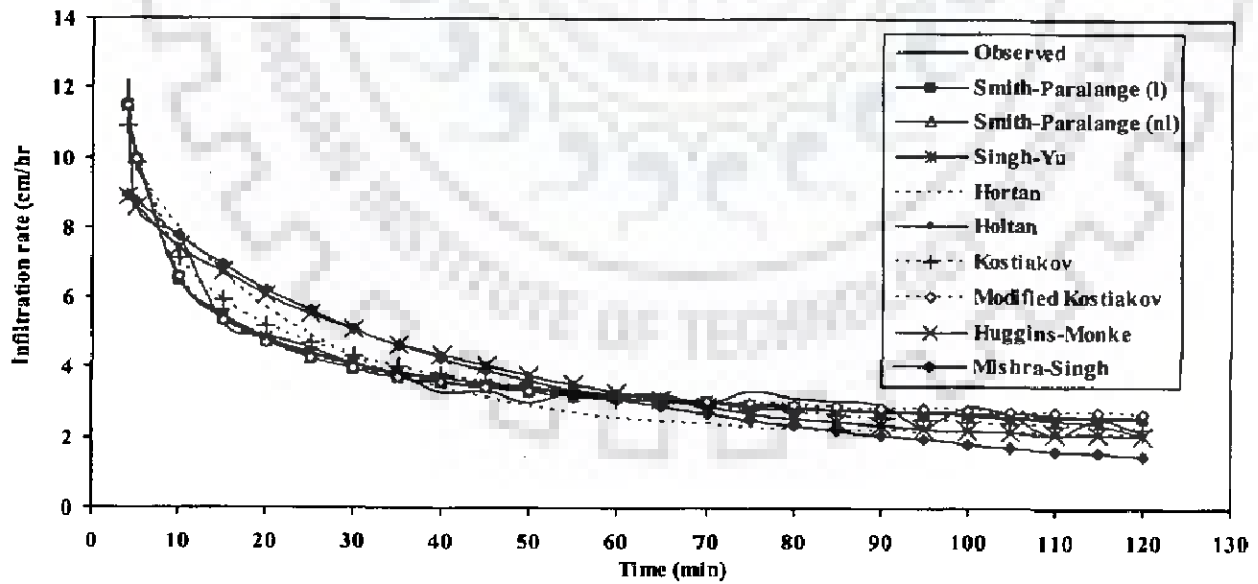


Fig. 3.2: Simulation of infiltration data of Robertsdale loamy sand (RLS)



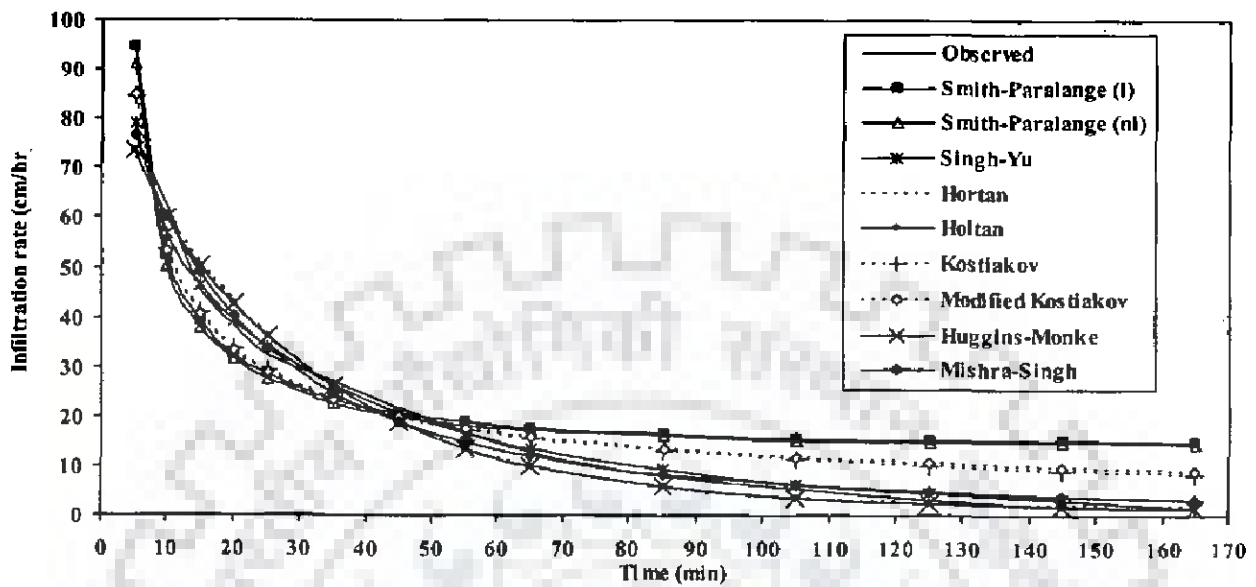


Fig. 3.3: Simulation of infiltration data of Dudhnai silty sand (DUSS)

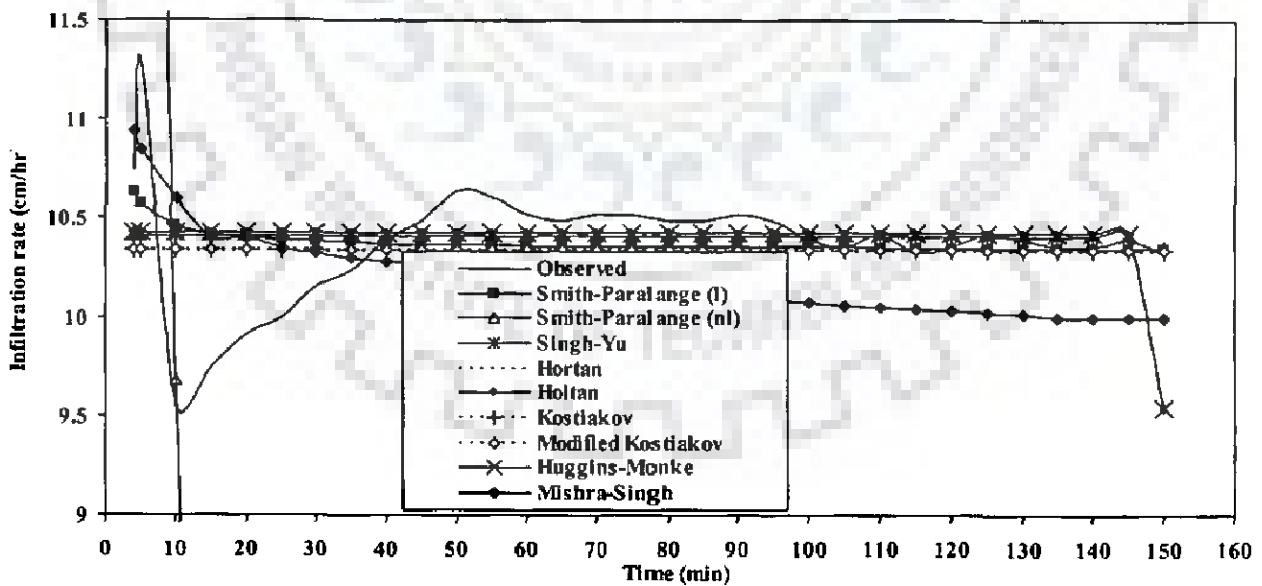


Fig. 3.4: Simulation of infiltration data of Cowarts loamy sand (COWLS)

# CHAPTER 4

## DESCRIPTION OF STUDY WATERSHEDS

---

### 4.1 GENERAL

The present research work aims at developing SCS-CN based lumped and temporal simple sediment yield models for small and medium-sized watersheds for application in field by conservation planners in watershed management. The accuracy of sediment yield models is largely determined by the availability and quality of the hydrologic and sediment yield data used for calibration. Equipment like automated rain gauge and stage level recorder are commonly used in watersheds for recording, respectively, the temporal rainfall and the variation of flow stage. The runoff hydrograph is generally computed by converting the stages into discharge rates using the discharge rating curve of the measuring station. However, in India, sampling for sediment rate is generally carried out manually, leaving a scope for some gaps at time intervals especially at odd hours, because the equipment like automatic pumping samplers are not commonly available. Also many a times, a record of only event's total rainfall from ordinary rain gauge is available due to non-functioning of automated equipment and delay in their repairing because of remote site location. Thus, the continuous record of rainfall, runoff, and sediment data is rare for most of the watersheds in India. Such data are available in plenty in developed countries, for example, USA. To test the general applicability of the proposed models, the watersheds for the present study were, therefore, selected from different river catchments of India and USA based on the availability of the hydrologic and sediment yield data of these watersheds. The watersheds vary in size, physiographic, climatic, soil and land use characteristics.

## 4.2 STUDY WATERSHEDS

Twelve watersheds were selected from India and USA for application of sediment yield models proposed in the study. These watersheds, depending on their monitoring agencies, are briefly described under three categories as follows. For a quick reference, a summary of these watersheds is presented in Table 4.1 and their drainage maps are shown in Figs. 4.1 to 4.12.

### 4.2.1 IGBP Watersheds

Nagwa watershed (92.46 km<sup>2</sup>), Karso watershed (27.93 km<sup>2</sup>) and Banha watershed (17.51 km<sup>2</sup>) in Hazaribagh district, Bihar, India, and Mansara watershed (8.70 km<sup>2</sup>) in Barabanki district, Uttar Pradesh, India, were monitored for rainfall, runoff and sediment yield under the 'Indo-German Bilateral Project (IGBP) on Watershed Management'. Rainfall was measured using tipping bucket rain gauges linked with a data-logger system, and also with ordinary rain gauges. Automatic stage level recorders were used to measure stream stage, and runoff was computed using relevant rating curves. The USDH-48 sampler and the Punjab bottle sampler were used to collect sediment samples. The hydrological data of these watersheds are available in SWCD (1991; 1993; 1994; 1995; and 1996).

The Nagwa watershed, located between 85° 16' 41" and 85° 23' 50" E longitudes and 23° 59' 33" and 24° 05' 37" N latitudes, lies in the Damodar river basin. It is drained by Upper Siwani stream that joins the river Konar, a tributary of Damodar river. The watershed is undulating in nature and its slope varies from 2.1 to 9.1%, the average slope being 2.3%. It falls in the sub-humid, tropical region of India, receiving an annual rainfall of 1,076 mm. The major soil type is sandy loam but silty clay, clay loam, loam and loamy sand soils are also found. The land use categories of agriculture, forest, open scrub, and waste land account for 64%, 6%, 9%, and 21% of the watershed area, respectively. Major crops grown in the watershed are paddy, maize, minor millets in summer, and mustard in winter season.

The Karso watershed is drained by Kolhuwatari stream that joins the Barhi nadi, a tributary of Barakar river. Geographically, the watershed lies between  $85^{\circ} 24' 20''$  and  $85^{\circ} 28' 06''$  E longitudes and  $24^{\circ} 16' 47''$  and  $24^{\circ} 12' 18''$  N latitudes. It lies in sub-humid, tropical climatic zone having an annual rainfall of about 1243 mm that occurs mostly during July to September. The watershed has extremely undulating and irregular slopes ranging from moderate 1.8% to steep 32%, the average slope being 7.3%. The soils in the watershed are primarily coarse granular. The texture of the soil is light sandy loam with the average percentage of coarse sand, fine sand, silt and clay as 30%, 28%, 17% and 25% respectively. The soils are low in organic matter content. The land use consists of agricultural lands, forests and open scrub which account for 49%, 41% and 10% of the watershed area respectively. Agricultural lands has paddy cultivation and mixed cultivation areas. Most of the cultivated area is treated with soil conservation measures like terracing, bunding etc.

Banha watershed in Upper Damodar Valley spreads between  $85^{\circ} 12' 02''$  and  $85^{\circ} 16' 05''$  E longitudes and  $24^{\circ} 13' 50''$  and  $24^{\circ} 17' 00''$  N latitudes. The topography of the major part of the watershed is nearly flat, with an average slope of about 3 to 4%. The soils of the watershed are sandy loam, loam, and clay loam covering approximately 47.7%, 28.5%, and 23.8% of the watershed area, respectively. The area has a sub-humid, tropical climate with a mean annual rainfall of 1,277 mm. About 90% of the rainfall occurs during June to October (monsoon months). The elevations of the highest and lowest points are 450 m and 406 m above the mean sea level, respectively. The geology of the watershed falls under the Archaean group, consisting of granite gneiss. The watershed comprises of 32% land under agriculture, 35% under forest, 18% under waste land, and 15% under grasses and others.

The Mansara watershed is a part of Gomti river basin and lies between  $81^{\circ} 23' 42''$  and  $81^{\circ} 26' 15''$  E longitudes and  $26^{\circ} 41' 04''$  and  $26^{\circ} 43' 15''$  N latitudes. Although the slope of the

watershed varies from flat to about 12%, the major area (93%) has a slope up to 1%. The watershed is bounded on top, right, and left by the minors of *Sarda Sahayak* irrigation project. The watershed has only one stream that receives runoff from overland flow. The watershed has a maximum relief of 7 m. The upper portion of the watershed is subjected to sheet erosion while rills are witnessed in the lower portion. The climate of the watershed is semi-arid subtropical and the temperature varies from 4.7° C in winter to 44° C in summer. The annual average rainfall of the watershed is about 1021 mm. The soils in the watershed are deep alluvial, grouped into three textural classes, viz., loam, sandy loam, and sandy soils. The watershed is predominantly comprised of agriculturally cropped lands. Mango gardens also occupy a sizeable area of the watershed. The major crops grown during *Kharif* (summer season) are maize, minor millets, paddy, groundnut, and pigeon pea, and during *Rabi* (winter season) these include wheat, gram, pea, and mustard, etc. (Agriculture Department, 1990). The watershed has been treated with soil and water conservation measures.

#### **4.2.2 USDA-ARS Watersheds**

Watershed W2 (0.33 km<sup>2</sup>) (ARS code 71002) is located near Treynor in IA, USA. It is one of the four experimental watersheds (W1, W2, W3, and W4) of the Deep Loess Research Station established by the US Department of Agricultural Research Service (USDA-ARS) in 1964 (Bradford, 1988; Vanliew and Saxton, 1984). Mean annual precipitation over the watershed is 814 mm. The topography consists of deeply incised channels, with slopes of 2-4% on the ridges and bottoms, and 12-18% on the sides. The watershed, with an average slope of 8%, is field contoured (Vanliew and Saxton, 1984; Kalin et al., 2003, 2004). The soil series in the watershed as described by the county soil series map are Monona (fine silty, mixed mesic typic Hapludolls), Napier (fine silty, mixed mesic cumulic Hapludolls), and Ida (fine silty, mixed calcareous mesic typic Udorthents) (Vanliew and Saxton, 1984). The surface soils consist of silt

loam and silty loam textures that are prone to erosion. 95% of the watershed area is grown in continuous corn and the remaining 5% consists of grassed waterways and active gullies at the watershed outlet. The Treynor experimental watersheds have been the subject of watershed studies for almost 30 years (Kalin et al., 2003, 2004). Simultaneous data of rainfall, runoff and sediment yield for six storms events on W2 watershed were collected for use in the present study. The data of two rain gauges 115 and 116 located around the watershed revealed some differences in measured precipitation and therefore, the average of the two rain gauges was taken as the mean watershed rainfall for use in the present study.

Three sub-watersheds of Goodwin Creek (GC) experimental watershed, namely, W6 (1.25 km<sup>2</sup>) (ARS code 62906), W7 (1.66 km<sup>2</sup>) (ARS code 62907), and W14 (1.66 km<sup>2</sup>) (ARS code 62914), located in the bluff hills of the Yazoo River basin near Batesville, MS, USA, were also utilized in the present study. The Goodwin Creek experimental watershed is operated by the National Sedimentation Laboratory (NSL), and it is organized and instrumented for conducting extensive research on upstream erosion, instream sediment transport, and watershed hydrology (Blackmarr, 1995). Terrain elevation ranges from 71 to 128 m above mean sea level, with an average channel slope of 0.004 in Goodwin Creek. The climate of the watershed is humid, hot in summer and mild in winter. The average annual rainfall during 1982-1992 was 1440 mm (Blackmarr, 1995). Mainly soybeans and small grains are grown in the cultivated areas. The watershed is divided into fourteen nested sub-watersheds with a flow measuring flume constructed at each of the drainage outlets. Twenty-nine standard recording rain gauges are located within and just outside the watershed. Instrumentation at each gauging site includes an electronic data acquisition and radio telemetry system that collects, stores and transmits the data to a central computer at the NSL for processing and archival. Measurements collected at each site include water stage, accounting of automatically pumped sediment samples, air and water

temperature, precipitation, and climatological parameters. The runoff, sediment, and precipitation data of Goodwin Creek sub-watersheds are available on WWW at URL: [http://msa.ars.usda.gov/ms/oxford/nsl/cwp\\_unit/Goodwin.html](http://msa.ars.usda.gov/ms/oxford/nsl/cwp_unit/Goodwin.html). The mean rainfall over the study sub-watersheds was computed as the average of rain gauges 6, 34, and 43 for W6 sub-watershed; 7 and 65 for W7 sub-watershed; and 14, 52, and 53 for W14 sub-watershed.

In addition, three North Appalachian Experimental Watersheds (NAEW) of USDA-ARS, namely, 123 ( $5.50 \times 10^{-3} \text{ km}^2$ ) (ARS code 26010), 129 ( $1.10 \times 10^{-2} \text{ km}^2$ ) (ARS code 26003), and 182 ( $0.28 \text{ km}^2$ ) (ARS code 26040) watersheds, near Coshocton, OH, USA, were utilized. Watershed 123 is cultivated and planted to a corn and soybean rotation. Watersheds 129 and 182 are predominantly pasture and are subjected to grazing. Watersheds 123 and 129 have relatively uniform slopes with no well-defined channels. Watershed 182 is subjected to two land uses, woods and pasture. There are two well-defined channels on this watershed. The soils of the three watersheds are mostly silt loam, with some sandy loam (Kelly et al., 1975). Most of these soils are in hydrologic group C, exhibiting slow infiltration and moderate runoff rates (Kelly et al., 1975; Wu et al., 1993). Precipitation data were collected at several locations in or adjacent to each watershed. Storm runoff and sediment data were collected at the outlets of the watersheds. Sediment was collected with coshocton wheels. On watersheds 123 and 129, the sediment that was deposited in the approach flume was also collected. This was not done on watershed 182 and some small bed load was not included in the measured sediment yield. The rainfall-runoff and sediment yield data of these watersheds are available in Wu et al. (1993).

#### **4.2.3 Cincinnati Watershed**

The rainfall-runoff-water quality data of Cincinnati watershed ( $3.0 \times 10^{-4} \text{ km}^2$ ) were collected during 1995-97 (Sansalone and Buchberger, 1997) on a 15x20 m asphalt pavement at milestone 2.6 of I-75 that is a major north-south interstate in Cincinnati, OH, USA. The details of

the site are available elsewhere (Sansalone and Buchberger, 1997; Soil, 1982). The runoff from the selected stretch was contributed by four southbound lanes, an exit lane, and a paved shoulder, all draining to a grassy v-section median at a transverse pavement cross-slope of  $0.020 \text{ m m}^{-1}$ . The runoff from the highway site (longitudinal slope = 0.004) finally drains to Mill Creek. The flow of the highway is primarily characterized by sheet flow, and the land use as urban (industrial, commercial, and residential) (Sansalone and Buchberger, 1997). The storm water runoff diverted through the epoxy-coated converging slab, a 2.54 cm diameter Parshall flume, and a 2 m long 25.4 cm diameter PVC pipe to a 2000 l storage tank, was measured at a regular 1-min interval using an automated 24 bottle sampler with polypropylene bottles. Rainfall was recorded in increments of 0.254 mm using a tipping bucket gauge. The water quality data at every 2 min interval were collected during rainfall-runoff events at the experimental site and samples were analyzed for dissolved and particulate bound metals for several rainfall-runoff events. The total solids which are the sum of dissolved and suspended solids represented the sediment yield (Sansalone and Buchberger, 1997; Sansalone et al., 1998; and Li et al., 1999).

### **4.3 DATA STATUS**

The hydrologic and sediment yield data of 98 storm events were compiled for all twelve watersheds from the respective sources mentioned above. The data of all the events on W2 Treynor watershed and Goodwin Creek (W6, W7, and W14) watersheds consisted of the temporal rates of rainfall, runoff and sediment yield. These temporal data were also available for most of the events on Karso, Banha and Mansara watersheds, except for a few events where the data consisted of a lumped value of event rainfall from the ordinary rain gauge. However, in the case of Nagwa watershed all the events consisted of lumped value of event rainfall. The reason for lumped values of rainfall was reportedly attributed to the malfunctioning or the non-functioning of the automated rain gauge system. The data available for NAEW (123, 129 and



182) watersheds in Wu et al. (1993), and for Cincinnati watershed in Sansalone and Buchberger (1997) consisted of lumped values of the event rainfall, runoff and sediment yield for all the events. Thus, among a total of 98 events, 49 events had temporal data of rainfall, runoff and sediment yield on Karso, Banha, Mansara, W2 Treynor, W6 GC, W7 GC, and W14 GC watersheds, and these were used in the application of time-distributed sediment yield model. Nevertheless, the data of 49 events provided a good data base for application of temporal sediment yield model, while the data of all 98 events on twelve watersheds were used in the lumped model. Table 4.1 (column 9) shows the total number of available events and the events available with temporal rates (in parentheses) for each of the study watersheds.



Table 4.1: Hydro-climatic characteristics of the watersheds selected for the study

S. No.	Watershed/size/location	Climate	Av. annual rainfall (mm)	Soils	Av. slope (percent)	Land use (percent)	Source of watershed details/rainfall-runoff-sediment yield data	No. of available events in the study
(1)	(2)	(3)	(4)	(5)	(6)	(7)	(8)	(9)
1.	Nagwa (92.46 km <sup>2</sup> ) Hazaribagh, Bihar, India (85° 16' 41" and 85° 23' 50" E) (23° 59' 33" and 24° 05' 37" N)	Sub-humid, tropical	1076	Sandy loam, silty clay, clay loam, loam	2.3	AG=64 FO=6 OS=9 WL=21	SWCD (1991; 1993; 1994)	7 (0)
2.	Karso (27.93 km <sup>2</sup> ) Hazaribagh, Bihar, India (85° 24' 20" and 85° 28' 06" E) (24° 16' 47" and 24° 12' 18" N)	Sub-humid, tropical	1243	Light sandy loam	7.3	AG=49 FO=41 OS=10	SWCD (1991; 1993; 1994; 1995; 1996)	9 (8)
3.	Banha (17.51 km <sup>2</sup> ) Hazaribagh, Bihar, India (85° 12' 02" and 85° 16' 05" E) (24° 13' 50" and 24° 17' 00" N)	Sub-humid, tropical	1277	Sandy loam, Loam, clay loam	3.5	AG=32 FO=35 WL=18 GR=15	SWCD (1993; 1994; 1995; 1996)	16 (7)
4.	Mansara (8.70 km <sup>2</sup> ) Barabanki, Uttar Pradesh, India (81° 23' 42" and 81° 26' 15" E) (26° 41' 04" and 26° 43' 15" N)	Semi-arid, sub-tropical	1021	Loam, sandy loam, sandy	1	AG=84 OS=16	SWCD (1994; 1996) Agriculture Dept. (1990)	11 (7)
5.	W2 Treynor (0.33 km <sup>2</sup> ) Treynor, IA, USA (95° 39' 00" W) (40° 10' 10" N)	Sub-tropical	814	Silt loam	8	AG=95 GR=5	Bradford (1988); Vanliew and Saxton (1984); Kalin et al., 2003; 2004)	6 (6)
6.	W6 Goodwin Creek (1.25 km <sup>2</sup> ) Batesville, MS, USA (89° 51' 44.665" E) (34° 16' 16.082" N)	Humid	1440	Silty, silt loam	5	AG=35 GR=23 Idle=10 FO=32	Blackmarr (1995); <a href="http://msa.ars.usda.gov/ms/oxford/ns/cwp/unit/Goodwin.html">http://msa.ars.usda.gov/ms/oxford/ns/cwp/unit/Goodwin.html</a>	7 (7)

Table 4.1: Hydro-climatic characteristics of the watersheds selected for the study (contd...)

S. No.	Watershed/size/location	Climate	Av. annual rainfall (mm)	Soils	Av. slope (percent)	Land use (percent)	Source of watershed details/rainfall-runoff-sediment yield data	No. of available events in the study
(1)	(2)	(3)	(4)	(5)	(6)	(7)	(8)	(9)
7.	W7 Goodwin Creek (1.66 km <sup>2</sup> ) Batesville, MS, USA (89° 51' 34.479" E) (34° 15' 10.342" N)	Humid	1440	Silty, silt loam	4	AG=28 GR=49 Idle=3 FO=20	Blackmarr (1995); <a href="http://msa.ars.usda.gov/ms/oxford/nsi/cwp/unit/Goodwin.html">http://msa.ars.usda.gov/ms/oxford/nsi/cwp/unit/Goodwin.html</a>	7 (7)
8.	W14 Goodwin Creek(1.66 km <sup>2</sup> ) Batesville, MS, USA (89° 52' 53.252" E) (34° 15' 07.040" N)	Humid	1440	Silty, silt loam	5	AG=34 GR=40 Idle=9 FO=17	Blackmarr (1995); <a href="http://msa.ars.usda.gov/ms/oxford/nsi/cwp/unit/Goodwin.html">http://msa.ars.usda.gov/ms/oxford/nsi/cwp/unit/Goodwin.html</a>	7 (7)
9.	Cincinnati (3.0x10 <sup>4</sup> km <sup>2</sup> ) Asphalt pavement at milestone 2.6 of I-75, Cincinnati, OH, U.S.A. (Not known)	Not known	1020	Asphalt pavement	0.4	urban=100	Sansalone and Buchberger (1997); Soil (1982); Sansalone et al. (1998); Li et al. (1999)	11 (0)
10.	123 NAEW (5.50x10 <sup>3</sup> km <sup>2</sup> ) Coshocton, OH, USA (81° 47' 20" E), (40° 22' 23" N)	Not known	Not known	Silt loam	0.1	AG=100	Wu et al. (1993); Kelly et al. (1975)	5 (0)
11.	129 NAEW (1.10x10 <sup>2</sup> km <sup>2</sup> ) Coshocton, OH, USA (81° 47' 52" E), (40° 22' 19" N)	Not known	Not known	Silt loam	17	GR=100	Wu et al. (1993); Kelly et al. (1975)	5 (0)
12.	182 NAEW (0.28 km <sup>2</sup> ) Coshocton, OH, USA (81° 46' 55" E), (40° 21' 36" N)	Not known	Not known	Silt loam	7	GR=90 FO=10	Wu et al. (1993); Kelly et al. (1975)	7 (0)

Note: AG = Agriculture; FO = Forest; OS = Open scrub; GR = Grass/Pasture; WL = Waste land; NAEW = North Appalachian Experimental Watersheds

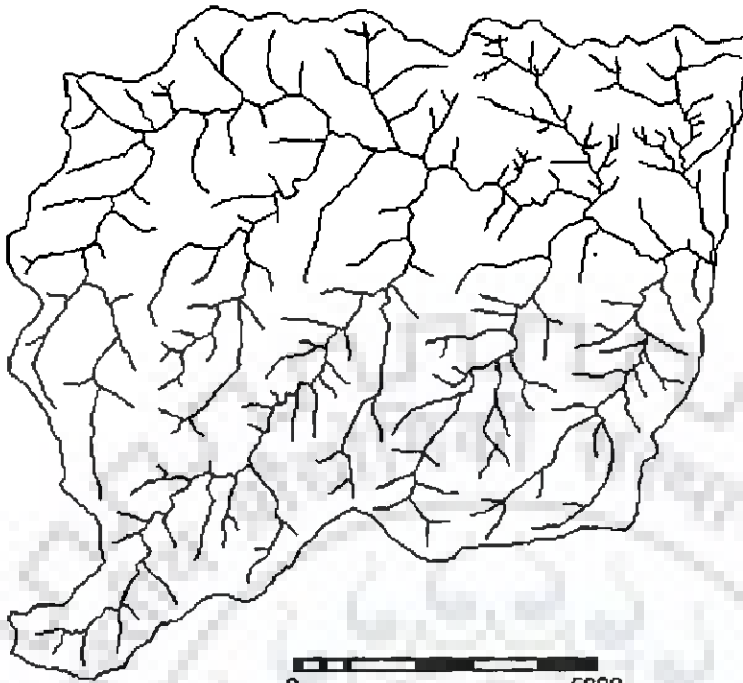


Fig. 4.1: Drainage map of Nagwa watershed

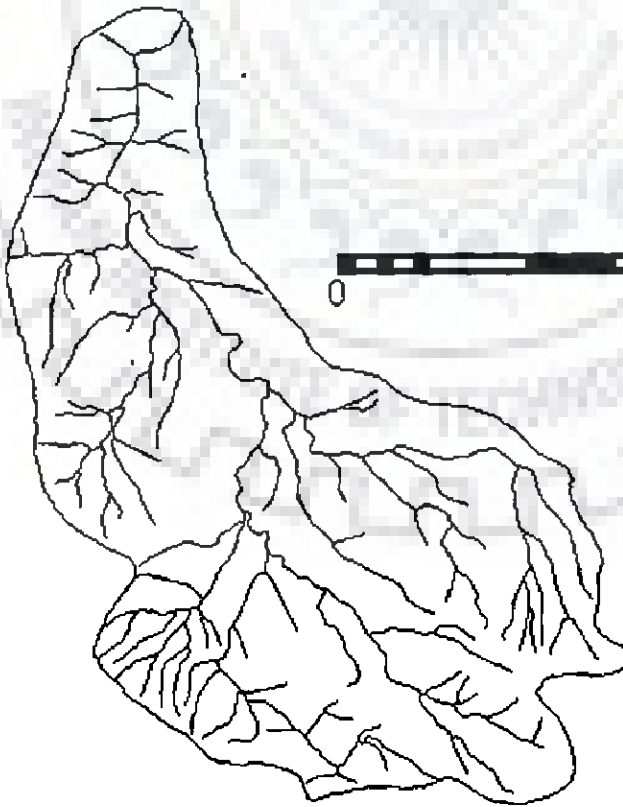


Fig. 4.2: Drainage map of Karso watershed

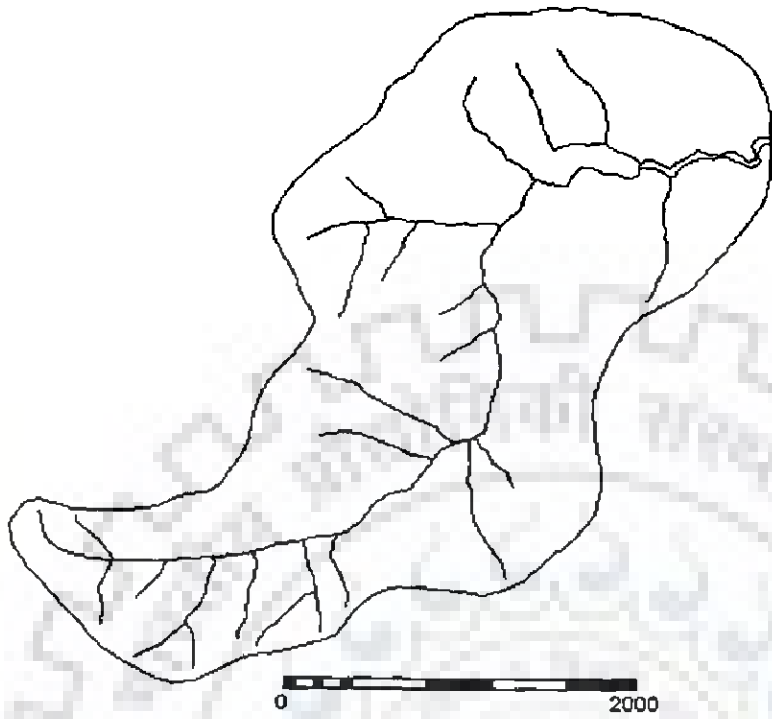


Fig. 4.3: Drainage map of Banha watershed

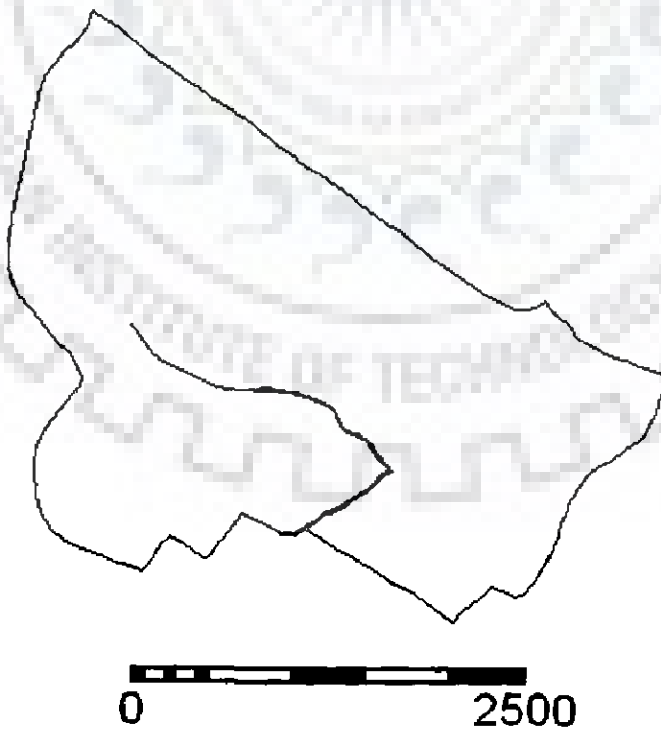


Fig. 4.4: Drainage map of Mansara watershed

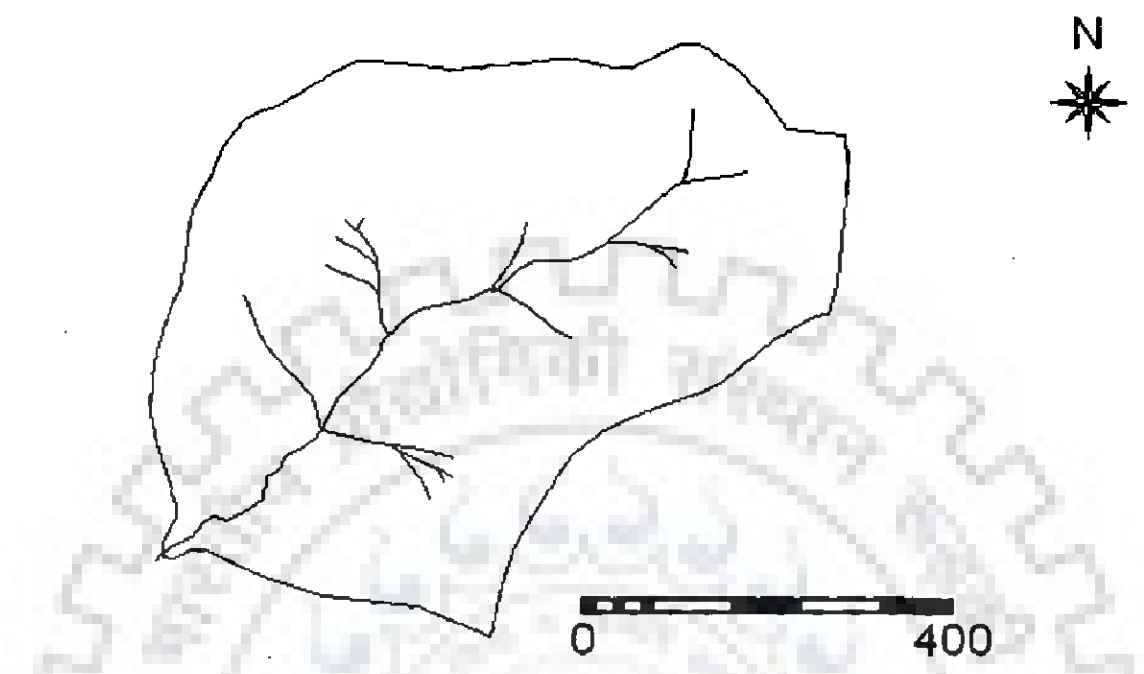


Fig. 4.5: Drainage map of W2 Treynor watershed

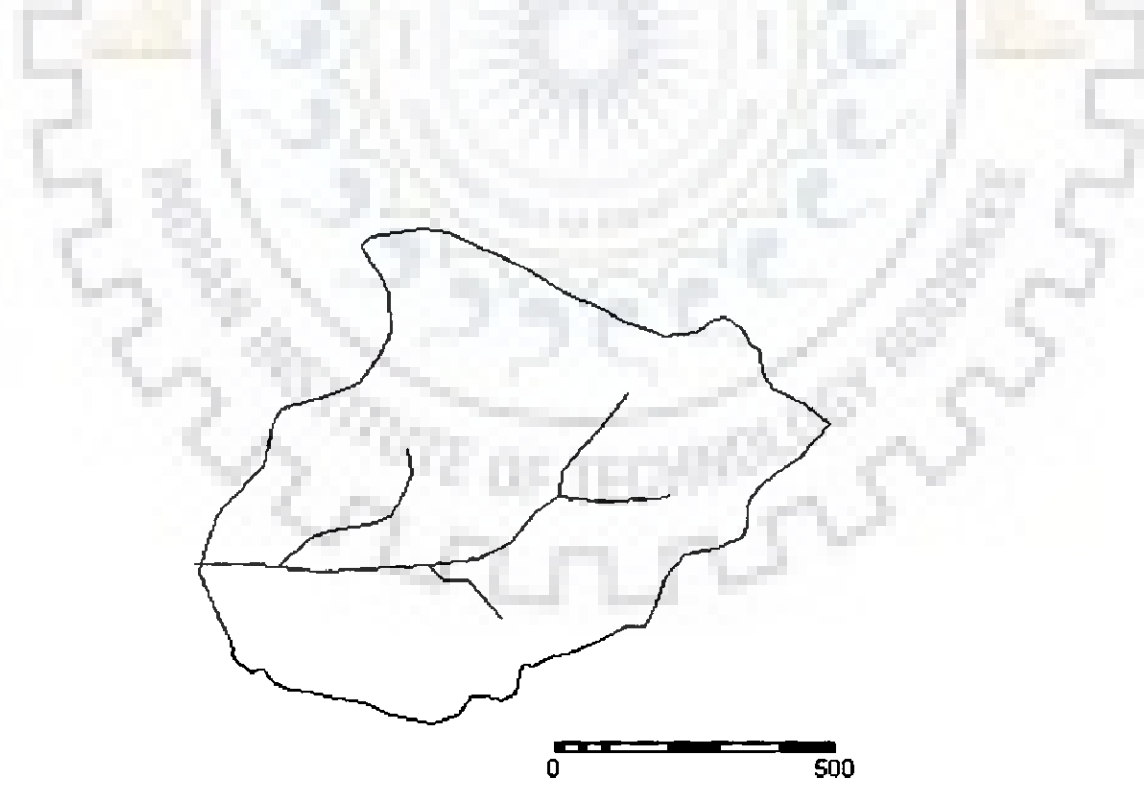


Fig. 4.6: Drainage map of W6 Goodwin Creek watershed

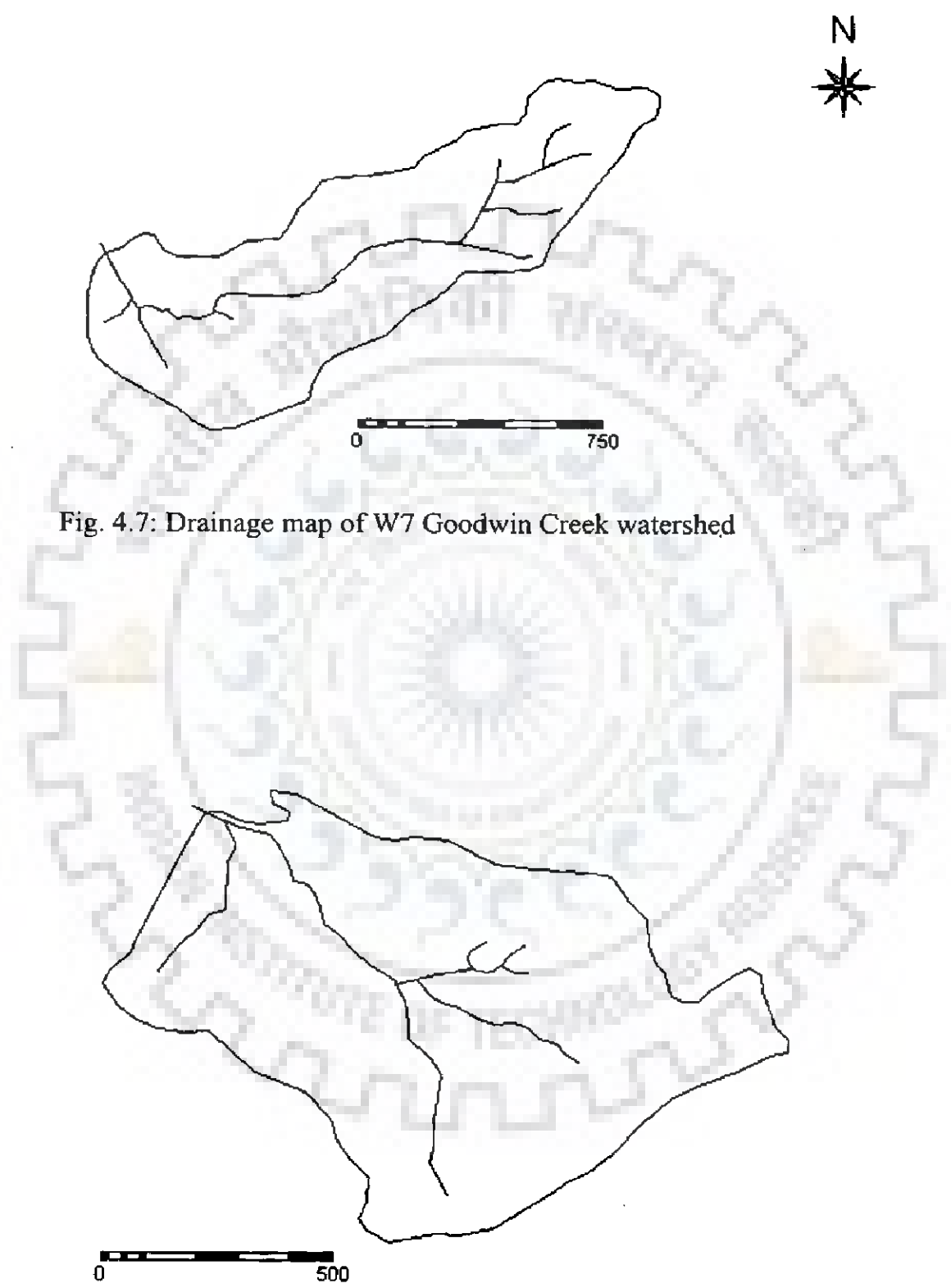


Fig. 4.7: Drainage map of W7 Goodwin Creek watershed

Fig. 4.8: Drainage map of W14 Goodwin Creek watershed



Fig. 4.9: Drainage map of Cincinnati watershed

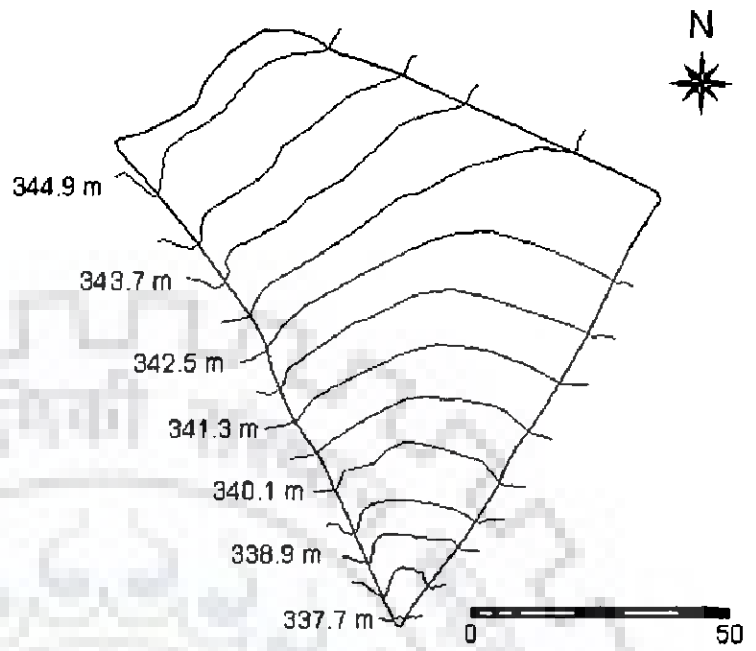


Fig. 4.10: Drainage map of 123 NAEW

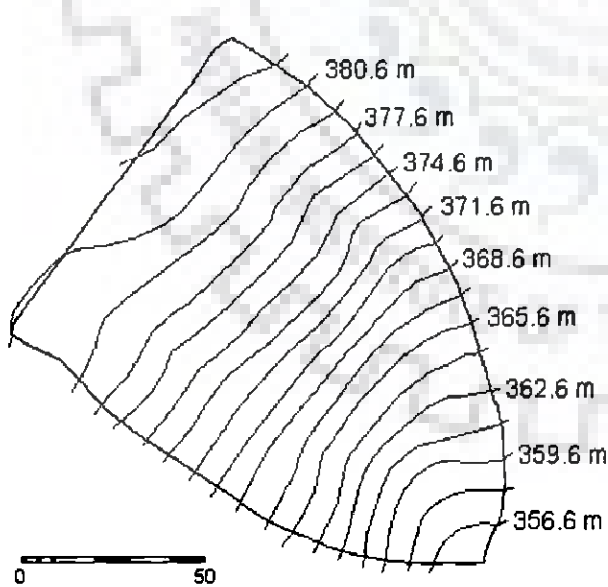


Fig. 4.11: Drainage map of 129 NAEW

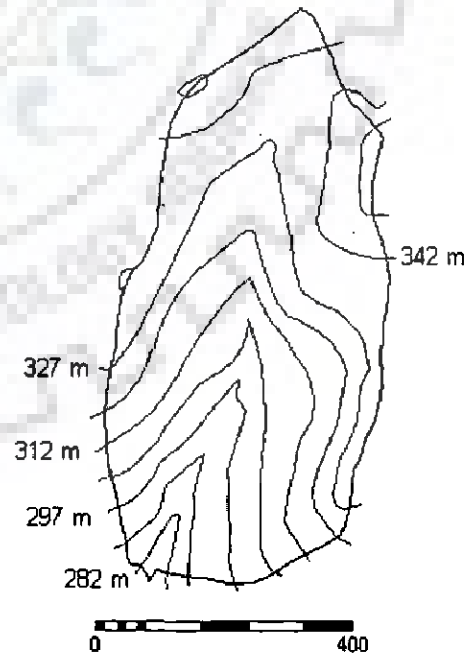


Fig. 4.12: Drainage map of 182 NAEW



## CHAPTER 5

### SCS-CN BASED LUMPED SEDIMENT YIELD MODEL

---

#### 5.1 INTRODUCTION

The Soil Conservation Service Curve Number (SCS-CN) method (SCS, 1956) and the Universal Soil Loss Equation (USLE) (Wischmeier and Smith, 1965) are widely used in hydrology and environmental engineering for computing the amount of direct runoff from a given amount of rainfall and the potential soil erosion from small watersheds, respectively. A great deal of published material on these methods along with their applications is available in hydrologic literature. The texts of Novotny and Olem (1994), Ponce (1989) and Singh (1988, 1992) are but a few examples. Since USLE was developed for estimation of the annual soil loss from small plots of an average length of 22 m, its application to individual storm events and large areas leads to large errors, but its accuracy increases if it is coupled with a hydrologic rainfall-excess model (Novotny and Olem, 1994). The current practice is to derive hydrologic information from a rainfall-runoff model and utilize it in the computation of potential erosion using USLE for determining the sediment yield (Knisel, 1980; Leonard et al., 1987; Rode and Frede, 1997; Young et al., 1987; Williams, 1975), which is of paramount importance in watershed management. The work of Clark et al. (1985) is noteworthy on the impact of erosion and sedimentation on the environment in general, and water quality in particular.

This discussion suggests that the SCS-CN method can be used as a rainfall-runoff model in sediment yield modelling. Furthermore, both the SCS-CN method and the USLE share a common characteristic in that they account for watershed characteristics, albeit differently. It is therefore conjectured that by coupling these two methods one can compute the sediment yield

from the knowledge of rainfall, soil type, land use and antecedent soil moisture condition. Thus, the present chapter aims at the development of an analytical model by coupling the SCS-CN method with USLE for computing total sediment yield from a storm event. This coupling has not yet been reported in the literature. The coupling is based on three hypotheses: (1) the runoff coefficient (C) is equal to the degree of saturation ( $S_r$ ), (2) USLE parameters can be expressed in terms of potential maximum retention (S), and (3) the sediment delivery ratio (DR) is equal to the runoff coefficient (C). The proposed sediment yield model is applied to a large set of rainfall-runoff-sediment yield data (98 storm events) obtained from twelve watersheds of different land uses (urban, agricultural, and forest), and varying in size from 300 m<sup>2</sup> to a few km<sup>2</sup>.

Before discussing the development of the sediment yield model, it is, however, relevant here to briefly revisit and reproduce from Chapter 2 the pertinent aspects of the SCS-CN method and the USLE method, which are crucial in the development and discussion of the proposed sediment yield model.

### 5.1.1 SCS-CN Method

The SCS-CN method couples the water balance equation (Eq. 2.1) with two hypotheses, which are given by Eq. 2.2 and Eq. 2.3, respectively, as:

$$P = I_a + F + Q \quad (2.1)$$

$$\frac{Q}{P - I_a} = \frac{F}{S} \quad (2.2)$$

$$I_a = \lambda S \quad (2.3)$$

where P is the total rainfall (mm),  $I_a$  is the initial abstraction (mm), F is the cumulative infiltration (mm), Q is the direct runoff (mm), S is the potential maximum retention (mm), and  $\lambda$  (= 0.2, taken as a standard value) is the initial abstraction coefficient. Eq. 2.2 is a proportionality concept (Fig. 5.1).

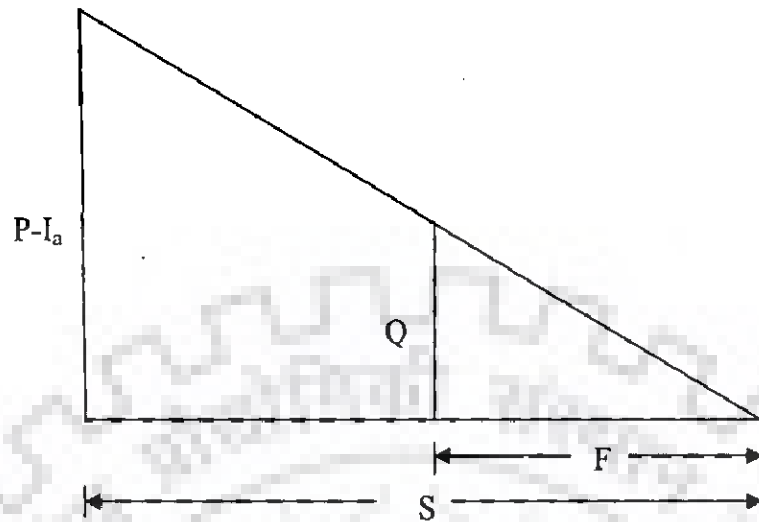


Fig. 5.1: Proportionality concept

Combination of Eqs. 2.1 and 2.2 leads to the SCS-CN method:

$$Q = \frac{(P - I_a)^2}{P - I_a + S} \quad (2.4)$$

which is valid for  $P > I_a$ ,  $Q = 0$ , otherwise. Coupling of Eq. 2.4 with Eq. 2.3 for  $\lambda = 0.2$  enables determination of  $S$  from the  $P$ - $Q$  data. In practice,  $S$  is derived from a mapping equation expressed in terms of the curve number (CN):

$$S = \frac{25400}{CN} - 254 \quad (2.6)$$

The non-dimensional CN is derived from the tables given in the National Engineering Handbook, Section-4 (NEH-4) (SCS, 1956) for catchment characteristics, such as soil type, land use, hydrologic condition, and antecedent soil moisture condition. Since CN indicates the runoff producing potential of a watershed, it should rely on several other characteristics, such as drainage density, slope length, gradient, etc. which significantly affect runoff (Gardiner and Gregory, 1981). The higher the CN value, the greater the runoff factor,  $C$ , or runoff potential of

the watershed, and vice versa. Michel et al. (2005) suggested  $S$  to be an intrinsic model parameter independent of initial moisture conditions. Though the simplification of SCS-CN method with  $I_a = 0.2S$  has found numerous successful applications the world over, Michel et al. (2005) found  $I_a$  and  $S$  to be independent of each other, for  $I_a$  is not an intrinsic parameter, rather it depends on initial moisture conditions.

### 5.1.2 Universal Soil Loss Equation

The Universal Soil Loss Equation (USLE) (Wischmeier and Smith, 1965) estimates the potential soil erosion (sheet and rill),  $A$ , from upland areas, and it is expressed as:

$$A = R K L S C P \quad (2.17)$$

Various terms of Eq. 2.17 are as explained in Chapter 2. Since the procedure for determining  $R$ -values suggested by Wischmeier and Smith (1965) is applicable for computation of annual erosion, its use in estimation of soil loss from a single storm would yield errors (Haan et al., 1994). Foster et al. (1977b) suggested a modification applicable to individual storm events as:

$$R = 0.5R_r + 0.35Qq^{1/3} \quad (2.21)$$

The terms of Eq. 2.21 are as explained in Chapter 2. Since the peak rate of runoff,  $q$ , is related to the detachment of soil particles more than is the runoff volume,  $Q$ , a reduction in peak discharge by the vegetative cover will also reduce sediment transport (Williams and Berndt, 1977). Renard et al. (1991) suggested the Revised USLE (RUSLE) incorporating a method for computing  $R$ -values for individual storm events. In another modification, Williams (1975) replaced the  $R$ -factor of the USLE by the runoff factor to estimate sediment yield for individual runoff events.

### 5.1.3 Computation of Sediment Yield

The sediment yield is determined from the above computed potential erosion using the sediment delivery ratio,  $DR$ . Erosion is distinguished from the sediment yield in that the former represents the potential erosion that is taken equal to the sum of sheet (upland) erosion and

channel erosion and the latter refers to the sediment measured in the receiving water body in a given time period. Vegetation dissipates rainfall energy, binds the soil, increases porosity by its root system, and reduces soil moisture by evapotranspiration to affect the sediment yield. DR is a dimensionless ratio of the sediment yield, Y, to the total potential erosion, A, in the contributing watershed. Expressed mathematically,

$$DR = \frac{Y}{A} \quad (2.23)$$

Eq. 2.23 is used to compute the sediment yield. Thus, the delivery ratio acts as a scaling parameter, varying from 0-1. It generally decreases with the basin size (Roehl, 1962).

Novotny and Olem (1994) equated the non-point pollution with soil loss and calibrated DR by minimizing the difference between the USLE-computed upland erosion and measured sediment yield estimates. According to Wolman (1977), the DR concept conceals a number of processes that contribute to temporal or permanent deposition of sediments in an eroding watershed, for these are highly variable, intermittent, and describable only statistically. The correlation of DR with the runoff coefficient (Novotny and Olem, 1994) indicates a significant effect of infiltration and other hydrologic losses on the magnitude of DR which is affected by the rainfall impact, overland flow energy, vegetation, infiltration, depression and ponding storage, change of slope of overland flow, drainage, and so on (Novotny et al., 1979, 1986; Novotny, 1980; Novotny and Chesters, 1989). Since these factors vary with time throughout the year, the sediment yield also varies with time.

The soil texture determines both permeability and erodibility of soils. Permeability describes infiltration, which, in turn, determines hydrologic activeness of the soil surface in terms of both runoff generation and soil erosion. Erosion is primarily driven by surface runoff (Gottschalk, 1964; Langbein and Schumm, 1958; Leopold et al., 1964; Singh, 1985; Walling and

Webb, 1983), if wind effects are ignored, and according to the SCS-CN method, the runoff generation is closely linked with infiltration. Thus, the processes of runoff generation and soil erosion are closely interrelated. In practice, the information on the volume of runoff and peak rate of runoff, for example, as utilized in the computation of erosion from USLE (Foster et al., 1977b) or in the computation of sediment yield from the Modified USLE (Williams, 1975), is derived separately using the SCS-CN method (Blaszczynski, 2003) or any other suitable hydrologic model.

## 5.2 DEVELOPMENT OF SEDIMENT YIELD MODEL

The sediment yield model is derived by integrating the SCS-CN method with USLE. The integration is based on three hypotheses: (1) the SCS-CN method can be reformulated using the  $C = S_r$  concept; (2) the USLE can be signified using the SCS-CN parameter  $S$ ; and, (3) the delivery ratio (DR) can be equated to  $C$  or  $S_r$ . These hypotheses are now described in what follows.

### 5.2.1 Hypothesis: $C = S_r$

For  $I_a = 0$  (i.e. immediate ponding situation), the SCS-CN proportionality hypothesis (Eq. 2.2) equates the runoff factor,  $C (= Q/P)$  to the degree of saturation ( $S_r$ ) that is defined using the terms shown in Fig. 5.2 as:

$$S_r = \frac{F}{S} = \frac{V_w}{V_v} \quad (5.1)$$

which is valid for  $S$  of a completely dry AMC, i.e. for  $V_v = S_1$ , where  $S_1$  is the potential maximum retention (=  $S$  of AMC 1). In Eq. 5.1,  $V_v$  is the void space, and  $V_w$  is the space occupied by the infiltrated moisture. In Fig. 5.2,  $V_a$  is the air space left after infiltration, and  $V_s$  is the volume of the solids. Thus, the total volume  $V$  is the sum of  $V_v$  and  $V_s$ . These quantities can also be expressed in terms of depth for a unit surface area.

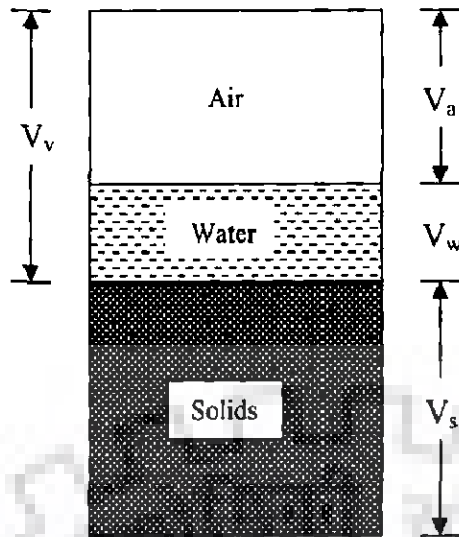


Fig. 5.2: Schematic diagram showing soil-water-air

### 5.2.2 Hypothesis: Physical Significance of S

Eq. 2.17 computes the potential soil loss ( $A$ ) from a watershed. Since  $A$  is the potential mass of soil per unit watershed area, it is equal to the product of the density of solids ( $\rho_s$ ) and the volume of solids per unit surface area ( $V_s$ ). Expressed mathematically,

$$A = V_s \rho_s \quad (5.2)$$

Eq. 5.2 can also be expressed as:

$$A = (V - V_v) \rho_s = \frac{V_v (1 - n)}{n} \rho_s \quad (5.3)$$

where  $n$  is the soil porosity (dimensionless). In Eq. 5.3, the term  $A$  represents the potential maximum erodible soil mass ( $= A_l$ ) corresponding to  $V_v$  ( $=$  potential maximum retention,  $S_l$ ). Considering the case of an initially wet soil having initial moisture as  $V_{w0}$ , and air space as  $V_{a0}$  that also represents the actual potential maximum retention,  $S$ , of the soil at the given initial moisture; Eq. 5.3, after its division by  $S$ , can be written as:

$$\frac{A_l}{S} = \frac{(V - V_v) \rho_s}{V_{a0}} \quad (5.4)$$

$V_{a0}$  can also be expressed as:

$$V_{so} = V_v - V_{wo} = V_v(1 - S_{ro}) \quad (5.5)$$

where  $S_{ro}$  is the initial degree of saturation. Substitution of Eq. 5.5 into Eq. 5.4 yields:

$$\frac{A_1}{S} = \frac{(V - V_v)\rho_s}{V_v(1 - S_{ro})} = \frac{(1 - n)}{n(1 - S_{ro})}\rho_s \quad (5.6)$$

For AMC I for which  $S_{ro} = 0$ , Eq. 5.6 shows that the  $A_1/S_1$  ratio depends on the type of soil and the density of soil particles, which are constant for a watershed. Furthermore, Eq. 5.6 can also be rearranged as:

$$\frac{A_1(1 - S_{ro})}{S} = \frac{(1 - n)}{n}\rho_s \quad (5.7)$$

where the term  $[A_1(1 - S_{ro})]$  is equivalent to the actual potential maximum erosion (A), corresponding to the actual potential maximum retention (S), which can be derived analytically. To this end, the actual potential maximum erosion (A) corresponding to actual potential maximum retention (S) can be, Similar to Eq. 5.3, expressed, as:

$$A = \frac{(V_v - V_{wo})(1 - n)}{n}\rho_s \quad (5.8)$$

Eq. 5.8 can be further manipulated to show that:

$$A = \frac{V_v(1 - S_{ro})(1 - n)}{n}\rho_s = A_1(1 - S_{ro}) \quad (5.9)$$

Therefore, Eq. 5.7 can be rewritten in terms of A and S as:

$$\frac{A}{S} = \frac{(1 - n)}{n}\rho_s \quad (5.10)$$

Thus, Eq. 5.10 shows that for a watershed the ratio of actual potential maximum erosion to actual potential maximum retention (= A/S ratio) is also a constant value. It further follows from Eq. 5.10 that,

$$A = \frac{S(1 - n)}{n}\rho_s \quad (5.11)$$



Coupling of Eq. 5.11 with Eq. 2.17 leads to:

$$R K L S C P = \frac{S(1-n)}{n} \rho_s \quad (5.12)$$

Thus, the actual potential maximum erosion of a watershed depends on  $n$ ,  $\rho_s$ , and  $S$ . It also implies that higher the potential retention of a watershed, the higher will be the potential erosion and vice versa. It is of common knowledge that highly porous soils (of high  $n$ ), such as sand, yield high  $S$ -values, whereas nonporous soils (of low  $n$ ), such as loam and clay, yield low  $S$ -values.  $S$  decreases with an increase in antecedent moisture, and vice versa. According to Eq. 5.10, heavy sediments (of high mass density) will yield low  $S$ -values and vice versa. Eq. 5.12 can also be written in terms of the actual potential maximum erodible soil depth,  $V_{pe}$  as:

$$V_{pe} = (1/\rho_s) R K L S C P + S \quad (5.13)$$

Thus, it is possible to determine the actual potential maximum erodible soil depth of a watershed using USLE and NEH-4 tables. Eq. 5.11 describes  $A$  in terms of the watershed characteristics explained by  $S$  and the material of the soil. Such an interpretation finds support from Novotny and Olem (1994): "For unconsolidated geological materials (soils, river deposits, sand dunes etc.), erodibility depends on particle size and texture of the material, water content, composition of the material, and the presence or absence of protective surface cover such as vegetation. Furthermore, loose soils with low chemical and clay content have highest erodibility." Eq. 5.12 shows an interdependence of USLE and SCS-CN parameter,  $S$ .

### 5.2.3 Hypothesis: $DR = C$

Similar to the SCS-CN proportional equality (or  $C = S_r$ ) concept, it is possible to extend it for sediment delivery ratio,  $DR$ , as:

$$C = S_r = DR \quad (5.14)$$

in which all variables range from 0 to 1.

## 5.2.4 Coupling of the SCS-CN Method with USLE

Eq. 5.14 can be expanded using the usual definitions and  $I_a = 0$  as:

$$\frac{Q}{P} = \frac{F}{S} = \frac{P}{P+S} = \frac{Y}{A} \quad (5.15)$$

Thus, Eq. 5.15 defines sediment yield,  $Y$  as,

$$Y = CA \quad (5.16)$$

Eq. 5.16 implies that the sediment yield is directly proportional to the potential maximum erosion  $A$ , and the runoff factor  $C$  is the proportionality constant. Alternatively,

$$Y = \frac{AP}{P+S} \quad (5.17)$$

For given watershed characteristics,  $A$  and  $S$ , the actual sediment yield  $Y$  increases with the rainfall amount, which confirms that higher the rainfall, higher will be the sediment erosion and its transport and hence higher the sediment yield, and vice versa. As  $S \rightarrow 0$  (or  $CN \rightarrow 100$ ),  $Y \rightarrow A$  since  $Q \rightarrow P$ . Similarly, as  $S \rightarrow \infty$  (or  $CN \rightarrow 0$ ),  $Y \rightarrow 0$  since  $Q \rightarrow 0$ . It also shows that direct surface runoff (or surface water) primarily drives sediment yield.

Furthermore, the  $A/S$  ratio, as shown by Eq. 5.10, is constant for a watershed. Thus, the basic thesis of the rainfall-sediment yield model can be described from Eq. 5.15 as a proportional equality which makes the ratio of actual potential maximum erosion ( $A$ ) to actual potential maximum retention ( $S$ ) equal to the ratio of actual erosion (sediment yield) to the actual retention (infiltration). Expressed mathematically,

$$\frac{A}{S} = \frac{Y}{F} = \text{constant} \quad (5.18)$$

where the ratio ('constant') depends on the soil material of the watershed. The availability of the values of this constant for various watersheds will enable the determination of  $A$  from NEH-4

tables. Eq. 5.17 integrates the SCS-CN method with USLE and can be modified for the following elements of the rainfall-runoff-erosion process.

**(i) Incorporation of  $I_a$**

The initial abstraction,  $I_a$  can be incorporated in Eq. 5.17 as:

$$Y = \frac{(P - I_a)A}{P - I_a + S} \quad (5.19)$$

Taking  $I_a = 0.2S$  which is a standard practice, Eq. 5.19 can be recast as:

$$Y = \frac{(P - 0.2S)A}{P + 0.8S} \quad (5.20)$$

which suggests that the sediment yield reduces with the increasing initial abstraction, and vice versa.

**(ii) Incorporation of antecedent moisture**

To incorporate antecedent moisture ( $M$ ) which represents the amount of moisture in the soil profile before the start of a storm, the SCS-CN proportionality (Eq. 2.2) can be modified according to the first hypothesis:  $C = S_r$  as:

$$\frac{Q}{P - I_a} = \frac{F + M}{S + M} \quad (5.21)$$

Combination of Eq. 5.21 with the water balance equation (Eq. 2.1) leads to,

$$\frac{Q}{P - I_a} = \frac{P - I_a + M}{P - I_a + M + S} \quad (5.22)$$

Thus, similar to the derivation of Eq. 5.19,  $Y$  can be derived using Eq. 5.22 as:

$$Y = \frac{(P - I_a + M)A}{P - I_a + S + M} \quad (5.23)$$

Similar to Eq. 5.20, Eq. 5.23 can also be expressed for  $I_a = 0.2S$  as:

$$Y = \frac{(P - 0.2S + M)A}{P + 0.8S + M} \quad (5.24)$$

Eq. 5.24 shows that the sediment yield will increase with increasing antecedent moisture amount (M), and vice versa.

### (iii) Incorporation of initial flush

Similar to the concept of initial abstraction, the concept of initial flush,  $I_f$  is quite popular in environmental engineering (Foster and Charlesworth, 1996; Sansalone and Buchberger, 1997). The initial abstraction is a loss of water primarily due to evaporation and it does not contribute to runoff. On the other hand, the initial flush is not a loss of sediment, rather it appears at the outlet of the watershed. For the most part, it is contributed by the initial runoff generated at the start of rainfall, after satisfying the initial abstraction requirements. To incorporate  $I_f$  in Eq. 5.24, the sediment delivery ratio (DR) is redefined as:

$$DR = \frac{Y - I_f}{A - I_f} \quad (5.25)$$

For simplicity, following the second SCS-CN hypothesis (Eq. 2.3),  $I_f$  can also be related to the potential erosion, A, as:

$$I_f = \lambda_1 A \quad (5.26)$$

Combination of Eq. 5.26 with Eq. 5.25 yields:

$$DR = \frac{Y - \lambda_1 A}{(1 - \lambda_1)A} \quad (5.27)$$

Thus, Eq. 5.24 can be further modified for the initial flush as:

$$Y = \left[ \frac{(1 - \lambda_1)[P - 0.2S + M]}{P + 0.8S + M} + \lambda_1 \right] A \quad (5.28)$$

From Eq. 5.28 it is possible to show that for  $M = 0$ , as  $S \rightarrow 0$ ,  $y \rightarrow A$  and as  $S \rightarrow \infty$ ,  $Y \rightarrow 0$ , for  $Y \geq 0$ . Eq. 5.28 represents the general form of the model, for  $\lambda = 0.2$ , for computation of the sediment yield from rainfall amount and catchment characteristics.

## **5.3 MODEL APPLICATION**

### **5.3.1 Data Used**

The proposed model, being lumped in nature, requires for its calibration and verification the observed data on total rainfall, runoff and sediment yield for the storm events. Therefore, as discussed in Chapter 4, the data of all 98 storm events for 12 watersheds (Table 4.1 and Figs. 4.1 through 4.12) were used for application of the model.

### **5.3.2 Model Formulations**

Based on the analytical development of Eq. 5.28 for the determination of sediment yield, seven models were formulated as shown in Table 5.1. In this table, Model S1 excludes the initial abstraction  $I_a$ , antecedent moisture  $M$ , and initial flush  $I_f$  components. Model S2 accounts only for initial abstraction with  $\lambda = 0.2$  (a standard value) and in Model S3,  $\lambda$  is allowed to vary. Model S4 accounts for both initial abstraction and antecedent moisture but allows the variation of  $\lambda$ . Model S5 is distinguished from Model S4 for  $\lambda = 0.2$ . Models S6 and S7 include all  $I_a$ ,  $M$ , and  $I_f$ , but the former assumes  $\lambda = 0.2$ .

### **5.3.3 Goodness of Fit Statistics**

The above formulated seven models were applied to the data of 98 events observed on twelve watersheds and their performance in computing the sediment yield was evaluated using the Nash and Sutcliffe (1970) efficiency, computed using the Eqs. 3.17 through 3.19 as discussed in Chapter 3.

## **5.4 RESULTS AND DISCUSSION**

### **5.4.1 Model Calibration and Verification**

The non-linear Marquardt algorithm of the least squares procedure of the Statistical Analysis System (SAS, 1988) was employed to estimate the parameters of the aforementioned models. Initially parameters were set as zero in all applications and the lower and upper limits were

Table 5.1: Formulation of rainfall-sediment yield and rainfall-runoff models

No.	Rainfall-sediment yield model	No.	Rainfall-runoff model
S1	$Y = \frac{AP}{P+S}$	R1	$Q = \frac{P^2}{P+S}$
S2	$Y = \frac{A(P-0.2S)}{P+0.8S}$	R2	$Q = \frac{(P-0.2S)^2}{P+0.8S}$
S3	$Y = \frac{A(P-\lambda S)}{P+(1-\lambda)S}$	R3	$Q = \frac{(P-\lambda S)^2}{P+(1-\lambda)S}$
S4	$Y = \frac{A(P-\lambda S+M)}{P+(1-\lambda)S+M}$	R4	$Q = \frac{(P-\lambda S)(P-\lambda S+M)}{P+(1-\lambda)S+M}$
S5	$Y = \frac{A(P-0.2S+M)}{P+0.8S+M}$	R5	$Q = \frac{(P-0.2S)(P-0.2S+M)}{P+0.8S+M}$
S6	$Y = \left[ \frac{(1-\lambda_1)[P-0.2S+M]}{P+0.8S+M} + \lambda_1 \right] A$	R6	$Q = \frac{(P-0.2S)(P-0.2S+M)}{P+0.8S+M}$
S7	$Y = \left[ \frac{(1-\lambda_1)[P-\lambda S+M]}{P+(1-\lambda)S+M} + \lambda_1 \right] A$	R7	$Q = \frac{(P-\lambda S)(P-\lambda S+M)}{P+(1-\lambda)S+M}$

decided by trial and error. If the computed value of a parameter in a run did not fall in the prescribed range, the limit was extended accordingly in the next run. If the subsequent runs produced the estimate within the prescribed range, the parameter estimate was assumed to be optimal globally.

The estimated values of parameters and the efficiencies resulting from computation of sediment yield for twelve study watersheds, viz., Nagwa, Karso, Banha, Mansara, W2, W6, W7,

W14, Cincinnati, 182, 129 and 123, are presented in Table 5.2(a-I), respectively. In these tables, efficiencies with superscripts 'a' and 'b' stand for the efficiency resulting from the computed sediment yield and runoff, respectively. Here, it is noted that Models S1-S7 determine sediment yield using rainfall and ignore a direct involvement of the observed runoff. In application of these models, variables A and M were also taken as parameters due to the lack of their observations. It is seen from Table 5.2(a) that for models S2 - S7, for the Nagwa watershed parameter S varied from 173.84 to 195.74 mm (or CN (Eq. 2.6) from 56 to 59),  $\lambda$  from 0.18 to 0.22, A from  $1.98 \times 10^5$  to  $2.16 \times 10^5$  KN, and M from 3.11 to 8.63 mm. The values of  $\lambda_1$ , wherever applicable, were obtained as 0.001. The ratio of A/S varied from 0.120 to 0.123 KN ha<sup>-1</sup> mm<sup>-1</sup>. Clearly, the variation of parameter values in a narrow range implicitly supports their credibility. The estimated low CN-values exhibit a low runoff potential of Nagwa watershed. The resulting efficiency (with superscript 'a') varying from 91.78 to 92.16% indicate a satisfactory model performance for the Nagwa watershed.

Similarly, parameters for all other watersheds generally vary in a close range. When allowed, the value of  $\lambda$  in Models S3, S4, and S7 varied from 0.10 to 0.225 for the study watersheds and these values lie in the range (0.1 - 0.3), which is consistent with Chen (1982) and SCD (1972). The curve numbers derived from S-values of Model S2 for the above watersheds varied from 52 - 97. The Cincinnati watershed with the highest CN (= 97) is the highest runoff producing watershed, which is consistent with the paved nature of the watershed. On the other hand, the Mansara watershed has the lowest runoff potential with the lowest CN (= 52), which is consistent with the watershed characteristics in terms of its subtropical, semi-arid climate, and alluvial soils. The other watersheds falling in between have fairly good to good runoff potential.

Table 5.2: Results of various model applications to study watersheds

(a) Nagwa watershed

Model No.	Parameters of rainfall-sediment yield models					Eff. <sup>a</sup> (%)	Eff. <sup>b</sup> (%)	A/S ratio (KN ha <sup>-1</sup> mm <sup>-1</sup> )
	S (mm)	$\lambda$	$\lambda_1$	A (KN)	M (mm)			
1	741.71	-	-	266766.960	-	50.20	7.50	0.039
2	173.84	-	-	197950.006	-	91.78	13.55	0.123
3	188.62	0.181	-	209931.842	-	92.00	10.92	0.120
4	193.13	0.213	-	214015.352	6.76	92.11	-2.00	0.120
5	195.15	-	-	215689.233	4.50	92.16	0.61	0.120
6	189.60	-	0.001	210913.430	3.11	92.07	3.61	0.120
7	195.74	0.220	0.001	216416.840	8.63	92.15	-6.24	0.120

(b) Karso watershed

Model No.	Parameters of rainfall-sediment yield models					Eff. <sup>a</sup> (%)	Eff. <sup>b</sup> (%)	A/S ratio (KN ha <sup>-1</sup> mm <sup>-1</sup> )
	S (mm)	$\lambda$	$\lambda_1$	A (KN)	M (mm)			
1	85.34	-	-	18986.372	-	55.31	75.82	0.080
2	71.84	-	-	31058.695	-	84.51	45.62	0.155
3	77.12	0.182	-	32130.673	-	84.86	43.47	0.149
4	79.55	0.202	-	32897.806	2.05	85.00	37.56	0.148
5	79.86	-	-	32872.054	2.02	85.01	37.59	0.147
6	75.70	-	0.008	31551.285	0.51	84.75	41.05	0.149
7	79.89	0.193	0.006	32850.158	0.97	85.00	38.00	0.147

(c) Banha watershed

Model No.	Parameters of rainfall-sediment yield models					Eff. <sup>a</sup> (%)	Eff. <sup>b</sup> (%)	A/S ratio (KN ha <sup>-1</sup> mm <sup>-1</sup> )
	S (mm)	$\lambda$	$\lambda_1$	A (KN)	M (mm)			
1	107.75	-	-	16978.432	-	69.60	10.21	0.090
2	55.31	-	-	13980.260	-	75.21	1.76	0.144
3	51.41	0.204	-	13273.264	-	75.00	14.18	0.147
4	62.30	0.182	-	14688.905	0.92	75.37	-10.40	0.135
5	75.25	-	-	16626.557	5.23	75.69	-49.04	0.126
6	68.38	-	0.000	15686.739	4.03	75.48	-30.49	0.131
7	62.63	0.180	0.000	14852.791	1.12	75.44	-9.67	0.135

(d) Mansara watershed

Model No.	Parameters of rainfall-sediment yield models					Eff. <sup>a</sup> (%)	Eff. <sup>b</sup> (%)	A/S ratio (KN ha <sup>-1</sup> mm <sup>-1</sup> )
	S (mm)	$\lambda$	$\lambda_1$	A (KN)	M (mm)			
1	336.31	-	-	4513.492	-	32.69	70.05	0.015
2	233.68	-	-	11180.957	-	81.45	58.78	0.055
3	237.13	0.196	-	11205.110	-	81.57	58.65	0.054
4	231.45	0.225	-	10967.678	5.78	81.41	53.41	0.054
5	239.73	-	-	11196.477	1.82	81.62	56.72	0.054
6	245.39	-	0.005	11474.620	1.31	81.75	52.93	0.054
7	238.31	0.201	0.000	11221.188	2.01	81.57	57.07	0.054



## (e) W2 Treynor watershed

Model No.	Parameters of rainfall-sediment yield models					Eff. <sup>a</sup> (%)	Eff. <sup>b</sup> (%)	A/S ratio (KN ha <sup>-1</sup> mm <sup>-1</sup> )
	S (mm)	$\lambda$	$\lambda_1$	A (KN)	M (mm)			
1	300.68	-	-	31109.580	-	61.76	-58.51	3.135
2	66.10	-	-	16122.176	-	85.43	-26.10	7.391
3	64.08	0.204	-	15582.008	-	85.34	-21.04	7.368
4	73.21	0.199	-	17253.897	1.62	85.78	-44.90	7.141
5	78.94	-	-	18269.065	2.81	86.00	-60.04	7.013
6	79.14	-	0.000	18400.431	3.00	85.97	-59.79	7.046
7	75.20	0.198	0.000	17680.877	1.99	85.85	-48.97	7.124

## (f) W6 Goodwin Creek watershed

Model No.	Parameters of rainfall-sediment yield models					Eff. <sup>a</sup> (%)	Eff. <sup>b</sup> (%)	A/S ratio (KN ha <sup>-1</sup> mm <sup>-1</sup> )
	S (mm)	$\lambda$	$\lambda_1$	A (KN)	M (mm)			
1	258.54	-	-	2966.324	-	64.92	15.41	0.092
2	74.12	-	-	1834.484	-	81.03	36.26	0.198
3	73.35	0.192	-	1766.312	-	81.12	41.77	0.193
4	76.43	0.207	-	1819.057	1.73	81.49	32.55	0.190
5	80.67	-	-	1903.572	1.93	81.96	27.06	0.189
6	80.21	-	0.001	1889.557	1.77	81.90	27.65	0.188
7	77.47	0.197	0.000	1839.661	1.30	81.60	33.84	0.190

## (g) W7 Goodwin Creek watershed

Model No.	Parameters of rainfall-sediment yield models					Eff. <sup>a</sup> (%)	Eff. <sup>b</sup> (%)	A/S ratio (KN ha <sup>-1</sup> mm <sup>-1</sup> )
	S (mm)	$\lambda$	$\lambda_1$	A (KN)	M (mm)			
1	446.08	-	-	10253.638	-	59.16	5.54	0.139
2	134.73	-	-	7071.485	-	80.20	15.97	0.316
3	133.22	0.195	-	6845.325	-	80.24	19.77	0.310
4	148.03	0.210	-	7481.055	4.86	81.06	3.56	0.304
5	142.35	-	-	7213.321	2.34	80.76	10.79	0.305
6	137.25	-	0.000	6994.857	1.54	80.47	15.25	0.307
7	135.67	0.221	0.000	6940.530	4.51	80.34	11.50	0.308

## (h) W14 Goodwin Creek watershed

Model No.	Parameters of rainfall-sediment yield models					Eff. <sup>a</sup> (%)	Eff. <sup>b</sup> (%)	A/S ratio (KN ha <sup>-1</sup> mm <sup>-1</sup> )
	S (mm)	$\lambda$	$\lambda_1$	A (KN)	M (mm)			
1	347.51	-	-	5619.130	-	57.20	-4.16	0.097
2	103.26	-	-	4358.002	-	90.04	-8.67	0.254
3	103.25	0.198	-	4310.703	-	90.06	-7.23	0.252
4	140.68	0.210	-	5524.721	9.19	91.28	-65.42	0.237
5	136.95	-	-	5410.200	6.97	91.19	-55.41	0.238
6	136.92	-	0.015	5332.590	5.02	91.14	-58.72	0.235
7	136.35	0.186	0.000	5390.837	5.10	91.17	-47.35	0.238

## (i) Cincinnati watershed

Model No.	Parameters of rainfall-sediment yield models					Eff. <sup>a</sup> (%)	Eff. <sup>b</sup> (%)	A/S ratio (KN ha <sup>-1</sup> mm <sup>-1</sup> )
	S (mm)	$\lambda$	$\lambda_1$	A (KN)	M (mm)			
1	15.52	-	-	1.203E-02	-	83.92	81.36	0.026
2	7.87	-	-	9.588E-03	-	76.15	87.33	0.041
3	7.25	0.100	-	9.102E-03	-	77.68	92.05	0.042
4	8.09	0.228	-	9.963E-03	0.81	79.51	86.65	0.041
5	7.98	-	-	9.550E-03	0.93	78.79	88.30	0.040
6	7.70	-	0.000	9.653E-03	0.95	77.43	89.09	0.042
7	7.85	0.207	0.000	9.525E-03	0.97	78.46	88.44	0.040

## (j) 182 watershed

Model No.	Parameters of rainfall-sediment yield models					Eff. <sup>a</sup> (%)	Eff. <sup>b</sup> (%)	A/S ratio (KN ha <sup>-1</sup> mm <sup>-1</sup> )
	S (mm)	$\lambda$	$\lambda_1$	A (KN)	M (mm)			
1	231.46	-	-	535.478	-	39.94	45.12	0.083
2	159.07	-	-	1023.017	-	81.20	-80.28	0.230
3	181.52	0.174	-	1137.857	-	81.43	-88.98	0.224
4	182.63	0.194	-	1143.641	3.86	81.44	-99.66	0.224
5	170.32	-	-	1078.829	2.35	81.32	-91.36	0.226
6	179.83	-	0.003	1127.115	3.81	81.41	-101.06	0.224
7	180.53	0.192	0.001	1132.677	2.99	81.42	-96.67	0.224

## (k) 129 watershed

Model No.	Parameters of rainfall-sediment yield models					Eff. <sup>a</sup> (%)	Eff. <sup>b</sup> (%)	A/S ratio (KN ha <sup>-1</sup> mm <sup>-1</sup> )
	S (mm)	$\lambda$	$\lambda_1$	A (KN)	M (mm)			
1	239.79	-	-	3.716	-	48.38	16.58	0.014
2	137.17	-	-	5.825	-	90.95	-102.95	0.039
3	137.00	0.199	-	5.813	-	90.92	-101.44	0.039
4	140.69	0.241	-	5.940	6.57	90.95	-128.40	0.038
5	149.12	-	-	6.201	2.46	90.96	-118.09	0.038
6	144.62	-	0.007	6.022	0.55	90.96	-115.15	0.038
7	138.80	0.199	0.002	5.855	0.15	90.95	-105.54	0.038

## (l) 123 watershed

Model No.	Parameters of rainfall-sediment yield models					Eff. <sup>a</sup> (%)	Eff. <sup>b</sup> (%)	A/S ratio (KN ha <sup>-1</sup> mm <sup>-1</sup> )
	S (mm)	$\lambda$	$\lambda_1$	A (KN)	M (mm)			
1	568.50	-	-	25.335	-	32.32	-23.24	0.081
2	153.51	-	-	31.274	-	84.04	-69.26	0.370
3	136.63	0.225	-	28.359	-	84.12	-63.75	0.377
4	140.75	0.219	-	29.082	0.12	84.10	-65.54	0.376
5	148.90	-	-	30.136	0.00	83.14	-63.00	0.368
6	149.56	-	0.000	30.506	0.00	83.28	-63.92	0.371
7	152.53	0.200	0.000	31.167	0.11	83.94	-67.95	0.372

Note: Superscript 'a' and 'b' in Table 5.2(a-l) stand for efficiency in computation of sediment yield and direct runoff, respectively.

To examine the validity of the above curve numbers derived from the rainfall-sediment yield model, these were correlated with those derived from the S-values computed using the rainfall-runoff data as (Hawkins, 1993):

$$S = 5[P + 2Q - \sqrt{Q(4Q + 5P)}] \quad (5.29)$$

The resulting median CNs for all the watersheds, when plotted against each other (Fig. 5.3), exhibited a quadratic relation:

$$y = -0.0106x^2 + 2.248x - 21.493; \quad (5.30)$$

$$R^2 = 0.916$$

Eq. 5.30 is valid only for the fitted region of data. Here, y is the CN-value corresponding to the P-Q data, x is the CN derived using the rainfall-sediment yield model (Model S2), and  $R^2$  is the coefficient of determination.  $R^2 = 0.916$  indicates a satisfactory fit, implying that the CN-values derived using the two entirely different approaches not only are consistent in their computation but also support the above analytical development and its application results. Fig. 5.3 shows that the sediment yield model underestimated the CN value. It is perhaps because of the deposition of sediment particles during their transport by runoff, yielding lesser amount of sediment at the watershed outlet than actually eroded in the watershed. It is also evident from the results of the Cincinnati watershed which is of high runoff potential and small in size and does not allow the process of sediment deposition to occur. On the other hand, this process might be quite dominant in other agricultural watersheds.

Since, Model S1 is the simplest of all the seven models (Table 5.1), the resulting low efficiency of 50.20% in its Nagwa application (Table 5.2a) is indicative of (a) the dependence of the sediment yield on the SCS-CN-generated runoff and (b) the applicability of the  $C = S_r = DR$  concept (Eq. 5.14). It is further supported by the efficiency (= 91.78%) of Model S2 that is

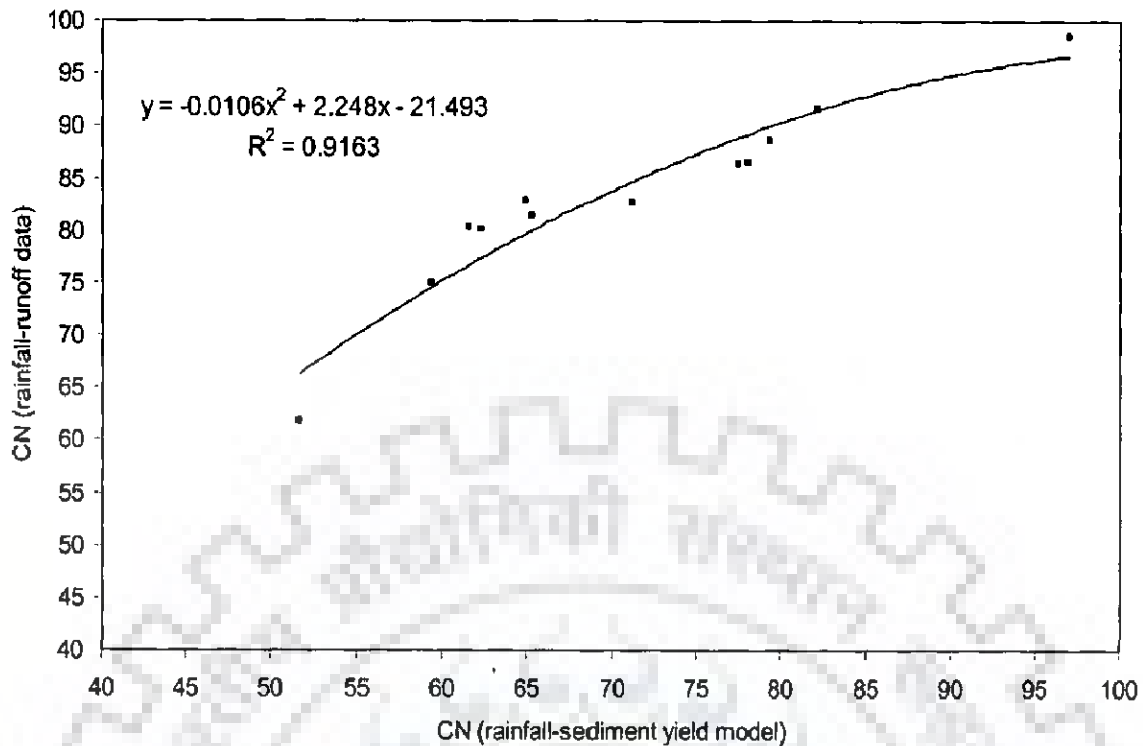


Fig. 5.3: Relationship between curve numbers derived from (a) the rainfall-sediment yield model and (b) the existing SCS-CN method (using rainfall-runoff data)

directly based on the existing SCS-CN method (Eq. 2.4 with  $I_a = 0.2S$ ). When  $\lambda$  was allowed to vary, as in Model S3, the efficiency improved to 92%. The incorporation of the antecedent moisture  $M$ , as in Models S4 and S5, further improved the resulting efficiency to 92.11% and 92.16%. The inclusion of the concept of initial flush (Models S6 and S7) and allowing the variation of  $\lambda$  in optimization (Model S7) slightly improved the efficiency to 92.15% over that of Model S4. Thus, a high value of efficiency supports the general applicability of the concept. Similarly, the results of model application to other watersheds can also be explained from Table 5.2(b-1). In general, the SCS-CN-based sediment yield models (S2 to S7) exhibited high efficiencies (more than 90%) on the data of Nagwa, W14, and 129 watersheds; and reasonably high efficiencies (75-90%) on the data of all other watersheds, indicating satisfactory model performance.

The above evaluation, however, excludes the observed runoff ( $Q$ ) in the estimation of the sediment yield. In practice, sediment yield from upland areas is generally better correlated with observed runoff (Singh and Chen, 1983) than with rainfall. Therefore, to further support the validity of coupling the SCS-CN method with USLE, it is appropriate to check the credibility of the estimated values of the parameters by computing direct surface runoff using these values and then comparing the computed runoff with the observed values.

For computation of direct runoff, the SCS-CN based models, designated as Models R1-R7 (Table 5.1) corresponding to Models S1-S7, were used. Models R1 to R3 are equivalent to Eq. 2.4 with  $I_a = 0$ ,  $I_a = 0.2S$ , and  $I_a = \lambda S$ , respectively. Models R4 and R5 are equivalent to Eq. 5.22 with  $I_a = \lambda S$  and  $I_a = 0.2S$ , respectively. Models R4 and R7 are the same in formulation, and so are Models R5 and R6.

Using the parameters of Table 5.2(a-1), direct runoff was computed, and the resulting model efficiencies are shown with superscript 'b' in these tables. It is seen that the simplest Model R1 and the most complicated Model R7 exhibited efficiencies of 7.50 and -6.24%, respectively, in the Nagwa application, indicating poor model performance in runoff computation. The efficiencies on all other watersheds were also quite low, except for the Cincinnati watershed on which these ranged from 81.36 to 92.05%, showing satisfactory model performance. The reason for low efficiencies in the computation of runoff for all other watersheds, except the Cincinnati, is the underestimation of their CN-values by the sediment yield model due to the sediment deposition. Therefore, it is necessary to transform the S-values of Table 5.2(a-1) to those corresponding to rainfall-runoff data using Eq. 5.30. To this end, it is appropriate to first evaluate the models for adoption for field use utilizing the Nagwa results (Table 5.2a).

The efficiencies varying from 91.78 to 92.16% for Models S2 - S7 suggest that any of these models is suitable. Since Model R2 (the existing SCS-CN method) shows the highest efficiency, though quite low (= 13.55%), among the runoff models, it is appropriate to consider it for further evaluation, also for the reason of its simplicity and possible use of NEH-4 tables in the sediment yield computation. Such an inference can also be generally derived from the results of other watersheds.

The S values derived from the application of Model S2 (Table 5.2(a-1)) were transformed using Eq. 5.30 to correspond to the P-Q data. The transformed S-values (Table 5.3) were then used to compute runoff from each watershed using Model R2. The resulting efficiencies (Table 5.3) in runoff computation showed a significant improvement from 13.55 to 91.75% for the Nagwa watershed, from 45.62 to 71.63% for Karso, from 1.76 to 90.23% for Banha, from 58.78 to 80.08% for Mansara, from -26.10 to 79.42% for W2, from 36.26 to 82.18% for W6, from 15.97 to 90.59% for W7, from -8.67 to 71.26% for W14, from -80.28 to 74.10% for 182, from -102.95 to 70.90% for 129, and from -69.26 to 81.22% for 123. Except for the Cincinnati watershed where the efficiency decreased, however marginally (from 87.33 to 85.95%), for all other watersheds there was significant improvement. These efficiencies, indicating satisfactory model performance on all the watersheds, support the rationale of the S-transformation for runoff computation. The results of the sediment yield computations using Model S2 (Table 5.2(a-1)) and runoff computations using Model R2 (Table 5.3) are depicted in Figs. 5.4 through 5.15 for all the twelve watersheds. The closeness of data points to the line of perfect fit indicates a satisfactory model performance (Figs. 5.4-5.15).

Table 5.3: Runoff computation using transformed S-values and Model R2

Sl. No.	Name of watershed	Transformed S values (mm) (corresponding to S values of Model S2)	Efficiency of runoff computation (%)
1.	Nagwa	86.46	91.75
2.	Karso	30.33	71.63
3.	Banha	23.21	90.23
4.	Mansara	128.55	80.08
5.	W2 Treynor	27.77	79.42
6.	W6 GC	31.37	82.18
7.	W7 GC	62.95	90.59
8.	W14 GC	45.69	71.26
9.	Cincinnati	8.32	85.95
10.	182	77.34	74.10
11.	129	64.36	70.90
12.	123	73.98	81.22

#### 5.4.2 Determination of the A/S Ratio

It is also appropriate to investigate the estimated values of A/S ratio (Table 5.2(a-l)), which, according to Eq. 5.10, should be a constant value for a watershed. Apparently, Models S2-S7 yield the A/S ratio in the range of (0.120-0.123)  $\text{KN ha}^{-1} \text{mm}^{-1}$  for Nagwa, (0.147-0.155) for Karso, (0.126-0.147) for Banha, (0.054-0.055) for Mansara, (7.013-7.391) for W2, (0.188-0.198) for W6, (0.304-0.316) for W7, (0.235-0.254) for W14, (0.040-0.042) for Cincinnati, (0.224-0.230) for 182, (0.038-0.039) for 129, and (0.368-0.377) for 123 watershed. It can be observed that these values vary in a very narrow range and therefore a constant value can be assumed for Model S2 as 0.123, 0.155, 0.144, 0.055, 7.391, 0.198, 0.316, 0.254, 0.041, 0.230, 0.039, and 0.370  $\text{KN ha}^{-1} \text{mm}^{-1}$  for the respective watersheds. Such determination of A/S ratio for various watersheds is useful for estimation of sediment yield using NEH-4 tables as follows:

- (a) Determine the AMC II CN value for a watershed from the NEH-4 tables.
- (b) Based on the antecedent 5-day rainfall, determine the AMC for the storm event.
- (c) Convert the AMC II CN value to the identified AMC using the NEH-4 table. Also Compute S using Eq. 2.6.
- (d) Transform the above computed S to obtain S-value relevant for the sediment yield model using Eq. 5.30.
- (e) Multiply the S-value of step (d) with the available A/S ratio to obtain A in  $\text{KN ha}^{-1}$ .

Such a procedure may help determine the sediment yield of ungauged watersheds using the concept of homogeneous watersheds (Singh et al., 2001). Furthermore, it may also help revise the empirically derived components of USLE using the SCS-CN method.

## 5.5 SUMMARY

Coupling the SCN-CN method with the USLE, a new model is proposed for the estimation of the rainstorm-generated sediment yield from a watershed. The coupling is based on three hypotheses: (1) the runoff coefficient is equal to the degree of saturation, (2) the USLE parameters can be expressed in terms of potential maximum retention, and (3) the sediment delivery ratio is equal to the runoff coefficient. The proposed sediment yield model is applied to a large set of rainfall-runoff-sediment yield data obtained from twelve watersheds of different land uses (urban, agricultural, and forest) and varying in size, climatic, physiographic and soil characteristics. For all watersheds the computed sediment yield is found to be in good agreement with the observed values. The results and analysis of model application show that the model has considerable potential for use in field.



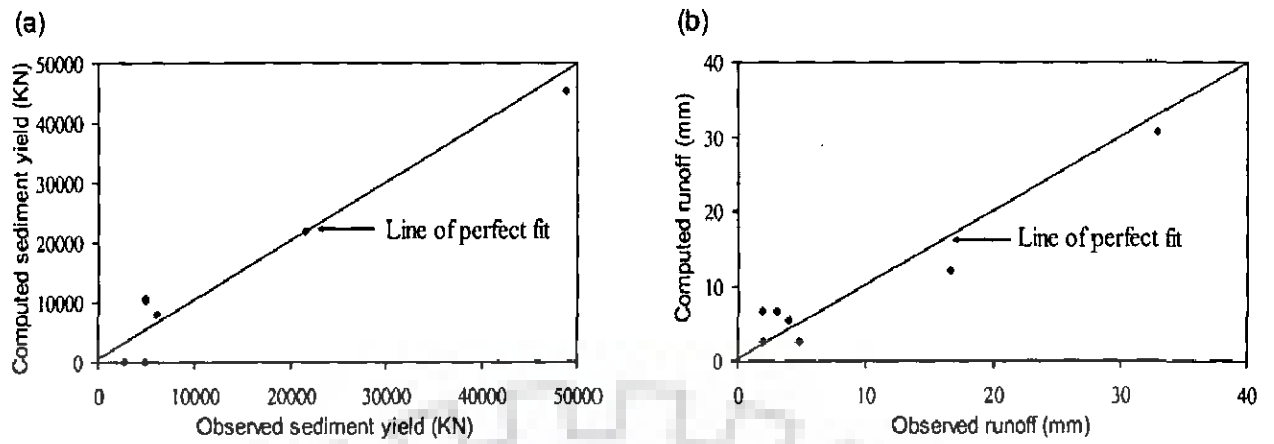


Fig. 5.4: Comparison of observed and computed (a) sediment yield (b) runoff using models S2 and R2, for Nagwa watershed

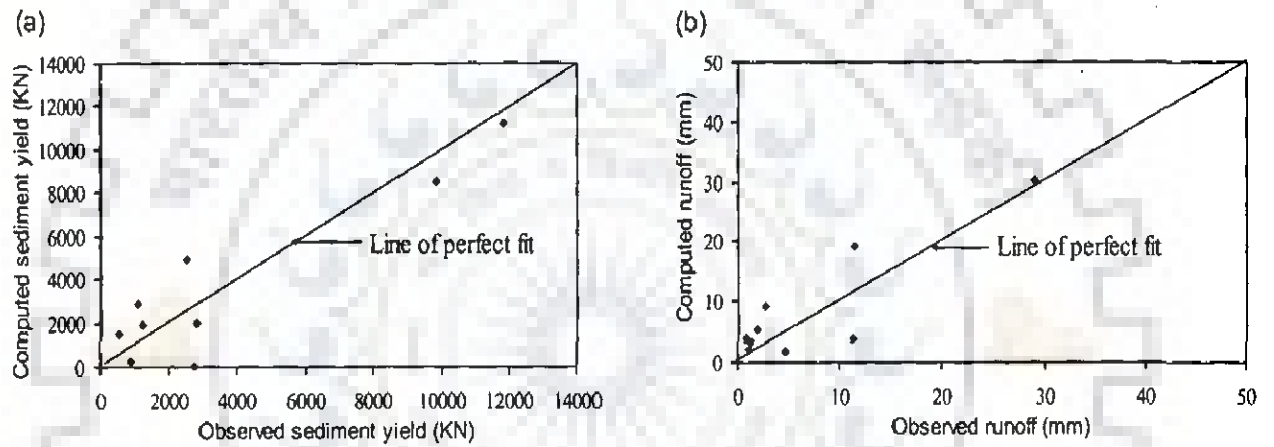


Fig. 5.5: Comparison of observed and computed (a) sediment yield (b) runoff using models S2 and R2, for Karso watershed

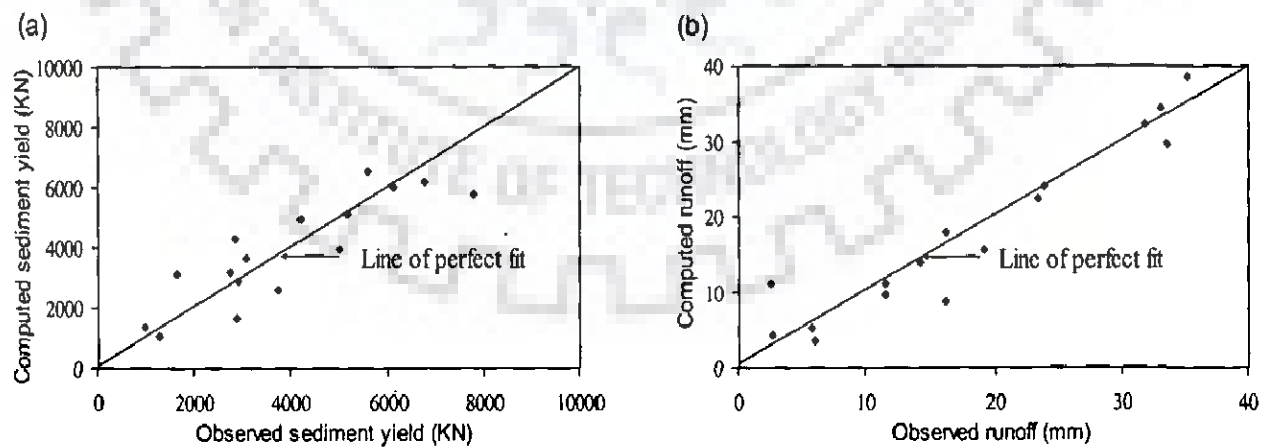


Fig. 5.6: Comparison of observed and computed (a) sediment yield (b) runoff using models S2 and R2, for Banha watershed

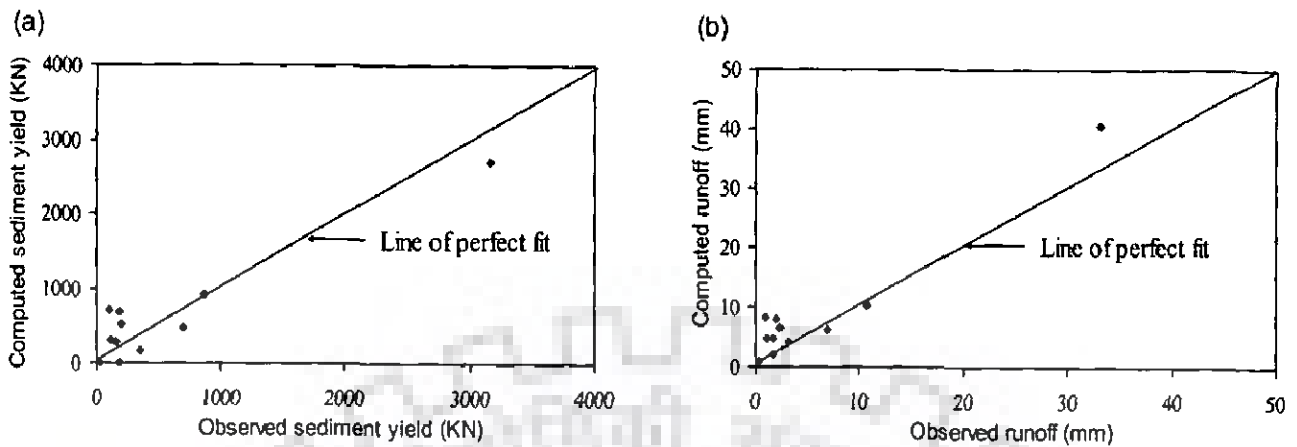


Fig. 5.7: Comparison of observed and computed (a) sediment yield (b) runoff using models S2 and R2, for Mansara watershed

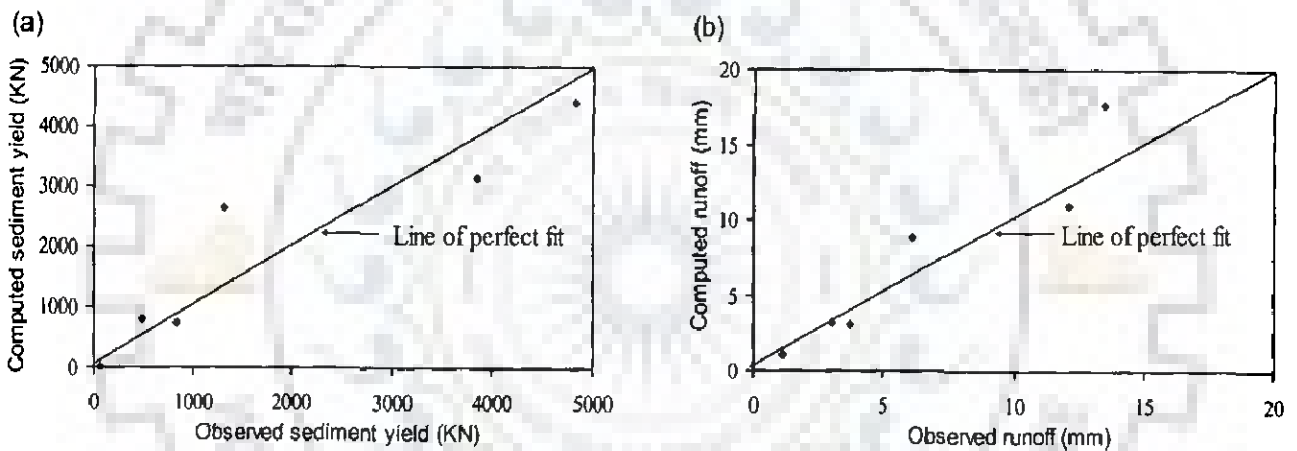


Fig. 5.8: Comparison of observed and computed (a) sediment yield (b) runoff using models S2 and R2, for W2 watershed

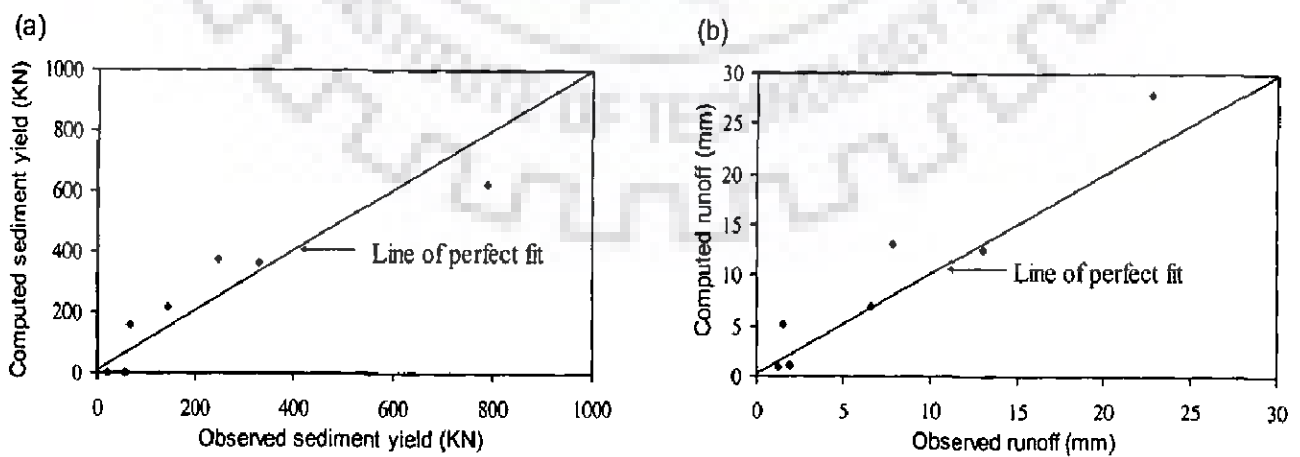


Fig. 5.9: Comparison of observed and computed (a) sediment yield (b) runoff using models S2 and R2, for W6 GC watershed

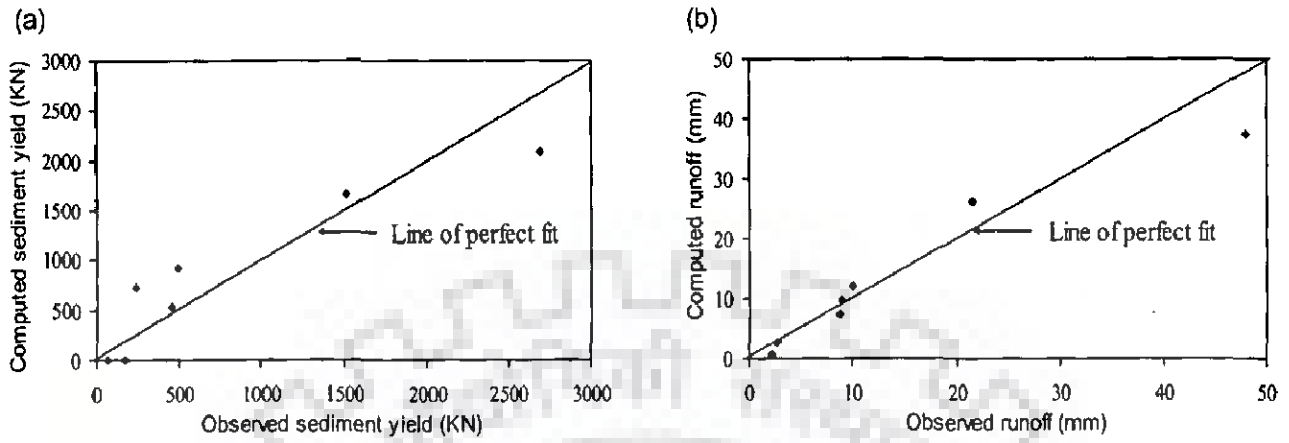


Fig. 5.10: Comparison of observed and computed (a) sediment yield (b) runoff using models S2 and R2, for W7 GC watershed

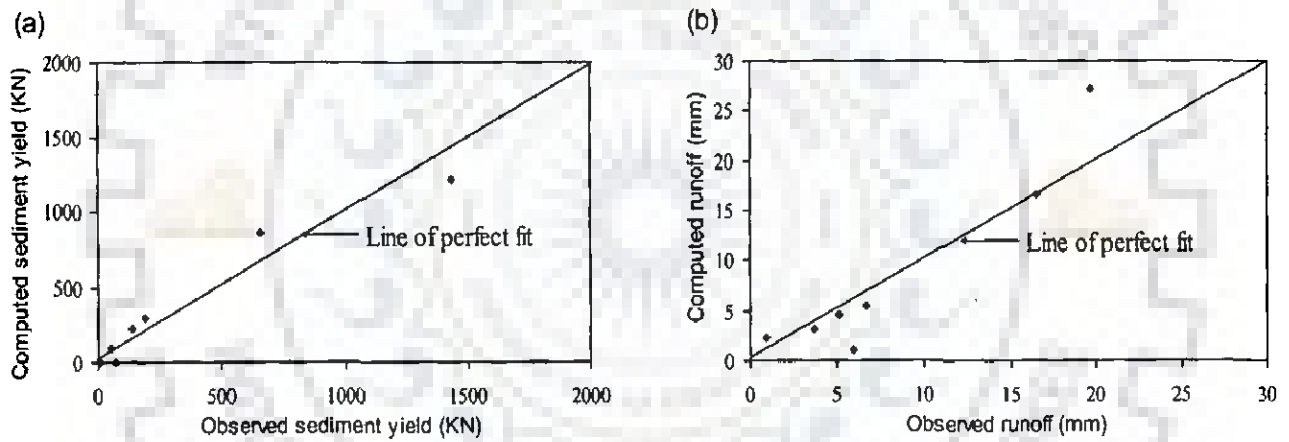


Fig. 5.11: Comparison of observed and computed (a) sediment yield (b) runoff using models S2 and R2, for W14 GC watershed

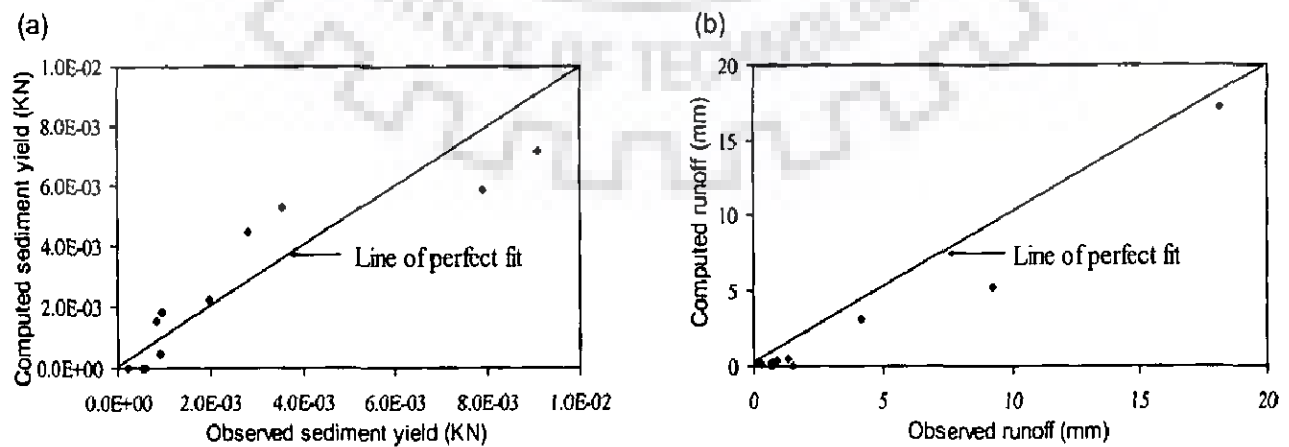


Fig. 5.12: Comparison of observed and computed (a) sediment yield (b) runoff using models S2 and R2, for Cincinnati watershed

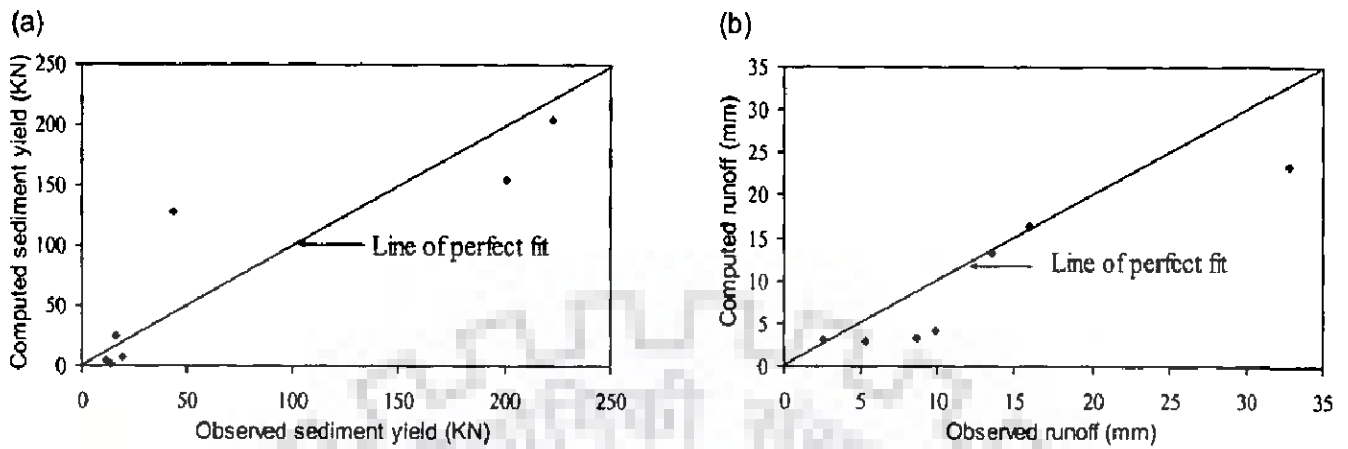


Fig. 5.13: Comparison of observed and computed (a) sediment yield (b) runoff using models S2 and R2, for 182 watershed

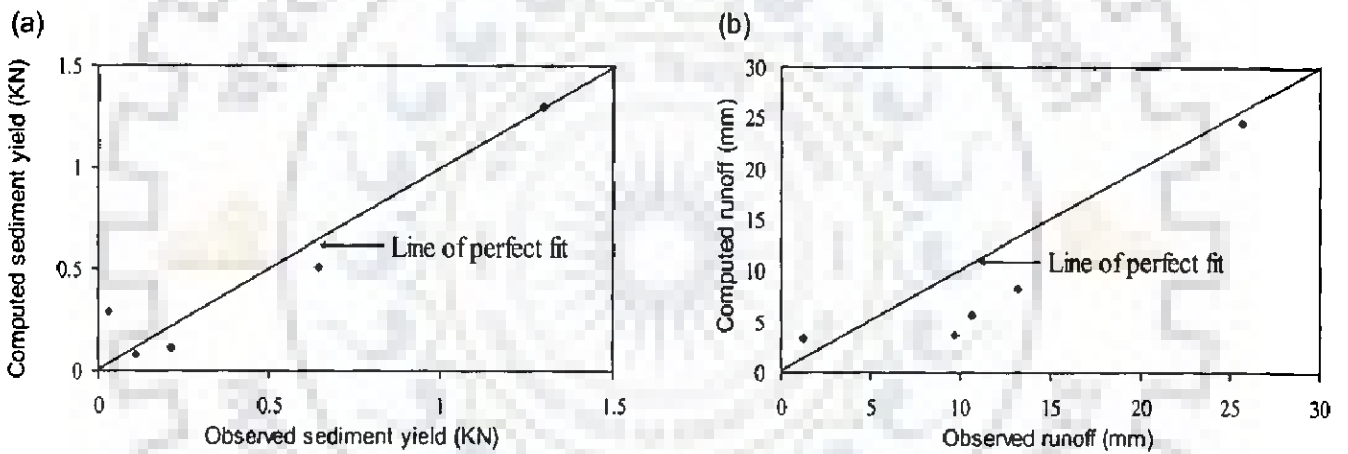


Fig. 5.14: Comparison of observed and computed (a) sediment yield (b) runoff using models S2 and R2, for 129 watershed

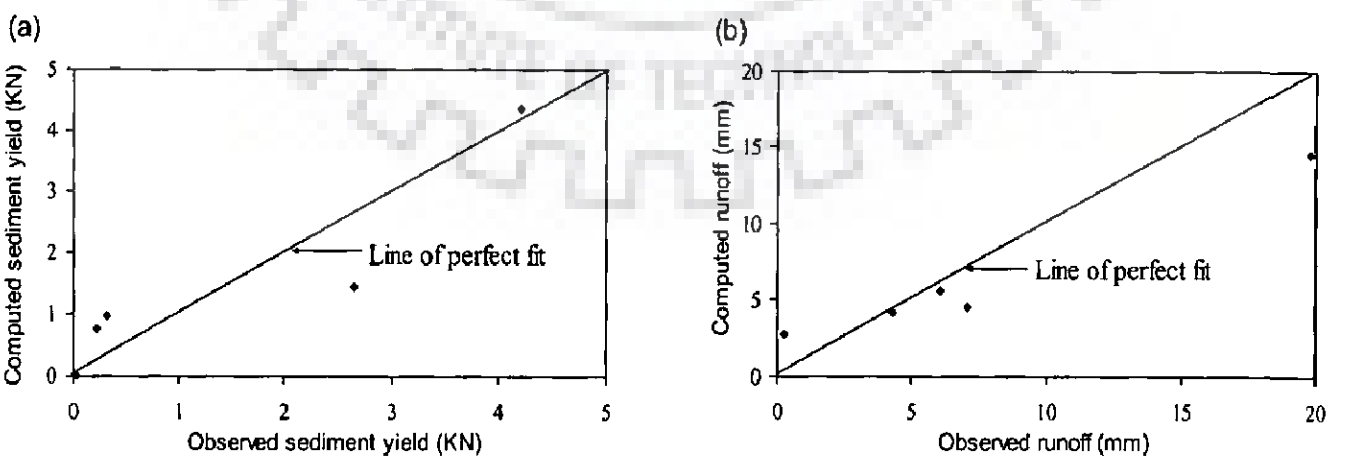


Fig. 5.15: Comparison of observed and computed (a) sediment yield (b) runoff using models S2 and R2, for 123 watershed

## CHAPTER 6

### SCS-CN BASED TIME-DISTRIBUTED SEDIMENT YIELD MODEL

---

#### 6.1 INTRODUCTION

Estimates of temporal variation of sediment yield are used to address a wide range of water quality and pollution problems through a variety of engineering, natural resource conservation planning, and land management methods. The process of sediment yield is extremely complex and mainly consists of detachment and transport of sediment particles by raindrops and runoff. The sediment particles, during their transport by overland flow, continuously fall due to gravity and are uplifted by the turbulence of flow, depending on the transport capacity of the flow which is largely governed by the rate of surface flow. Review of literature reveals that both empirical and physically based approaches are employed to estimate the rate of surface runoff and the associated sediment yield. The complex physically based models are expected to provide reliable estimates of the sediment yield. However, these models require the coordinated use of various sub-models related to meteorology, hydrology, hydraulics, and soil erosion. As such, the large input parameter requirement and uncertainty in estimation of these parameters limit the practical applications of physically based models to those areas which have little or no data.

In the present study, an SCS-CN based simple sediment yield model is proposed for computing the temporal rates of sediment discharge from a rainfall event on natural watersheds to suit the data availability in developing countries like India. The model is assessed for its field applicability using rainfall-runoff-sediment yield data from a variety of watersheds located in India and USA.

## 6.2 MODEL DEVELOPMENT

Development of an event based time-distributed sediment yield model is based on (i) the relationship of Universal Soil Loss Equation (USLE) with the potential maximum retention parameter of the SCS-CN method; (ii) SCS-CN based infiltration model; (iii) coupling of rainfall-excess rate with upland erosion for computation of sediment-excess rate; and (iv) routing of the sediment-excess rate for computation of sediment yield rate or event sedimentograph.

### 6.2.1 Relationship of USLE with S

Using the volumetric concept, an analytical relation between the USLE and the potential retention parameter of SCS-CN method was developed in Chapter 5. The relationship is expressed by the Eq. 5.10 as:

$$\frac{A}{S} = \frac{(1-n)}{n} \rho_s \quad (5.10)$$

It shows that for a watershed the ratio of actual potential maximum erosion (A) to actual potential maximum retention (S) (= A/S ratio) is a constant value that depends on soil porosity and density of solids, which are normally constant for a watershed under a given land use and tillage practices.

### 6.2.2 Derivation of Infiltration Model and Computation of Rainfall-Excess Rate

Before the derivation of the SCS-CN based infiltration model, it is in order to first derive the Mockus method (Mockus, 1949) from the Horton model using the proportionality concept (Eq. 2.2) of the SCS-CN method. The Horton infiltration model (Horton, 1938) is expressed as:

$$f = f_c + (f_0 - f_c)e^{-kt} \quad (6.1)$$

where  $f$  is the infiltration rate ( $LT^{-1}$ ) at time  $t$ ,  $f_0$  is the value of  $f$  at  $t = 0$ ,  $k$  is infiltration decay constant, and  $f_c$  is final infiltration rate. Eq. 6.1 is valid for the time,  $t$ , past ponding. Integration of Eq. 6.1 leads to the cumulative infiltration,  $F$ , at time  $t$ , as:

$$F - F_c = \frac{f_o - f_c}{k} (1 - e^{-kt}) \quad (6.2)$$

where  $F_c (=f_c t)$  is the steady portion of infiltration, and  $(F - F_c)$  represents the dynamic portion of infiltration,  $F_d$ . Thus, as  $t \rightarrow \infty$ ,  $F_d \rightarrow (f_o - f_c)/k$ . From Eq. 2.2, as  $Q \rightarrow (P - I_a)$ ,  $F_d \rightarrow S_d$ , which is valid for time  $t$  approaching infinity. Therefore,

$$S_d = \frac{f_o - f_c}{k} \quad (6.3)$$

where  $S_d$  is the potential maximum storage space available for dynamic portion of infiltration,  $F_d$ . It follows that  $S = S_d + S_c$ , where  $S_c$  is the potential maximum storage space available for steady portion of infiltration. It is common experience that  $f_o = i$ , where  $i$  is the uniform rainfall intensity ( $L T^{-1}$ ) at time  $t$  (time past ponding) = 0. Its substitution into Eq. 6.3 yields:

$$f_o - f_c = i - f_c = i_e = kS_d \quad (6.4)$$

where  $i_e$  is effective uniform rainfall intensity. Eq. 6.4 defines the Horton parameter  $k$  equal to the ratio of  $i_e$  to  $S_d$ . It implies that  $k$  increases as  $i_e$  increases and decreases as  $S$  increases or CN decreases, and vice versa. Thus  $k$  depends on the magnitude of the rainfall intensity and soil type, land use, hydrologic condition, antecedent moisture condition that affect  $S$  and it is consistent with the description of Mein and Larson (1971). Further substitution of Eq. 6.3 into Eq. 6.2 and the resulting expression into Eq. 2.2 (for  $I_a = 0$ ) yields:

$$\frac{Q}{P} = (1 - e^{-kt}) \quad (6.5)$$

Assuming that the effective rainfall,  $P_e (= P - F_c)$  grows linearly with time  $t$ , which is a valid and reasonable assumption for infiltration rates derived from field/laboratory tests, it follows that:

$$P_e = i_e t \quad (6.6)$$

Eq. 6.6 asserts the general notion that  $P$  grows unbounded (Ponce and Hawkins, 1996).

Substitution of Eq. 6.4 into Eq. 6.6 yields:

$$\frac{P_e}{S_d} = kt \quad (6.7)$$

With the assumption that P in Eq. 6.5 also excludes  $F_c$  (or  $f_c=0$ ), it follows from Eq. 6.5 that:

$$\frac{Q}{P_e} = (1 - e^{-P_e/S_d}) \quad (6.8)$$

which, for  $I_a = 0$ , is an equivalent form of the Mockus equation:

$$Q = P_e [1 - 10^{-bP_e}] \quad (6.9)$$

in which  $b = 1/[S_d \ln(10)]$ . Allowing for  $I_a$ , the effective rainfall,  $P_e$  in Eq. 6.9 can be taken as  $(P - I_a - F_c)$ . It is evident from the above derivation that both the SCS-CN and Mockus methods exclude the static portion of infiltration,  $f_c$ , and thus, underestimate infiltration.

Eqs. 6.4 through 6.7 permit derivation of the time distribution of infiltration rate from the SCS-CN method. To that end, Eqs. 2.1 and 2.2 are combined to recast the SCS-CN equation for  $F_d$  as below.

$$F_d = \frac{P_e S_d}{P_e + S_d} \quad (6.10)$$

which holds for  $I_a = 0$ . Coupling of Eq. 6.7 with Eq. 6.10 leads to:

$$F_d = \frac{kS_d t}{(1 + kt)} \quad (6.11)$$

Differentiation of Eq. 6.11 with respect to  $t$  yields dynamic rate of infiltration,  $f_d$ :

$$f_d = \frac{kS_d}{(1 + kt)^2} \quad (6.12)$$

Adding non-zero  $f_c$  term on both sides of Eq. 6.12 and coupling it with Eq. 6.4 leads to:

$$f = f_c + \frac{(i - f_c)}{(1 + kt)^2} \quad (6.13)$$



where  $f$  is the total infiltration rate (or infiltration capacity). For time to ponding,  $t_p = 0$ , Eq. 6.13 represents the infiltration loss equation proposed by Mishra (1998) and Mishra and Singh (2002b). Eq. 6.13 can be further developed to incorporate rainfall,  $P$ , and watershed characteristics through  $S$ . To this end, Eq. 6.13 can, alternatively, be expressed as:

$$f = f_c + \frac{(i - f_c)S^2}{[S + kSt]^2} \quad (6.14)$$

From Eqs. 6.4 and 6.6, expression  $[(i - f_c)t = kS_d t]$  represents  $(P - F_c)$ . Further, consideration of  $[kSt = k(S_d + S_c)t]$  and  $(kS_c t = F_c)$  makes  $kSt = P$ . Therefore, Eq. 6.14 is rewritten as:

$$f = f_c + \frac{(i - f_c)S^2}{(S + P)^2} \quad (6.15)$$

Here, the quantity  $(i - f_c)S^2$  is constant for a given uniform rainfall intensity and, therefore,  $f$  decays as rainfall ( $P$ ) grows (Eq. 6.15). Incorporating initial abstraction,  $I_a (= \lambda S)$ , which represents the portion of infiltration abstracted before time to ponding,  $t_p$ , besides other field losses (Ponce and Hawkins, 1996; Mishra and Singh, 2002b), Eq. 6.15 leads to:

$$f = f_c + \frac{(i - f_c)S^2}{(P + S - \lambda S)^2} \quad (6.16)$$

which is applicable for  $P > \lambda S$ . Eq. 6.16 forms the expression for computation of infiltration rate,  $f$  ( $L T^{-1}$ ), at time  $t$  from the natural rainfall events on a watershed. It is noted that in Eq. 6.16, the term  $P$  is the cumulative rainfall up to time  $t$ . During any time interval with rainfall intensity,  $i \leq f_c$ , both  $f_c$  and  $f$  equal  $i$ .

The rainfall-excess rate ( $q$ ) ( $L T^{-1}$ ) (or the direct surface runoff rate) at any time  $t$  can be computed by subtracting the infiltration rate ( $f$ ) (Eq. 6.16) from the rainfall intensity ( $i$ ). The resulting rainfall-excess rate ( $q$ ) can be expressed as:

$$q = i - \left[ f_c + \frac{(i - f_c)S^2}{(P + S - \lambda S)^2} \right] = (i - f_c) \left[ 1 - \frac{S^2}{(P + S - \lambda S)^2} \right] \quad (6.17)$$

which is valid for  $P > \lambda S$ ,  $q = 0$  otherwise.

### 6.2.3 Coupling of Rainfall-Excess Rate with Upland Erosion

The sediment-excess rate can be computed by coupling the rainfall-excess rate ( $q$ ) (Eq. 6.17) with the potential maximum erosion using the proportionality concept of SCS-CN method as follows:

$$\frac{y_t}{A} = \frac{q_t}{P_{\Delta t}} \quad (6.18)$$

where  $y_t$  = sediment-excess rate ( $M T^{-1}$ ) at time  $t$  during any time interval  $\Delta t$ ;  $q_t$  = rainfall-excess rate ( $L T^{-1}$ ) at time  $t$ ;  $A$  = actual potential maximum erosion ( $M$ ) of the watershed, dependent on soil properties and the actual potential maximum retention,  $S$  (Eq. 5.10); and  $P_{\Delta t}$  = rainfall amount ( $L$ ) during the time interval  $\Delta t$ . Alternatively, Eq. 6.18 can be expressed as:

$$\frac{y_t}{q_t} = \frac{A}{P_{\Delta t}} \quad (6.19)$$

Eq. 6.19 describes that during any time interval  $\Delta t$ , the ratio of actual erosion rate (sediment yield rate) to actual runoff rate equals the ratio of actual potential maximum erosion to actual potential maximum runoff. Combining with Eq. 6.17, Eq. 6.19 can be rearranged for  $y_t$  as:

$$y_t = \frac{Aq_t}{P_{\Delta t}} = \frac{A}{P_{\Delta t}} \left[ 1 - \frac{S^2}{(P + S - \lambda S)^2} \right] (i - f_c) \quad (6.20)$$

Eq. 6.20 enables determination of sediment-excess rate from watershed characteristics and temporal distribution of rainfall. It also shows that as the rate of runoff increases, the rate of sediment yield also increases and vice versa. In the present study, the value of  $\lambda$  is taken as 0.2, a standard value.

#### 6.2.4 Routing of Sediment-Excess Rate

To compute sedimentograph at the watershed outlet, the sediment-excess rate (Eq. 6.20) is routed using a simple single linear reservoir technique. In discrete form, the continuity equation and the storage equation of single linear reservoir can be expressed, respectively, as:

$$I - O = \Delta V / \Delta t \quad (6.21)$$

and

$$V = K O \quad (6.22)$$

In application of these equations to sediment flow,  $V$  denotes the storage of sediment reservoir;  $K$  is the sediment storage coefficient (different from infiltration decay constant,  $k$  in Eq. 6.1);  $\Delta t$  is the time interval;  $I$  is the sediment inflow rate (or sediment-excess rate,  $y_t$  in Eq. 6.20), and;  $O$  is the sediment outflow rate (or sediment yield rate) at the outlet of the watershed. Using finite difference scheme,  $O$  at different time steps can be computed as follows:

$$O_{(t+1)} = c_o I_t + c_1 I_t + c_2 O_t \quad (6.23)$$

where  $t$  and  $t+1$  are the time steps at  $\Delta t$  interval and,

$$c_o = \frac{\Delta t / K}{2 + \Delta t / K} \quad \text{and,} \quad c_o = c_1 \quad (6.24)$$

$$c_2 = \frac{2 - \Delta t / K}{2 + \Delta t / K} \quad (6.25)$$

To avoid the problem of negative sediment outflows,  $K \geq \Delta t / 2$ .

### 6.3 HYDROLOGICAL DATA FOR MODEL APPLICATION

The proposed SCS-CN based time-distributed sediment yield model is tested on temporal rainfall-runoff-sediment yield data of 49 rainfall events from seven watersheds. These included Karso, Banha, and Mansara watersheds in India; and W2 Treynor, W6 GC, W7 GC, and W14 GC watersheds in USA (Table 4.1 and Figs. 4.1 through 4.12).

## 6.4 RESULTS AND DISCUSSION

The available events for each watershed were randomly divided into two sets: one set consisting of 28 events was used for model calibration and the other set of 21 events for model validation.

### 6.4.1 Model Calibration

With  $\lambda = 0.2$ , the proposed sediment yield model has four parameters, viz., potential maximum erosion (A), potential maximum retention (S), steady state infiltration rate ( $f_c$ ), and storage coefficient (K). The value of parameter S can be estimated from watershed characteristics and the AMC of rainfall events using NEH-4 tables (SCS-1956). However, this value of S is applicable for runoff and its applicability to sediment discharge, as discussed later, is yet to be examined. Since soil properties vary spatially, a representative value of parameter A for the watershed needs to be determined through calibration. The observed hydrograph and the knowledge of soil types may provide an idea of the estimates of K and  $f_c$  values. In the present study, all four parameters of the model were optimized during calibration using the non-linear Marquardt algorithm of least squares procedure of the statistical analysis system (SAS, 1988). The Nash and Sutcliffe (1970) efficiency criterion was used for evaluating the model performance in simulating the sediment yield. The criterion can be expressed as:

$$\text{Efficiency} = \left( 1 - \frac{\sum_{j=1}^N (O_o - O_c)_j^2}{\sum_{j=1}^N (O_o - O_{\text{mean}})_j^2} \right) \times 100 \quad (6.26)$$

where N is the number of ordinates in an event, j is an integer varying from 1 to N,  $O_o$  and  $O_c$  are the observed and computed rates of sediment yield at the  $j^{\text{th}}$  ordinate, and  $O_{\text{mean}}$  is the mean rate of observed sediment yield. The efficiency varies on the scale 0-100. Higher the model

efficiency, the better will be the agreement between the computed and observed sediment yield, and vice versa.

The model parameters, optimized using calibration data sets, are presented in Table 6.1. It can be observed from the table that for various calibration events the value of parameter A varied from 2572.25 to 15129.63 KN for Karso; 4371.83 to 10072.50 KN for Banha; 3858.20 to 8213.97 KN for Mansara; 9710.05 to 15298.89 KN for W2 Treynor; 207.68 to 492.43 KN for W6 GC; and 290.08 to 785.0 KN for W14 GC watershed. Apparently, the minimum and maximum values of A exhibit a consistent correspondence with those of S which are, respectively, 15.75 and 61.04 mm for Karso watershed; 18.62 and 70.21 mm for Banha; 147.60 and 253.63 mm for Mansara; 43.53 and 61.31 mm for W2 Treynor; 33.41 and 62.20 mm for W6 GC; and 28.41 and 69.23 mm for W14 GC watershed. This shows the dependence of the actual potential maximum erosion, A on the actual potential maximum retention, S (Eq. 5.10), and supports the validity of the model derivation. However, the W7 GC watershed is an exception, i.e. the minimum (356.50 KN) and maximum (798.84 KN) values of A do not match with their counterpart values of S (60.45 and 87.16 mm, respectively). It is worth noting here that the land use of W7 GC watershed consists of an exceptionally high area, i.e., about half of the watershed area (49 %) under grass (pasture) cover. The values of storage coefficient, K, and the steady infiltration rate,  $f_c$ , were found to vary, respectively, in the range of (0.89 - 5.93 h) and (2.88 - 6.69 mm h<sup>-1</sup>) for Karso; (0.43 - 1.17 h) and (2.95 - 10.94 mm h<sup>-1</sup>) for Banha; (0.64 - 2.82 h) and (3.59 - 24.72 mm h<sup>-1</sup>) for Mansara; (0.15 - 0.20 h) and (10.10 - 27.91 mm h<sup>-1</sup>) for W2 Treynor; (0.38 - 1.45 h) and (7.62 - 17.50 mm h<sup>-1</sup>) for W6 GC; (0.55 - 0.79 h) and (0.85 - 8.62 mm h<sup>-1</sup>) for W7 GC; and (0.29 - 1.57 h) and (6.07 - 27.66 mm h<sup>-1</sup>) for W14 GC watershed. A close investigation of data showed that the high values of  $f_c$  generally correspond to storm events of high rainfall intensity.

Table 6.1: Optimized values of parameters of sediment yield model for calibration events

Event	A (KN)	S (mm)	K (h)	$f_c$ (mm h <sup>-1</sup> )	A/S ratio (KN mm <sup>-1</sup> ha <sup>-1</sup> )	Average A/S ratio (KN mm <sup>-1</sup> ha <sup>-1</sup> )
<b>Karso watershed</b>						
28.07.1991	6676.489	23.19	2.91	4.90	0.103	0.081
17.08.1991	2572.247	15.75	5.93	4.94	0.058	
14.06.1994	15129.630	61.04	0.89	2.88	0.089	
04.08.1995	11267.180	54.75	4.09	6.69	0.074	
<b>Banha watershed</b>						
31.08.1993	7143.344	45.19	1.01	2.95	0.090	0.114
05.09.1993	8301.880	31.95	1.17	9.24	0.148	
17.07.1996	10072.500	70.21	0.43	10.94	0.082	
23.08.1996	4371.833	18.62	1.00	3.31	0.134	
<b>Mansara watershed</b>						
23.06.1994	8213.969	253.63	1.07	24.72	0.037	0.037
03.08.1994	4519.071	155.27	0.64	3.59	0.033	
08.08.1994	7794.760	188.47	2.82	5.50	0.048	
10.08.1994	3858.198	147.60	2.67	9.46	0.030	
<b>W2 Treynor watershed</b>						
12.06.1980	9710.047	43.53	0.15	26.49	6.759	7.107
05.09.1980	10855.310	45.38	0.20	27.51	7.249	
30.05.1982	10930.240	48.30	0.19	10.10	6.857	
30.06.1982	15298.890	61.31	0.17	27.91	7.562	
<b>W6 GC watershed</b>						
02.01.1982	317.139	44.56	0.82	7.62	0.057	0.054
15.03.1982	207.679	33.41	1.45	10.09	0.050	
25.05.1982	492.428	62.20	0.46	17.50	0.063	
27.08.1982	297.700	50.26	0.38	11.66	0.047	
<b>W7 GC watershed</b>						
25.05.1982	361.150	73.03	0.64	0.85	0.030	0.039
03.06.1982	798.838	79.35	0.55	8.47	0.061	
11.08.1982	356.495	87.16	0.79	8.62	0.025	
27.08.1982	406.839	60.45	0.60	3.63	0.041	
<b>W14 GC watershed</b>						
08.04.1982	290.086	28.41	1.14	6.63	0.062	0.064
16.06.1982	784.998	69.23	1.57	6.07	0.068	
17.07.1982	449.991	45.97	0.29	27.66	0.059	
12.09.1982	711.008	64.59	0.82	13.60	0.066	

The characteristics of the observed and computed sedimentographs for calibration events are summarized in Table 6.2. For evaluating the model performance in computation of the peak sediment yield rate, time to peak, and the total sediment yield due to a rain storm, relative errors (RE) were computed as:

$$\text{Relative error (RE)} = \frac{Y_c - Y_o}{Y_o} \times 100 \quad (6.27)$$

where  $Y_c$  and  $Y_o$  are the computed and observed quantities, respectively. The overall model performance in the derivation of the sedimentograph is explained by the Nash-Sutcliffe efficiency (Eq. 6.26). From the RE values (Table 6.2), it is seen that the peak rate of sediment yield is overestimated by 26 % (maximum) in Mansara watershed, while on other watersheds, it is generally underestimated (maximum RE = 42 %). The time to peak was found to match well with the observed values in most of the events. Out of 28 calibration events, RE in peak rate and time to peak rate estimation was found within 10 % for 11 and 15 events, respectively; and within 25 % for 22 and 23 events, respectively. The model also satisfactorily conserved the mass of total sediment yield which was computed within 10 % error for 20 events and within 25 % error for all 28 events. The overall efficiency of simulation of sedimentographs varied from 70 to 99 %, with 12 events showing efficiency above 90 %, 23 events showing above 80 %, and 25 events showing the efficiency above 75 %. These efficiencies indicate a more than satisfactory performance of the proposed model in simulation of the temporal variation of sediment yield.

The observed and computed sedimentographs for the calibration events were plotted for visual comparison. These graphs exhibited that the computed and observed rates of sediment yield match satisfactorily in most of the events. As an illustration, Fig. 6.1 depicts some of the typical graphs representing single and multi-peaked events, events simulated with lowest, highest, and average efficiencies, and events of different periods.

Table 6.2: Characteristics of observed and computed sedimentographs for calibration events

Event	Peak rate of sediment yield (KN h <sup>-1</sup> )			Time to peak (min)			Total sediment yield (KN)			Nash-Sutcliffe Efficiency of simulation (%)
	Obs.	Comp.	R.E. (%)	Obs.	Comp.	R.E. (%)	Obs.	Comp.	R.E. (%)	
<b>Karso watershed</b>										
28.07.1991	1076.44	754.74	-29.89	120	110	-8.33	2784.43	2570.65	-7.68	91.79
17.08.1991	650.81	420.56	-35.38	530	450	-15.09	2823.63	2769.99	-1.90	72.53
14.06.1994	761.57	759.00	-0.34	120	120	0.00	1218.52	1139.14	-6.51	99.72
04.08.1995	129.75	126.07	-2.84	210	150	-28.57	504.53	570.42	13.06	82.84
<b>Banha watershed</b>										
31.08.1993	759.05	519.51	-31.56	120	120	0.00	966.37	949.53	-1.74	73.65
05.09.1993	1265.43	1306.45	3.24	300	300	0.00	4184.42	3310.54	-20.88	91.94
17.07.1996	1440.79	1415.16	-1.78	90	90	0.00	1626.45	1523.86	-6.31	99.31
23.08.1996	1337.02	1008.90	-24.54	240	300	25.00	3744.09	2813.33	-24.86	86.02
<b>Mansara watershed</b>										
23.06.1994	52.06	65.43	25.68	180	180	0.00	102.98	103.54	0.54	91.64
03.08.1994	20.35	23.74	16.66	90	120	33.33	29.85	29.20	-2.18	95.15
08.08.1994	24.71	23.87	-3.40	180	150	-16.67	123.23	110.13	-10.63	69.60
10.08.1994	54.96	55.24	0.51	240	210	-12.50	179.84	183.93	2.27	95.16
<b>W2 Treynor watershed</b>										
12.06.1980	9608.49	9542.56	-0.69	30	40	33.33	3840.56	4029.36	4.92	94.67
05.09.1980	272.01	209.16	-23.11	50	50	0.00	73.80	83.37	12.98	86.55
30.05.1982	892.85	884.44	-0.94	110	110	0.00	500.82	415.57	-17.02	84.55
30.06.1982	5129.84	3861.01	-24.73	60	60	0.00	1312.03	1465.91	11.73	84.08
<b>W6 GC watershed</b>										
02.01.1982	160.55	136.37	-15.06	130	110	-15.38	142.25	151.12	6.23	84.64
15.03.1982	13.25	11.65	-12.08	90	50	-44.44	19.79	19.41	-1.95	82.28
25.05.1982	295.49	294.29	-0.41	100	100	0.00	247.95	235.73	-4.93	97.65
27.08.1982	778.97	632.65	-18.78	90	100	11.11	789.52	733.01	-7.16	94.09
<b>W7 GC watershed</b>										
25.05.1982	526.93	471.82	-10.46	80	70	-12.50	449.98	524.30	16.52	89.48
03.06.1982	470.09	484.55	3.08	60	50	-16.67	496.27	483.93	-2.49	98.80
11.08.1982	282.69	178.01	-37.03	180	190	5.56	235.20	213.97	-9.03	86.46
27.08.1982	2324.87	1344.96	-42.15	100	140	40.00	2688.15	2679.46	-0.32	76.69
<b>W14 GC watershed</b>										
08.04.1982	70.63	51.96	-26.43	220	200	-9.09	69.66	75.72	8.69	78.84
16.06.1982	3.14	2.77	-11.78	50	50	0.00	4.68	4.55	-2.74	80.88
17.07.1982	282.40	247.23	-12.45	30	30	0.00	138.65	139.65	0.72	97.09
12.09.1982	45.29	42.95	-5.17	130	120	-7.69	54.99	57.74	5.00	81.14



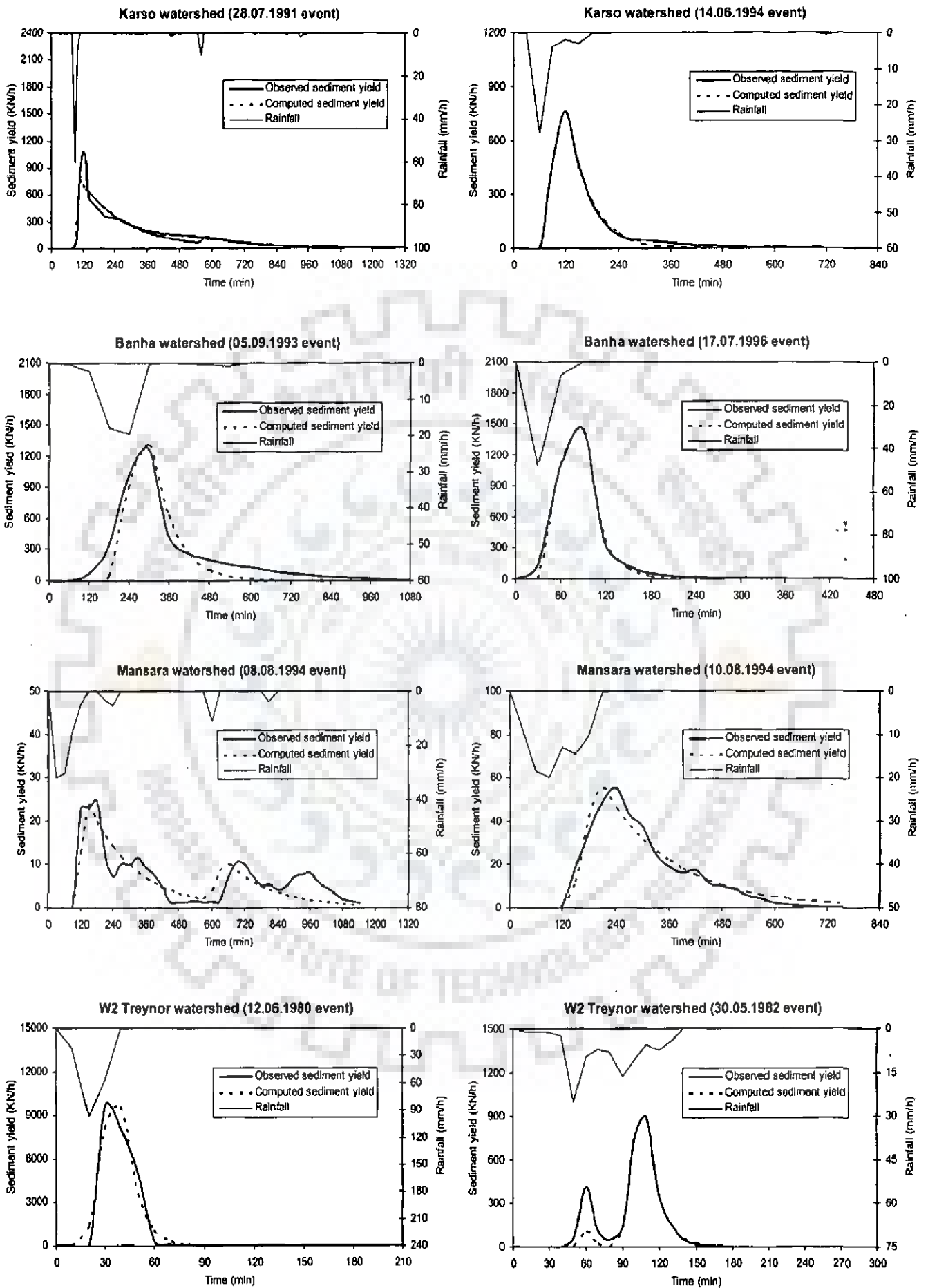


Fig. 6.1: Comparison of observed and computed sedimentographs for the calibration events

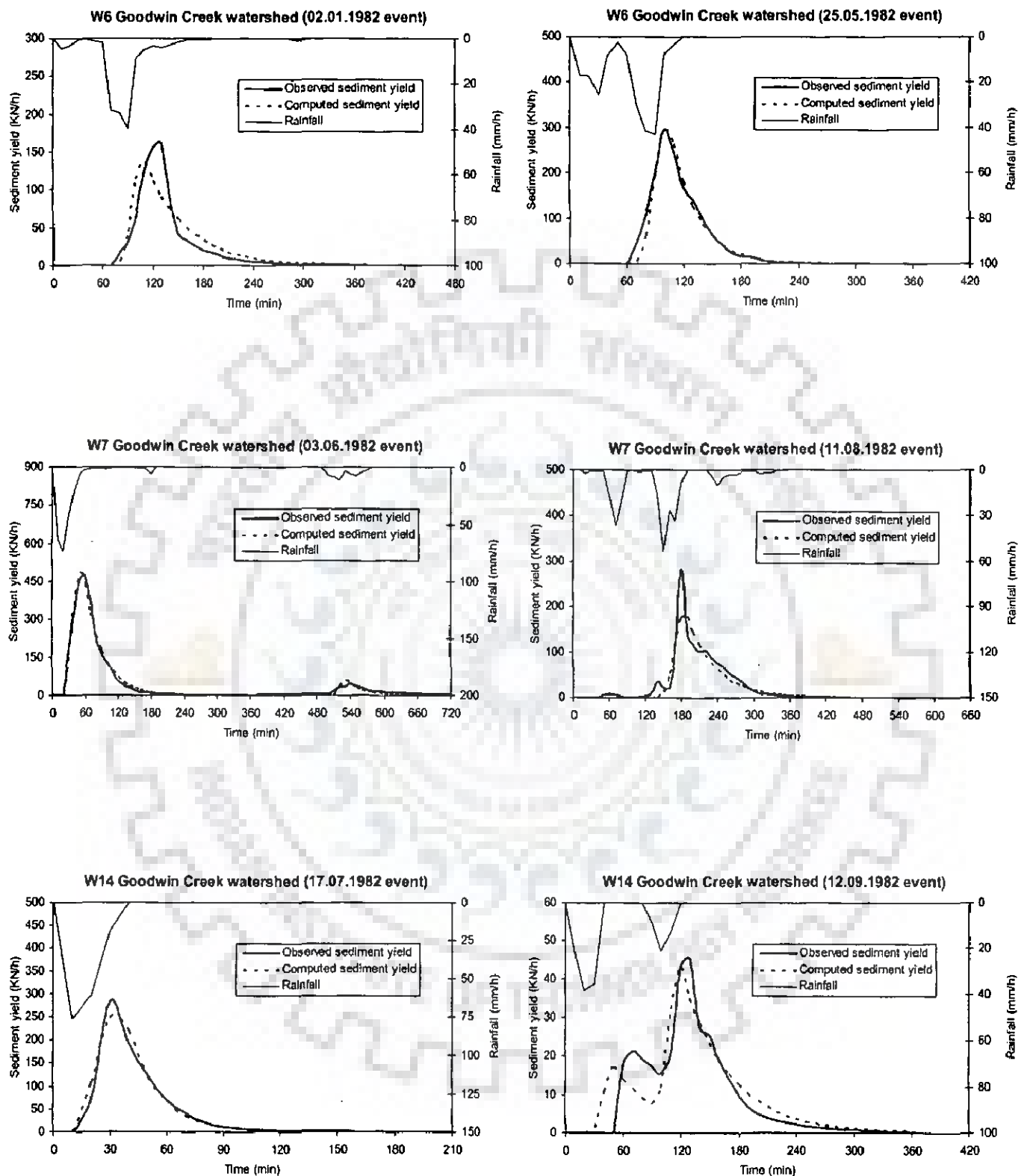


Fig. 6.1: Comparison of observed and computed sedimentographs for the calibration events (contd...)

The S values (Table 6.1) computed from the rainfall-sediment yield model are further examined for their validity and consistency. For each of the calibration events, the computed S values were converted to curve numbers (CN) using Eq. 2.6. The Mansara watershed with lowest CN values (ranging from 50 - 63.25) exhibits the lowest runoff generating potential, which is consistent with the watershed characteristics in terms of its alluvial soils, treatment with mechanical soil and water conservation measures, and subtropical, semi-arid climate. The event CN values for other study watersheds were obtained in the range of (80.62 - 94.16) for Karso, (78.34 - 93.17) for Banha, (80.55 - 85.37) for W2 Treynor, (80.33 - 88.37) for W6 GC, (74.45 - 80.77) for W7 GC, and (78.58 - 89.94) for W14 GC watershed, indicating an average runoff generating potential of these watersheds. For further analysis, the model computed CN values for each watershed were plotted against those derived from the S-values computed using the event rainfall (P) and runoff (Q) data as (Hawkins, 1993):  $S = 5[P + 2Q - \sqrt{Q(4Q + 5P)}]$ . The relations exhibited by these plots (Fig. 6.2) for study watersheds are given as:

$$\text{Karso watershed: } y = 0.6986 x^{1.085} ; R^2 = 0.9952 \quad (6.28)$$

$$\text{Banha watershed: } y = 0.6066 x^{1.1199} ; R^2 = 0.9897 \quad (6.29)$$

$$\text{Mansara watershed: } y = 0.9827 x^{1.0097} ; R^2 = 0.9721 \quad (6.30)$$

$$\text{W2 Treynor watershed: } y = 2.7012 x^{0.7911} ; R^2 = 0.9986 \quad (6.31)$$

$$\text{W6 GC watershed: } y = 1.4966 x^{0.917} ; R^2 = 0.9611 \quad (6.32)$$

$$\text{W7 GC watershed: } y = 0.549 x^{1.1492} ; R^2 = 0.8196 \quad (6.33)$$

$$\text{W14 GC watershed: } y = 1.5339 x^{0.9116} ; R^2 = 0.8322 \quad (6.34)$$

where x is the CN-value corresponding to rainfall-sediment yield model, y is the CN-value derived from the P-Q data (Hawkins, 1993), and  $R^2$  is the coefficient of determination.

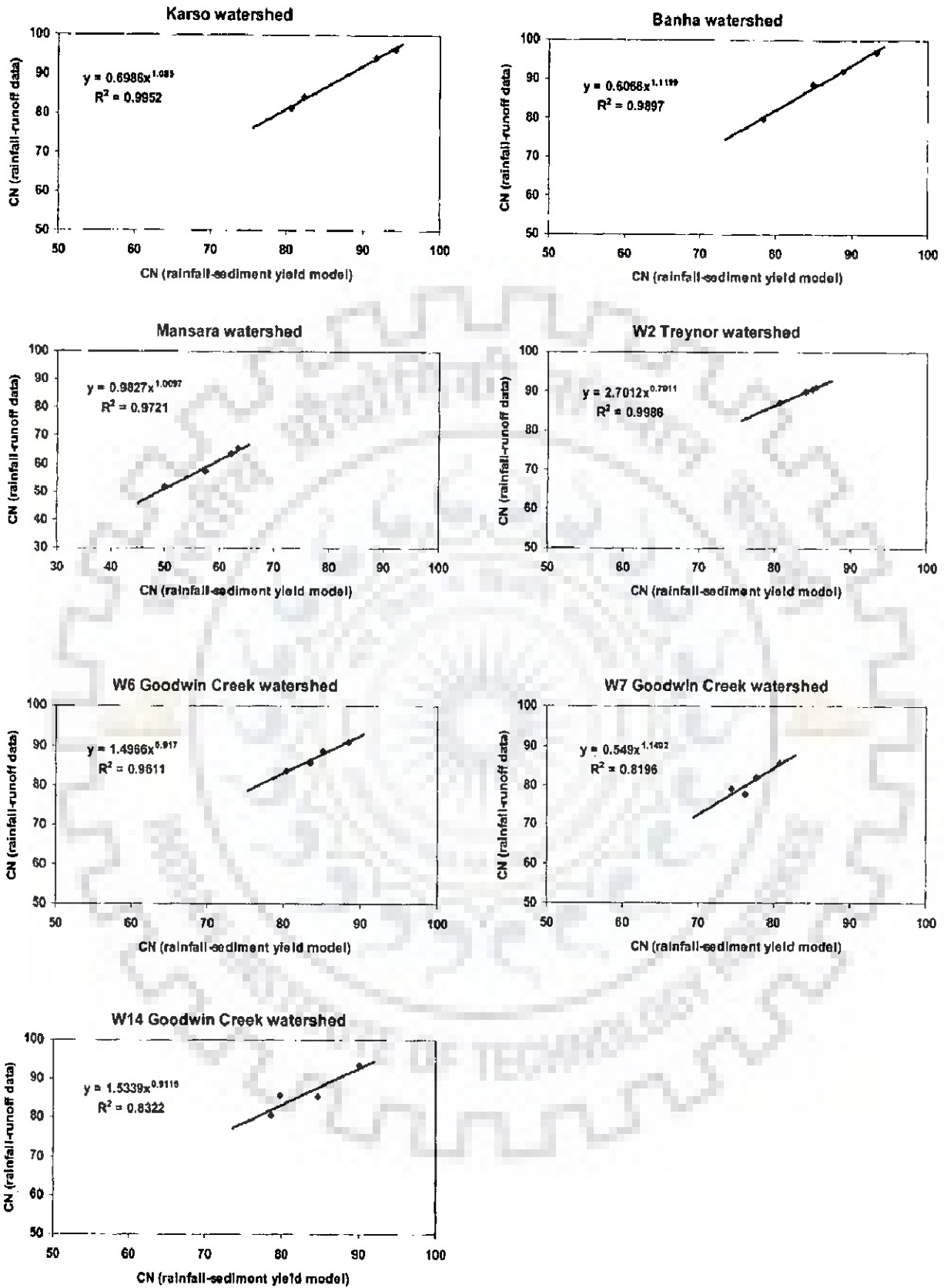


Fig.6.2: Relationship between curve numbers derived from (a) the time-distributed rainfall-sediment yield model and (b) the existing SCS-CN method (using rainfall-runoff data)

The value of  $R^2 > 0.95$  for Karso, Banha, Mansara, W2 Treynor, and W6 GC watersheds indicates an adequate fit of the CN values. Though the plots for W7 GC and W14 GC watersheds show some scattering of data points, still the values of  $R^2$  as 0.82 and 0.83, respectively, for these watersheds indicate a satisfactory fit. It implies that the CN values computed from the sediment yield model are consistent with those derived from P-Q data, and thus, also support the analytical coupling of rainfall-runoff-sediment yield in the model development. It can be further observed from Fig. 6.2 that the CN values are underestimated by the sediment yield model (as in the case of lumped model, Chapter 5), which can be, perhaps, ascribed to the deposition of the sediment particles during their transport by runoff, yielding lesser amount of sediment at the outlet than actually eroded in the watershed. The W7 GC and W14 GC watersheds have respectively 49% and 40% area under grasslands, which acts as a filtering mechanism for sediment, and probably behaves differently with different rainfall amount in allowing the passage of runoff and sediment through its filtering action, and therefore, these watersheds show some scattering in the plots of CN values.

#### 6.4.2 Determination of A/S Ratio

Eq. 5.10 provides that the A/S ratio for a watershed is constant, which is further examined using the calibration results. The A/S ratios computed for individual calibration events on all the study watersheds are presented in Table 6.1. It can be observed that the ratio varied in the range of (0.058 - 0.103  $\text{KN mm}^{-1} \text{ha}^{-1}$ ) for Karso; (0.082 - 0.148  $\text{KN mm}^{-1} \text{ha}^{-1}$ ) for Banha; (0.030 - 0.048  $\text{KN mm}^{-1} \text{ha}^{-1}$ ) for Mansara; (6.759 - 7.562  $\text{KN mm}^{-1} \text{ha}^{-1}$ ) for W2 Treynor; (0.047 - 0.63  $\text{KN mm}^{-1} \text{ha}^{-1}$ ) for W6 GC; (0.025 - 0.061  $\text{KN mm}^{-1} \text{ha}^{-1}$ ) for W7 GC; and (0.059 - 0.068  $\text{KN mm}^{-1} \text{ha}^{-1}$ ) for W14 GC watershed. A small variation in the values of A/S ratio, exhibited by individual events for a watershed, can be largely attributed to the fact that the rainfall events used in the study represent different growing seasons/years. Temporal variations in the root

development of plants and the use of different kinds of tillage implements at different crop stages affect soil porosity (Brakensiek and Rawls, 1988) which, in turn, affects the A/S ratio. The variation of A/S ratios in a small range, however, supports the constancy of this ratio for a watershed. Therefore, a representative value of the A/S ratio (Table 6.1) was determined as the average of A/S-values of individual events for each study watershed, and it was used in model validation.

### 6.4.3 Model Validation

For model validation, the CN values for individual validation events were derived from the watershed CN value for AMC II ( $CN_{II}$ ) and the AMC criterion of 5-day antecedent rainfall. The weighted  $CN_{II}$  values for Mansara, W2 Treynor, W6 GC, W7 GC, and W14 GC watersheds were computed as 77, 86, 85, 83, and 84, respectively. For Karso and Banha watersheds, these values were estimated as 86.5 and 87, respectively, by Rao et al. (2003) using the NEH-4 procedure. The AMC for an individual event was determined by taking a 5-day antecedent rainfall as: less than 12.7 mm for AMC I; above 12.7 but less than 38 mm for AMC II; and above 38 mm for AMC III. The CN values thus computed for individual events were converted to those corresponding to sediment yield model using Eqs. 6.28 to 6.34 for respective watersheds. The converted CN values were then used to compute the S-values for validation events using Eq. 2.6.

Parameter A was computed from the representative A/S ratio for a watershed (Tables 6.1 & 6.3) and the above computed S-values. Parameters K and  $f_c$ , which vary with individual events, were adjusted by trial and error observing their range derived by calibration. The event AMC and the values of parameters A, S, K, and  $f_c$  computed for 21 validation events are presented in Table 6.3. As can be seen from Table 6.3, the validation events represent all three AMCs which demonstrate the applicability of the proposed model for computing sediment yield from a watershed for an applicable range of S values.

Table 6.3: Parameter values of sediment yield model for validation events

Event	Average A/S ratio (KN mm <sup>-1</sup> ha <sup>-1</sup> )	5-day antecedent rain (mm)	A M C	CN for the event (based on CN <sub>II</sub> and AMC)	Model parameters			
					Transformed S-values (corresponding to SY model from CN-CN plot) (mm)	A (KN)	K (h)	f <sub>c</sub> (mm h <sup>-1</sup> )
1	2	3	4	5	6	7=(2x6)	7	8
<b>Karso watershed</b>								
30.08.1993	0.081	2.70	I	73	95.87	21690.271	2.60	1.61
02.09.1993		54.40	III	95	20.45	4628.565	1.03	4.87
14.10.1993		84.70	III	95	20.45	4628.565	1.79	8.23
17.06.1994		34.90	II	87	43.64	9872.361	4.23	6.99
<b>Banha watershed</b>								
14.06.1994	0.114	65.50	III	95	24.60	4898.393	1.55	3.09
20.08.1996		61.90	III	95	24.60	4898.393	4.59	3.10
30.08.1996		25.30	II	87	47.37	9430.021	0.78	5.67
<b>Mansara watershed</b>								
19.07.1994	0.037	10.80	I	59	186.04	5999.087	2.35	19.80
25.07.1994		4.80	I	59	186.04	5999.087	0.94	26.84
16.08.1994		30.10	II	77	84.03	2709.837	1.90	23.90
<b>W2 Treynor</b>								
18.06.1980	7.107	39.10	III	94	31.88	7477.920	0.10	21.42
14.06.1982		14.10	II	86	65.91	15456.640	0.12	25.95
<b>W6 GC watershed</b>								
20.01.1982	0.054	14.20	II	85	56.26	382.224	0.09	14.20
16.06.1982		13.90	II	85	56.26	382.224	0.15	5.30
01.07.1982		57.02	III	94	24.01	163.139	0.69	3.34
<b>W7 GC watershed</b>								
17.10.1981	0.039	3.54	I	67	134.34	867.617	0.41	7.10
30.11.1981		27.36	II	83	68.32	441.233	0.86	3.28
30.06.1982		13.30	II	83	68.32	441.233	0.79	4.79
<b>W14 GC watershed</b>								
17.10.1981	0.064	4.20	I	68	141.33	1496.364	0.09	11.34
11.08.1982		16.50	II	84	59.50	629.890	0.45	15.50
27.08.1982		0.00	I	68	141.33	1496.364	0.19	5.28

It is seen from the computation results of the validation (Table 6.4) that, similar to the calibration results, the model overestimated the peak rate of sediment yield for Mansara watershed, and underestimated for all other watersheds. Out of 21 events, the RE in the peak rate of sediment yield computation varies within 10 % for 6 events, and within 25 % for 18 events. The maximum RE for time to peak simulation is obtained as  $\pm 33$  % for Karso, Banha and Mansara watersheds. The model conserved the mass of sedimentographs within 10 % error for 11 events, and within 25 % error for 17 events. The efficiencies resulting from the simulation of the overall sedimentographs showed that the model simulated 6 events with an efficiency above 90 %; 16 events with an efficiency above 80 %; and 17 events with an efficiency above 75%; the minimum efficiency being 66 % on an event from Karso watershed. A graphical comparison of observed and simulated sediment yields (Fig. 6.3) also indicated a satisfactory agreement between the observed and computed rates for the validation events.

From the simulation results discussed above, it is evident that the proposed model simulated the sediment yield rates for the rainfall events on the study watersheds with a reasonable degree of accuracy. The efficiencies in both calibration and validation were reasonably high to show satisfactory model performance. An accurate determination of a representative value of A/S ratio from a large data set forms the key to better prediction of sediment yield rates from rainfall rates and the prevailing S determinable from NEH-4 procedure.

## **6.5 SUMMARY**

A sediment yield model is developed to estimate the temporal rates of sediment yield from rainfall events on natural watersheds. The model utilizes the SCS-CN based infiltration model for computation of rainfall-excess rate, and the SCS-CN-inspired proportionality concept for computation of sediment-excess rate. For computation of sedimentographs, the sediment-



excess rate is routed to the watershed outlet using a single linear reservoir technique. Analytical development of the model shows the ratio of the actual potential maximum erosion (A) to the actual potential maximum retention (S) of the SCS-CN method is constant for a watershed. The encouraging results from calibration and validation of the proposed simple four parameter model exhibit its potential in field application.



Table 6.4: Characteristics of observed and computed sedimentographs for validation events

Event	Peak sediment discharge (KN h <sup>-1</sup> )			Time to peak (min)			Total sediment yield (KN)			Nash-Sutcliffe Efficiency of simulation (%)
	Obs.	Comp.	R.E. (%)	Obs.	Comp.	R.E. (%)	Obs.	Comp.	R.E. (%)	
<b>Karso watershed</b>										
30.08.1993	2970.88	2083.21	-29.88	240	300	25.00	9815.50	8280.09	-15.64	66.05
02.09.1993	458.02	361.44	-21.09	240	240	0.00	886.78	945.69	6.64	85.32
14.10.1993	344.57	282.58	-17.99	180	240	33.33	1058.56	997.00	-5.82	87.15
17.06.1994	565.01	469.02	-16.99	420	300	-28.57	2534.59	2670.68	5.37	76.53
<b>Banha watershed</b>										
14.06.1994	1337.63	1268.09	-5.20	150	120	-20.00	2852.67	3210.54	12.54	95.16
20.08.1996	244.00	188.74	-22.65	180	240	33.33	1256.03	1180.88	-5.98	82.63
30.08.1996	1159.63	899.95	-22.39	240	240	0.00	2882.62	2181.45	-24.32	87.72
<b>Mansara watershed</b>										
19.07.1994	63.11	64.52	2.23	180	120	-33.33	160.45	172.67	7.62	80.58
25.07.1994	97.01	114.12	17.64	90	120	33.33	191.70	170.92	-10.84	87.72
16.08.1994	117.34	115.76	-1.35	120	120	0.00	361.39	301.70	-16.52	91.55
<b>W2 Treynor watershed</b>										
18.06.1980	2588.73	2448.55	-5.42	90	90	0.00	847.61	840.21	-0.87	99.35
14.06.1982	17948.1	13667.4	-23.85	50	50	0.00	4815.75	5191.48	7.80	81.74
<b>W6 GC watershed</b>										
20.01.1982	485.99	447.93	-7.83	110	110	0.00	330.83	229.75	-30.55	91.81
16.06.1982	121.30	103.66	-14.54	50	60	20.00	68.07	46.16	-32.18	88.55
01.07.1982	60.26	52.94	-12.15	60	60	0.00	57.93	57.99	0.12	96.10
<b>W7 GC watershed</b>										
17.10.1981	1146.11	959.49	-16.28	140	160	14.29	1506.10	1390.00	-7.71	87.23
30.11.1981	57.51	41.07	-28.59	260	240	-7.69	67.95	63.70	-6.24	72.23
30.06.1982	253.36	197.42	-22.08	80	80	0.00	173.80	239.31	37.69	72.98
<b>W14 GC watershed</b>										
17.10.1981	2800.76	1490.44	-46.78	90	90	0.00	1432.98	869.24	-39.34	68.03
11.08.1982	318.42	268.03	-15.83	90	100	11.11	188.39	203.54	8.04	94.74
27.08.1982	895.10	907.79	1.42	130	140	7.69	659.74	519.53	-21.25	84.55

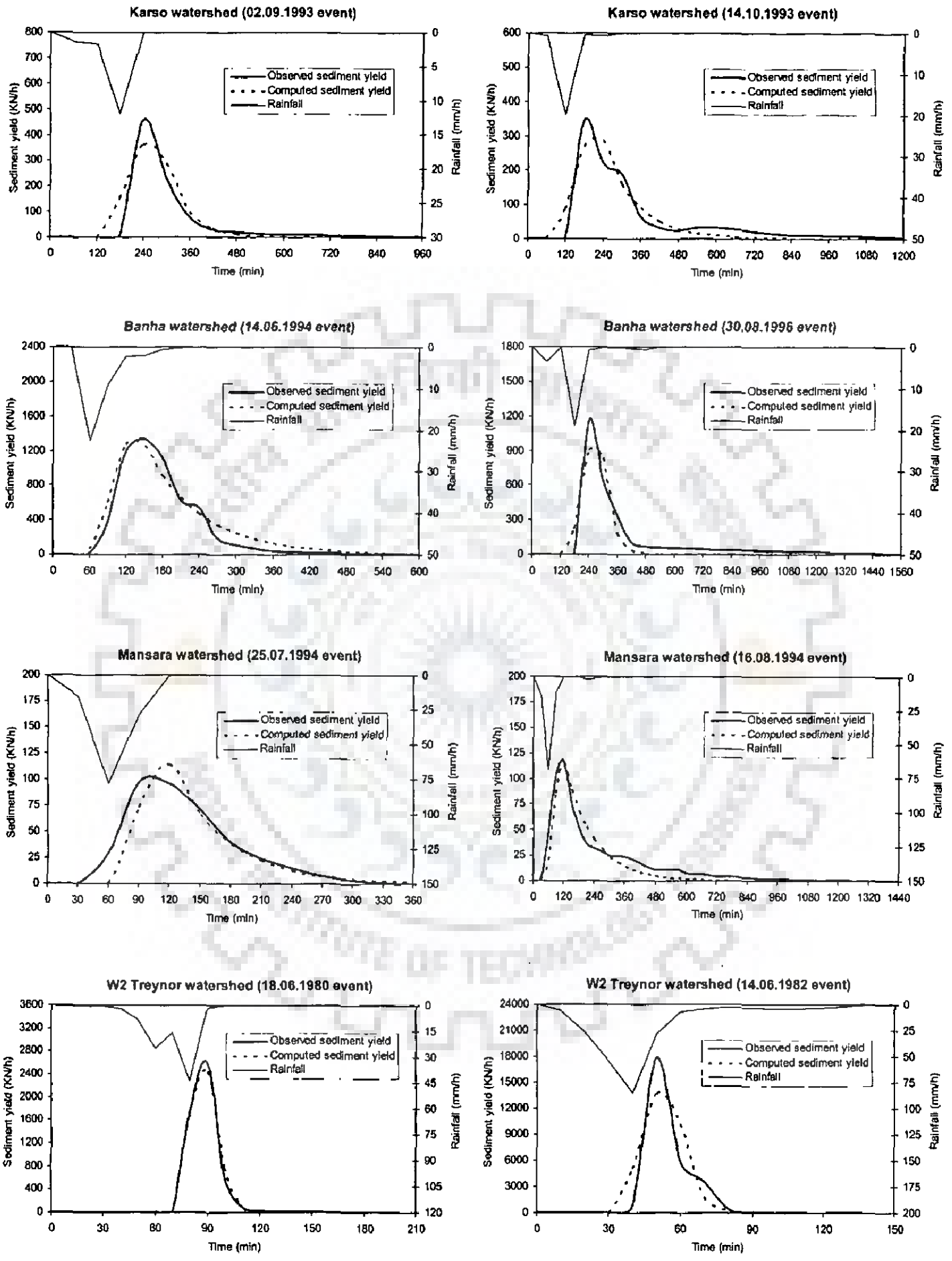


Fig. 6.3: Comparison of observed and computed sedimentographs for the validation events

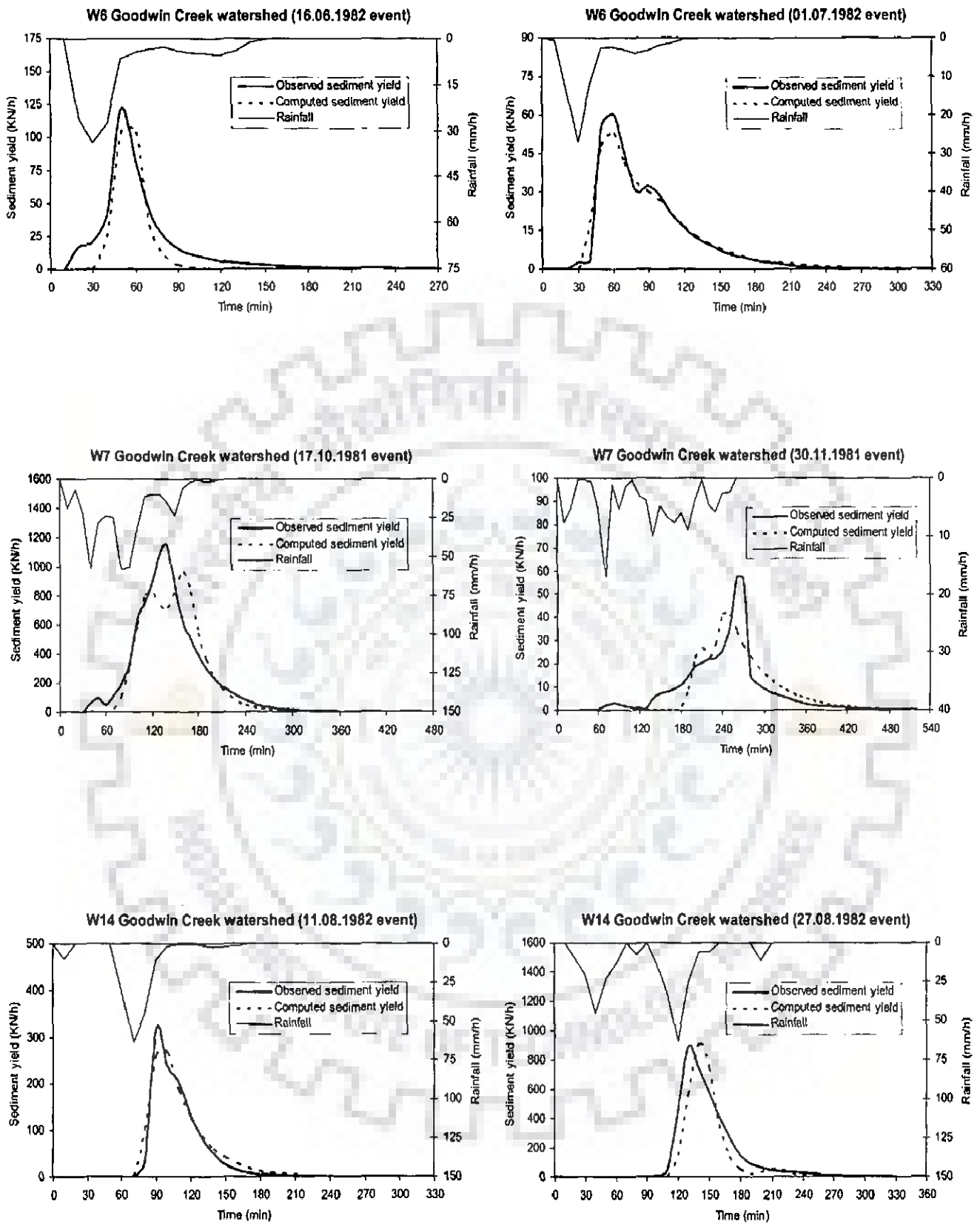


Fig. 6.3: Comparison of observed and computed sedimentographs for the validation events  
(contd...)

## CHAPTER 7

### SUMMARY AND CONCLUSIONS

---

Sediment delivery is regarded as one of the most problematic off-site consequences of soil erosion, which is an extremely complex process. Since the early attempts to model soil erosion, many new and more sophisticated models have been developed using different concepts. Most of these models can be used only at the field scale or in small homogeneous watersheds. Physically based models are expected to provide reliable estimates of sediment yield. However, these models require a large number of input parameters and, therefore, the practical application of these models is still limited. Keeping in view the scarce data availability for most of the watersheds in a developing country, simple models are needed for use in field by conservation planners.

The main objective of the present research work was to develop lumped and time-distributed simple sediment yield models for computation of sediment yield resulting from storm events on natural watersheds. The models were developed using the well-accepted proportionality hypothesis of the SCS-CN method that is widely used for computing direct surface runoff, because of its simplicity and requiring estimation of only one parameter from easily available watershed and meteorological characteristics. The SCS-CN generated direct surface runoff and the upland potential erosion which is normally estimated by erosion equations, such as USLE, are closely interrelated as both the methods account for major watershed characteristics, viz., soil type, land use, surface condition and antecedent moisture condition. The proportionality hypothesis of the SCS-CN method was therefore extended to the sediment delivery ratio for developing the new sediment yield models. In developing the time-

distributed sediment yield model, the rainfall-excess rate was computed using the SCS-CN based infiltration model. In order to have confidence in its simulation ability, the model was first evaluated for its performance in comparison with other popular infiltration models. The general applicability of the proposed sediment yield models was tested on the hydrologic and sediment yield data compiled from a number of watersheds located in India and USA. A summary of the research work and the conclusions arrived at are presented below in sequence of the development of models.

### **7.1 EVALUATION OF SCS-CN BASED INFILTRATION MODEL**

The SCS-CN based infiltration model was utilized for the development of time-distributed sediment yield model. With the aim to evaluate the performance of SCS-CN based infiltration model in comparison to other popular models, a total of fourteen infiltration models including Philip Model, Green-Ampt model, linear and nonlinear Smith-Parlange models, Singh-Yu model, SCS-CN based Mishra-Singh model, Smith model, Horton model, Holtan model, Overton model, Kostiakov model, modified Kostiakov model, Huggins-Monke model, and Collis-George model were applied to 243 sets of infiltration data collected from field and laboratory tests conducted in India and USA on soils ranging from coarse sand to fine clay. The following conclusions were drawn from the study.

1. The semi-empirical Singh –Yu general model outweighed and far surpassed other models in performance on most soils examined.
2. The semi-empirical Singh-Yu, Holtan and Horton models; empirical Huggins-Monke, modified Kostiakov, Kostiakov, and SCS-CN based models, and; physically based Smith - Parlange (linear and non-linear) models exhibited a satisfactory to very good

performance on laboratory-tests and poor to very good on field tests in India. The performance of other models was found to be poorer than these models.

3. The physically based models generally performed better on the data sets derived from laboratory tests than those derived from the field.
4. All the models generally performed poorly on Georgia sandy soils for the possible reason of existence of macro-pores or secondary pores.
5. The SCS-CN based infiltration model exhibited satisfactory to very good performance on both laboratory-test data (USA) and field-test data (India), exhibiting the Nash-Sutcliffe efficiency  $\geq 75\%$  on these soils. Based on the results of the study, it was concluded that the SCS-CN based infiltration model, with its performance comparable with other frequently used models, can be used satisfactorily for further applications.

## **7.2 SCS-CN BASED LUMPED SEDIMENT YIELD MODEL**

Coupling the SCS-CN method with the USLE, a lumped model was developed for computation of rain-storm generated sediment yield from a watershed. The coupling is based on three hypotheses: (i) the runoff coefficient ( $C$ ) is equal to the degree of saturation ( $S_r$ ), (ii) the USLE parameters can be expressed in terms of potential maximum retention ( $S$ ), and (iii) the sediment delivery ratio ( $DR$ ) is equal to the runoff coefficient. The proposed sediment yield model was applied to a large set of rainfall-runoff-sediment yield data obtained from twelve watersheds of different land uses, size, climatic, physiographic and soil characteristics. The following conclusions were drawn from the study.

1. The hypothesis  $C = S_r = DR$  enables determination of direct surface runoff and sediment yield using rainfall data and watershed characteristics.

2. USLE can be described in terms of the SCS-CN parameter potential maximum retention, S, and the potential erodible depth can be determined from USLE and S.
3. In application to the rainfall-runoff-sediment yield data of twelve watersheds, the recommended Models S2 and R2 computed sediment yield and runoff, respectively, with efficiencies of 91.78 and 91.75% for Nagwa, 84.51 and 71.63% for Karso, 75.21 and 90.23% for Banha, 81.45 and 80.08% for Mansara, 85.43 and 79.42% for W2, 81.03 and 82.18% for W6, 80.20 and 90.59% for W7, 90.04 and 71.26% for W14, 76.15 and 85.95% for Cincinnati, 81.20 and 74.10% for 182, 90.95 and 70.90% for 129, and with 84.04 and 81.22% for 123 watershed. These efficiency values indicate satisfactory performance of both the models on all the watersheds.
4. The ratio of potential maximum erosion to potential maximum retention (A/S) for a watershed is constant. The values of the A/S ratio for Nagwa, Karso, Banha, Mansara, W2, W6, W7, W14, Cincinnati, 182, 129, and 123 watersheds are 0.123, 0.155, 0.144, 0.055, 7.391, 0.198, 0.316, 0.254, 0.041, 0.230, 0.039, and 0.370 KN ha<sup>-1</sup> mm<sup>-1</sup> respectively. Determination of this ratio for watersheds of varying complexity may be of value in the estimation of sediment yield from ungauged watersheds using the concept of homogeneous watersheds.

### **7.3 SCS-CN BASED TIME-DISTRIBUTED SEDIMENT YIELD MODEL**

A sediment yield model for computation of event sedimentograph was developed using the SCS-CN based infiltration model for computation of rainfall-excess rate, and the SCS-CN-inspired proportionality concept for computation of sediment-excess rate. The sediment-excess rate was routed using simple single linear reservoir technique to obtain event sedimentograph at the outlet of the watershed. The following conclusions were drawn from the analytical



development of the time-distributed sediment yield model and its application to 49 rainfall events derived from seven watersheds.

1. The SCS-CN proportionality concept can be extended for determination of sediment yield rates from rainfall intensity and watershed characteristics.
2. The computed rates of sediment yield were in good agreement with the observed rates for most of the events of the study watersheds.
3. The ratio of potential maximum erosion to potential maximum retention (A/S) for a watershed can be determined from rainfall-runoff-sediment yield data for gauged watersheds. For determination of sediment yield rates from rainfall events, the representative value of A/S ratio for Karso, Banha, Mansara, W2 Treynor, W6 GC, W7 GC, and W14 GC watersheds are computed as 0.081, 0.114, 0.037, 7.107, 0.054, 0.039, and 0.064 KN ha<sup>-1</sup> mm<sup>-1</sup>, respectively.
4. The proposed time-distributed sediment yield model is simple, has only four parameters, and is easy to apply in field for conservation planning.

#### **7.4 MAJOR CONTRIBUTIONS OF THE STUDY**

The major contributions of the study can be summarized as follows.

1. Collection and compilation of (a) large set of infiltration data derived from laboratory and field tests conducted in India and USA on soils ranging from coarse sand to fine clay, and (b) hydrological and sediment yield data of twelve watersheds from different river catchments of India and USA that vary in size, physiographic, climatic, and land use characteristics. These data were collected from monitoring agencies, available literature and the internet resources.

2. Performance evaluation and comparative assessment of the SCS-CN based infiltration model on a comprehensive set of infiltration data.
3. Development of an event based lumped sediment yield model and A/S ratio concept.
4. A simple procedure for estimating sediment yield using the A/S ratio of the watershed.
5. Development of a simple, four-parameter time-distributed sediment yield model for computing event sedimentographs.
6. Assessment of the applicability of the proposed sediment yield models on a number of watersheds varying in complexity and characteristics.
7. Development of software for the above models.



## REFERENCES

---

- Agriculture Department (Soil Conservation Section) (1990). Project on hydrological and sedimentation monitoring - Mansara watershed, Flood prone river Gomti. unpub. Govt. of Uttar Pradesh, India.
- Alberts, E.E., Moldenhauer, W.C., and Foster, G.R. (1980). Soil aggregates and primary particles transported in rill and interrill flow. *Proc. Soil Sci. Soc. Am. J.*, 44: 590-595.
- Andrews, R.G. (1954). The use of relative infiltration indices for computing runoff. Unpub, Soil Conservation service, Fort Worth, Texas.
- ARS. (1976). Calibration of selected infiltration equations for the Georgia coastal Plain. Agricultural Research Service, ARS - S - 113, U.S. Department of Agriculture.
- Arnold, J.G., Allen, P.M., and Bernhardt, G. (1993). A comprehensive surface-groundwater flow model. *J. Hydrology*, 142: 47-69.
- Arnold, J. G., Srinivasan, R., Muttiah, R. S., and Williams, J. R., (1998). Large area hydrologic modeling and assessment, Part I: Model development. *J. Am. Water Resour. Assoc.*, 34(1): 73-89.
- Aron, G., Miller, A.C. Jr., Lakatos, D.F. (1977). Infiltration formula based on SCS curve number. *J. Irrig. and Drain. Div., ASAE*, 103(IR4), 419-427.
- Banasik, K., and Walling, D.E. (1996). Predicting sedimentographs for a small catchment. *Nordic Hydrology*, 27(4):275-294.
- Beasley, D.B., Huggins, L.F., and Monke, E.J. (1980). ANSWERS: A model for watershed planning. *Trans. ASAE*, 23: 938-944.
- Beasley, D.B., and Huggins, L.F. (1981). ANSWERS Users Manual. EPA-905/9-82-001: USEPA. Chicago, IL.
- Bennett, J.P. (1974). Concept of mathematical modeling of sediment yield. *Water Resources Research*, 10(3): 485-492.

- Bhunya, P. K., Mishra, S. K., and Berndtsson, R. (2003). Discussion on estimation of confidence interval for curve numbers. *J. Hydrol. Engg., ASCE* 8(4): 232-233.
- Bhuyan, S.J., Mankin, K.R., and Koelliker, J.K. (2003). Watershed-scale AMC selection for hydrologic modeling. *Trans. ASAE*, 46(2): 303-310.
- Black, T.A., Gardner, W.R., and Thurtell, G.W. (1969). The prediction of evaporation, drainage, and soil water storage for a bare soil. *Proc. Soil Sci. Soc. Am.* 33: 655-660.
- Blackmarr, W.A. (1995). Documentation of hydrologic, geomorphic, and sediment transport measurements on the Goodwin creek experimental watershed, Northern Mississippi, for the period 1982-1993: preliminary release. Research report No. 3, U.S. Dept. of Agriculture, ARS, Channel and Watershed Processes Research Unit, National Sedimentation Laboratory, Oxford, MS.
- Blau, J.B., Woolhiser, D.A., and Lane, L.J. (1988). Identification of erosion model parameters. *Trans. ASAE*, 31(3): 839-845.
- Blaszczynski, J. (2003). Estimating watershed runoff and sediment yield using a GIS interface to curve number and MUSLE models. Soils and Geology, Resources Notes No. 66, National Science and Technology Center, Denver, Colorado, U.S.
- Bonta, J.V. (1997). Determination of watershed curve number using derived distributions. *J. Irrig. and Drain., Engg., ASCE*, 123(1), 28-36.
- Bosznay, M. (1989). Generalisation of SCS curve number method. *J. Irrig. and Drain. Engg., ASCE*, 115(1): 139-144.
- Bouraoui, F., and Dillaha, T.A. (1996). ANSWERS-2000: Runoff and sediment transport model. *J. Envir. Engrg., ASCE*, 122(6): 493-502.
- Bradford, J.M. (1988). Erosional development of valley bottom gullies in the upper western United States. lecture notes, Training course on Soil Erosion and its Control, IRTCES, Beijing, China.
- Brakensiek, D. L., and Onstad, C.A. (1977). Parameter estimation of the Green-Ampt equation. *Water Resources Research*, 13(2): 335-359.
- Brakensiek, D. L., Engleman, R.L., and Rawls, W.J. (1981). Variation within texture classes of soil water parameters. *Trans. ASAE*, 24(2): 335-339.

- Brakensick, D.L., and Rawls, W.J. (1988). Effects of agricultural and rangeland management systems on infiltration. In: *Modelling Agricultural, Forest, and Rangeland Hydrology*, ASAE, St. Joseph, Mich. P. 247.
- Brown, L.C., and Foster, G.R. (1987). Storm erosivity using idealized intensity distributions. *Trans. ASAE*, **30**(2): 379-386.
- Browning, G.M., Parish, C.L., and Glass, J.A. (1947). A method for determining the use and limitation of rotation and conservation practices in control of soil erosion in Iowa. *Proc. Soil Sci. Soc. of Am.* **23**.
- Cahoon, J. (1998). Kostiaikov infiltration parameters from kinematic wave model. *J. Irrig. and Drain. Engg.*, **124**(2): 127-130.
- Cazier, D.J., and Hawkins, R.H. (1984). Regional application of the curve number method. *Proc. Conf. on Water Today and Tomorrow, Irrigation and Drainage Division Special Conf.*, ASCE, New York.
- Chahinian, N., Moussa, R., Andrieux, P., and Voltz, M. (2005). Comparison of infiltration models to simulate flood events at the field scale. *J. Hydrology*, **306**(1-4):191-214.
- Chen, Cheng-lung (1982). An evaluation of the mathematics and physical significance of the soil conservation service curve number procedure for estimating runoff volume, In: Singh, V.P. (ed.), *Rainfall-Runoff Relationship*, Water Resour. Pub., Littleton, CO.
- Chen, V.J. and Kuo, C.Y. (1986). A study of synthetic sediment graphs for ungauged watersheds. *J. Hydrology*, **84**:35-54.
- Chow, V.T. (1959). *Open Channel Hydraulics*. McGraw-Hill, New York.
- Chow, V.T., Maidment, D.R., and Mays, L.W. (1988). *Applied Hydrology*. McGraw Hill, New York.
- Clark, E.H., Haverkamp, J.A., and Chapman, W. (1985). *Eroding soils—The Off-Farm Impacts*. The Conservation Foundation, Washington D.C.
- Cogo, N.P., Moldenhauer, W.C., and Foster, G.R. (1984). Soil loss reductions from conservation tillage practices. *Proc. Soil Sci. Soc. of Am.* **48**(2): 368-373.

- Collis-George, N. (1977). Infiltration equations for simple soil systems. *Water Resources Research*, **13**: 395- 403.
- Cooley, K.R. (1980). Erosivity values for individual design storms. *J. Irrig. and Drain. Div., ASCE*, **106**(IR2):135-145.
- Cook, H.L. (1936). The nature and controlling variables of the water erosion process. *Soil Sc. Soc. of Am., Proc.* 1.
- Croley, II, T.E. (1982). Unsteady overland sedimentation. *J. Hydrology*, **56**: 325-346.
- Croley, II, T.E., and Foster, G.R (1984). Unsteady sedimentation in nonuniform rills. *J. Hydrology*, **70**: 101-122.
- David, W.P., and Beer, C.E. (1975a). Simulation of soil erosion-Part I. Development of a mathematical erosion model. *Trans. ASAE*, 126-129, 133.
- David, W.P., and Beer, C.E. (1975b). Simulation of soil erosion-Part II. Stream flow and suspended sediment simulation results. *Trans. ASAE*, 130-133.
- Dendy, F.E. (1982). Distribution of sediment deposits in small reservoirs. *Trans. ASAE*, **25**:100-104.
- Dickey, E.C., Shelton, D.P., Jasa, P.J., and Peterson, T.R. (1985). Soil erosion from tillage systems used in Soybean and Corn residue. *Trans. ASAE*, **28**(4): 1124-1129, 1140.
- Dudal, R. (1981). An evaluation of conservation needs. In: Morgan, R.P.C. (ed.), *Soil conservation, problems and prospects*, p 3-12, John Wiley & Sons, Chichester, England.
- Einstein, H.A. (1950). The bed load function for sediment transportation in open channel flows. U.S. Department of Agriculture, Tech. Bull. No. 1026.
- Elliot, W.J., and Laflen, J.M. (1993). A process-based rill erosion model. *Trans. ASAE*, **36**(1): 65-72.
- Ellison, W.D. (1944). Studies of raindrop erosion. *Agricultural Engineering*, **25**:131-136, 181-182.
- Ellison, W.D. (1947). Soil erosion studies. *Agricultural Engineering*, **28**: 145-156, 197-201, 245-248, 297-300, 349-351, 402-405, 442-444.

- Elrick, D.E. and Bowman, D.H. (1964). Note on an improved apparatus for soil moisture flow measurements. *Proc. Soil Sci. Soc. Am.* **28**: 450-453.
- Evans, R. (1980). Mechanics of water erosion and their spatial and temporal controls: an empirical viewpoint. In: Kirkby, J. and Morgan, R.P.C. (eds.), *Soil Erosion*, Wiley: 109-128.
- Flaxman, E.M. (1972). Predicting sediment yield in western United states. *J. of Hydr. Div., ASCE*, **98**(HY12): 2073-2085.
- Fok, Y.S. (1975). A comparison of the Green-Ampt and Philip two-term infiltration equations. *Trans. ASAE*, **18**: 1073-1075.
- Foster, G.R. (1976). Sedimentation, general. Proc. of the National Symposium on Urban Hydrology, Hydraulics, and Sediment Control. Univ. of Kentucky. Lexington: 129-138.
- Foster, G.R. (1982). Modelling the Erosion Processes. In: Haan, C.T., Johnson, H., and Brakensiek, D.L. (eds.), *Hydrological Modelling of Small Watersheds*, ASAE Monograph No. 5, American Society of Agricultural Engineers, St. Joseph, Michigan: 297-380.
- Foster, G. R., Lane, L. J., Nowlin, J. D., Laflen, J. M., and Young, R. A. (1981). Estimating erosion and sediment yield on field-sized areas. *Trans. ASAE*, **24**: 1253-1263.
- Foster, G.R., and Lane, L.J. (1983). Erosion by concentrated flow in farm fields. In: Proc. D.B. Simons symp. on Erosion and Sedimentation, Colorado State Univ., Fort Collins, CO: 9.65-9.82.
- Foster, G.R., and Meyer, L.D. (1972a). A closed form soil erosion equation for upland areas. In: Shen, H.W. (ed.), *Sedimentation (Einstein)*, Chapter 12, Colorado State University, Fort Collins, CO.
- Foster, G.R., and Meyer, L.D. (1972b). Transport of soil particles by shallow flow. *Trans. ASAE*, **15**(1): 99-102.
- Foster, G.R., and Meyer, L.D. (1975). Mathematical simulation of upland erosion by fundamental erosion mechanics. In: *Present and Prospective Technology for Predicting Sediment Yields and Sources*. ARS-S 40. USDA-Agricultural Research Service: 190-207.
- Foster, G.R., Meyer, L.D., and Onstad, C.A. (1977a). An erosion equation derived from basic erosion principles. *Trans. ASAE*, **20**(4): 678-682.

- Foster, G.R., Meyer, L.D., and Onstad, C.A. (1977b). A runoff erosivity factor and variable slope length exponents for soil loss estimation. *Trans. ASAE*, **20**(4): 683-687.
- Foster, G.R., Flanagan, D.C., Nearing, M.A., Lane, L.J., Risse, L.M., and Finkner, S.C. (1995). Hillslope erosion component. In: Flanagan, D.C., and Nearing, M.A. (eds.) USDA-Water Erosion Prediction Project (WEPP) - Hillslope Profile and watershed Model Documentation, Chap. 11, USDA-ARS, NSERL Report No. 10. West Lafayette, Ind.: National Soil Erosion Research Laboratory.
- Foster, G.R., and Wischmeier, W.H. (1974). Evaluating irregular slopes for soil loss prediction. *Trans. ASAE*, **17**(2):305-309.
- Foster, I.D.L., and Charlesworth, S.M. (1996). Heavy metals in the hydrological cycle: Trends and explanation. *J. Hydrol. Process.*, **10**: 227-261.
- Franti, T.G., Foster, G.R., and Monke, E.J. (1996). Modeling the effects of incorporated residue on rill erosion , Part I: Model development and sensitivity analysis. *Trans. ASAE*, **39**(2):535-542.
- Freebairn, D.M., Gupta, S.C., Onstad, C.A., and Rawls, W.J. (1989). Antecedent rainfall and tillage effects upon infiltration. *J. Soil Sci. Soc. Am.* **53**: 1183-1189.
- Garde, R.J., and Kothiyari, U.C. (1987). Sediment yield estimation. *J. Irrigation and Power, CBIP, India*, **44**(3):97-123.
- Garde, R.J., Ranga Raju, K.G., Swamee, P.K., Miraki, G.P., and Molanezhad, M. (1983). Mathematical modeling of sedimentation processes in reservoirs. Hydraulics Engg. Report No. HYD 8304, Univ. of Roorkee, India.
- Gardiner, V., and Gregory, K.J. (1981). Drainage density in rainfall-runoff modeling. In: Singh, V.P. (ed.), Int. Symp. on Rainfall-Runoff Modelling, Mississippi State University, Mississippi: 449-476.
- Gifford, G.F. (1976). Applicability of some infiltration formulae to range land infiltrometer data. *J. Hydrology*, **28**: 1-11.
- Gilley, J.E., Finkner, S.C., Spomer, R.G., and Mielke, L.N. (1986). Runoff and erosion as affected by corn residue: Part II. Rill and interrill components. *Trans. ASAE*, **19**(1):161-164.



- Gosain, A.K., and Rao, S. (2004). GIS-based technologies for watershed management. *Current Science*, Special Section: Application of S&T to Rural Areas, Current Science Association in Collaboration with Indian Academy of Sciences, Bangalore, India, **87(7)**: 948-953.
- Gottschalk, L.C. (1964). Sedimentation, Part I: Reservoir sedimentation. In: Chow, V.T.(ed.), *Handbook of Applied Hydrology*, McGraw Hill, New York.
- Govindaraju, R.S., and Kavvas, M.L. (1991). Modeling the erosion process over steep slopes: Approximate analytical solutions. *J. Hydrology*, **127**: 279-305.
- Green, R.E. (1962). Infiltration of water into soils as influenced by antecedent moisture. Unpub. Ph.D. Thesis, Iowa State Univ., Iowa.
- Green, W.H., and Ampt, C.A. (1911). Studies of soil physics, I. Flow of air and water through soils. *J. Agric. Science*, **4**: 1-24.
- Grigorjev, V.Y., and Iritz, L. (1991). Dynamic simulation model of vertical infiltration of water in soil. *J. Hydrological Sciences*, **36(2)**: 171-179.
- Haan, C.T., Barfield, B.J., and Hayes, J.C. (1994). *Design Hydrology and Sedimentology for Small Catchments*. Academic Press, New York.
- Hadley, R.F., Lal, R., Onstad, C.A., Walling, D.E., and Yair, A. (1985). Recent Developments in Erosion and Sediment Yield Studies. UNESCO, (IHP) Publication, Paris: 127.
- Hawkins, R.H. (1978). Runoff curve numbers with varying site moisture. *J. Irrig. and Drain. Div. ASCE*, **104(IR4)**: 389-398.
- Hawkins, R.H. (1984). A comparison of predicted and observed runoff curve numbers. Proc. special conf., Irrig. and Drain. Div., ASCE, New York, NY: 702-709.
- Hawkins, R.H. (1993). Asymptotic determination of runoff curve numbers from data. *J. Irrig. And Drain. Engg., ASCE* **119** (2), 334-345.
- Hawkins, R. H., Hjelmfelt, A. T. Jr., and Zevenbergen, A. W. (1985). Runoff probability, storm depth, and curve numbers. *J. Irrig. And Drain. Engg., ASCE*, **111(4)**: 330-339.
- Hirschi, M. C., and Barfield, B. J. (1988). KYERMO-A physically based research erosion model Part I: Model development. *Trans. ASAE*, **31(3)**: 804-813.

- Hjelmfelt, A. T. Jr. (1980). Curve-number procedure as infiltration method. *J. Hydraulics Engg., ASCE*, **106**(HY6): 1107-1111.
- Hjelmfelt, A.T. Jr. (1982). Closure to Empirical investigation of the curve number technique. *J. Hydraulics Div., ASCE*, **108**(HY4):614-616.
- Hjelmfelt, A. T. Jr. (1991). Investigation of curve number procedure. *J. Hydraulics Eng., ASCE* **117**(6), 725–737.
- Hjelmfelt, A.T. Jr., Peist, R.F., and Saxton, K.E. (1975). Mathematical modeling of erosion on upland areas. Proc. 16<sup>th</sup> Cong., Int. Assoc. for Hydraulic Res., Sao Paulo, Brazil, **2**: 40-47.
- Hjelmfelt, A. T. Jr., and Wang. M. (1999). Modeling hydrologic and water quality response to grass waterways. *J. Hydrol. Engg, ASCE*, **4**(3): 251-256.
- Hogarth, W.L., Rose, C.W., Parlange, J.Y., Sander, G.C., and Carey, G. (2004a). Soil erosion due to rainfall impact with no inflow: a numerical solution with spatial and temporal effects of sediment settling velocity characteristics. *J. Hydrology*, **294**: 229-240.
- Hogarth, W.L., Parlange, J.Y., Rose, C.W., Sander, G.C., Steenhuis, T.S., and Barry Andrew. (2004b). Soil erosion due to rainfall impact with inflow: an analytical solution with spatial and temporal effects. *J. Hydrology*, **295**: 140-148.
- Holtan, H.N. (1961). A concept of infiltration estimates in watershed engineering. ARS 41-51, U.S. Department of Agriculture, Washington, D.C.
- Horton, R.I. (1938). The interpretation and application of runoff plot experiments with reference to soil erosion problems. Proc. *Soil Sci. Society Am.*, **3**: 340-349.
- Hsu, Nien-Sheng, Kuo, Jan-Tai, and Chu, Wen-Sen (1995). Proposed daily streamflow-forecasting model for reservoir operation. *J. Water Resou. Planng. and Mangmnt, ASCE*, **121**(2).
- Huber, W.C., Heaney, J.P., Bedient, B.P., and Bender, J.P. (1976). Environmental resources management studies in the Kissimmie river basin. Report no. ENV-05-76-3, Dept of Environ. Engg. Sc., Univ. of Florida, Gainesville, FL, May.
- Huggins L.F., and Monke, E.J. (1966). The mathematical simulation of the hydrology of small watersheds. Tech. Rep. No. 1, Purdue Water Resources Research Centre, Lafayette.

- Hussein, M.H., and Laflen, J.M. (1982). Effect of crop canopy and residue on rill and interrill soil erosion. *Trans. ASAE*, **25**(5):1310-1315.
- Idike, F. I., Larson, C.L., Slack, D.C. and Young, R.A. (1980). Experimental evaluation of two infiltration models. *Trans. ASAE*, **23**(6):1428-1433.
- Innes, G. (1980). Comparison of infiltration models on disturbed soils using parameter optimization. Unpub. M.S. thesis, 83 p., Univ. of Tennessee, Knoxville, Tennessee.
- Jain, M.K., and Kothyari, U.C. (2000). Estimation of soil erosion and sediment yield using GIS. *J. Hydrol. Sciences*, **45**(5): 771-786.
- Jain, M.K., Kothyari, U.C., and Ranga Raju, K.G. (2005). Geographic information system based distributed model for soil erosion and rate of sediment outflow from catchments. *J. Hydrol. Engg., ASCE*, **131**(9): 755-769.
- Jain, M.K., Mishra, S.K., and Singh, V.P. (2006a). Evaluation of AMC-dependent SCS-CN-based models using watershed characteristics. *Water Resources Management*, **20**: 531–552.
- Jain, M.K., Mishra, S.K., Babu, P.S., Venugopal, K., and Singh, V.P. (2006b). Enhanced runoff curve number model incorporating storm duration and a nonlinear  $I_a$ -S relation. *J. Hydrol. Engg., ASCE*, **11**(6):631-635.
- Jansen, J.M.L., and Painter, R.B. (1974). Predicting sediment yield from climate and topography. *J. Hydrology*, **21**:371-380.
- Johnson, J.W. (1943). Distribution graph of suspended matter concentration. *Trans. ASAE*, **108**:941-964.
- Judson, S. (1981). What's happening to our continents. In: Skinner, B.J. (ed.), *Use and Misuse of Earth's Surface*. William Kaufman Inc., Los Altos, California: 12-139.
- Kalin, L., Govindaraju, R. S., and Hantush, M.M (2003). Effect of geomorphologic resolution on modeling of runoff hydrograph and sedimentograph over small watersheds. *J. Hydrology*, **276**: 89-111.
- Kalin, L., Govindaraju, R. S., and Hantush, M.M (2004). Development and application of a methodology for sediment source identification. I: Modified unit sedimentograph approach. *J. Hydrol. Engg., ASCE*, **9**(3): 184-193.

- Kelly, G.E., Edwards, W.M., Harrold, L.L. (1975). *Soils of the North Appalachian experimental watersheds*. Misc. Pub. No.1296, U.S. Dept. of Agriculture, Agricultural Research Service, Washington, D.C.
- Kincaid, D. C., Heerman, D.F., and Kruse, E.G. (1969). Application rates and runoff in center-pivot sprinkler irrigation. *Trans. ASAE*, **12**(6).
- Knisel, W.G. (ed.) (1980). *CREAMS: A field scale model for chemicals, runoff and erosion from agricultural management system*. Cons. Res. Report, No. 26, USDA-SEA, Washington, D.C., 643p.
- Kostiakov, A.N. (1932). On the dynamics of the coefficients of water percolation in soils. Sixth Commission, Int. Soil Science Society, Part A: 15-21.
- Kothyari, U.C., Jain, S.K. (1997). Sediment yield estimation using GIS. *J. Hydrol. Sciences*, **42**(6), 833-843.
- Kothyari, U.C., Tiwari, A.K., and Singh R. (1996). Temporal variation of sediment yield. *J. Hydrol. Engg., ASCE*, **1**(4): 169-176.
- Kothyari, U.C., Tiwari, A.K., and Singh, R. (1997). Estimation of temporal variation of sediment yield from small catchment through the kinematic method. *J. Hydrology*, **203**: 39-57.
- Kumar, S., and Rastogi, R.A. (1987). A conceptual catchment model for estimating suspended sediment flow. *J. Hydrology*, **95**: 155-163.
- Kumar, S.R., Patwari, B.C., and Bhuniya, P.K. (1995). *Infiltration studies: Dudhnai sub-basin (Assam and Meghalaya)*. Tech. Report, CS(AR)-183, Case Study, National Institute of Hydrology, Roorkee-247 667, India.
- Laflen, J. M., and Colvin, T.S. (1981). Effect of crop residue on soil loss from continuous row cropping. *Trans. ASAE*, **24**(32): 605-609.
- Laguna, A., and Giraldez, J.V. (1993). The description of soil erosion through a kinematic wave model. *J. Hydrology*, **145**: 65-82.
- Lal, R. (1976). Soil erosion problems on an alfisol in western Nigeria and their control. *Int. Ints. of Tropical Agriculture*, Ibadan, Nigeria, **1**:208.

- Laliberte, G.E., Corey, A.T., and Brooks, R.H. (1966). Properties of unsaturated porous media. Hydrol. Paper 17, Colorado State Univ., Fort Collins, Colorado.
- Lane, L.J., Shirley, E.D., and Singh, V.P. (1988). Modelling erosion on hillslopes. In: Anderson, M.G. (ed.), *Modelling Geomorphological Systems*, John Wiley and Sons Ltd.: 287-308.
- Langbein, W.B., and Schumm, S.A. (1958). Yield of sediment in relation to mean annual precipitation. *Trans. Am. Geophys. Union* **39**: 1076-84.
- Laws, J.O., and Parsons, D.A. (1943). The relation of raindrop size to intensity. *Trans. Am. Geophys. Union*, **24**: 452-460.
- Leonard, R.A., Knisel, W.G., and Still, D.A. (1987). GLEAMS: Groundwater loading effects on agricultural management systems. *Trans. ASAE*, **30**(5):1403-1428.
- Leopold, L.B., Wolman, M.G., and Miller, J.P. (1964). *Fluvial Processes in Geomorphology*. W.H. Freeman, San Francisco.
- Li, R.M. (1979). Water and sediment routing from watersheds. In: Shen, H.W. (ed.) *Modelling of Rivers*. Wiley, New York: 9.1 - 9.8.
- Li, Y., Buchberger, S.G., and Sansalone, J.J. (1999). Variably saturated flow in storm-water partial exfiltration trench', *J. Environ. Engg., ASCE*, **125**(6): 556-565.
- Linsley, R.K., Kohler, M.A., and Paulhus, J.L.H. (1975). *Hydrology for Engineers*. 2<sup>nd</sup> Ed., McGraw Hill, 482 p.
- Liu, B.Y., Nearing, M.A., and Risse, L.M. (1994). Slope gradient effects on soil loss for steep slopes. *Trans. ASAE*, **37**(6): 1835-1840.
- Lloyd, C.H., and Eley, G.W. (1952). Graphical solution of probable soil loss formula for northeastern region. *J. Soil and Water Conservation*, **7**.
- Maidment, D.R. (ed. in chief) (1993). *Handbook of Hydrology*, Mc-Graw Hill, Inc., New York.
- McCool, D.K., Brown, L.C., Foster, G.R., Mutchler, C.K., and Meyer, L.D. (1987). Revised slope steepness factor for the Universal Soil Loss Equation. *Trans. ASAE*, **30**(5): 1387-1396.
- McCuen, R. H. (1982). *A Guide to Hydrologic Analysis Using SCS Methods*. Prentice-Hall Inc., Englewood Cliffs, New Jersey.

- McCuen, R. H. (2002). Approach to confidence interval estimation for curve numbers. *J. Hydrol. Engg., ASCE*, 7(1): 43-48.
- Mein, R.G., and Larson, C.L. (1971). Modeling the infiltration component of the rainfall-runoff process. WRRC Bull. 43, Water Resources Research Center, Univ. of Minnesota, Minneapolis, Minnesota.
- Mein, R.G., and Larson, C.L. (1973). Modeling infiltration during a steady rain. *Water Resources Research*, 9(2): 384-394.
- Meyer, L.D. (1964). Mechanics of soil erosion by rainfall and runoff as influenced by slope length, slope steepness, and particle size. Ph.D. thesis, Purdue Univ., W. Lafayette, IN.
- Meyer, L.D. (1981). How rain intensity affects interrill erosion. *Trans. ASAE*, 24: 1472-1475.
- Meyer, L.D., and Wischmeier, W.H. (1969). Mathematical simulation of the process of soil erosion by water. *Trans. ASAE*, 12(6): 754-758, 762.
- Meyer, L.D., Foster, G.R., and Nikolov, S. (1975a). Effect of flow rate and canopy on rill erosion. *Trans. ASAE*, 905-911.
- Meyer, L.D., Foster, G.R., and Romkens, M.J.M. (1975b). Source of soil eroded by water from upland slopes. In: Present and Prospective Technology for Predicting Sediment Yields and Sources. ARS-S 40. USDA-Agricultural Research Service, 177-189.
- Michel, C., Andreassian, V., and Perrin, C. (2005). Soil conservation service curve number method: how to mend a wrong soil moisture accounting procedure. *Water Resources Research*, 41, W02011, doi:10.1029/2004WR003191.
- Miller, N., and Cronshey, R.C. (1989). Runoff curve numbers, the next step. Proc. Int. conf. on Channel flow and catchment runoff, Univ. of Virginia, Charlottes, Va.
- Mishra, S.K. (1998). Operation of a multipurpose reservoir. Unpub. Ph.D. Thesis, Univ. of Roorkee, Roorkee, India.
- Mishra, S.K., and Singh, V.P. (1999). Another look at the SCS-CN method. *J. Hydrol. Engg., ASCE*, 4(3): 257-264.
- Mishra, S. K., and Singh, V. P. (2002a). SCS-CN method Part-I: Derivation of SCS-CN based models. *Acta Geophysica Polonica* 50(3): 457-477.

- Mishra, S.K., and Singh, V.P. (2002b). SCS-CN-based hydrologic simulation package, Ch. 13 In: Singh, V.P., and Frevert, D.K. (eds.) *Mathematical Models in Small Watershed Hydrology*, Water Resources Publications, P.O. Box 2841, Littleton, Colorado 80161.
- Mishra, S. K., and Singh, V. P. (2003). *Soil Conservation Service Curve Number (SCS-CN) Methodology*, Kluwer Academic Publishers, Dordrecht, The Netherlands, ISBN 1-4020-1132-6.
- Mishra, S. K., Singh, V. P. (2004a). Long term hydrological simulation based on the soil conservation service curve number. *J. Hydrol. Process.*, **18**(7): 1291–1313.
- Mishra, S. K., Singh, V. P. (2004b). Validity and extension of the SCS-CN method for computing infiltration and rainfall-excess rates. *J. Hydrol. Process.*, **18**: 3323-3345.
- Mishra, S.K., Sahu, R.K., Eldho, T.I., and Jain M.K. (2006). An improved  $I_a$ -S relation incorporating antecedent moisture in SCS-CN methodology. *J. Water Resources Management*, **20**(5): 643–660.
- Mockus, V. (1949). Estimation of total (peak rates of) surface runoff for individual storms. Exhibit A of Appendix B, Interim Survey Report Grand (Neosho) River Watershed, USDA, December 1.
- Mockus, V. (1964). Letter to Orrin Ferris, March 5, 6 p. In: Rallison, R.E. Origin and evolution of the SCS runoff equation, Proc. ASCE Symp. Watershed management, Boise, Idaho, July, 1980.
- Moldenhauer, W.C., and Long, D.C. (1964). Influence of rainfall energy on soil loss and infiltration rates: I. Effect over a range of texture. *Soil Sci. Soc. Am. Proc.*: 813-817.
- Moore, R.E. (1939). Water conduction from shallow water tables. *Hilgardia* **12**(6): 383-426.
- Morgan, R.P.C. (1979). *Soil Erosion*, Longman Group Ltd., London.
- Morgan, R.P.C. (1995). *Soil Erosion and Conservation*. Second ed., Longman Group Ltd., England.
- Morgan, R.P.C., Quinton, J.N., Smith, R.E., Govers, G., Poesen, J.W.A., Auerswald, K., Chisci, D., and Styczen, M.E. (1998). The European Soil Erosion Model (EUROSEM): a dynamic approach for predicting sediment transport from fields and small catchments. *Earth Surface Processes and Landforms*, **23**: 527-544.

- Musgrave, G.W. (1947). The quantitative evaluation of factors in water erosion, a first approximation. *J. Soil Cons.*, **2**(3): 133-138.
- Mutchler, C.K., and Young, R.A. (1975). Soil detachments by raindrops. In: Present and Prospective Technology for Predicting Sediment Yields and Sources. ARS-S-40. USDA-ARS: 113-117.
- Muttiah, R.S., and Wurbs, R.A. (2002). Scale-dependent soil and climate variability effects on watershed water balance of the SWAT model. *J. Hydrology*, **256**:264-285.
- Nachabe, M. H., Illagasekare, T.H., Morel-Seytoux, H.J., Ahuja, L.R., and Ruan, H. (1997). Infiltration over heterogeneous watershed: influence of rain excess. *J. Hydrol. Engg., ASCE* **2**(3): 140-143.
- Narayana, V.V.D. (1993). Estimation of soil Loss. Ch. 4 In: Soil and Water Conservation Research in India, p. 30-56, Indian Council of Agricultural Research, New Delhi.
- Narayana, V.V.D., and Babu, R. (1983). Estimation of soil erosion in India. *J. Irrig. and Drain. Engg., ASCE*, **109**(4): 419-434.
- Narula, K.K., Bansal, N.K., and Gosain, A.K. (2002). Hydrological sciences and recent advances: a review. *TERI Information Digest on Energy and Environment* **1**(1):71-93.
- Nash, J.E., and Sutcliffe, J.V. (1970). River flow forecasting through conceptual models Part I-a discussion of principles. *J. Hydrology*, **10**: 282-290.
- Nearing, M.A., Foster, G.R., Lane, L.J., and Finkner, S.C. (1989). A process-based soil erosion model for USDA-water erosion prediction project technology. *Trans. ASAE*, **32**(5): 1587-1593.
- Norton, L.D., Cogo, N.P., and Moldenhauer, W.C. (1985). Effectiveness of mulch in controlling soil erosion. In: Soil Erosion and Conservation, Maidson, Wis.: *Soil Sci. Soc. of Am*: 598-606.
- Novotny, V. (1980). Delivery of suspended sediment and pollutants from non-point sources during overland flow. *Water Resources Bull.*, **16**(6): 1057-1065.
- Novotny, V., and Chesters, G. (1989). Handbook of Nonpoint Pollution: Sources and Management. Van Nostrand Reinhold, New York.



- Novotny, V., and Olem, H. (1994). *Water Quality: Prevention, Identification, and Management of Diffuse Pollution*. Wiley, New York.
- Novotny, V., et al. (1979). *Simulation of Pollutant Loadings and Runoff Quality*. EPA 905/4-79-029, U.S. Environmental Protection Agency, Chicago, IL.
- Novotny, V., Simsim, G.V., and Chesters, G. (1986). Delivery of pollutants from nonpoint sources. In: *Proc., Symp. on Drainage Basin Sediment Delivery*, Int. Assoc. Hydrol. Sci., Publ. No. 159, Wallingford, England.
- Ogden, F. L., and Sagafian, B. (1997). Green and Ampt infiltration with redistribution. *J. Irrig. and Drain. Engg., ASCE* 123(5): 386-393.
- Ogrosky, H.O. (1956). *Service objectives in the field of hydrology*. Unpub., Soil Conservation Service, Lincoln, Nebraska.
- Onstad, C.A., and Foster G.R. (1975). Erosion modeling on a watershed. *Trans. ASAE*, 18(2):288-292.
- Onstad, C.A., and Bowie, A.J. (1977). Basin sediment yield modeling using hydrological variables. *Proc. symp. on Erosion and Solid Matter Transport in Inland Waters*, IAHS, Paris, 122:191-202.
- Overton, D.E. (1964). *Mathematical refinement of an infiltration equation for watershed engineering*. ARS 41-99, U.S. Department of Agriculture, Washington, D.C.
- Parlange, J.Y. (1971). Theory of water movement in soils 2. One-dimensional infiltration. *Soil Science*, 111(3): 170-174.
- Philip, J.R. (1957). Theory of infiltration: 4. Sorptivity and algebraic equations. *Soil Science*, 84: 257-265.
- Philip, J.R. (1969). Theory of infiltration. In: Chow, V.T. (ed.) *Advances in Hydrosience*, Academic Press, New York, N.Y.: 215-296.
- Piest, R.F., Bradford, J.M., and Spomer, R.G. (1975). Mechanics of erosion and sediment movement from gullies. In: *Present and Prospective Technology for Predicting Sediment Yields and Sources*. ARS-S 40. USDA-Agricultural Research Service: 130-141.

- Ponce, V.M. (1989). *Engineering Hydrology: Principles and Practices*. Prentice Hall, Englewood Cliffs, NJ, 07632.
- Ponce, V. M., and Hawkins, R. H. (1996). Runoff curve number: has it reached maturity? *J. Hydrol. Engg. ASCE*, 1(1): 11–19.
- Raghuwanshi, N.S., Rastogi, R.A., and Kumar S. (1994). Instantaneous-unit sediment graph. *J. Hydr. Engg., ASCE*, 120(4): 495-503.
- Rao, B.K., Singh, D.K., Bhattacharya, A.K., and Singh, A. (2003). Derivation of curve numbers from the observed rainfall and runoff data for Banha and Karso watersheds of Upper Damodar Valley in Jharkhand state. *J. Soil and Water Conservation, Soil Conservation Society of India*, 2(3&4): 136-145.
- Rawls, W.J. (1983). Estimating soil bulk density from particle size analysis and organic matter content. *Soil science*, 135(2):123-125.
- Rawls, W.J., Yates, B., and Asmussen, L. (1976). Calibration of selected infiltration equations for Georgia coastal plain. ARS-S-113, U.S. Department of Agriculture.
- Rawls, W. J., Brakensiek, D.L., and Miller, N. (1983). Green-Ampt infiltration parameters from soils data. *J. Hydr. Engg.*, 109(1): 62-70.
- Renard, K.G., Simanton, J.R., and Osborn, H.B. (1974). Applicability of the universal soil loss equation to semi-arid rangeland conditions in the southwest. Proc. AWRS and Arizona Academy of Science, Arizona.
- Renard, K.G., Foster, G.R., Weesies, G.A., and Porter, J.P. (1991). RUSLE: Revised Universal Soil Loss Equation, *J. Soil and Water Cons.*, 46(1): 30-33.
- Rendon-Herrero, O. (1978). Unit sediment graph. *Water Resources Research*, 14: 889-901.
- Rode, A.A. (1965). *Theory of soil moisture*, Vol. 1, (Translated from Russian). Pub. for USDA and N.S.F. by the Israel Program for Scientific Translation, Jerusalem, (1969).
- Rode, M., and Frede, H.G. (1997). Modification of AGNPS for agricultural land and climate conditions central Germany. *J. Environ. Qual.* 26 (1): 165–172.
- Roehl, J.W. (1962). Sediment source areas, delivery ratios, and influencing morphological factors. Publ. No.59, Int. Assoc. Hydrol. Sci.: 202-213.

- Roy, B.P. and Singh, H. (1995). Infiltration study of a sub-basin, Case Study, CS(AR) 170, National Institute of Hydrology, Roorkee-247 667, India.
- SAS (1988). SAS/STAT User's Guide. Release 6.03 Edition, Statistical Analysis System Institute Inc., SAS Circle, Box 8000, Cary, NC 27512-8000.
- SCD (1972). Handbook of Hydrology. Soil Conservation Department, Ministry of Agriculture, New Delhi.
- SCS (1956, 1964, 1971, 1972, 1985, 1993). Hydrology, National Engineering Handbook, Section 4. Soil Conservation Service, US Department of Agriculture, Washington DC.
- SWCD (Soil and Water Conservation Division) (1991, 1993, 1994, 1995, 1996). Evaluation of Hydrologic Data. Indo-German Bilateral Project on Watershed management, Ministry of Agriculture, Govt. of India, New Delhi, India.
- Sahu, R.K., Mishra, S.K., Eldho, T.I., and Jain, M.K. (2006). An advanced soil moisture accounting procedure for SCS curve number method. *J. Hydrol. Process.*, HYP-06-0016. (Published online).
- Sander, G.C., Hairsine, P.B., Rose, C.W., Cassidy, D., Parlange, J.Y., Hogarth, W.L., and Lisle, I.G. (1996). Unsteady soil erosion model, analytical solutions and comparison with experimental results. *J. Hydrology*, **178**: 351-367.
- Sansalone, J.J., and Buchberger, S.G. (1997). Partitioning and first flush of metals in urban roadway storm water. *J. Environ. Engg., ASCE*, **123**(2):134-143.
- Sansalone, J.J., Koran, J.M., Smithson, J.A., and Buchberger, S.G. (1998). Physical characteristics of urban roadway solids transported during rain events. *J. Environ. Engg., ASCE*, **125**(6): 556-565.
- Schneider, L.E., and McCuen, R. H. (2005). Statistical guidelines for curve number generation. *J. of Irrig. and Drain. Engg., ASCE*, **131**(3): 282-290.
- Schultz, J.P. (1985). Detachment and splash of a cohesive soil by rainfall. *Trans. ASAE*, **28**(6):1878-1884.
- Schumm, S.A. (1954). Relation of drainage basin relief to sediment loss. Symp. on Continental Erosion, IAHS, **36**(1):216-219.

- Sharda, V.N., and Singh, S.R. (1994). A finite element model for simulating runoff and soil erosion from mechanically treated agricultural lands 1. Governing equations and solutions. *Water Resources Research*, **30**(7): 2287-2298.
- Sharda, V.N., Juyal, G.P., and Singh, P.N. (2002). Hydrologic and sedimentologic behavior of a conservation bench terrace system in a sub-humid climate. *Trans. ASAE*, **45**(5): 1433-1441.
- Sherman, L.K. (1949). The unit hydrograph method. In: Meinzer, O.E. (ed.), *Physics of the Earth*, Dover Publications, Inc., New York: 514-525.
- Shirley, E.D., and Lane, L.J. (1978). A sediment yield equation from an erosion model. *Proc. Hydrology and Water Resour.*, **8**: 90-96.
- Singh, V.P. (1985). A mathematical study of erosion from upland areas. Water Resources Report, Dept. of Civil and Env. Engrg., Louisiana State University, Baton Rouge, LA 70803-6405.
- Singh, V.P. (1988). *Hydrologic Systems, Vol. 2: Watershed Modeling*. Prentice Hall, Englewood Cliffs, New Jersey.
- Singh, V.P. (1992). *Elementary Hydrology*. Prentice Hall, Englewood Cliffs, New Jersey.
- Singh, V.P., Banicekiewiez, A., and Chen, V.J. (1982). An instantaneous unit sediment graph study for small upland watersheds. In: Singh, V.P. (ed.), *Modeling Components of Hydrologic cycle*, Littleton, Colo., Water Resources Publications:539-554.
- Singh, V.P. and Chen, V.J. (1983). The relationship between storm runoff and sediment yield. Tech. Rep.3, Water Resources Program, Dept. of Civil and Environmental Engineering, Louisiana State University, Baton Rouge, LA 70803.
- Singh, P., Narda, N.K., and Singh, A. (1992). Evaluation of Horton and Philip infiltration functions for determining optimum slope of graded check borders, *J. of Agric. Engg., ISAE*, **29**(1-4): 1-9.
- Singh, P., and Singh, V.P. (2001). *Snow and Glacier Hydrology*. Kluwer Academic Publishers, P.O. Box 322, Dordrecht, The Netherlands.
- Singh, R.D., Mishra, S.K., and Chowdhary, H. (2001). Regional flow duration models for 1200 ungauged Himalayan watersheds for planning micro-hydro projects. *J. Hydrol. Engg., Tech. Note, ASCE*, **6**(4).

- Singh, V.P., and Prasad, S.N. (1982). Explicit solutions of kinematic equations for erosion on an infiltrating plane. In: Singh, V.P. (ed.) Modeling Components of Hydrologic Cycle. Water Resources, Littleton, CO, pp. 515-538.
- Singh, V.P. and Regi, R.R. (1983). Analytical solutions of kinematic equations for erosion on a plane: I. Rainfall of indefinite duration. *Advances in Water Resources*, 6(1): 2-10.
- Singh, V.P., and Yu, F.X. (1990). Derivation of infiltration equation using systems approach. *J. Irrig. and Drain. Engg., ASCE*, 116(6): 837-857.
- Skaggs, R.W., Huggins, L.E., Monke, E.J., and Foster, G.R. (1969). Experimental evaluation of infiltration equations. *Trans. ASAE*, 12(6): 822-828.
- Smith, D.D. (1941). Interpretation of soil conservation data for field use. *Agricultural Engineering*, 22.
- Smith, D.D., and Whitt, D.M. (1947). Estimating soil losses from field areas of claypan soil. *Soil Sci. Soc. Proc.*, 12: 485-490.
- Smith, D. D., and Whitt, D.M. (1948). Evaluating soil loss from field areas. *Agriculture Engineering*, 19:394-396, 398.
- Smith, R.E. (1972). The infiltration envelopes: Results from a theoretical infiltrometer. *J. Hydrology*, 17: 1-21.
- Smith, R.E., and Parlange, J.Y. (1978). A parameter efficient hydrologic infiltration model. *Water Resources Research*, 14(3): 533-538.
- Snyder, G. (1980). Computer usage in making watershed management decisions. Proc. of Symp. on Interior West Watershed Management, Washington.
- Soil survey of Hamilton County (1982). U.S. Dept. of Agriculture, Washington D.C.:1-220.
- Soni, B., Mishra, G.C. (1985). Soil water accounting using SCS hydrologic soil classification, case study. National Institute of Hydrology, Roorkee (India).
- Springer, E.P., McGurk, B.J., Hawkins, R.H., and Goltharp, G.B. (1980). Curve numbers from watershed data. Proc. Symp. on Watershed Management, Irrigation and Drainage Div., ASCE, New York, 2: 938-950.

- Steenhuis, T.S., Winchell, M., Rossing, J., Zollweg, J.A., and Walter, M.F. (1995). SCS runoff equation revisited for variable-source runoff areas. *J. Irrig. and Drain. Engg., ASCE*, **121**(3), 234-238.
- Su, B., Kazama, S., Lu, M., and Sawamoto, M. (2003). Development of a distributed hydrological model and its application to soil erosion simulation in a forested catchment during storm period. *J. Hydrol. Process.* **17**: 2811-2823.
- Swartzendruber, D., and Youngs, E.G. (1974). A comparison of physically based infiltration equations. *Soil Science*, **117**(3): 165-167.
- Tayfur, G. (2001). Modeling two-dimensional erosion process over infiltrating surface. *J. Hydrol. Engg., ASCE*, **6**(3): 259-262.
- Tayfur, G. (2002). Applicability of sediment transport capacity models for nonsteady state erosion from steep slopes. *J. Hydrol. Engg., ASCE*, **7**(3): 252-259.
- Tayfur, G., and Kavvas, M.L. (1994). Spatially averaged conservation equations for interacting rill-interrill area overland flows. *J. Hydr. Engrg., ASCE*, **120**(12): 1426-1448.
- Taylor, B.D. (1983). Sediment rates in coastal southern U.S. *J. Hydr. Div., ASCE*, **109**(1):71-85.
- USFS (1959). Forest and Range Hydrology Handbook. U.S. Forest Service Publication, Washington, D.C.
- Vanliew, M.W., and Saxton, K.E. (1984). Dynamic simulation of sediment discharge from agricultural watersheds. *Trans. ASAE*, **27**(4): 678-682.
- Van Doren, C.A., and Bartelli, L.J. (1956). A method of forecasting soil losses. *Agricultural Engineering*, **37**.
- Van Genuchten, M.Th. (1980). A closed form equation for predicting the hydraulic conductivity of unsaturated soils. *J. Soil Sc. Soc. Am.*, **44**(5): 892-898.
- Van Mullem, J.A. (1989). Runoff and peak discharges using Green-Ampt infiltration model. *J. Hydr. Engg., ASCE*, **117**(3), 354-370.
- Walling, D.E. (1983). The sediment delivery problems. *J. Hydrology*, **65**:209-237.
- Walling, D.E. (1988). Erosion and sediment yield research - some recent perspectives. *J. Hydrology*, **100**: 113-141.

- Walling, D.E., and Webb, B.W. (1983). Patterns of sediment yield. In: Gregory, K.J. (ed.), *Background to Paleohydrology*, Wiley, New York.
- Watson, D.A., and Laflen, J.M. (1986). Soil strength, slope and rainfall intensity effects on interrill erosion. *Trans. ASAE*, **29**: 98-102.
- Whisler, F.D., and Bower, H. (1970). Comparison of methods for calculating vertical drainage and infiltration for soils. *J. Hydrology*, **10**: 12-19.
- White, I., and Sully, M.J. (1987). Macroscopic and microscopic capillary length and time scales from field infiltration. *Water Resources Research*, **23**:1514-1522.
- Wicks, J.M., and J.C. Bathurst (1996). SHESED: a physically based, distributed erosion and sediment yield component for the SHE hydrological modelling system. *J. Hydrology*, **175**: 213-238.
- Williams, J.R. (1975). Sediment yield prediction with Universal equation using runoff energy factor, In: Present and Prospective Technology for Predicting Sediment Yields and Sources, USDA-ARS, S-40, USDA: 244-252.
- Williams, J.R. (1978). A sediment graph model based on an instantaneous unit sediment graph. *Water Resources Research*, **14**: 659-664.
- Williams, J.R., and Berndt, H.D. (1972). Sediment yield computed with universal soil loss equation. *J. Hyd. Div., ASCE*, **98**(HY12):2087-2098.
- Williams, J.R., and Berndt, H.D. (1977). Sediment yield prediction based on watershed hydrology, *Trans. ASAE*, **20**: 1100-1104.
- Williams, J.R. and Hann, R.W. (1978). Optimal operation of large agricultural watersheds with water quality constraints. Texas Water Resources Institute, Texas A&M Univ., Tech. Rep. No. 96.
- Williams, J. R., and LaSeur, V. (1976). Water yield model using SCS curve numbers. *J. Hydraulics Engg., ASCE*, **102**(HY9): 1241-1253.
- Williams, J. R., Dyke, P. T., and Jones, C. A. (1983). EPIC: a model for assessing the effects of erosion on soil productivity. In: Laurenroth, W. K., Skogerboe, G. V., and Flug, M. (ed.), *Analysis of Ecological Systems: state-of-the-art in ecological modeling*, Amsterdam, Elsevier Science:553-572.

- Wilson, B. N., Slack, D.C., and Young, R.A. (1982). A comparison of three infiltration models. *Trans. ASAE*, **25**: 349-356.
- Wilson, L. (1973). Seasonal sediment yield patterns of U.S. rivers. *Water Resources Research*, **8**.
- Wischmeier, W.H. (1975). Estimating the soil loss equation's cover and management factor for undistributed areas. In: Present and Prospective Technology for Predicting Sediment Yields and Sources. ARS-S-40. USDA-ARS: 113-117.
- Wischmeier, W.H. (1976). Use and misuse of universal soil loss equation. *J. Soil and Water Conservation*, **33**(1): 5-9.
- Wischmeier, W.H., and Mannering, J.V. (1969). Relation of soil properties to its erodibility. *Soil Sci. Soc. Am. Proc.*, **33**: 131-137.
- Wischmeier, W.H., and Smith, D.D. (1958). Rainfall energy and its relationship to soil loss. *Trans. Am. Geophysical Union*, **39**(3):285-291.
- Wischmeier, W.H., and Smith, D.D. (1965). Predicting rainfall-erosion losses from cropland east of Rocky Mountains, USA Agricultural Handbook No. 282, Washington, DC.
- Wischmeier, W.H., and Smith, D.D. (1978). Predicting rainfall erosion losses-A guide to conservation planning. USDA, Agriculture Handbook 537, Washington, D.C.
- Wischmeier, W.H., Johnson, C.B., and Cross, B.V. (1971). A soil erodibility nomograph for farmland and construction sites. *J. Soil and Water Cons.*, **26**: 189-193.
- Wolman, M.G. (1977). Changing needs and opportunities in the sediment field. *Water Resources Research*, **13**: 50-54.
- Woolhiser, D.A. (1977). Unsteady free-surface flow problems in mathematical models of surface water hydrology. In: Criani, T.A., Marions, V., and Wallis, J.R. (eds.), A Wiley Interscience publication: 195-213.
- Woolhiser, D.A., Smith, R.E., and Goodrich, D.C. (1990). KINEROS: a kinematic runoff and erosion model: documentation and users manual. USDA Agriculture Research Service, ARS-77, USA.
- Wu, T.H., Hall, J.A., and Bonta, J.V. (1993). Evaluation of runoff and erosion models. *J. Irrig. and Drain. Engg., ASCE*, **119**(4): 364-382.



- Wurbs, R.A. (1994). Computer Models for Water Resources Planning and Management. U.S. Army Corps of Engineers, IWR Report 94-NDS-7.
- Yalin, Y.S. (1963). An expression for bed load transport. *J. Hydr. Div., ASCE*, **89**: 221-250.
- Young, R.A., Onstad, C.A., Bosch, D.D., Anderson, W.P. (1987). AGNPS: An agricultural non-point source pollution model: A large water analysis model. U.S. Dept. of Agri., Cons. Res. Report No.35.
- Yu, B. (1998). Theoretical justification of SCS method for runoff estimation. *J. Irrig. and Drain. Engg., ASCE*, **124**(6): 306-310.
- Yuan, Y., Mitchell, J.K., Hirschi, M.C., and Cooke, R.A.C. (2001). Modified SCS curve number method for predicting subsurface drainage flow. *Trans. ASAE*, **44**(6): 1673-1682.
- Zeng, W. (2000). A model for understanding and managing the impacts of sediment behavior on river water quality. Ph.D. Dissertation, Univ. of Georgia, Athens, Ga.
- Zeng, W., and Beck, M. B. (2001). Development and evaluation of a mathematical model for the study of sediment-related water quality issues." *Water Sci. Technol.*, **43**(7): 47-54.
- Zhang, G.H., Liu, B.Y., Nearing, M.A., and Zhang, K.L. (2002). Soil detachment by shallow flow. *Trans. ASAE*, **45**(2): 351-357.
- Zingg, A.W. (1940). Degree and length of land slope as it affects soil loss in runoff. *Agricultural Engineering*, **21**: 59-64.

## LIST OF PUBLICATIONS

---

### PUBLISHED

1. Mishra, S.K., Tyagi, J.V., and Singh, V.P. (2003). Comparison of infiltration models. *J. Hydrol. Process.*, **17**:2629-2652.
2. Mishra, S.K., Tyagi, J.V., Singh, V.P., and Singh, R. (2006). SCS-CN-based modeling of sediment yield. *J. Hydrology*, **324**: 301-322.

### COMMUNICATED AND UNDER REVIEW

3. Tyagi, J.V., Mishra, S.K., Singh, R., and Singh, V.P.: SCS-CN based time-distributed sediment yield model. *J. Hydrology* (under review).